The design, development and characterization of a self-replicating DNA expression technology.

By

Warren Ralph Josephus de Moor
DMRWAR001

A thesis submitted to the University of Cape Town in fulfilment of the requirements for the degree

Doctor of Philosophy

in Medical Virology

2020

Supervisor: Professor Edward Rybicki

Co-supervisors: Dr Guy Regnard and Professor Anna-Lise Williamson

In the Department of Pathology

Faculty of Health Sciences, University of Cape Town, South Africa

These are some quotes that have inspired me

"To see a World in a Grain of Sand

And a Heaven in a Wild Flower

Hold Infinity in the palm of your hand

And Eternity in an hour"

~ William Blake ~

The truth is rarely pure and never simple.

~Oscar Wild~

This is your last chance. After this, there is no turning back. You take the blue pill—the story ends, you wake up in your bed and believe whatever you want to believe. You take the red pill—you stay in Wonderland, and I show you how deep the rabbit hole goes.

~Morpheus: The Matrix~

DECLARATION

The work described in the thesis below was done at the Division of Medical Virology, Department of Pathology at the University of Cape Town, Health Sciences campus under the supervision and guidance of Professor Edward Rybicki Professor Anna-Lise Williamson, Dr Guy Regnard. This is my own work, and where use has been made of others, their contribution has been acknowledged.

Signed by candidate

Warren Ralph Josephus de Moor

Signed: 25/09/2019

Table of Contents

Appendicies

Abstract

High quality T-cell immunogenicity can be an elusive type of immunity to generate and one that is often sought after by virologists, immunologists and cancer researchers alike. When T-cell immunity is generated using current methodologies the quality and magnitude of the immunological response achieved is often weak and unable to create protective immunity. Among current methods, DNA vaccines, generate highly specific T-cell immunity towards targeted antigens, and do not suffer from issues like misdirected vector targeted immunity, like viral based vectors. DNA vaccines, however, face a variety of their own weaknesses. These include, inefficient delivery, high biological loss inside the body, and the inability to counteract or avoid immediate innate cellular defence mechanisms, which limit their ability to persist inside a host cell. For these reasons, DNA vaccines are usually combined with more conventional viral vaccines in what is known as a DNA prime and viral boost regiment strategy. Combining them works well and results in improved immunity towards targeted antigens that is superior to what is obtained when either DNA or recombinant vaccines are used alone.

To address many of the core issues faced by DNA vaccines, I report here on the design, development and characterization of a self-replication DNA gene expression technology. This novel DNA expression system employs a form of DNA replication (known as rolling circle replication) to generate a self-replicating DNA amplicon that can amplify its own copy number and the relative localised levels of antigen expression inside transfected mammalian cells in tissue culture and within Balb/cJ mice. These capabilities help effectively mitigate many of the core issues faced by DNA vaccines.

The technology developed was shown to significantly increase gene expression for eGFP and Luciferase reporter genes, with an overall average increase in expression of approximately two-fold by 48 h post transfection in HeLa S3 cells. More specifically, an increase of at least two-fold in the absolute maximum level of the gene of interest per cell was also observed. Such localised doubling in antigen expression, at the cellular level, is believed to enhance innate immune activation and improve the overall immune response. Experimental results indicated that gene expression levels by this technology is non static in nature and appears to increase in magnitude within affected cells over time as was hypothesised. This provided strong evidence that the replication technology appears to be functioning as was expected and was able to demonstrate the ability to elevate antigen expression over time, potentially starting from extremely low and otherwise ineffective starting concentrations. This ability has potential to effectively mitigate many of the issues associated DNA vaccines such as low and ineffective delivery.

This capability was observed in tissue culture as a steady increase in reporter gene expression levels across the entire range of DNA transfection levels. Furthermore, the increases in gene expression were observed to continue to amplify over time, eliminating the presence of weakly fluorescing cells in tissue culture. By 11 days post transfection, every observable cell transfected with the replication expression

system, was observed to have extremely high levels of fluorescence. With recorded fluorescence levels being as bright or brighter than the highest levels obtained under normal transfections with non-replicative plasmids (~48-72 h).

Unique cellular responses to the presence of the replicating gene expression technology were also observed. These included an apparent slowdown in cellular metabolic activity and growth among cells transfected with replicating vectors. This was observed as a decrease in cellular division and total cell number by ~50%, by 48 h post transfection. This was accompanied by significant increases in cell size, internal cellular granularity, and gene-of-interest expression per cell. These changes were observed among all cells regardless of their relative DNA transfection level. This was demonstrated by assessment of the change in the range, mean, median, skewness and standard deviation of the cellular distribution curves for eGFP expression, cell size and internal cellular granularity. These observations provided further evidence of the dynamically changing and active nature of this technology. This also provided evidence that the replicating gene expression technology has a definitively different kind of cellular impact and effect on transfected cells compared to non-replicating DNA expression systems.

Pilot studies to test the technology in Balb/cJ mice indicated, the technology appears to be functional within this animal model and was able to increase gene of interest (eGFP) expression levels compared to an equivalent non-replicating DNA expression vector control. Furthermore, these animal experiments also demonstrated significant increases in the maximum possible level of expression achieved within localised ‘hot spots’ of muscle fibre bundles. This effect appeared to increase following transient addition of additional replication associated protein (Rep), giving further evidence this technology appears to be functional within the Balb/cJ animal model. Suggesting that the rate at which the replication amplification process occurs, may also be manipulated by adjusting Rep concentration.

Finally, an antiviral response gene array was run to look for evidence that the replicating gene expression technology could increases antiviral response gene activation, to possibly improve T-cell activation and immunity. The array provided evidence improved antiviral response gene activation was occurring however the data was inconclusive in nature and further investigation is needed to verify these preliminary findings. The array also showed significant evidence of Rep induced Caspase 10 (CASP10), gene suppression. This suggests that Rep may play a role in the survival and virulence of BFDV by acting as a suppressor of cellular apoptosis in a concentration-dependant manner and is worth investigating further.

Acknowledgements

Firstly, I would like to thank my supervisors Professor Anna-Lise Williamson, Professor Edward Rybicki and Dr Guy Regnard for their consistent encouragement and support of my work despite many setbacks and changes that were undertaken to develop into the project presented here.

I also want to thank my family Ferdinand and Irene de Moor and my sister Robyn Bandey for their continuous help and support in every way as well as their patience and understanding since my MSc. To Lindi Swart for always being there for me and having the patience and perseverance to stick with me through thick and thin throughout the duration this project.

I would like to extend my gratitude to Professor Anna-Lise Williamson, National Research Foundation (NRF) and the Poliomyelytis Research Foundation (PRF) as well as the University of Cape Town (UCT) for all their assistance in terms of the financial aid and support given to me and this project.

Special thanks go to Mr Rodney Lucas, the UCT animal technologist and his team who performed all animal inoculations, feeding, maintenance, euthanasia and tissue harvesting procedures for the mice experiments conducted. I could not have done this work without his expertise and professionalism.

Additional thanks go to Mrs Susan Cooper for all her help with work done using the confocal microscope as well as Miss Hayley Tomes for her assistance with histology sectioning and staining.

Finally, I would like to thank all my lab collages for their advice and support throughout this journey, with a special thanks to Godfrey Dzhivhuho for his help with ELISpot experimental protocols and training, and Gerald Chenge for supplying reagents for these experiments. To all my lab colleagues for their advice, wisdom and friendship and all the interesting conversations, stories and jokes to help lighten up PhD life.

List of Abbreviations

%	- percentage
#	- number
°C	- degrees Celsius
µl	- microlitre
µM	- micromolar
aka	- also known as
AD5	- Adenovirus 5
ADCC	- antibody dependent cellular cytotoxicity
AEC	- Animal Ethics Committee
AIM2	- absent in melanoma 2
ALRs	- AIM-like receptors
APC	- antigen presenting cell
ATCC	- American Type Culture Collection
ATP	- adenosine triphosphate
BFDV	- beak and feather disease virus
bp	- base pair
CARD9	- caspase recruitment domain family member 9
CASP 8/10	- caspase 8/10
CCL5	- C-C motif chemokine ligand 5
CD4/8+	- cluster of differentiation 4/8 positive
CDC	- Centers for Disease Control
CENP-A/B/C	- centromeric protein A/B/C
cGAMP	- cyclic guanosine monophosphate adenosine monophosphate
cGAS	- cyclic guanosine monophosphate adenosine monophosphate synthase
CMV	- cytomegalovirus
cp / CP	- capsid protein gene / capsid protein
CpG	- cytosine phosphate guanine nucleotide pairs
CTL	- cytotoxic T-lymphocytes (aka CD8+)
CXCL 8/11	- C-X-C motif chemokine ligand 8/11
DAMPs	- damage associated molecular patterns
Daxx	- death associated domain protein
DHX58	- DExH-box helicase 58
DMEM	- Dulbecco's modified Eagle's medium
df	- dilution factor
DNA	- deoxyribonucleic acid
dNTP’s	- deoxy-nucleotide triphosphates
dsDNA	- double-stranded deoxyribonucleic acid
EDTA	- ethylenediaminetetraacetic acid
EtOH	- ethanol
FBS	- foetal bovine serum
g	- gram
Gag	- Group-specific antigen
gp	- glycoprotein
GTP	- guanosine triphosphate
h	- hours
H5N1	- Influenza A virus subtype H5N1 (hemagglutinin 5 neuraminidase 1)
HBV	- hepatitis B virus
HIN200	- hematopoietic interferon-inducible nuclear protein with a 200-amino-acid repeat
HIV	- human immunodeficiency virus
HLA	- human leukocyte antigen

HPXV	- horsepox virus
HSV	- herpes simplex virus
IAV	- influenza A virus
ICD	- immunogenic regulated cell death
iCDR	- interphase centromere damage response
IFI16	- interferon-inducible protein 16
IFNB1	- Interferon beta 1
IL12B	- Interleukin 12 beta
IRF3/5	- interferon regulatory/response factor 3/5
kbp	- kilo-base pair
kDa	- kilo-Daltons
LACV	- La Crosse virus
LAV	- live attenuated vaccines/viruses
LB	- lysogeny broth (aka Luria broth, Lennox broth, or Luria-Bertani medium)
MEFV	- Mediterranean fever, aka pyrin innate immunity regulator
MHCI/II	- major histocompatibility complex class I or II
min	- minutes
ml	- millilitre
mM	- millimolar
MOI	- multiplicity of infection
mol	- molar
mRNA	- messenger ribonucleic acid
mTOR	- mammalian target of rapamycin
MVA	- modified vaccinia virus Ankara
MX1	- MX dynamin like GTPase 1
MyD88	- myeloid differentiation primary response gene 88
Na*Cl*	- sodium chloride
ND10	- nuclear domain 10
Nef	- negative regulatory factor
NF-κB	- nuclear factor kappa beta
NK	- natural killer cell
nm	- nanometre
nmol	- nanomolar
NRF	- National Research Foundation
OAS2	- 2'-5'-oligoadenylate synthetase 2
PAMPs	- pathogen associated molecular patterns
PCR	- polymerase chain reaction
pmol	- picomolar
pt	- post transfection
PBFD	- psittacine beak and feather disease
PCV	- porcine circovirus
PrEP	- pre-exposure prophylaxis
PRF	- Poliomyelytis Research Foundation
PRR	- pattern/pathogen recognition receptors
pUC19	- plasmid University of California number 19
PVDF	- polyvinylidene fluoride
PY	- pyrin domain
rAD5	- recombinant adenovirus 5
RAF	- Research Animal Facility
RCA	- rolling circle amplification
RCR+/-	- rolling circle replication (positive or negative capability)
Rep	- replication associated protein
rep	- replication associated protein gene
RIG-1	- retinoic acid-inducible gene 1
RNA	- ribonucleic acid

rpm	- revolutions per minute
SDS-PAGE	- sodium dodecyl sulphate polyacrylamide gel electrophoresis
sec	- seconds
SP100	- speckled protein of 100 kDa
ssDNA	- single-stranded deoxyribonucleic acid
STEP	- HIV vaccine study and Phambili trial
STING	- stimulator of interferon genes
SUMOs	- small ubiquitin-like modifiers
SV40	- simian vacuolating virus 40
TBK-1	- serine/threonine protein kinase TANK-binding kinase 1
THOV	- Thogoto virus
TLR	- toll like receptor
TR	- transfection reagent
Tris	- tris(hydroxymethyl)aminomethane
tRNA	- transfer ribonucleic acid
UCT	- University of Cape Town
UV	- ultraviolet
V	- volts
VACV	- vaccinia virus
WHO	- World Health Organisation
x g	- times gravity
YF-D17	- yellow fever virus D17 strain

1. Literature review

1.1 The history of medicine and immunization

The Rod of Asclepius, a type of Caduceus (or snake around a stick) is the ancient emblem of the medicinal arts. It is used all around the world, a truly ancient symbol which dates back as far as 3000-4000 BCE (Ward, 1910). Coincidentally, this is also roughly the same time frame that recent phylogenetic analysis has associated with the emergence of the smallpox variola virus VARX, the first virus to ever be vaccinated against (Babkin and Babkina, 2015).

The story of vaccines, immunization and how they relate to the practice of medicine is an interesting one. The first medicinal practitioners, it seems, were snake charmers, shamans and witchdoctors. These very first practitioners of medicine were aware of the concept of immunity and even had some idea of influencing its development. Many diseases, including smallpox, do not afflict people a second time after they survived a previous infection. The desire to manufacture and transfer this 'immunity' to others was actively pursued by these medicine men (Babkin and Babkina, 2015; Lawson, 2004).

At the time snake handlers had at least some concept of how immunity was generated, as they knew that repeated small exposures of snake venom could give them an immunity to snake venom doses that were normally lethal, and that this could save their lives if they were bitten by the same snake. From this knowledge they developed concoctions and potions, often using snake venom as an ingredient, and sold their wares for profit - and so the first 'snake oil' sales/medicine men were born. The practice of self-immunizing with snake venom, is still practiced by snake handlers today (Benoit, 2010; Stone et al., 2013).

As we look back to these historical practices of old, which gave birth to the medical quest to grant us immunity from disease, we can see that the history of medicine is often a history of attempting to boost the immune system. Most of the time these medicinal practitioners had no idea of what might work or not; however, snake venom and the idea of combining the suspected causative agent into a medical concoction that weakens the effect of the venom, seems to have persisted. There are Egyptian papyrus medical scrolls from 380-343 BCE which contain recipes for such medical concoctions and antidotes, which were usually a mixture of mud, herbs and crushed up medicinal plants, saliva, and animal blood and parts. Importantly though, they often included the suspected causative agent with a bit of snake venom for good measure (Lawson 2004, Anderson 2005). One of the preferred delivery methods for such concoctions was the scarification method, whereby a small incision or scratch was made in the skin and the medical concoction rubbed into it (Lawson 2004, Anderson 2005). Through the lens of modern science, we now know that many useful medicinal compounds have been derived from these ancient known medicinal plants. We also know now that the act of mixing things like viruses and snake

venoms with the chemically active compounds found in freshly crushed plant matter, such as plant phenols and various other plant compounds, oils and enzymes, could easily have had the effect of chemically inactivating or denaturing whatever disease or toxins present within them, making them safer for human exposure. Similarly, heating or aging the disease-causing agents and toxins and exposing them to sunlight (UV inactivating), are also viable methods of denaturing proteins or inactivating viruses. Furthermore, the compounds and micro-organisms found in these ingredients may well have had adjuvant-like effects.

From these stories and recipes, we can discern a philosophy about immunity beginning to emerge. A simple and age-old one, retold in diverse cultures around the world but one that essentially acknowledges the same truth: that which does not kill you, makes you stronger. An example of this philosophy in practice in ancient times is 'Mithridatism', whereby one ingests small amounts of known poisons to develop an immunity to them (Swiderski, 2010).

1.1.1 Immunization technology from smallpox to vaccine science

In the ancient medicine book, and encyclopaedia of plant knowledge, known as the 'Grete Herball', one of the first recorded methods for immunization against smallpox is described (Treveris, 1526). The method involved taking the pus from a person with a 'favourable' form of the disease and transferring or inoculating it intra-nasally to a healthy individual. This resulted in the transference of a 'milder' form of the disease, and development of immunity. Examples of this basic method have been found in Chinese texts dating back as far as the 10th century CE. Later Chinese texts go on to describe an even more mild transference of the disease, whereby the pox material should be aged by carrying it at body temperature for a period of one month before its use (Gross and Sepkowitz, 1998). The method also stated that if this could not be done, due to time constraints, the pox material could alternatively, be mixed with herbs and heated with steam (Boylston, 2012). A similar method was also reportedly used by the Arabs and Ottomans around the same time. It is therefore difficult to trace its true origins. In any event, such procedures arguably describe the first methods of inactivating the smallpox virus wholly or partially for immunization purposes. The method recounted in the 'Grete Herball' goes further still, by suggesting that powdered 'cow ice' (which was not characterized) can be used as alternative, if suitable smallpox material could not be obtained (Gross and Sepkowitz, 1998). Could this have been the first use of cowpox material to vaccinate for smallpox? We now know the smallpox vaccine, used to eradicate the disease and developed from the method famously published by Edward Jenner, is a live preparation of the vaccinia virus (VACV) originally obtained from cow lymph which supposedly derives from cowpox pustules. It is therefore possible that 'cow ice' may be referring to cowpox material (Gross and Sepkowitz, 1998; Treveris, 1526).

Other examples of its use recorded in history include its use by Lady Mary Wortley Montagu who learned about its use in Constantinople. At her behest and the Prince of Wales the technique was tested

with a follow up challenge experiment in 1721 on prisoners and abandoned children who were inoculated under the skin. Then after a period of several months later, these patients were deliberately exposed to smallpox. At which point the procedure was deemed to be safe and members of the royal family were subsequently inoculated. The procedure then became fashionable in Europe. Cotton Mather from Massachusetts also reportedly promoted and publicised the technique after being introduced to it by one of his African slaves, Onesimus. Resulting in its use during the Boston smallpox epidemic of 1721 (National Institutes of Health, 2002).

Jenner's contribution to vaccinology was not the discovery that the inoculum from cowpox pustules could be used to safely immunize against smallpox, using widespread variolation techniques. As the method was known to be in common use in the early as 1700's long before Jenner "vaccinated" James Phillips and even in the UK, it had been publicised by a man named Benjamin Jesty who had performed the procedure on his own children, and also tested by challenging them with smallpox (Gross and Sepkowitz, 1998; Pead, 2006). It is likely that the practice was around sometime before then, which explains the reason why these men appeared to be so confident that the practice worked: they were willing to stake their reputations and wellbeing on their convictions, by openly and publicly performing dangerous smallpox challenge experiments, to prove the method worked and publicise their results. The real question is, if they knew it worked, why did they feel the need go to such effort to test it publicly at great risk to themselves? These publicised treatments it would seem were made in an attempt to document this knowledge for public use, however until Jenner it appears the dissemination of this knowledge largely failed. Indicating the difficulty of officially challenging the medical establishments dogma of the time. In this sense Jenner does indeed deserve a fair share of recognition and acclaim, for two important reasons. First, he carefully recorded and properly documented his experiment by meticulously following and applying the scientific method. This gave him the hard evidence and data he needed to properly and professionally publish the knowledge in a manner that could not be ignored by the medical establishment of the time. This forced them to consider new ideas and practices that challenged the establishment dogma. Jenner staked his reputation and career when he did this and he stood firm when the inevitable medical and scientific community backlash came for him (Gross and Sepkowitz, 1998). Part of Jenner's success lies not only with his solid adherence to scientific method, which made challenging his claims very difficult for his opponents, but also with the way he marketed his findings to the public. His rebranding of the legitimately controversial practice of variolation (done using smallpox pus at the time) with a new term 'vaccination' (which he coined) for essentially the same procedure using cowpox inoculum instead, was a brilliant marketing move.

1.1.2 Improving technology and methods

The history of immunization can thus be regarded as a progression: from rudimentary practices of warrior scarification rituals for immunity using snake venom concoctions, to Mithridatism for immunizing oneself from poisoning, to variolation, and then to vaccination by inoculation of cowpox to immunize against smallpox. How far have we come? Ironically, in some ways a full circle it might seem, as Liu. *et al* (2010) have shown that the scarification method actually produces a superior immune response when compared to intramuscular inoculation using a syringe and needle. Their study showed that inoculations using the scarification method with either vaccinia virus (VACV) or modified vaccinia Ankara virus (MVA) produced vastly better T-cell immunogenicity than intramuscular inoculations did (by generating a more complete level of protection which was independent of neutralizing antibodies titres in subsequent challenge experiments). In this context, it should be noted that VACV and MVA are some of the most widely used, and successful, vaccine vectors available today. These vaccine vectors are essentially safer and attenuated versions of the same cowpox virus used by Jenner that brought about the eradication of smallpox. Phylogenetically, however, the 'cowpox' used at the time, and which later went on to become the VACV vaccine strain identified from these vaccine stocks, appears to be genetically closer to wild horsepox strains of the orthopoxvirus genus which includes smallpox and cowpox. As all of these viruses are able to infect horses, cows and humans, and develop the same symptoms, and can vaccinate against smallpox, this becomes somewhat of a moot point (Esparza et al., 2018). Today MVA, VACV and other poxviruses are used as vaccine vectors for a diverse set of diseases by being genetically modified to express antigens from other pathogens.

As for the scarification method, its superior immunogenicity was attributed to skin-resident effector memory T cells. Amazingly, scarification was also able to confer immune protection in B cell-deficient mice, whereas intra-peritoneal injections could not (Liu et al., 2010). Vaccine delivery to the skin via micro-needling and tattoo gun methods has similarly been shown to induce superior immunogenicity for DNA vaccines as well, where the many minor mechanical injuries produced by the tattooing microneedle induce natural haemorrhaging, cellular necrosis and inflammation to occur, followed eventually by cellular regeneration. This sequence of events serves to naturally stimulate the immune system in a manner similar to scarification and is believed to help contribute towards the superior immunogenicity generated thereafter (Hu et al., 2016; Pokorna et al., 2008).

This is where the vaccine research field may arguably be stuck. The vaccine development methods and techniques that worked well for polio and smallpox are not sufficient for the chronic infecting viruses like HIV and herpes simplex virus (HSV), which require strong T-cell immunogenicity for a vaccine to work - as indicated by the fact that the correlates of protection for these viruses indicate that T-cell immunogenicity is a critical part of their biological control. To be fair, the current vaccine development tools, and especially live-attenuated vaccines such as poxvirus vaccines, do generate T-cell based

immunity. It is however recognised that this area of vaccine research has significant room for improvement. One approach, used in HIV vaccine trials, is a prime-boost vaccine strategy, which often starts with a DNA prime followed by a poxviral boost. Although this strategy is promising, there is a need for further improvements and stronger developmental tools that can target and improve specific types or areas of the immune response generated. This is particularly true when it comes to the CDCs list of prevalent communicable diseases, most of which have proven especially difficult to vaccinate against and treat (Garber et al., 2012; Hongo et al., 2015; Nolz and Harty, 2011). Similarly, the cancer vaccine research field is also seeking the ability to generate targeted T-cell immunogenicity, which, if achieved, offers the potential to cure a wide variety of difficult-to-target cancers (Makkouk and Weiner, 2015; McNeel et al., 2012; Tokunaga et al., 2018; Vermaelen, 2019; Vyas et al., 2016; Walther and Stein, 2009). To develop vaccine strategies capable of achieving these ever more demanding immunological outcomes, necessary to combat these diseases, will require researchers to leverage the most advanced knowledge available concerning the ways in which the immune system works in order to discover new ways of directing immune function, which is required to generate the powerful, targeted immune responses needed. The nuanced ways in which immunogenic outcomes can be altered, often with great effect, demonstrates that a gap in knowledge still exists and that a more precise and detailed understanding of the immune system and how it is engaged by vaccines, is crucial and key to controlling this complex system to direct it towards desired immunogenic outcomes (Georg and Sander, 2019).

1.2 The Immune system – The author of immunity

What is mammalian immunity and where does it come from? The answer is the incredibly complex and interconnected immune system, an army of cells that recognise pathogens and can attack and destroy them, to maintain a state of health and hygiene.

The Merriam-Webster online dictionary (Merriam-Webster, 2019), defines the Immune system as: *"the bodily system that protects the body from foreign substances, cells, and tissues by producing the immune response and that includes especially the thymus, spleen, lymph nodes, special deposits of lymphoid tissue (as in the gastrointestinal tract and bone marrow), macrophages, lymphocytes including the B cells and T cells, and antibodies."* Although this is a reasonably good definition, it falls short of defining the vast array of activity and functionality that is the immune system.

If one considers the many ways in which the immune system can interact, recognise, and communicate, with all the cells of the host, then one must inevitably conclude that such a system is not only of critical importance for complex cellular life to exist, but also the director of it and any other symbiotic life that accompanies such life. The immune system is the system that maintains the collective co-operation and homeostasis for the entire complex living organism including all the resident organisms, commensal-microbes and even viruses, that fall under its protection (Diner *et al.*, 2015; Lee and Mazmanian, 2010).

It is now known that the microbiome, the virome, the metabolome and the brain all intercommunicate with the immune system and play a role in how the immune system registers and responds to threats and manages and directs the processes of life. While this may seem rather broad, it is important to understand these aspects and roles of the immune system as they can be highly influential in determining immunological outcomes under the right circumstances (Sompayrac, 2019).

The immune system provides the metaphorical 'glue' that allows complex living systems to stick and work together. In the gut and skin the immune system functions as the steward and guardian of the extracellular matrix in these tissues, maintaining their adhesion, repairing and reconnecting them when these barriers routinely break down in their harsh environment (Badylak, 2019; Richmond and Harris, 2014; Tomlin and Piccinini, 2018).

Recent research into cross-talk communication between the immune system and the gut microbiota has made a strong case that healthy gut microflora are more than just symbiont cohabitants but rather an active extension of the immune system itself (Burcelin, 2017; Pomié *et al.,* 2016). This notion is further supported by the wealth of knowledge that has been generated in the burgeoning field of neuroimmunology, where the important intercommunication systems between the brain and the immune system have been shown to be highly influential in mental health and a variety of areas that have not been traditionally encompassed by immunology. For example, the immune system can support an injured brain, and aids in its correct functioning through times of stress, assisting in learning, and even how we deal with social interactions (Chen *et al.,* 2017; Louveau *et al.,* 2015). The brain, in turn, responds to immunological information which can alter its circuitry. The nature of this immunological surveillance and intercommunication between the brain and immune system has been called the body's 'seventh sense'. It is non-trivial in nature, and cannot be easily dismissed (Kipnis, 2018). After all, the brain and immune system together provide all the executive function of the body. Together they function as the metaphorical CEO, director, manager, organiser and guardian of the processes of life: deciphering the cellular language of communication which they use, is key to joining in on this metaphorical conversation. This is something that the development of vaccines and advanced medicines for the treatment of cancer is essentially attempting to do, particularly when such methodologies seek to direct and alter immunogenic outcomes.

The rules that govern the immune system are incredibly complex, and are arguably among the most complex aspects of living systems and life itself. Part of this complexity lies in the incredible dynamism of the immune system. Its actions and defence mechanisms vary greatly at different times, under different situations, and in different cellular locations. The nature and circumstances under which various immunological triggers become activated are important in determining the direction, focus and scope of the resulting immune response that is generated.

Decisions by the immune system can lead it to nurture, and even protect, beneficial symbiotic microbiota present in all complex living animals. Yet at the same time, it routinely seeks out and destroys native host cells that are not functioning optimally or have become damaged (Parham, 2014). It is critical to think about the immune system in this way, as the guardian of the system as a whole, when attempting to understand it. Exploring and developing a deeper understanding behind the philosophy and mechanisms that drive the immune system, allows us to design better and novel vaccines that have greater capacity to engage this system and improve immunological outcomes.

1.2.1 Types of Immunity

There are two main arms of the immune system that dominate immune responses. These are the antibody-mediated responses driven by B-cells, and the cytotoxic T-cell mediated responses. Both arms can participate in adaptive and innate responses, which ultimately intersect in elegant ways (Parham, 2014). In many cases these two systems work together, but in certain cases and notably for chronic viral infections, control of infection and the dominant response is often CTL and T-cell weighted. This is demonstrated by looking at the correlates of protection among some well-known chronic viral infections Table 1 (Pantaleo and Koup, 2004).

Table 1: Correlates of immune protection in different virus infections. Taken from Pantaleo and Koup, (2004).

Virus	Type of vaccine	Vaccine-induced protective immunity	Mechanisms of immune control during virus infection
Smallpox	Live	Antibodies, CTL	CTL
Rabies	Killed virus	Antibodies	Antibodies, CD4, CTL
Polio	Live or killed virus	Antibodies	Antibodies
Measles	Live	Antibodies; CTL	Antibodies, CD4, CTL
Mumps	Live	Antibodies	Antibodies
Rubella	Live	Antibodies	Antibodies
Varicella zoster	Live	Antibodies; CTL	Antibodies, CTL
Influenza	Protein	Antibodies	Antibodies, CD4, CTL
Hepatitis A	Killed virus	Antibodies	Antibodies, CD4, CTL
Hepatitis B	Protein	Antibodies	Antibodies, CD4, CTL
Human papillomavirus	VLP	Antibodies	CD4, CTL
Hepatitis C	–	–	CD4, CTL
Cytomegalovirus	–	–	CD4, CTL
Epstein-Barr virus	–	–	CD4, CTL
Herpes simplex virus types 1 and 2	–	–	CTL
HIV-1 and HIV-2	–	–	CD4, CTL
Human herpesvirus 6			Antibodies, T cells

A look through Table 1 above paints an interesting picture. First, our most successful vaccines are predominantly antibody-based. Second, only the live vaccines appear to be capable of generate

protective CD8+ or cytotoxic T-lymphocyte (CTL)-mediated immunity. Third, the mechanism of immune control for all the most problematic chronic viruses (like HIV and herpes) appear to require strong CD4 and CTL responses to be controlled naturally (Pantaleo and Koup, 2004).

CD4+ or helper T-cell responses are generated upon immune control during viral infection, because this process takes time to develop and mature. Generation of CTL immunogenicity is most likely due to a variety of highly complex immune tolerance mechanisms which increase the amount of time and complexity for the generation of a mature focused T-cell response (Parham, 2014; Sompayrac, 2019). For vaccine researchers to improve the abilities of vaccines in this area requires a more in depth understanding of precisely how this type of immunity is generated, and more specifically why current vaccine development methods are failing to achieve this.

To understand the challenges for vaccine design, one needs to take a closer look at the different types of vaccines and the viruses for which they confer protection.

Typically, two classes of viruses exist. 1) Acute viruses that can be cleared during natural infection: these include smallpox, polio, measles, mumps, rubella and influenza. 2) Chronically infecting viruses, such as Epstein-Barr virus (EBV), cytomegalovirus (CMV), hepatitis virus (B and C), herpes simplex virus (HSV) and human immunodeficiency virus (HIV). These different viruses have varying levels of susceptibility to different components of the immune system. Neutralizing antibodies, for example, are great at preventing infection and combating acute viral infection, and also work in limiting the spread of chronic viruses, but are typically less capable of identifying or destroying infected host cells (Pantaleo and Koup, 2004). Antibodies can sometime identify surface antigens on infected host cells in a process known as antibody dependant cellular cytotoxicity (ADCC), which is effective in some circumstances and can spot cells with replicating and budding viruses (Parham, 2014; Pollara et al., 2013). However, when it comes to many of the known chronic viral infections (i.e. EBV, CMV, hepatitis viruses (B and C), HSV and the HIV-1 latent reservoir), the ability of these viruses to establish latency within cells allows them to avoid the immune system, giving them a safety inside host cells where they can wait and adapt to circumstance with little to no exposure of viral protein for antibodies to bind. Thus, it is imperative that both a strong population of memory CD8+ cytotoxic T-lymphocyte (CTL) cells and a neutralising antibody response are induced by vaccines aimed at targeting latent and chronic type viruses such as HIV or HSV. If a latent virus is completely inactive, no part of the immune system will be able to respond. However, background expression of low amounts of viral protein can be spotted by CD8+ cells if they are suitably primed to identify MHCI-presented viral peptides (Parham, 2014; Sompayrac, 2019), (Figure 1). The ability of the CTL response to identify and respond decisively to as little as a single peptide from any possible viral protein, presented by an infected host cell, makes a suitably primed CD8+ T-cell an extremely powerful and potent immunological force for a virus to reckon with. However, most viruses that use latent strategies have adapted their life cycle strategy to

ensure that such well primed and armed T-cell responses are limited or prevented from maturing. As potent as these responses can be, the slow and tedious process of how these cells are generated (which is fraught with cellular checks and balances) serves to limit the likelihood that they ever get generated at all (Sompayrac, 2019). These latent capabilities are difficult to contend with for vaccine developers attempting to develop improved T-cell activating vaccines (Ebina et al., 2013; Parham, 2014; Sompayrac, 2019). However, when these potent cells are generated, and demonstrate their capabilities, the results are often spectacular (Gilbert, 2012; Miliotou and Papadopoulou, 2018). For this reason, it is important and necessary that future vaccines elicit strong CTL immune responses, to be effective at defeating these problematic dormant and latent viral infections. Our current knowledge of viral latency and how T-cell versus antibody mediated responses fundamentally work (Figure 1), as well as real world evidence from the correlates of protection detected for these viruses, suggests that developing vaccines capable of meeting all these desired immunological expectations, represents the optimum strategy (Pantalio and Koup 2004, Haynes & Shattock, 2008).

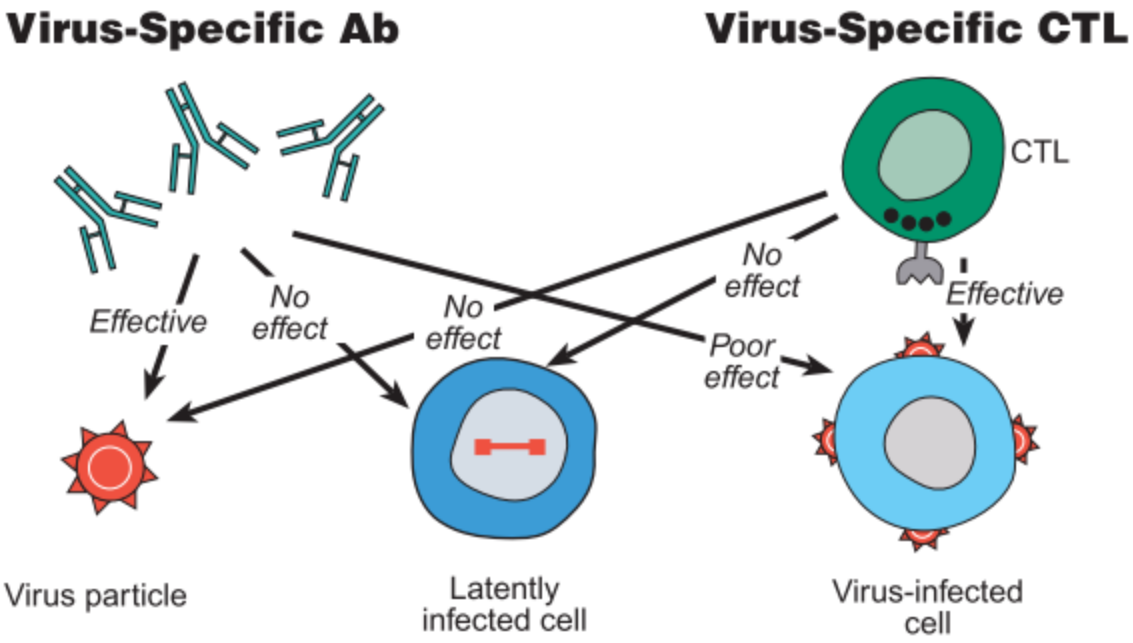

Figure 1: Components of the antiviral immune system (Pantalio and Koup 2004).

Further review will focus specifically on the genesis of T-cell immunogenicity, as this is an area of vaccine design that is arguably less developed and well understood than that of antibody-eliciting immunogenicity, and as such is also where novel methods for improvements for vaccine designs may be found.

1.2.2 T-cell immunity - Why quality responses are difficult to obtain

T-cell immunity is required for the identification and destruction of intracellular pathogens that are inaccessible to antibodies. For various reasons, this type of immunity is complex while some studies have shown it can be detected rapidly highly effective mature T-cell responses are usually slow to develop (Panagioti et al., 2018). The fine balances that control T-cells and that help them differentiate 'self' from 'pathogen' lies at the heart of this issue. The immune system evolved to generate a rapid and overwhelming response to attack invading pathogens. It does this exceedingly well in most cases, where invading viruses or bacteria pathogens only generate an acute infection which is dealt with relatively rapidly within days or weeks. Otherwise, the immune system is overwhelmed, and the pathogen kills the host (Parham, 2014). It is important to note that T-cell responses are also extremely complex and are not yet as understood as antibody mediated immunity. Despite various promising vaccines being capable of stimulating robust T cell responses, the key factors that mediate T cell-immune protection against chronic infections still need to be clearly defined. In many cases the memory response induced by these vaccines is not sustained and typically diminishes over time (Panagioti et al., 2018). Generating durable T-cell responses of appropriate magnitude and quality to effectively contribute to pathogen clearance and defining the mechanisms by which antigen-specific T cell populations able to mediate long-term protection against viruses is an important goal, in the quest to develop more effective and safe prophylactic T cell-eliciting vaccines (Panagioti et al., 2018).

This system's power comes partly from having a large resident population of sophisticated immune cells containing an arsenal of pathogenic attack modalities waiting 'primed and ready to go'. The system can very rapidly activate this resource through a complex series of positive feedback mechanisms maintained by the various immune system cell types (Parham, 2014). An ideal immune response should be rapid and effective, overwhelming the invasive pathogen, while simultaneously also being proportionate, and most importantly, finite. After the invading pathogen is destroyed, positive activation feedback loops must be shut down. Failure to do this can result in chronic inflammation autoimmunity, which can be devastating or even fatal to the host (Kempen et al., 2015; Toubi and Vadasz, 2019). In order to achieve this, the mechanisms that are responsible for the termination of activation need to be capable of halting and countering the positive feedback mechanisms in a manner that is ultimately more powerful than they are. Moreover, these systems are crucial to the healthy operation of the immune system and intricately integrated with the mechanisms of immune activation. The balancing role played by the termination component of this system remains permanently active, at the same time this arm of the immune system is also permanently primed for rapid activation. Ultimately, these immunological control systems acting against one another manage to find balance as well as control the magnitude of immune activation when it occurs. This system is also responsible for preventing overactivation during an active immune response and infection.

Ensuring a proportional immune response is crucial in minimising the health risk and lethargy of the host during illness. Understanding how immune termination mechanisms are intricately interwoven with immune activation is significantly relevant and important to vaccine researchers who seek to control the size and scope of immune activation in response to new vaccines. This is an area that has often been overlooked, but one that is being increasingly researched and recognised as an integral part of any immune response. This increased interest comes directly from experimentation and research into termination signalling, which has mapped many of the termination signalling and molecular interactions to many of the very same pathogen recognition receptors and biochemical pathways involved in activation. This is a key indicator relating to how closely integrated immune activation and termination are. This has spurred greater efforts by researchers to investigate the intracellular processes that drive these processes to better understand the nature of how they operate and interact with one another. To improve vaccine designs and develop novel therapies, it is necessary to understand and appreciate the nature of these immunological activation and termination mechanisms, and how they integrate with one another in a multivariate system that maintains the health of the host (Kane et al., 2014; Marrack et al., 2010).

To be effective, the immune system must have various ways of defending against a variety of pathogenic attacks from all the potential biological threats that it faces. In addition to these, the system also requires some capacity to indiscriminately attack novel pathogens without specific recognition. This is achieved, in part, by having a sophisticated means of identifying self, which facilitates the indiscriminate attack on anything not able to pass the self-identification process. Similar screening processes also exist for B-cell mediated antibody immunity (Parham, 2014). The complexities of how the immune system manages this differentiation process, particularly for T-cell immunogenicity, are substantial. There are no fewer than five self-tolerance inducing mechanisms associated with MHC restriction processes involving a variety of positive and negative selection mechanisms including; tolerance by ignorance, peripheral tolerance induction, tolerance due activation-induced cell death, as well as T-cell inactivation processes that create neutered or anergized T-cells. These incredible processes are well described elsewhere (Parham, 2014; Sompayrac, 2019). The amount of cellular energy and effort these mechanisms expend to develop these types of immunity and tolerance mechanisms is interesting from an evolutionary standpoint. Indeed, with the attrition rate and multiple ways in which T-cells are prevented from working by the known tolerance mechanisms, it is a wonder that they work at all. However, when created, a fully-activated T-cell has managed to pass the numerous checks and balances inflicted upon it during its extensive ‘training’ and is able to become an incredibly lethal force that can repeatedly and tirelessly identify and kill cells that expose its target peptide antigen. This system can be so effective that it is able to completely eradicate and destroy large and numerous cancerous tumours throughout the body in a matter of days in near-miraculous recoveries of terminal cancer patients who received activated T-cell immunotherapies that can target their cancers (Cosma and Eisenlohr, 2018;

Feins et al., 2019; Galluzzi et al., 2016; Makkouk and Weiner, 2015; Miliotou and Papadopoulou, 2018; Vermaelen, 2019).

As we attempt to understand the successes of T-cell immunogenicity, we must also consider what happens when this system goes wrong. The severe and dangerous side-effects of hyper over-activation of T-cells demonstrate precisely why the body makes this type of immunity so difficult to generate (Arellano et al., 2016; Behrens and Koretzky, 2017; Penaloza-MacMaster et al., 2015). Strong immune activation is something we are all familiar with, it is something we literally feel when we catch the flu or get sick (Lee and Mazmanian, 2010; Luo et al., 2016). These familiar aches and pains when sick and the areas and organs in which they felt, are intricately linked to T-cell immunogenicity and its destructive capabilities, which can result in it attacking healthy cells as well as diseased ones. Understanding why certain tissue types are targeted, informs us in many ways about how this system operates and how the T-cell 'training process' occurs. Being mindful of how this occurs is important and relevant when considering new T-cell targeted vaccine development strategies (Kempen et al., 2015; Kobie et al., 2011; Parham, 2014; Toubi and Vadasz, 2019).

T-cell immunogenicity is arguably one of the most powerful weapons of the immunological arsenal – and this is demonstrated when this type of immune response becomes unrestricted. For example, the severe effects of what is known as 'cytokine storm syndrome', where a loss of negative feedback occurs, causing hyper immune activation, results in severe and often lethal autoimmunity. Development of this syndrome has been associated with the most lethal cases of the avian influenza such as the H5N1 strain, which emerged in 1997 and again in 2005 (Behrens and Koretzky, 2017; Penaloza-MacMaster et al., 2015; Tisoncik et al., 2012).

The above discussion helps to explain two very important aspects of T-cell immunity and viral infection. First, because a wide variety of highly specialised and diverse cell types exist, which must be protected and therefore tolerated by T-cell immunity, a high level of basal tolerance must be achievable for this system to be allowed to exist. This creates an opportunity that viral infections can exploit. A sufficiently low/basal level of metabolic activity ca be an effective immune avoidance strategy, which is often used by latently infectious viruses like HIV which can maintain a notoriously difficult to eliminate latent viral reservoir. Limiting metabolic activity by adopting a minimal replication cycle and maintaining sufficiently low levels of protein expression can be effective strategies for avoiding T-cell activation. To see examples of these strategies in action one only need look at the life cycles of the well-known and recognised chronic viral infections such as: HIV, CMV and HSV which all are able to effectively avoid T-cell detection (Collins et al., 2017; Deeks et al., 2015; Walton et al., 2014). Understanding how T-cell tolerance is generated also helps to explain why highly effective T-cell vaccines are difficult to create. To make an effective T-cell vaccine, all the built-in mechanisms that maintain host cell self-tolerance, balance and control must be overcome for the new vaccine to become truly be effective and

create a population of highly specific and fully activated T-cells. At present, we don't fully understand how these activation, termination and self-tolerance inducing mechanisms really work: by themselves, or together? What we do know, however, is that they do work together and there appears to be more of them than were originally thought existed or have been described (Luo et al., 2016; Makkouk and Weiner, 2015; Sompayrac, 2019).

Understanding how these mechanisms of tolerance work has become an area of intensive research for scientists trying to generate immune activation and vaccine development strategies in both cancer research and virology fields. While the primary mechanisms of immune response and upregulation are well researched (Parham, 2014; Sompayrac, 2019), the nuances behind the molecular triggers of immune activation, and the conditions under which they function, is of particular interest for vaccine designers. As this field grows it has become recognised that the immune system, and particularly T-cell immunity, may only become truly activated when it is released from its complex biological constraints (Sompayrac, 2019). Simply applying powerful and pure immunogenic stimulation alone consistently fails to result in T-cell immune activation. In recent years it has become clear that a combination of multiple immunogenic and internal biological genetic responses creating the right set of immunogenic signalling and stimulation are actually necessary for a fully activated T-cell response to be generated (Bednarski and Sleckman, 2019; Chen et al., 2013; Collins et al., 2017; Georg and Sander, 2019; Kobiyama et al., 2013a; Pennock et al., 2013; Rose et al., 2015).

Decoding the subtle complexities of initial pathogen recognition from a state of naïveté to the eventual full activation of T-cell immunogenicity has become a rapidly evolving area of scientific research (Diner et al., 2015; Georg and Sander, 2019; Sompayrac, 2019). While the driving forces behind these systems are incredibly complex and an exception for every rule seems to exist, a motivating philosophy behind what drives immune activation is emerging, and from this philosophy new approaches and methodologies are being developed (Sompayrac, 2019).

The immune system, is not easily tricked into initiating a powerful T-cell activation when confronted with an inanimate or artificial stimulus such as dead/inactivated virus, DNA, protein or other inactive components used as vaccines. Singular immunogenic stimuli -- for example, adding adjuvant such as alum or bacterial flagella which are highly immunogenic but also are incapable, on their own, of generating what is considered a fully activated immune response (Hajam et al., 2017). So, crude immunogenic stimulation alone, is often insufficient to elicit full T-cell activation. Investigation into this matter has overturned conventional wisdom on how many of these adjuvating agents really work and spurred a re-evaluation of the old theories about them while simultaneously spurring new research into developing novel adjuvants that target different mechanisms of action, for stimulating immunogenicity (Bourgeois-Daigneault et al., 2018; Kuroda, 2018; Vermaelen, 2019). Alum, a commonly-used adjuvant, for example, has had its effects linked to its induction of the release of uric

acid *in-vitro*, which then acts to induce DNA damage-associated molecular patterns (DAMPs) (Kuroda, 2018; Marrack et al., 2009) This is a vastly different mode of action to the one originally put forward, which suggested the adjuvant effect was caused by a sustained and prolonged exposure of antigen to the immune system, on account of it trapping and releasing the antigen over time (Marrack et al., 2009). This complements other research into DAMPs and immunogenicity, particularly in association with immunogenic-regulated cell death (Kepp et al., 2014). Importantly, the DNA damage response and detection mechanisms come up with increasing frequency when discussing immune activation pathways and the activation of T-cells required for the genesis of this type of immunity (Galluzzi et al., 2018, 2016; Georg and Sander, 2019; Kepp et al., 2014).

While some studies have reported early T-cell differentiation can be induced by vaccines (Maeto et al., 2014), the quality of these early responses and whether this type of early induction is important for vaccine efficacy and long-term protection is unclear. Ideally more mature forms of T-cells such as stem cell memory T-cells are necessary to elicit protection and vaccines capable of generating these kinds of T-cells responses need further exploration (Panagioti et al., 2018).

In live attenuated vaccines, the vaccine-induced T cell subsets are observed to be highly similar to those generated by natural viral infection (Karrer et al., 2004). This is not true for inactivated, synthetic or subunit vaccines, which indicates there are stimulatory processes such as inflation, that occur during infection and that are necessary for the development of potent and mature T-cell immunity. The T-cell subsets that develop upon immunization with these kinds of vaccines are also highly dependent on the addition of adjuvants as well as the method of administration (Panagioti et al., 2018).

An alternative mechanism known as T cell “inflation” which has been shown to lead to a durable increase of memory T cells is observed for certain viral-specific responses following infection by cytomegalovirus (CMV). During inflation an antigen-specific set of T cells that target specific viral peptides expand gradually over time and are maintained at high frequencies as effector memory T cells (Karrer et al., 2003). Critically, these inflationary responses maintain their effector functions, and unlike exhausted CD8 T cells, can provide protective immunity against pathogen re-challenge (Karrer et al., 2003). Memory inflation is was also observed for CMV-specific antibodies, however the rules that characterise this kind of inflation have not been fully determined. It is clear that for inflation to occur viral antigen must persist long term, appearing to require T cell costimulation (Panagioti et al., 2018).

1.2.3 Intracellular pathogen detection and T-cell activation

Part of the problem in deciphering the genesis of T-cell immunity lies in the complexity and difficulty of observing and deciphering how the intracellular triggers and pathogen-detecting molecules translate

into gene activations. These molecules interact rapidly and are readily recycled. It is therefore the levels at which they recycle and the degree to which they are stimulated in combination of other cellular and extracellular signalling, that ultimately determines immunogenic outcomes.

When it comes to T-cell immunogenicity, it is the intracellular pathogen detection receptors that lead to the extracellular communication and immune signalling via MHCI complexes and cytokines that generate this immunity (Parham, 2014). Determination of the magnitude of the response seems to occur predominantly at the intracellular level. It is also here where the intersection between the adaptive and innate immune systems exists. Mounting evidence in this area also suggests that an intersection between DNA damage response mechanisms and adaptive T-cell immunity also exists, and is crucial in determining different cellular outcomes. These may vary from no affect at all, to some immunogenic signalling, to apoptosis, and even highly immunogenic forms of regulated cell death (Bednarski and Sleckman, 2019; Georg and Sander, 2019; Kepp et al., 2014; Li and Chen, 2018; Parham, 2014). When DNA damage response mechanisms become activated, they create a cascade of damage associated molecular patterns DAMPs (Giglia-Mari et al., 2011). Similarly, when pathogens are identified via a variety of pathogen recognition receptors and detection mechanisms, another set biochemical responses and gene activation cascades occur. These are collectively referred to as the pathogen-associated molecular patterns (PAMPs) (Kumar et al., 2011; Takeda and Akira, 2015).

Many of the PAMP triggers and PRRs are self-explanatory, being linked to the very nature and unique characteristics of the type of pathogen they identify. For example, bacterial flagella are unique to bacteria, and their identification by PRRs induces a particular combination of responses best suited to combating a bacterial type of infection. In this manner, the particular PRRs activated, and the PAMPs associated with various combinations of PRRs, can tailor the immunogenic response in a way that is best suited to the type of threat being detected. In many cases, overall response tends to converge on either a Th1 or Th2 response (Berger, 2000; Cortés et al., 2017; Mestas and Hughes, 2004; Wells et al., 1997). That said, the combination of immunogenic signalling by different PRRs is far more nuanced than simply shifting the overall response in either of these directions. The nature of a response may also differ quite dramatically, depending on cell type, extracellular signalling and even metabolic energy signalling — all of which have been shown to be influential in determining outcomes (Pomié et al., 2016).

1.2.4 Pathogen recognition receptors and evolution

Innate resident molecular receptors -- often referred to as the pattern recognition receptors (PRRs) - are able to identify invading pathogens by the very nature of their origin and activity. These receptors act as *'the tip of the immunological spear'* by being the first molecules that interact with, and respond to,

invading pathogens based on certain specific, definitive characteristics that define them. As mentioned above, receptors that bind bacterial flagella or peptidoglycans are obvious targets for immediate identification of foreign invaders. In other cases, such as for viruses, the distinction may be more difficult, and more sophisticated mechanisms are involved. The full extent and nature of all the PRRs that exist have not yet been fully identified. Several families have been well characterised, such as the Toll-like receptors (TLRs), the NOD-like receptors (NLRs), C-type lectin receptors, the RIG-I-like receptors and the AIM2 like receptors (Brice et al., 2007; Kumar et al., 2011; Lugrin and Martinon, 2018; Rathinam and Fitzgerald, 2011; Takeda and Akira, 2015). In many cases, the primary target of pathogen recognition is the genomic material of the invading pathogen, whether it is RNA or DNA, and single or double-stranded. In addition to this, the longer a pathogen has co-evolved with a host, the better-adapted and well-regulated its control and recognition by the host the immune system becomes. This relationship between pathogens and hosts is a powerful driver of evolutionary adaptation: for example, one can date the origins of retroviruses as far back as the evolution of vertebrates, >450 million years ago (Aiewsakun and Katzourakis, 2017; Moelling and Broecker, 2019). The integration of vast amounts of retroviral DNA within human and vertebrate genomes serves as a testament to these observations (Aiewsakun and Katzourakis, 2017; Hayward, 2017; Magiorkinis *et al.*, 2017).

1.2.5 Toll like receptors (TLRs)

The TLRs were some of the first PRRs responsible for influencing the activation of PAMPs. This group of transmembrane protein receptors, that are ubiquitously expressed, are capable of immediately recognizing highly conserved structural motifs native to commonly encountered pathogens. This group includes receptors for critical and common molecules and structures of bacterial or pathogen origins, such as lipopolysaccharides, peptidoglycans and lipopeptides as well as bacterial DNA and double stranded viral RNA (Takeda and Akira, 2015). In humans, there are ten classified TLRs with relatively well-defined functions. For example, TLR3, TLR7, TLR8 and TLR9 have been shown to play important roles in the recognition of viral RNA and DNA, and induce type I interferon responses through interaction with the MyD88 adaptor protein. These responses are responsible for the activation of interferon regulatory factors (IRF's), such as IRF3, IRF5 and IRF7, which trigger the activation of canonical antiviral response pathways for interferon production (Kumar et al., 2011; Takeda and Akira, 2015). Recently, these signalling processes have also been linked with altering the activity of the highly influential protein kinase mammalian target of rapamycin (mTOR), a key regulator of cellular and bodily function. This enzyme's activity has been shown to influence cellular physiology and the biological control of growth, aging, and metabolic regulation, making it influential in disease progression. Functioning as a serine-threonine protein kinase, mTOR sits at a critical checkpoint maintaining biochemical cellular homeostasis and responding to extracellular stimuli such as nutrient levels and external growth factors (Costa-Mattioli and Sonenberg, 2008). The ability to respond to intracellular metabolic and pathogen detection cues and regulate cellular growth and metabolism, makes

the control of this pathway influential in determining the availability of cellular resources, and it is therefore a key target for antiviral activity and immune control. These links directly connect the detection of pathogens via PRRs to meaningful biochemical responses - not only in alerting the immune system, but also in regulating and controlling the rate of infection by restricting cellular resources and slowing metabolism (Kumar et al., 2011; Morita et al., 2015).

Cellular DNA health and activation of DAMPs blurs together with the viral and pathogenic DNA detection and PAMPs at the biochemical level. It is likely that many of the DNA damage detection mechanisms serve a dual role, also functioning as pathogen detection elements (Diner et al., 2015; Lugrin and Martinon, 2018). DNA structural elements, codon usage to the type and nature of the promoter used varies from different cells and is often unique to different families of organisms, species, bacteria and viruses. As such, unique characteristics (like structural features such as stem loops or high frequency codon usage patterns like CpG rich motifs and islands) can be used to help inform the cell of pathogenic infection. Cells that closely monitor their own state -- assessing nuclear homeostasis and rates of gene expression through biochemical pathways -- are thus able to evaluate the balance of gene expression activity (Takeda and Akira, 2015). These pathways and the observation that they intersect through enzymes like mTOR (among others), provide a robust array of mechanisms which have the potential to facilitate the detection of intracellular pathogens. Furthermore, the integral roles that these molecules play in regulating cellular activities, such as gene expression programs, make them ideal tools or 'weapons' by which the immune system may act to limit a pathogenic threat. In this way, the greater the strength of a stimuli and the more ways biochemical activity is altered, the higher the likelihood that a pathogen's activity will trigger a greater number of cellular responses and the more likely those will be detrimental to the pathogen (Nishimoto, 2004).

The pathogen detection activities by the TLRs appear to be important when it comes to DNA vaccines. CpG motifs which are present in human and vertebrate genomes at a significantly lower frequency than in viral genomes where they are often found in high frequency in viral promoter sequences. In humans, their genomes are confined to the nucleus, and the CpG motifs found there are largely methylated. A process that occurs over time is responsible for down regulating expression activity and has also been linked to aging (Illingworth and Bird, 2009). In viral and bacterial genomes, CpG motifs are both, more abundant, and unmethylated (both properties associated with increased expression levels). The tendency of viral or bacterial infections to rapidly increase their genome copy number drastically increases the abundance of these unmethylated DNA motifs. By simply monitoring the abundance of this type of DNA the non-specific nature of the detection mechanism employed by TLR-9 is renders it capable of detecting active infection and pathogen replication and generating a proportional response. The location of detection also matters: while its possible detection may occur in the nucleus or cytoplasm, the extent of antiviral response gene activation is greater for DNA detected in the cytoplasm (Latz et al., 2004; Motwani et al., 2019).

As a non-specific type of foreign DNA detection, CpG islands are likely tolerated up to a specific threshold. When these genetic motifs were discovered, statistical characterization was performed to investigate their influential frequency. In their first paper characterising CpG islands, Gardiner-Gardner and Frommer (1987) developed the following definition:

"For the purpose of this survey, regions of DNA with a moving average of %G+C over 50 and Obs/Exp CpG over 0.6 have been classed as CpG-rich regions. CpG-rich regions over 200 bp in length are unlikely to have occurred by chance alone, so, as a working definition, have been labelled as CpG islands." (Gardiner-Garden and Frommer, 1987).

This definition was built upon a wide analysis of vertebrate genomes. CpG islands are also known to be binding sites for ubiquitous transcription factors, which explains their high frequency in viral genomes. While the actual thresholds of TLR-9 CpG detection mechanisms remain unknown, it is clear that, through this type of detection, the immune system possesses an ability to directly monitor and, in a manner, quantify viral DNA replication and differentiate it from native host unmethylated CpG islands. This distinction has been noted by DNA vaccine designers who optimise to maximise the number of CpG islands on DNA vaccines, in an effort to improve their efficacy for improving T-cell responses (predominantly mediated through TLR-9 activity) (Illingworth and Bird, 2009; Williams, 2013).

Typically, TLRs are predominantly expressed by cells of the immune system but, more recently, it has been shown that they can be upregulated in other cell types, such as skeletal muscle, which are known to be capable of becoming facultative antigen presenting cells particularly during times of cellular stress (Afzali et al., 2018; Marino et al., 2011).

1.2.6 Pathogenic nuclear DNA detection and immune signalling by IFI16

Until recently, the methods by which mammalian cells recognise the entry and presence of viral DNA within the nucleus has been poorly understood. This recognition, however, is a crucial part of viral detection and the initiation of the antiviral response to DNA viruses and bacteria. The interferon-inducible protein 16 (IFI16) has been identified as a nuclear viral DNA sensor and acts as an important antiviral response factor. It is able to selectively identify and bind pathogenic viral and bacterial DNA on account of its ability to preferentially bind supercoiled DNA compared to other DNA structures. Supercoiled DNA is frequently found in bacteria, viruses and plasmids and is often the default DNA conformation of their genetic material and genomes. The key distinction here made by IFI16 is that because the host genomic DNA uses histones to package and organise itself in eukaryotes, it remains in a dsDNA form. This allows IFI16 to simply screen for something as natural as supercoiled DNA to identify pathogenic DNA (Hároníková et al., 2016). It is however worth noting that the telomeres of each chromosome also exist as quadruplex DNA. Therefore, there must exist some native tolerance

level to this DNA form. IFI16 is also likely a DNA damage-detection sensor, as it is also able to detect broken genomic DNA fragments that can become detached from the genome and may become supercoiled without the structural stabilizing effect of histones while it was safely 'packaged' in the chromosomes (Knipe, 2015).

Research into the PRRs IFI16 has revealed much about cellular tolerance mechanisms and the complex range of interactions mediated by IFI16 in the nucleus that are highly pertinent to T-cell vaccine design. IFI16 has been shown to localise preferentially at the periphery of the nuclear envelope, driven predominantly by association with nuclear envelope matrix protein structures such as the nucleopore complex. By localising and concentrating at the site of viral and bacterial pathogenic DNA entry into the nucleus, IFI16 is able to screen molecular trafficking into the nucleus for pathogenic DNA. These interactions have been tracked in real time in HSV infected live cells. Upon the entry of HSV DNA into the nucleus, IFI16 immediately binds invading pathogenic DNA and forms foci in the nucleus adjacent to the labelled HSV viral nucleocapsid binding site on the exterior side of the nuclear envelope. Importantly, the size of these foci was shown to be dependent on the viral multiplicity of infection (MOI), indicating that the IFI16 signalling was proportional to the level of infection. As IFI16 is a dsDNA binding PRR protein, the more DNA present in the nucleus the stronger the IFI16 mediated response can become (Diner et al., 2016, 2015).

Proteomics experiments indicated that, in addition to IFI16's pyrin (PY) domain aiding localization with the nucleopore complex, the PY domain also appears to be responsible for the oligomerization of the IFI16, and its recruitment of nuclear domain 10 (ND10) bodies. These are spherical bodies of 0.2-1.0 μM in diameter with approximately 10 distributed throughout the nucleus. These structures form primarily through favourable associations with other ND10 resident proteins and molecules which include protein-protein, protein-DNA and protein-RNA associations that are associated with these bodies. ND10 bodies are also associated with SUMOylated proteins, which is a form of post translational modification whereby SUMOs (small ubiquitin-like modifiers) are added. This process alters protein structure and specifically, subcellular localization (Rivera-Molina, 2013).

Known SUMOylated proteins prominently associated with ND10 bodies are the Death associated domain protein (Daxx) and Speckled protein of 100 kDa (SP100), both of which play important roles in the inflammasome and are upregulated by interferon. These bodies and proteins have also been shown to have repressive effects on viral replication cycles (Rivera-Molina, 2013). In addition to this, most nuclear DNA replicating viruses encode immediate-early proteins responsible for the disruption and dispersion of these complexes, which, in the absence of those viral proteins, results in severe viral replication inhibition (Rivera-Molina, 2013). Furthermore, it has been observed that viral replication for some viruses occurs at the periphery of ND10 complexes, indicating that these complexes are associated with a favourable environment for DNA transcription and replication. A lot is still not known

about ND10 bodies, but it is believed that these protein bodies act as aggregation sites functioning as a nexus of certain biological activities when protein complexes are created, and biological molecules are deposited or sequestered away. By concentrating a variety of specific proteins in localized hotspots within the nucleus, ND10 bodies can facilitate protein degradation, post translational modification and the genesis and regulation of transcription complex formation. This is backed up by the association of ND complexes with high levels of transcriptional activity and nascent RNA around them (Maul, 1998; Rivera-Molina, 2013; Wang et al., 2004).

These mechanisms create direct links between pathogenic nuclear DNA, upregulated antiviral responses which include increasing IFI16 production and thus help cellular efforts to combat pathogenic DNA replication by directing bound pathogenic DNA to ND10 bodies. This process also appears to be proportional to the amount of pathogenic DNA present and, therefore, has the capacity to track the developing viral infection and its replication processes (Rivera-Molina, 2013).

After IFI16 foci formation and association with ND10 the HSV infected cells were shown to enter a state of relaxation, which was marked by further enrichment of IFI16 and its diffuse distribution in a manner similar to that observed from uninfected cells. However, during the second phase of HSV infection, IFI16 was recruited into nuclear puncta which were distributed throughout the nucleus and in greater numbers than before. These nuclear foci/puncta were observed to assemble directly adjacent to the chromosomal centromeres with their localization believed to have been conferred by IFI16s HIN200 domains.

Proteomics helped identify an association of IFI16 with the HSV ICP0 protein which has been shown to facilitate the degradation of centromeric proteins such as CENP-A, CENP-B and CENP-C during HSV-1 infection. This in turn induces activation of the interphase centromere damage response (iCDR) pathway (Gross et al., 2012). The link between IFI16's DNA binding HIN200 domain with the initiation of iCDR signalling, expands the role of IFI16 to initiation of DAMPs associated signalling and other cellular stress-related pathways and responses (Diner et al., 2016). In HSV infections no further activity by IFI16 was detectable once the HSV had become established. This is because HSV is known to expresses proteins responsible for the degradation and destruction of IFI16. Viral counter measures responsible for the destruction or inactivation of IFI16 are common, among chronically infecting viruses. This arguably demonstrates the importance IFI16 plays as a PRR that aids in the genesis of T-cell immunogenicity. Cytomegalovirus, for example, inactivates IFI16 before the second phase of CMV infection begins (Diner et al., 2016).

IFI16 overexpression has also been shown to be influential during the early stages of inflammation that precede the onset of autoimmune disease (Dell'Oste et al., 2013).

Given what we now known about IFI16 and how it progressively stimulates stronger immunogenic responses as it detects increasing concentrations of pathogenic nuclear DNA, it becomes clear that the detection of increasing concentrations of pathogenic genomic DNA and RNA is a critical trigger of PAMP signalling associated with T-cell activation.

A key takeaway from the above discussion is not only the important links between pathogenic DNA sensing and immune activation, but also the proportional and sequential nature of how this occurs. It develops in response to the level of stimulation received. The activation process is not switched on or off in a binary manner, but is rather a dynamic and actively-changing self-feedback response system that can continuously amplify in response to amplifying stimuli. An internally amplifying stimulus, able to mimic the way a virus actively and increasingly stimulates these PRR which trigger the activation of cellular immunity. It may well be what is required to generate a fully activated T-cell immune response. The fact that the level of HSV infection influences this progression in terms of viral MOI is direct evidence this may be the case (Diner et al., 2016; Rivera-Molina, 2013).

Ultimately, a proportional response to a viral infection must track the development and progression of that infection. What better way is there for the immune system to do that, than to link its response to the level of viral replication occurring inside infected host cells, and doing this by directly detecting pathogenic DNA and/or genomic material? At low levels of infection, and in the absence of significant replication, this relatively generalized and non-specific technique of pathogen detection, might allow a pathogen to go unnoticed by the host initially. However, as a pathogen starts its pathogenic replication cycle (which is a hallmark trait of pathogens and viruses), the replication process and the many pathogenic genomes that are created in it can become a powerful signal of an infection that must be urgently dealt with by the immune system.

The above research indicates that IFI16 is likely one of the known PRRs that has the ability to directly facilitate the cellular distinction between viable and non-viable pathogens. This distinction, and the proportional immunogenic signalling it can generate, is in all likelihood a major determinant of the magnitude of the resulting cellular immune response (Dell'Oste et al., 2013; Diner et al., 2016; Knipe, 2015). This makes massive IFI16 stimulation a good PRRs to target immunologically.

1.2.7 STING-TBK-IRF3 activation by cGAS–cGAMP–STING signalling

The induction of interferon-β (IFN- β) and its association with the differentiation of T-cells into T-helper cells, natural killer T-cell and cytotoxic T lymphocytes (CTLs) has been linked to the detection of pathogenic DNA motifs and the propagation of antiviral signalling through the activation of the stimulator of interferon genes (STING) pathway. This process begins with the formation of the serine/threonine protein kinase TANK-binding kinase 1 (TBK-1) and subsequent activation of the interferon response factor 3 (IRF-3) transcription factor. This gene activation cascade is responsible for

the induction and activation of several critically important antiviral transcription regulators that induce cytokine production through a family of transcription factors known as the Nuclear Factor kappa-light-chain-enhancer of activated B cells (NF-κB). This cascade is known to be especially important and influential in regulating the immune responses to viral and intracellular pathogens and initiating responses that lead to inflammation and cellular processes of autophagy, apoptosis and necrosis (Motwani et al., 2019).

The pathway becomes activated when cyclic guanosine monophosphate (GMP)–adenosine monophosphate (AMP) synthase (cGAS), a dsDNA sensor, binds cytosolic pathogenic dsDNA and covalently links monomers of GMP and AMP to form cyclic GMP-AMP (cGAMP), which subsequently strongly binds and activates the STING adaptor protein initiating signal transduction and gene activation through the STING-TBK-IRF3 pathway (Li and Chen, 2018). Diner *et al* (2016) also showed that IFI16 may also be an unrealised downstream component of this canonical pathway or a secondary independent activator of the same set of antiviral response genes. If this proves to be the case, it would imply that the dual activation of these viral DNA detection mechanisms may complement each other in a manner that facilitates the determination of pathogenic viability. cGAS-cGAMP-STING has also been implicated in the detection of DNA damage, cellular senescence and cancer (Diner et al., 2016; Li and Chen, 2018; Material et al., 2013; Motwani et al., 2019).

The DNA detection by cGAS is activated by dsDNA, irrespective of specific sequence. This is not an issue for cGAS activity in the cytoplasm, where host cell DNA is not present, but is potentially problematic within the nucleus where self-activation of cGAS from genomic DNA could occur for nuclear resident cGAS. Interestingly, nuclear resident free/unbound cGAS has also been shown to preferentially localise at ND10 domains (Diner et al., 2016). It has also been shown that genomic DNA damage leads to the activation of this pathway generating inflammatory responses (Li and Chen, 2018). Targeting the cGAS-cGAMP-STING pathway has been an area of intense research by cancer researchers, pharmaceutical companies and virologists, due to the potent immunogenic effects associated with this pathway. Furthermore, the ability of pathogenic DNA to stimulate this pathway has been shown to correlate the size of the stimulating DNA fragment as well as its abundance where small fragments <25 bp are less immunogenic but larger fragments >45 bp are more readily identified as pathogenic and bind strings of cGAS molecules to generate stronger immunogenic stimulation (Motwani et al., 2019). The length and abundance of pathogenic DNA have clear links to pathogen viability, in the sense that viable pathogens create abundant large-to-genome-size DNA fragments, while natural DNA damage, such as genome ss-ds DNA breakages, are associated with small free-floating DNA fragments of low abundance. Intact genomic DNA is protected by chromatin-associated proteins and histones (Diner et al., 2016; Georg and Sander, 2019; Motwani et al., 2019).

Until recently, it was assumed that cGAS avoided constitutive activation by host DNA by being isolated to the cytoplasm. However, new research has shown that cGAS predominantly localizes inside the nucleus, while most nuclear resident cGAS is tightly genomic DNA bound where it is maintained in an inactive state by nuclear chromatin (Motwani et al., 2019; Volkman et al., 2018). Thus, only non-chromatin-bound free nuclear DNA I.E. (pathogenic DNA) is catalytically active to cGAS within the nucleus, meaning genomic DNA is safe by virtue of its chromatin association. Similarly, resident inactive and genome associated cGAS is present in the nucleus, in high concentrations, and in a state of readiness. It is able to become active upon detection of nuclear dsDNA as soon as it disassociates with nuclear chromatin. This may occur when genomic DNA damage occurs, particularly when dsDNA breakage occurs, or when any free floating dsDNA, (I.E. pathogenic DNA), is detected. This corroborates with the other well described role of cGAS, as a DNA damage detection receptor associated with DAMPs (Li and Chen, 2018). These DNA damage responses are also associated with the nuclear export of DNA into the cytoplasm, where cGAS is always active and STING is activated. Furthermore, nuclear DNA export is also associated with active viral infections. This shows how pathogenic nuclear DNA replication can generate cytoplasmic viral DNA, which is then able to induce cytoplasmic-mediated antiviral defences (Diner et al., 2016, 2015; Galluzzi et al., 2016; Knipe, 2015; Paludan and Bowie, 2013; Volkman et al., 2018; Wenzel et al., 2012).

STING antagonists have been proposed for several therapeutic uses, including use as a vaccine adjuvant as well as the management of chronic viral and bacterial infections. As an adjuvant bacterial cyclic dinucleotides, as well as human cGAMP have demonstrated improved vaccine efficacy and been shown to improve IgG responses (Motwani et al., 2019). Recently, STING antagonists have demonstrated the ability to carry out reactivation of latent SIV in macaques, and enhance SIV specific responses, giving hope that stimulating this pathway with STING specific antagonists may offer a new way of purging latently infected T cells of virus and boost CTL, NK cellular responses, outcomes that are required for a functional HIV cure to be developed (Yamamoto et al., 2019).

1.2.8 The AIM2 inflammasome

Another interferon-inducible protein, known as absent in melanoma 2 (AIM2), serves as another important PRR which is able to detect both pathogenic and host DNA, and initiate signal transduction cascades that activate the Type I interferon and NF- κB inflammatory transcription factors. AIM2 is quite similar to IFI16 but contains only one HIN200 domain and a single pyrin PY domain. Collectively, these form into a loosely defined greater family of DNA binding receptors known as the aim-like receptors (ALRs). Unlike IFI16, AIM2 localises to the cytoplasm and binds predominantly dsDNA. Its signalling pathway is similar to IFI16 and is also upregulated by the type I interferon response in phases. This self-feedback system of pathogenic DNA binding PPRs, which recognise and respond to the presence of pathogenic DNA, forming part of a powerful antiviral defence system that is able to

recognise and respond proportionally to the detection of pathogenic genomic replication, whether it is occurring inside or outside of the nucleus. Furthermore, this system, which also functions to hinder pathogenic replication, may become activated in response to extracellular signalling, which in turn can also help initiate upregulation of Type I interferon response genes (Lugrin and Martinon, 2018; Motwani et al., 2019; Wenzel et al., 2012).

In the second phase of AIM2 activation, post-translational assembly of the AIM2 inflammasome occurs to create high molecular weight cellular protein complexes that recruit and activate inflammatory caspases to initiate programmed cell death decision pathways (Lugrin and Martinon, 2018; Yuan et al., 2016). Several other immunogenic DNA sensors have been described, but these are not as well researched and understood as the ones listed. It is likely that still more mechanisms (including redundant mechanisms) exist and are yet to be discovered (Paludan and Bowie, 2013).

1.2.9 DNA damage and immunogenicity

Genotoxic agents often used in chemotherapeutics have been shown to produce highly immunogenic T-cell responses, most notable of which is the induction of so-called immunogenic regulated cell death (ICD), whose induction occurrence correlates well with the success rate of chemotherapy cancer treatments. Indeed, it is likely that the very capability of these genotoxic agents to work in cancer therapy originates from their ability to initiate ICD (Galluzzi et al., 2016; Kepp et al., 2014). The nature of how this is process is initiated has been linked to the activation of DNA sensing PRRs. For this reason, a great deal of research effort has been put into the development of so-called cancer vaccines. These vaccines target the same T-cell immunogenicity that vaccinologists seek for controlling HIV and other chronic viral infections. These pathogens are adept at ‘hiding’ and avoiding the immune system, effectively making them like cancer in this regard. By establishing latent reservoirs within a host cell reservoir, chronically-infectious viruses like HIV, HSV and CMV are able to dramatically limit exposure to the immune system, enabling them to vastly extend their life cycle within their hosts and become active at opportune times which may be signalled by stress hormones or other possible biological signals that can signify a weakened immunological state. These viruses often employ complex intracellular defence mechanisms that can further limit immune detection often by directly counteracting known innate antiviral biochemical pathways that are able to detect them (Gilbert, 2012; Motwani et al., 2019; Virgin et al., 2009).

1.2.10 Is threat severity and T-cell activation determined by detection of genomic replication as a signal of pathogenic life?

As mentioned before, the immune system exists in a perpetually primed state, always ‘raring to go’, but it is also continually being biologically restrained. Understanding the nature of these restraints is crucial if we are to unleash the largely untapped power of T-cell immunogenicity. Recently, research into

cancer vaccines and autoimmunity conditions has begun to reveal some of the secrets behind these immunological shackles. As it turns out, multiple biological systems work to restrain the activation of T-cell immunogenicity. These restraints exist for a variety of excellent evolutionary and safety reasons, and some are even passive in nature (Parham, 2014). In most cases, a single stimulus is insufficient to release the multiple immunological constraints required for effectively developing strong T-cell immunogenicity. For this reason, many vaccines rely on additional stimuli, such as adjuvants, which aid inactivated and inanimate vaccines which appear more threatening to the immune system, often by stimulating DNA damage responses. By providing this additional stimulus, adjuvants are able to greatly enhance the magnitude of the developing immune response. This helps ensure that the response generation is strong enough to be useful and effective.

Research into adjuvants, the most well-known add-on immunogenic stimuli for vaccines, have revealed some amazing insights into how these agents work and how this compares with live attenuated vaccines (LAVs). Subunit vaccines, like HBV, require multiple booster shots to develop effective immunogenicity (Georg and Sander, 2019). In contrast, live vaccines, such as the yellow fever YF-D17 vaccine, can confer a highly effective lifelong immunity from a single inoculation. Because of its impressive immunogenicity, YF-D17 has been studied in greater depth than most other vaccines and this research has brought new insights, particularly into the more nuanced complexities of generating immunogenicity. The YF-D17 vaccine was shown to activate TLR2, -7 and -9 in mice, and in humans TLR8 was also shown to become activated. In humans, these TLR activations are accompanied by transcriptional signalling of the interferon pathways through the TLR7 and RIG-I receptors which sense viral RNA which is created by live virus in plasmocytoid dendritic cells (Georg and Sander, 2019). Furthermore, cytokine responses generated by this LAV were abrogated in experiments using UV inactivated viruses, indicating that it is the molecular processes and activity of the living virus that are responsible for enhancing the immunogenic response. Similar immunogenic observations have been made when comparing live versus dead bacteria, where the actions of TLR8 were shown to be able to determine the viability of microbes by detecting the presence and/or activity of their cellular machinery (Ugolini et al., 2018). The mechanisms by which an immune system is able to discriminate between live and dead immunogenic stimuli, have been loosely defined as a subset of PAMPs, known as the ‘viability associated PAMPs’ (*vita*-PAMPs). These PAMPs and their associated PRRs are able to determine whether an invading pathogen is viable or not. The *vita*-PAMPs are therefore associated with hallmark traits of pathogenic vitality, such as rapid genome replication and abnormally high levels of gene expression, from a limited number of genes, such as capsid proteins. The *vita*-PAMPs, therefore, help the host cell distinguish between detecting foreign DNA and RNA, and determining whether it is a significant threat by monitoring and responding to the level of presence of crucial components of the detected threat. Viable pathogens, by definition, are replicative which means they have the capacity to radically increase their genome copy number and gene expression levels. Documenting and quantifying

this activity on multiple levels, by detection of increasing abundance of pathogenic RNA and DNA, reveals the nature of the pathogenic threat (Georg and Sander, 2019).

The benefit of LAVs and adding adjuvants apparently relate to the same processes. This is demonstrated by the fact that adding adjuvants like alum has limited benefit, or no benefit, when used in conjunction with LAV. In addition to this, research into adjuvants has linked the mode of action of several of these directly with their ability to cause DNA damage and thereby initiate DAMPs. This activity has also been shown to facilitate cells in affected areas enter into necrotic states, which are known to greatly boost immunogenicity (Georg and Sander, 2019; Jacobson et al., 2013; Marrack et al., 2009). The question that must be asked is what do LAV and DNA damage have in common? As I have discussed above, we know that the PRRs that identify DNA damage are also responsible for identifying pathogenic replication. In this way alum can help an inanimate vaccine present more like a live one. In this scenario the ability to replicate genomic can be both the animus of life itself and a biochemical signal that a pathogen is animate, and therefore a threat to be responded to with extreme prejudice and maximum force. This arguably makes the detection of genomic replication the true animus that differentiates a weak and strong innate immune response. This logic explains why LAV are animate vaccines and why adding alum in their formulations adds little to no immunogenic benefit (Jacobson et al., 2013; McKee et al., 2013).

When one considers what pathogenic replication entails, at the molecular and sub-cellular level, it makes a great deal of sense for the immune system to have means of actively seeking out and detecting this type of activity. Determining the viability of an unknown pathogen can be hugely beneficial to the host. The ability to limit or prevent a destructive, energy-intensive, potentially dangerous, and ultimately unnecessary, immune response means the host stands to gain a clear evolutionary advantage from such a distinction. Pathogenic replication and abnormal gene overexpression are logical targets on which to make viability determinations, as the pathogenic life cycle differs substantially from a host cell's normal homeostasis and life cycle. This distinction also ties directly to immune tolerance mechanisms. If non-viable pathogens do not necessitate the risk of full aggressive immune activation, a tolerance for the kind of disruption they bring must logically exist. We see evidence for this from the weak levels of immunogenicity generated by DNA vaccines and inactivated vaccines used without adjuvant (Bolhassani and Yazdi, 2009; Georg and Sander, 2019). While a T-cell immune response may begin upon pathogenic detection by various PRRs and other mechanisms, determination of that pathogen's viability is probably what drives the magnitude, scope and breadth of the response. It is also important to note that no additional biochemistry is necessarily required for a viability determination function to exist. It comes automatically from proportional and progressive self-amplification of the PRRs, which increase their own concentrations and the strength of their immunogenic stimulation by simply binding more and more pathogenic DNA and RNA, as the pathogen proceeds to hijack the host cell. This self-feedback mechanism is essentially able to link the level of immunogenic stimulation to

pathogen replication and gene expression level. It even makes evolutionary sense that the DNA damage detection and response mechanisms (responsible for maintaining cellular homeostasis) should be involved in assisting this determination. This is because they are already present and require an extremely high level of sensitivity to be capable of detecting and responding to natural DNA damage. In evolution it is common for advanced systems and biological capabilities to be repurposed in the aid of other goals that are beneficial to the host. This is one of the hallmarks of complex living systems.

Detection of a pathogens' viability by detecting its genomic replication cycle is perhaps the single most obvious and clear biochemical signal and process available for a cell to detect dangerous infections and an unmistakable sign that it has a serious problem. There is now also substantial scientific evidence indicating that this does occur and that it is highly influential in determining the magnitude of the immune response (Diner et al., 2015; Georg and Sander, 2019; Hu et al., 2016; Kobiyama et al., 2013b; Lugrin and Martinon, 2018; Wenzel et al., 2012).

1.3 Viral infections – Chronic viruses and those difficult to vaccinate

T-cell immunity is especially important for chronically infectious pathogens, such as the human immunodeficiency virus (HIV) or herpes simplex virus (HSV), as a key part of their life cycle is the long-term avoidance of the immune system. These pathogens maintain chronic persistent infections by hiding from, inactivating, or avoiding the numerous and varied components and cells of the immune system. In terms of T-cell immunity this is achieved by limiting T-cell maturation and/or refinement or inhibiting activation in the first place. By doing this they can persist in an individual for a lifetime. Controlling and eliminating these viruses requires a strong and directed T-cell response. This is demonstrated by their correlates of protection established during natural infection and control (Table 1). Therefore, a great research interest and need exists for new innovative and novel approaches to develop effective means of generating this type of immunity, while refining and improving on older methods to maximise their effects.

It is, however, unfortunate that current methods have proven largely inadequate at achieving this goal. There has been some success in terms of the HIV-1 RV144 vaccine trial, which showed a modest ~31% immunity in its participants by its end point, which was 31% higher than all previous trials of HIV vaccines (Rerks-Ngarm *et al.*, 2009). It does however give hope to the field that an effective vaccine can be developed. Many believe that a more effective HIV vaccine will require both strong T-cell and antibody-mediated immune responses (Hsu and O'Connell, 2017; Stephenson et al., 2016). Methods for generating antibodies are numerous and great progress has been made in this field, however, attempts at developing efficient and effective methods of generating T-cell immunity have not been unsuccessful. The only highly effective T-cell vaccine vector available (a recombinant Adenovirus 5 (rAD5) vector), showed problematic results in the widely discussed Phambili / STEP trials that were

stopped prematurely due to ineffectiveness and demonstrated a possible increased likelihood of contracting HIV by some patients who had AD5 immunity (Buchbinder et al., 2008; Sekaly, 2008). The high seroprevalence of AD5 antibodies and immunity among humans proved to be a deciding factor in the problems faced in this trial, which also determined that AD5 is probably not a suitable T-cell vaccine vector for HIV (Buchbinder et al., 2008; Fitzgerald et al., 2011).

It is worth discussing T-cell immunogenicity and HIV in greater depth, as HIV has a multitude of mechanisms that help it evade the immune system. It has arguably the most comprehensive and complete attack and evasion strategy of any virus studied to date, with specific strategies and methods of evading every part of the immune system. This is also why it may require every part of the immune system to combat it.

In terms of T-cell evasion, HIV uses its *Nef* protein to initially downregulate expression of MHC class I proteins, allowing it to hide from and evade T-cell immunity early on, while later it ultimately kills T-cells, effectively eliminating their threat and their ability to mature into a form that could threaten the virus, resulting in acquired immunodeficiency syndrome (AIDS) (Blagoveshchenskaya et al., 2002). Because HIV has a defence strategy against every part of the immune system, it becomes relevant as to how effective each of these defence mechanisms are. Antigen presentation by MHC-I and subsequent destruction of infected cells by CD8+ cytotoxic T lymphocytes (CTL) is a powerful mechanism used by the immune system to detect intracellular pathogens and clean up the remnants of viral infections. This mechanism forms a crucial part of both the innate and adaptive immune systems, which makes it an ideal target for HIV to target early on, as it begins to cripple the immune system. Nearly every step in the assembly and trafficking of MHC-I class proteins can be a potential target for immune evasion. Poxviruses, for example, encode multiple inhibitors that target MHCI presentation mechanisms for downregulation or ablation (Ploegh, 1998). HIV, on the other hand, only has one gene, *Nef*, that it uses to achieve this goal. HIV's *Nef* works by accelerating the process of MHC-I endocytosis and sequestration to the trans-Golgi apparatus. Data generated on this process has indicated that *Nef* is not particularly adept at achieving this effect. This inefficiency is more than made up for, however, by strengths in other areas that also attack the CTL network, not least of which is the viral targeting of this network itself, preventing the generation of mature CD8+ cells (Blagoveshchenskaya et al., 2002; Collings et al., 1999; Tähtinen et al., 2001).

HIV elite controllers are a subset of <1% of infected individuals who naturally control HIV to extremely low levels that are undetectable by conventional assay (<50 RNA copies per ml). Studies on elite controllers have shown that they commonly exhibit strong enrichment of particular types of human leukocyte antigen (HLA) class I genes (which are responsible for antigen presentation via MHCI complexes), as well as immune presentation and CTL training through MHCII presentation on antigen presenting cells (APC), which present antigens to CD4+ T cells via MHCII (Deeks *et al.*, 2015; Fellay

et al., 2007; Jia *et al.*, 2011). This strong association between elite controllers and MHC / HLA genes emphasises the importance and capability that T-cell immunity has to combat and control HIV infections. Moreover, the observations that this mechanism is a strong correlate of protection for elite controllers is powerful evidence that a vaccine will need to include a strong T-cell immunogenicity. Having a particular set of HLA genes does not necessarily mean only the lucky individuals with the right genes will ever be able to be elite controllers: it more realistically means that people without those genes will simply take a substantially longer period of time and a greater number of T-cell maturation rounds to get there. Once HIV has been contracted, the number of T-cell maturation rounds is limited by the virus-destroying T-cells, preventing a sufficiently long enough life time for this to ever develop (Parham, 2014; Sompayrac, 2019). That said, a preventative vaccine will have the necessary time and lack of inhibition frame for this process to occur.

It is important to note however that HIV does not entirely eliminate MHCI complexes, as this results in a process called 'missing self-regulation' which results in immediate destruction by natural killer cells, which have inhibitory "do not kill" receptors that recognise MHCI complexes. These receptors are polymorphic in nature and have their own entire screening process during natural killer (NK) cell development. Only NK cells that have demonstrated their ability to recognise self-cells are given 'licence to kill', and any cell that fails this highly important self-recognition test whereby MHCI complexes cause the stimulation of the 'do not kill' signal to the NK "licence to kill" receptors, is eliminated (Sompayrac, 2019). HIV evasion of T-cell immunogenicity is two-phased and highly sophisticated, as the virus uses *Nef* to limit, but not eliminate, self-exposure by downregulating MHCI exposure, delaying the development of a suitably specific and mature T-cell response, and then eliminate T-helper cells from living long enough to ever be capable of developing a fully mature response. In this sense, the generation of a fully mature T-cell response might only be possible through the development of an effective T-cell vaccine. However, once a full complement of mature memory CD-8 T-cells has been generated they are no longer dependent on the presence of a function of CD4+ helper T-cell population, which is required for their genesis (Parham, 2014; Sompayrac, 2019). The limiting of MHCI exposure has also been identified in cancer research as a mechanism by which cancerous cells also evade attack by CTLs, as such vaccines capable of generating enhanced and mature T-cell immunogenicity are of high interest for combating and treating a variety of cancers as well (Angell et al., 2014; Motwani et al., 2019).

HIV with its RNA genome of ~10 kb effectively also avoids many of the subcellular innate immune defences discussed above, by being an RNA virus and integrating a DNA copy of itself into the human genome with integrase protein. By performing much of its replication as RNA after the genetic material has been reverse transcribed into DNA and incorporated into the genome where it is safe, it effectively avoids most of the pathogenic DNA replication detection mechanisms and receptors. This greatly decreases its likelihood of eliciting a strong T-cell response (Rathinam and Fitzgerald, 2011). While

HIV is highly effective at avoiding the creation of T-cell immunogenicity, it still only down-regulates MHCI, as it cannot eliminate it. Any T-cell vaccine that is highly effective at creating a powerful and focussed CTL-mediated immunogenicity will therefore pose a significant threat to HIV. If this were not the case, HIV would not need such an advanced strategy for avoiding CTLs. While the retroviral life cycle strategy is highly effective at minimising exposure to T-cell activation processes, other viral replication cycles are not. Using these to generate this type of immunity is therefore a viable design strategy for the development of novel rational vaccine design (Jia et al., 2011; Williamson and Swanstrom, 2015).

1.4 Vaccinology in our modern world

Vaccinology is defined as the science of vaccines: this includes everything from basic science to immunogens, the host immune response, delivery strategies and technologies, manufacturing techniques and clinical evaluation. Aspects such as safety, regulatory concerns, ethical, legal and economic aspects are also included. Recently, ethical issues have been shunted to the foreground, with the successful synthetic recreation of infectious horsepox virus (HPXV) from synthesised DNA using basic molecular biology techniques (Noyce *et al.,* 2018). Horsepox has been shown to be the parent virus of the vaccinia virus vaccine strain. This is still widely used today in the form of the modified vaccinia virus Ankara (MVA) (Noyce et al., 2018; Sánchez-Sampedro et al., 2015). This demonstration showed that synthetic engineering of large DNA viruses is possible, and opens up a world of possibilities for creating novel vaccine vectors with enhanced efficacy, breadth, reduced costs and better safety.

However, the ability to synthesise DNA and the relative ease of reanimating dangerous viruses like smallpox (which have their genomes freely available to download on the internet from Genbank® has created a new means by which viruses can spread and evolve. This is also one that cannot be easily dismissed as the means, knowledge and finances do exist among known terrorist factions, making the threat of bioterrorism frighteningly real. Researchers have already published articles that detail how only five mutations can make the highly lethal H5N1 influenza virus strain transmissible via the airborne route (Imai et al., 2012; McKee et al., 2013). The publication of the details of how this potentially life threatening *in-silico* evolution of a deadly virus was hotly debated. However, the reality of the situation was that multiple groups were already aware, and had the knowledge and capability of creating such mutants. The research is however primarily focussed on developing effective vaccines in advance, so as to combat this type of mutation. Therefore, while there is some risk of bioterrorism, and the risk of mutant virus escaping from the labs is not zero, the promise of an effective vaccine capable of preventing both acts of terrorism and the threat of the virus naturally evolving, this capability is worth the risk (which would not be eliminated from not publishing). This has already led to the development

of several clinical and experimental H5N1 vaccines, including some made in plants (Clegg et al., 2013; Mortimer et al., 2013; Richard et al., 2017; Tisoncik et al., 2012).

The first-generation viral vaccines were exclusively live pathogens (Pantalio and Koup 2004). Due to safety concerns, second-generation vaccines were created by simply chemically or physically inactivating the viral pathogens. The use of purified or synthetic proteins created a third generation of vaccines, and recently advances in molecular biology and genetic engineering have led to the development of fourth generation vaccines, using isolated DNA and virus delivery vectors for vaccines and prime-boost regiments (Pantalio and Koup 2004). However, until recently, most vaccine candidates entering clinical trials would do so in the context of a limited knowledge about exactly how they work to stimulate immune responses, and a poor understanding of the types of immune responses that they create and how these in turn confer protective immunity (Pantalio and Koup 2004). This situation is beginning to change with the advanced techniques being developed and advanced research techniques that investigate the inner workings of the immune system and its function. We now know more than ever about the specific proteins, molecules and biochemical pathways that generate immunity, and have a variety of advanced and sophisticated tools and methods to work with, for the purpose of developing and improving vaccines. This has helped develop many new experimental vaccines and some improved ones, yet in many cases the knowledge has proven difficult to translate into effective novel vaccines for hard-to-vaccinate-against targets like HIV. Despite all the knowledge gained and progress made, there remains only approximately 50 vaccines available for use in humans, of which only 30-40 are licenced in the USA and Europe (Barrett A, 2016).

Research has recently shifted heavily towards understanding the genesis of immunity within living systems as a whole. Conventional inactivated or attenuated vaccines which exhibit short-lived antigen expression profiles and a limited time of immune exposure previously favoured for their safety, are being replaced with ever more advanced live vectors or combinations of inanimate vaccine technologies to generate the necessary combination of stimuli desired for high immunogenicity (Haynes *et al.,* 2014). Live replicative vaccines generate significantly better immunogenicity with far stronger T-cell responses and sustained antigen expression resulting in better presentation, which is critical for T-cell immunogenicity (Collins *et al.,* 2017). Live vaccines result in a more natural exposure to vaccine antigens over time, which allows T-cells and B-cells to evolve and hone the immune response into a strong and mature one (involving multiple rounds of immune cell maturation and complex interactions with antigen presenting cells (APC) and other necessary immune system cells) (Nolz *et al.,* 2011, Williams 2013, Collins *et al.*, 2017).

1.4.1 DNA vaccines

DNA vaccines have several advantages when it comes to eliciting cell-mediated defences. The blueprint-like nature of DNA enables a single gene to synthesis many target antigen molecules, and to

do this within the host's native cellular environment. This mimics the natural expression process and characteristics of the target virus, ensuring that protein folding, post-transcriptional and post-translational modifications and other cellular-level events, will occur in the same manner that they do for the real vaccine target virus (Haynes *et al.,* 2014). Foreign plasmid DNA also presents as pathogenic DNA to the host cell; moreover, it can have immunogenic-optimised codon usage, including high concentrations of CpG motifs, and exists in a supercoiled DNA form which is readily identified by resident PRRs as foreign. This allows DNA vaccines to stimulate canonical antiviral defence pathways, triggering a cascade of PAMPs that result in the upregulation of type I interferon response genes and increasing critical T-cell mediated response mechanisms such as upregulation of the toll-like receptors and MHC class I and II antigen presentation receptors and release of cytokines, and immunogenic signals responsible for generating T-cell immunity (Williams, 2013; Hasson *et al.,* 2015). For these reasons, DNA vaccines are seeing an increase in usage, particularly in prime-boost vaccination strategies where DNA is useful for specifically priming the cellular immune response to identify specific antigens. Moreover, DNA vaccines negate vector-based immunity being created, while boosting targeted immunogenicity to the antigen of interest, when combined with conventional vaccine vectors such as MVA.

When DNA vaccines were first produced there were great hopes for major breakthroughs, given that one manufacturing technique could theoretically be used to make vaccines for any target. Today however, DNA vaccines are rapidly approaching more widespread use and some DNA vaccines have already been approved for clinical use by the FDA in a veterinary setting. These include a vaccine against West Nile Virus in horses, indicating use in large animals is possible (Dauphin and Zientara, 2007). Furthermore, in US over 500 clinical trial that utilise DNA vaccination have been registered targeting viral infections and as cancer therapies. Important optimization steps to improve DNA transfection efficiency include the introduction of DNA-complexing nano-carriers aimed to prevent extracellular DNA degradation, enabling APC targeting, and enhanced endo/lysosomal escape of DNA. Attachment of virus-derived nuclear localization sequences facilitates nuclear entry of DNA. Some of the latest improvements in DNA vaccine design include the use of antigen presenting cell specific promotors, arrangement of multiple antigen sequences, co-delivery with molecular adjuvants for preventing cellular tolerance induction, as well as a variety of strategies designed to prevent cellular inhibitory effects associated with DNA vector backbone sequences (Hobernik and Bros, 2018).

There are many considerations and optimisations that must be carefully considered when it comes to DNA vaccine design. These include more obvious things like codon usage and promoter sequence design but may also include gene sequence regions that promote the creation of immunogenic dsRNA and the elimination of bacterial backbone components that can promote silencing of the DNA. These considerations are outlined well in the several reviews available on this topic (Kobiyama et al., 2013a; Rangarajan, 2014; Saade and Petrovsky, 2012; Wahren and Liu, 2014).

Upon a critical evaluation of the abilities of DNA vaccines, it becomes clear that there are two fundamental areas where DNA vaccines require improving. In the most basic sense, these relate to quality and strength. Quality can be characterised in terms of DNA sequence, codon optimisation, addition of CpG motifs, the use of different promoters and enhancer sequences, and the presence of essential elements in mRNAs such as introns, poly-A tails, Kozak-sequences and even the addition of genetic adjuvants, co-expressed cytokines/chaperones and immunogenic dsRNA. All of these can help drive higher levels of mRNA and antigen expression, improve immunogenic signalling, help stimulate various PRRs, and enhance PAMP responses to improve efficacy. In terms of strength, the delivery or uptake of 'naked' DNA into cells after inoculation is exceedingly poor. This remains a substantial issue with DNA vaccine development and technology. At the core of this issue lies a basic truth: that DNA is readily and actively degraded in the body. There are many cellular and subcellular barriers for it to pass to reach a cell nucleus, all of which naked DNA is ill equipped to do (Illingworth and Bird, 2009). Even inside the nucleus, DNA is not truly safe from destruction or from having its genes silenced (Knipe, 2015).

Recent research has focused on improving plasmid DNA delivery by employing methods such as electroporation, microneedle 'tattoo' application or encapsulation. However, these new methods are often expensive and do not offer the desired levels of improvement that are technically needed (Hu et al., 2016). Still more methods exist that look at using things like ultrasound to form microbubble that enhance plasmid DNA uptake (Rong et al., 2018). A whole field of research exists that explores a variety of encapsulation methods that can incorporate plasmid DNA or drugs for targeted delivery to therapeutic areas. Encapsulation methods used include creation of liposomes or similar self-assembling molecules, or using proteins that self-assemble to encapsulate biologically active elements from viruses to various biological transport vesicles and chemical nanostructures such as nanotubes (Carboni et al., 2019; Jiang et al., 2019; Masoomi Dezfooli et al., 2018). These methods are often effective in terms of protecting their encapsulated contents, but may suffer from other issues, such as not targeting the right cell types. Their development and use tend to also be prohibitively expensive.

These problems associated with DNA vaccines help explain, to a significant extent, why DNA vaccines have not yet been able to generate any particularly strong, or long-lived levels of immunogenicity (Saade *et al.,* 2012). The DNA vaccines that have been developed have demonstrated they function quite well in animal models associated with developing highly desirable, T-cell immunogenicity (Gilbert, 2012; Hu et al., 2016; McMichael and Koff, 2014; Nchinda et al., 2008; Wahren and Liu, 2014). Yet, in practice this has not translated well from animal studies, mostly in mice, to human studies, as had been expected (Saade *et al.,* 2012, Hasson *et al.,* 2015). This has been linked to exceptionally poor delivery in large animals and humans, and currently no DNA vaccines, aside from experimental ones, have been approved for use in humans (Hobernik and Bros, 2018). However many DNA vaccines have gone into the clinical trials phase of research and are becoming ever more prominent in prime

boost trial regiments (Li et al., 2016). There is also a limit to how much DNA can be injected before the body actively targets it for degradation, at which point any additional DNA inoculated would probably just increase its destruction and decrease the desired effects (Bai et al., 2017; Rose et al., 2015; Wahren and Liu, 2014).

Over the last two decades DNA vaccines have gained prominence as potentially powerful therapeutics for treating infectious diseases, cancer and autoimmune disorders and extensive efforts and have been made to attempt to address or mitigate many of their major shortcomings. Some of the more common approaches use biomaterial-based adjuvants to enhance antigen delivery and immune responses. These include alum, saponins, microspheres, nanoparticles, liposomes, polymers, etc. Which are commonly used in traditional vaccine formulations. However, other molecular adjuvants such as: cytokines, chemokines and heat shock proteins have also shown promise for enhancing DNA vaccine efficacy. The review by Gulce-Iz and Saglam-Metiner, (2019) details the merits and rational behind these various approaches in depth. While the review by Li et al., (2016) elaborates on the molecular mechanisms and pathways engaged by DNA vaccines and how these mechanisms might be more intelligently targeted by new DNA vaccine designs to improve immunogenicity. New approaches have led to many successes for DNA vaccines and new optimised delivery methods have shown dramatically improved response rates that are often dependant on delivery methods. In mice DNA vaccines have been able to induce protective immunity to the severe acute respiratory syndrome (SARS) corona virus of 2003 which were mediated by CD4 and CD8 cells as well as significant antibody titres (Yang et al., 2004). While such efficacy has been difficult to translate to human models research indicates much of the reasons for this can likely be overcome by improved delivery methods and enhancements of the technology (Li et al., 2016).

In summary, DNA vaccines have both a great deal of potential, and a long list of failures. Their potential lies with the inherently adjuvant-like nature of DNA, and the limitless possibilities of engineering it. The failures lie largely with an intrinsic failure of DNA to be effectively delivered to its target location at useful, relevant, or immunogenic levels. This failure is compounded by its failure to then persist within the nucleus in a meaningful manner without been silenced or destroyed, in part due to its desirable immunogenic effects, which cause both its recognition by cellular and nuclear PRRs, followed by its destruction by activation of anti-pathogen responses (Bai et al., 2017; Diner et al., 2015; Hobernik and Bros, 2018; Motwani et al., 2019).

The elusiveness of the highly desired T-cell immunity and the demonstrated capability and link to the genesis of this type of immunity by DNA vaccines, however continues to spur renewed efforts and interest in creating new and improved DNA vaccines (Hu et al., 2016; Wahren and Liu, 2014; Yi et al., 2018). This is where the idea of a self-replicating DNA expression system and vaccine development technology comes in. The ability to replicate within the nucleus potentially solves all of the known and

defined problems faced by DNA vaccines. While a replicating and non-replicating DNA vaccine, upon inoculation into skeletal muscle, both deliver a relatively low and mostly ineffective dosage of antigen gene copies to targeted cell nuclei. Once there however, this is where the ability to replicate has potential to generate significant and meaningful effects and change immunological outcomes. The non-replicating vaccine will most likely result in a short-lived duration and magnitude of antigen gene expression before it is silenced, destroyed or inactivated. As soon as a self-replicating DNA vaccine enters into a nucleus and expresses its replication genes, however, it will begin to copy itself, amplifying both its immunogenic adjuvant-like presence in terms of copy number, and its gene expression levels and capacity at the cellular level. This ever-increasing nuclear ss- and dsDNA presence is highly immunogenic and will help trigger powerful DAMPs and PAMPs and their associated immunogenicity-inducing response mechanisms. These will be continually, and increasingly, stimulated as the replication process continues. In addition to this ever-increasing DNA immunogenic stimulus, the increasing levels of heterologous antigen gene expression from the increasing copy numbers of plasmid will result in increased mRNA and antigen presence, which themselves will also begin stimulating immunogenic responses by tripping the cytoplasmic pathogenic viability associated PRRs (discussed earlier). This, in turn, should increase the likelihood of the activation of the *vita*-PAMPs, which in combination with the increased antigen expression levels, effectively mimic and recapitulate the progression and gene expression of a real viral infection. If achieved this should make a replicating DNA expression system substantially different and better than a non-replicating one, and presumably more immunogenic (Cheung, 2015; Diner et al., 2016; Georg and Sander, 2019; Huang et al., 2016; Motwani et al., 2019).

DNA vaccines also have the unique capability of not inducing any vector-based immunity, which is an issue for all other killed and live viral or bacterial vaccine vectors. This ability to avoid misdirection of the immune system to targets not associated with the agent the vaccine was developed for, is very useful, and grants any successfully developed DNA vaccine vector the ability to be reused for different viral targets.

1.4.2 Localization - Where do DNA vaccines go?

After inoculation, DNA vaccines primarily locate into lymph nodes and skeletal muscle, where they are expressed. Their distribution greatly influences their immunogenicity, particularly in large animals and humans (Bai et al., 2017; Dupuis et al., 2000). The lymph nodes are integral parts of the immune system and full of all the types of cells necessary for eliciting an immunogenic response. However, localisation in skeletal muscle deserves further discussion in terms of the relationship between immunogenicity and this abundant cell type.

DNA vaccines are readily absorbed into cells of skeletal muscles through microtubules which are prominent in skeletal muscle, and grant the free-floating DNA relatively easy access into cellular

cytoplasm and possible guidance to the nucleus (Bai et al., 2017; Hobernik and Bros, 2018; Marino et al., 2011). Skeletal muscles themselves are a major component of the mammalian body, and consist mainly of two stable cell types: myofibers and adult multipotent stem cells, which can multiply and repair damaged tissues. Traditionally, study of skeletal muscle was mostly focussed on locomotion, and these cells were somewhat ignored from an immunological standpoint. More recently though, it has been shown that these cells are in fact active participants in the immune system, capable of playing a wide variety of immunogenic roles, which include a complex level of intercommunication with various immune system cell types, some of which maintain a permanent residence specifically inside muscle tissue. Indeed, there is a growing body of evidence that a complex and comprehensive range of immunological type actions can be taken by myofibers, particularly during inflammatory and autoimmune responses. Myoblasts and myocytes within skeletal muscle have been shown to have intrinsic antigen presenting cell (APC) capabilities under these conditions as well as the ability to respond to, and endogenously produce, a range of cytokines and chemokines. They have been shown to express Toll-like receptors as well as both classes of major histocompatibility complexes (MHCI and MHCII). This makes DNA vaccine adsorption into skeletal muscle a desirable, and not an unwanted, side effect (Englund et al., 2001; Hobernik and Bros, 2018; Ljungberg and Liljestrom, 2015; Marino et al., 2011; Pokorna et al., 2008).

1.5 Aims and objectives

The aim of this study was to develop a self-replicating DNA vaccine vector from a ssDNA avian virus, and to investigate and compare its capabilities for gene expression with an otherwise equivalent traditional non-replicating DNA vaccine vector.

Specific aims:

- To design and develop a self-replicating DNA expression technology by studying and utilising the RCR system from beak and feather disease circovirus (BFDV).
- To characterise the vector's heterologous gene expression capabilities, and monitor for the induction of unique cellular effects associated with pathogen responses and immunogenicity.
- To investigate and compare expression longevity and strength of replicating and non-replicating vectors in a Balb/cJ Jax mice, by confocal analysis of histology sections of mice inoculated with replicating and non-replicating eGFP expression vectors
- To characterize and compare differences in cellular immune responses from replicating and non-replicating expression vectors in cell culture, by analysing for changes in gene expression of 84 select antiviral response genes.
- To investigate changes in immunogenicity from replicating and non-replicating vectors in Balb/cJ mice by performing interferon ɣ ELISpot assays.

1.6 Hypotheses

1. A self-replicating DNA expression system will create a stronger overall and longer lasting antigen or gene of interest expression profile than a non-replicating DNA expression system.

    a. (Null hypothesis 1) The self-replicating DNA expression system exhibits no difference to the non-replicating DNA expression system.

2. A self-replicating vaccine will persist longer than a non-replicating vaccine, creating a more stable, higher and more consistent level of foreign gene expression.

    a. (Null hypothesis 2) The self-replicating vaccine shows no noticeable improvement in longevity and long-term gene expression levels.

3. A self-replicating DNA vaccine will induce a stronger gamma interferon response.

    a. (Null hypothesis 3) There are no differences in the interferon gamma response.

4. Replicating intranuclear DNA of foreign origin will be identified by nuclear pathogenic DNA sensors and trigger antiviral responses to a greater extent than non-replicating DNA.

    a. (Null hypothesis 4) Replicating intranuclear foreign DNA will not activate antiviral responses differentially to non-replicating nuclear plasmid DNA.

2. Development of a Rolling Circle Replication Expression System

2.1 Introduction

A self-replicating DNA expression technology, derived from a virus, for use as a vaccine is something that lends itself naturally to the enhancement of immunogenicity. As discussed in the review of the literature, many of the biochemical mechanisms that are influential in the generation of T-cell immunity are activated by foreign DNA. Processes such as exogenous DNA replication occurring within the nucleus should, in all likelihood, aid in triggering recognition by key DAMPs and PAMPs associated receptors (Knipe, 2015; Paludan and Bowie, 2013). Furthermore, these systems are known to be of particular importance in generating the kind of T-cell immunity that is sought after when contending with many of the more pervasive and problematic diseases such as HIV, HSV, CMV among others, for which there are currently no available vaccines (Pantaleo and Koup, 2004; Saez-Cirion *et al.*, 2016).

Despite extensive research into the development of replicon-based DNA expression systems (Faurez *et al.,* 2010), no available literature has demonstrated the incorporation of a self-replicating DNA system into a functional DNA vaccine. The closest example to date is of DNA vaccines that deploy a self-replicating RNA system derived from an alphavirus (Knudsen *et al.,* 2015; Ljungberg and Liljestrom, 2015). This system has shown great promise, demonstrating improved immunogenicity and antigen expression levels over more conventional non-replicating DNA vaccines. However, as discussed earlier, there are key PRR targets present within the nucleus, such as IFI16 and possibly others, which can trigger the generation of critical PAMPs associated with the creation of T-cell immunogenicity. These PRRs specifically can be targeted by exogenous replicating DNA in the nucleus, in ways that replicating RNA, which targets PRRs within the cytoplasm, cannot (Knudsen *et al.,* 2015; Leitner *et al.,* 2003; Ljungberg and Liljestrom, 2015). Intriguingly, with the design and development of the replicating DNA system explored here, and existence of the replicating RNA-based system described above, there exists a future possibility of hybridising these two vaccine-targeted gene expression systems for even more enhancement of effects.

Circoviruses are small (14-23 nm in diameter) ssDNA animal viruses that replicate in the nuclei of their host cells and are highly dependent on host genetic machinery to do so. They employ a DNA replication process known as rolling circle replication (RCR) which is dependent on only two viral elements (Crowther *et al.,* 2003; Koonin *et al.,* 2015). The first is a complex protein known as 'replication-associated protein' (Rep) and the second is a region of non-coding DNA, referred to as the long intergenic region (LIR), which contains both a ssDNA and a dsDNA origin of replication, and a conserved stem loop structure. This contains a conserved nucleotide motif of between eight to nine base

pairs where DNA cleavage occurs during RCR. Interestingly, there are several similarities between circoviruses (which infect vertebrates) and nanoviruses (which infect plants). Genetic analysis of *rep* indicates that it is likely to have made the host switch from plants to vertebrates in the distant past. The switch was probably aided by a genetic recombination event which appears to have appended the C-terminal RNA-binding protein fragment (protein 2C), from a picorna-like virus, onto the N-terminal replication initiator Rep of a nanovirus (Gibbs and Weiller, 1999). This created an entirely new class of animal viruses dependent on a unique and complex mode of replication known as RCR, adopted from plant-infecting nanoviruses.

RCR is an efficient mechanism by which circoviruses recruit host genetic DNA polymerase machinery and use it to replicate their circular ssDNA genomes. This allows these viruses to have small and simple genomes, often only encoding two critical proteins. These are the Rep protein, which is responsible for initiating RCR, and the capsid protein (Cp), which varies greatly from host to host.

RCR is a natural example of a self-replicating DNA expression system at work. Its elegance and simplicity as well as the small genome size of circoviruses make the latter an ideal candidate for adaptation and development into a novel self-replicating DNA expression and vaccine vector.

2.1.1 Beak and feather disease virus and rolling circle replication

Beak and feather disease virus (BFDV) was first described by Ritchie *et al.,* (1989). It belongs to the genus *Circovirus* of the family *Circoviridae* and has an ssDNA genome of ~1993 bp contained within a 14-21 nm icosahedral capsid (Crowther *et al.*, 2003; Finsterbusch and Mankertz, 2009). The virus is the causative agent of psittacine beak and feather disease (PBFD), which was first described as possibly being a viral disease in 1984 (Pass and Perry, 1984). BFDV is known to be non-infectious to humans, and is a member of a viral family that is known to have highly restricted host ranges (Niagro *et al.*, 1998). It was recently demonstrated by our group, however, that the BFDV genome is capable of undergoing RCR within mammalian HEK-293TT cells, if introduced as a genomic clone with two LIRs (Regnard et al., 2017).

The RCR mechanism of BFDV has not been extensively studied; however, that of its closest genetic relative, the porcine circovirus (PCV) has been the subject of many studies. The high amino acid similarity of the critical ~33.3 kDa Rep between BFDV and PCV is a strong indication that the RCR mechanism employed by BFDV is probably very similar to that used by PCV (Bassami *et al.,* 1998). This is further emphasised by conservation between the two viruses of four conserved amino acid motifs that have been linked to RCR functionality (Bassami *et al.,* 1998; Crowther *et al.,* 2003; Niagro *et al.,* 1998; Regnard *et al.,* 2015). While the genetic similarities between BFDV and PCV are well documented and their phylogenetic history well established, their genomes only share an overall similarity of 64.3%, while their capsid proteins share a sequence identity of just 29.1% (Bassami *et al.,*

1998; Crowther *et al.*, 2003; Niagro *et al.*, 1998). Furthermore, the *rep* of PCV includes an intron, allowing for two transcriptional mRNA species and Rep protein variants known as Rep and Rep′; the BFDV Rep sequence does not include this. A phylogenetic map of these two viruses, in comparison with the other circoviruses, is depicted in Figure 2.1.

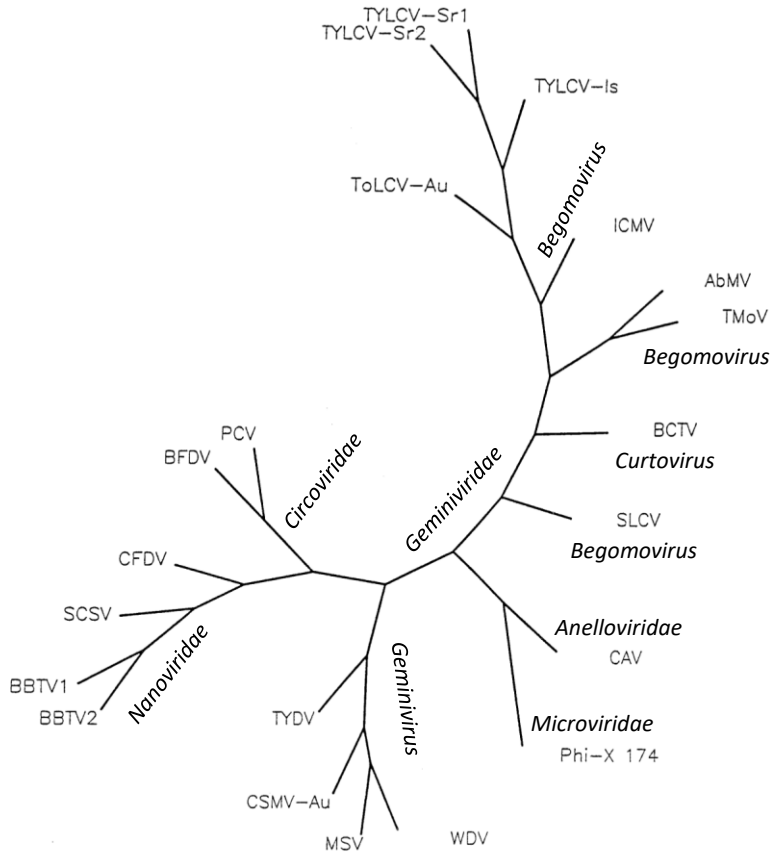

Figure 2.1: Unrooted phylogenetic tree depicting the relationships among the Rep proteins for various viruses. AbMV abutilon mosaic virus; BBTV1 banana bunchy top virus component 1; BBTV2 banana bunchy top virus component 2; BCTV beet curly top virus; BFDV beak and feather disease virus; CAV chicken anaemia virus; CFDV coconut foliar decay virus; CSMV-Au Australian isolate of chloris striate mosaic virus; ICMV Indian cassava mosaic virus; MSV maize streak virus; PCV porcine circovirus; Phi-X 174 bacteriophage φX 174; SCSV subterranean clover stunt virus; SLCV squash leaf curl virus; TmoV tomato mottle virus; ToLCV-Au Australian isolate of tomato leaf curl virus; TYDV tobacco yellow dwarf virus; TYLCV-SR Spanish isolates of tomato yellow leaf curl virus; TYLCV-IS Israeli isolate of tomato yellow leaf curl virus; WDV wheat dwarf virus. Adapted from (Niagro *et al.,* 1998), with family and genus names added.

To understand the utility of the RCR mechanism for use in a vaccine, one must first come to understand the process by which RCR occurs. This complex process has been well studied and reviewed in detail (Cheung, 2015; Faurez *et al.*, 2009; Finsterbusch and Mankertz, 2009). There are two current theories on exactly how RCR occurs. The original theory, referred to as the rolling circle cruciform model, was first described in 1989 as a selection of DNA sequences essential for replication of the tomato golden mosaic virus (Revington *et al.*, 1989). The theory developed rapidly over time to the more detailed and complete one that exists today (Cheung, 2015, 2012; Faurez et al., 2010, 2009; Finsterbusch and Mankertz, 2009; Gutierrez, 1999; Heyraud-Nitschke et al., 1995; Laufs et al., 1995; Palmer and Rybicki, 1998; Stenger et al., 1991).

Cheung (2015) wrote an excellent overview of the complete process, which is depicted in Figure 2.2 below.

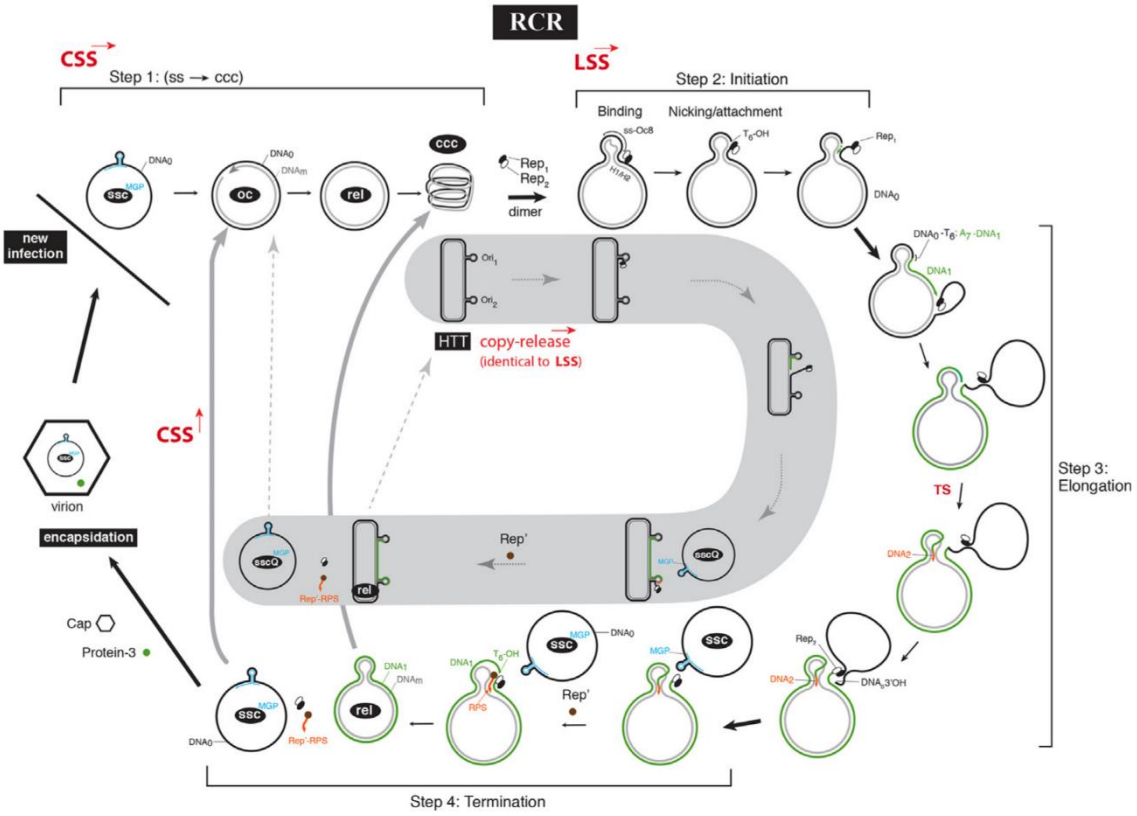

Figure 2.2: A model for copy-release replication and RCR. For the copy-release pathway (shaded inside cycle) supercoiled double stranded (ds) closed circular genome (ccc) is utilized as a head to tail tandem genomic construct. Initiation begins at the upstream Ori1 and termination ends at the downstream Ori2. For leading strands synthesis (LSS) of RCR, only one Ori sequence is involved. As indicated, the copy-release mechanism is identical to the LSS mechanism. At the end of both processes, in addition to the regeneration of the parent ds ccc molecule, a minus genome primer (MGP) couples to a single stranded circular (ssc) molecule (sscMGP) and a Rep'–DNA forms a hybrid with the right palindromic sequence. The sscMGP molecules may undergo complementary strand synthesis to become ccc and yield more sscMGP or it may be encapsidated by Cp in the presence of Protein-3 to become infectious virions. The virion-strand genome (DNA_0) is represented by a solid line circle and the complementary-strand or minus-strand (DNAm) is represented by a grey circle. The first round DNA (DNA_1) is indicated in green and the second round DNA (DNA_2) is indicated in orange. TS indicates template-strand switching. Long dotted arrow indicates recycling of the DNA species derived from copy-release replication and long shaded arrow indicates recycling of the DNA species derived from LSS. Adapted from (Cheung, 2015).

This process, as detailed above (Figure 2.2), involves complex activity with intermediate states involving ssDNA and dsDNA in both linear and circular forms, with protein bound and free floating intermediary DNA forms (Cheung, 2015). Developing this into a self-replicating DNA vaccine potentially benefits from all these states and unique characteristics as each one of them offers a unique form of DNA that can potentially interact with an ever-increasing array of newly discovered immunogenic-associated intracellular and intranuclear PRRs. These interactions with PRRs are believed to act as primary innate immune system triggers, that are either capable of directly activating, or contributing to, an array of immunogenic biochemical signal cascades that drive the different and distinct types of possible immunogenic responses. These trigger mechanisms and the complex biochemical signalling pathways with which they are associated (known as DAMPs and PAMPs) are

not yet fully understood. Intriguingly, however, it appears that RCR activity and its various replicating DNA forms and intermediaries, may be ideal biochemical stimulants for these pathways, possibly creating various adjuvant-like effects. RCR includes both nicked and linear DNA forms that may, at any point in time, exist as either ssDNA or dsDNA (Cheung, 2015). The very nature of these DNA forms and the RCR process amplifying their presence, gives them a high potential to strongly and directly interact and stimulate the DAMPs and PAMPs through known associated activation receptors for these pathways. A growing body of research also indicates that the activation of these pathways is of critical importance for the effective induction and generation of a strong Type I interferon response and the associated biochemical pathways. These in turn are closely associated with the generation of T-cell immunogenicity (Diner et al., 2015; Kepp et al., 2014; Kutzler and Weiner, 2008; Li et al., 2012; Marino et al., 2011; Material et al., 2013; Paludan and Bowie, 2013; Takeda and Akira, 2015). As is the natural immune control of most circoviruses which are considered to be T-cell activating and targeting viruses (Fort et al., 2009; Hakimuddin et al., 2016; Huang et al., 2016; Robino et al., 2014).

To summarise, self-replicating DNA offers several key advantages over non-replicating DNA expression systems. These are as follows:

- The ability to amplify gene copy number in cell nuclei, and thereby boost intracellular gene expression levels and relative localised heterologous gene concentrations within cells that have taken up the DNA vaccine.
- The ability to maintain sustained and elevated levels of foreign gene expression over an extended period.
- DNA replacement, repair and redundancy afforded by self-replication offers the potential to compensate for intracellular and *in vivo* DNA degradation and serves to mitigate against possible gene silencing mechanisms that can minimise foreign gene expression and reduce desired immunological responses.
- The unique possibility of interacting with, and triggering, critical DAMPs and PAMPs associated with subcellular innate immune PRRs and DNA damage recognition receptors to trigger and boost the immunogenic biochemical signal cascades associated with type I interferon response.
- The ability to recapitulate natural viral infection in terms of metabolic stress and dynamic genotoxic biochemical cellular strain through the dynamic activity of an active DNA replication process and non-static gene expression profile.

2.1.2 Aim

The aim of work reported in this chapter was to develop and test the core components from BFDV (required for RCR) in order to create a novel self-replicating DNA expression system, and to demonstrate both RCR functionality and effective gene expression from it.

2.2 Materials and methods

2.2.1 *In silico* design

DNA plasmids were all designed, analysed and tested *in silico* using CLC-Main Workbench by Qiagen (Netherlands,) before any subcloning was performed.

2.2.2 Subcloning procedure

All subcloning procedures were performed using standard methodology. Typical steps involved performing a PCR reaction (section 2.2.10) or restriction endonuclease digestion (section 2.2.6) to obtain linearized of insert and vector DNA. The DNA products were separated using agarose gel electrophoresis (section 2.2.7) followed by DNA gel extraction/purification (section 2.2.16). DNA concentration was then determined using a Nanodrop 1000C (Thermo Fisher Scientific; USA) for subsequent DNA ligation reaction calculations (section 2.2.3). In some instances, PCR reactions using oligonucleotides designed to introduce specific restriction sites (specified for each instance) were used to allow for precise isolation of a DNA insert fragment and ensure its correct orientation and easy ligation into a designated target location. For all experiments, at least one restriction endonuclease site, producing a sticky end, was incorporated to ensure correct DNA orientation during ligation. Ligation reactions always used a 3:1 insert to vector ratio. After DNA ligation (section 2.2.3), the ligation mix containing the newly created plasmid was transformed (section 2.2.4) into *E. coli* DH5α cells and spread plated LB agar containing 50 ng/ml Ampicillin for plasmid selection. This was then incubated overnight at 37 °C and transformants on the plates were screened via colony PCR (section 2.2.10) and confirmed using restriction endonuclease digestion (section 2.2.7). PCR-positive transformants were grown in lysogeny broth (LB) (Bertani, 2004) containing the selective antibiotic (typically ampicillin 100 µg/mL) overnight. Thereafter plasmid DNA was prepared (section 2.2.5). Post screening glycerol stocks (two-parts culture to one-part 50% glycerol) (section 2.2.18) were prepared for each confirmed plasmid and stored at -80 °C.

2.2.3 General molecular techniques

DNA Ligations

DNA ligations were performed per manufacturer instructions using T4 DNA ligase (Thermofisher Scientific).

Transformation procedure

Commercial E. cloni® 10G chemically competent *Escherichia coli* DH5α cells (Lucigen, USA) were used for plasmid transformations as per manufacturer's instructions. Selection of transformed cells was

done using selective LB agar plates using either ampicillin (100 µg/mL) or carbenicillin (100 µg/mL) with overnight incubation at 37 °C.

Plasmid DNA extractions

Plasmid DNA used for subcloning and early transfections was extracted using mini or midi Zyppy™ (Zymogen, USA) endotoxin free plasmid extraction kits, as per manufacturer's instructions. For sensitive transfections that involved expression quantification or animal inoculations ZymoPUREII™ Maxi prep kits (Zymogen, USA) were used as per manufacturer's instructions. DNA quality (Typical >98% supercoiled) was assessed on agarose gels and purity, A260/A280, via Nanodrop™ 1000 (Thermofisher Scientific) readouts.

Restriction digestion of DNA

All restriction endonuclease digestions used endonucleases supplied by Thermofisher (USA) or New England Biolabs (USA) as per manufacturer's instructions.

DNA separation and extraction using agarose gel electrophoresis

DNA products were separated by electrophoresis on tris(hydroxymethyl) aminomethane (Tris), borate, ethylene diaminetetra acetic acid (EDTA), aka (TBE) agarose gels (0.8% unless stated otherwise) run using 1x TBE buffer (89 mM Tris-borate and 2 mM EDTA, pH 8.3) with (0.5 µg/mL) ethidium bromide, (Sigma-Aldrich, USA). This was imaged under 302 nm UV light using a Gel Doc™ XR+ system (BioRad, USA).

DNA extractions were done under blue light at 470 nm using a Blook blue LED transilluminator (GeneDireX, USA) and purified using the DNA IsolateII PCR and Gel Purification Kit (Bioline, USA) as per manufacturer's instructions.

Tissue culture DNA extractions

Total DNA extractions from transfected mammalian cells were performed using a DNeasy Blood & Tissue kit (Qiagen, USA) as per manufacturer's instructions for cultured cells.

2.2.4 PCR oligonucleotide design

A list of primers that were designed is shown in Table 2.2.4.

Table 2.2.4 List of oligonucleotides used. The restriction endonuclease site is underlined in the sequence.

Name	Sequence (5′ → 3′)	Length
BFDV LIR1 For-EcoRI	GGTGGTGAATTCAGAGGTGCCCCACAGGC	29
BFDV LIR1 Rev-BamHI	GGTGGTGGATCCTGTTCCCGGGCGACTGTG	30
BFDV LIR2 For-NotI	GGTGGTGCGGCCGCAGAGGTGCCCCACAGGC	31
BFDV LIR2 Rev-AscI	GGTGGTGGCGCGCCTGTTCCCGGGCGACTGTG	32
BFDV Rep For-HindIII	GGTGGTAAGCTTATGCCGTCCAAGGAG	27
BFDV Rep Rev-BamHI	GGTGGTGGATCCTCAAAAATTGATGGGGTG	30
BFDV Rep3 Rev-SphI	GGTGGTGCATGCTCAAAAATTGATGGGGTG	30
BFDV Rep3 Rev-XhoI	GGTGGTCTCGAGTCAAAAATTGATGGGGTG	30
LIR-Rep Forward	AGGCCTAGGCGCGCCCTG	18
SIR-Rep Reverse	TCCCGCCCTGCGCCATCG	18
LIR2-CP Forward	GGGGCACCTCTAACTGCG	18
SIR-CP Reverse	GAAGGCCAGGCCGTAGTG	18
eGFP-For-HindIII	GGTGGTAAGCTTATGGTGAGCAAGGGCGAG	30
eGFP-Rev-BamHI	GGTGGTGGATCCTTACTTGTACAGCTCGTCCATGC	35

2.2.5 PCR Protocols

A high fidelity *Pfu Phusion* (Thermo Fisher) DNA polymerase was used for cloning purposes. The thermocycling conditions were 98 °C for 30 s followed by 30-45 cycles of 98 °C for 10-15 s, T_a (dependent on the oligonucleotide pair) for 10-15 s and 72 °C for 15 s/'kilo base pair' (kbp) (dependent on the expected PCR product size). A final extension of 5 minute at 72 °C was included. The reaction mix was prepared as per manufacturer's instructions. A touch down PCR method similar in methodology to the protocol developed for difficult AT rich genes was used for oligonucleotides with a T_a difference of greater than 5 °C (Su et al., 1996).

OneTaq DNA polymerase (New England Biolabs) was used for screening of transformants instructions. The thermocycling parameters were as follows: 94 °C for 30 s, followed by 30 cycles of 94 °C for 15 s, T_a (dependent on the oligonucleotide pair) for 15 s and 68 °C for 60 s/kbp (dependent on the expected PCR product size). A last step of 5 minutes at 68 °C was included. The PCR reaction mix was prepared as per manufacturer's instructions. Each reaction contained cells from an identified transformed colony. Screened colonies were also transferred to a numbered square on an agar plate with selection, for temporary storage.

2.2.6 Rolling Circle Amplification (RCA) screening

Amplification of circular DNA fragments for detection and screening was performed using a TempliPhi™ 100 Amplification Kit (GE Healthcare, USA) as per the manufacturer's instructions.

2.2.7 DNA sequencing

The RCA DNA for sequencing was linearised using *EcoRV* – which cuts once in the viral sequence - and resolved by electrophoresis on a 0.8% TBE agarose gel and gel purified. The linearised DNA was then subcloned into the CloneJET PCR cloning kit (Thermofisher Scientific) as per manufacturer's instructions. The ligation DNA was then transformed into competent *E. coli* DH5-α and the plasmid was isolated from overnight cultures. Isolated plasmid DNA was then sequenced at Stellenbosch University (Figure 2.7). Sequence alignments were done using CLCBio (Qiagen).

2.2.8 Source of eukaryotic cells and cell culture

All cell lines were obtained from the American Type Culture Collection (ATCC, USA), these included HEK-293 (ATCC® CRL-1573™), HEK-293T (ATCC® CRL-3216™), and HeLa S3 (ATCC® CCL-2.2™). All mammalian cells were cultured at 37 °C, 5% CO^2 with 80%-95% humidity in 75 cm^2 tissue culture flasks. Growth media consisted of Dulbecco's modified Eagle's medium (DMEM) containing 10% foetal bovine serum (FBS) and penicillin with streptomycin (Pen/Strep) at (100 U/ml). Cells were passaged every 2-3 days at which point they were washed twice with PBS and treated with 3 mL Gibco 0.25% Trypsin containing 0.02% EDTA (Sigma-Aldrich) to free the cells. Growth media was added to neutralise the trypsin reaction and a cell count performed using a haemocytometer. Flasks were then seeded at approximately 12.5-25% confluency, depending on cell type. All handling was done in biosafety Level 2 cabinets using good laboratory practice.

2.2.9 Transfections

Tissue cultured cells were transfected with DNA plasmids by seeding 6, 12, or 24 well plates at a confluency of 30-50%. The cells were then cultured to ~60-80% confluency which took ~24-48 h before transfections were performed. Roche X-tremeGENE™ HP DNA (manufacturer?) transfection reagent (TR) was used to transfect DNA into cells and optimised per cell line used as per manufacturer instructions. In most cases this was 1 µg DNA to 1 µL transfection reagent per 100 µL DMEM with a 30-40 minute equilibration step. The transfection mix was then added directly to the growth media in TC plates and left for the duration of the experiment. Time-limited transfections were also performed whereby a transfection step of 4-6 h was used before aspirating the growth media, washing 3 × with PBS, and adding fresh growth media.

Transfections based on plasmid copy number used the same ratio of DNA to transfection reagent to DMEM. The plasmid concentration (pmols) was calculated and converted to DNA concentration with the use of Equation 2.2.9 below.

Equation 2.2.9

$$\mu gDNA = pmolDNA \times (660 pg/pmol) \times (1 \mu g/10^6 pg) \times N (\# bp)$$

2.2.10 Luciferase assays

The luciferase assays were performed using the Luciferase Assay System (Promega, USA), using the kit pGL4.13 expression vector as a positive control, and our customised luciferase-expressing vectors, designed in house, from this vector. The assay was optimized for transfection efficiency in BHK, HEK-293, HEK-293T and HeLa S3 cells. Varying transfection concentrations were calculated by determining the pmol concentrations of plasmid DNA to normalize plasmid and therefore gene copy number when using plasmids of varied sizes. Transfections were performed as described above. High purity plasmid DNA was used in transfections. This DNA was >95% supercoiled, endotoxin free and supplied from Aldevron (USA) or purified using the ZymoPURE II DNA Maxiprep kits (Zymogen). Characterization assays were repeated multiple times using a high number of replicates (typically n=6) and performed as per manufacturer's instructions. Luminescence was recorded in relative luminescence units (RLU) using a Promega GloMax® luminometer.

2.3 Results

All plasmid constructs used in this chapter are presented below, with depiction of their relevant expression cassettes (Figure 2.3). All vectors contain the pUK57 simple backbone (not depicted).

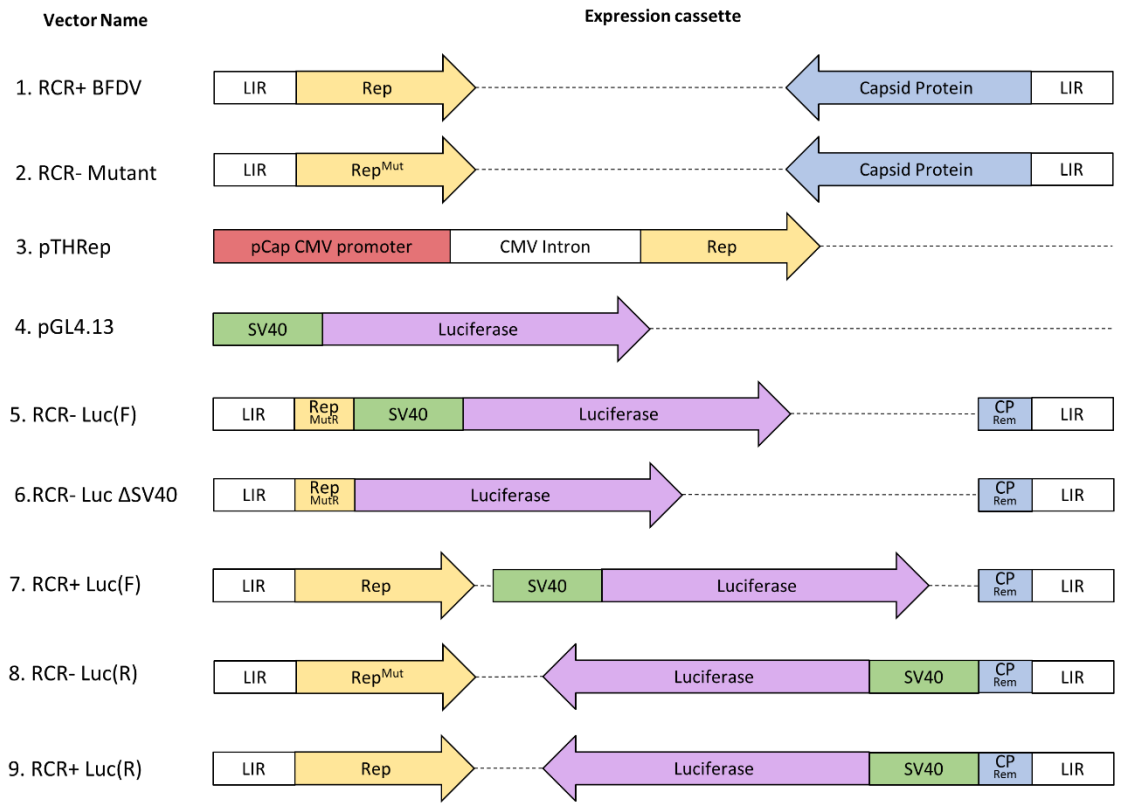

Figure 2.3: Expression cassettes of experimental plasmid constructs. 1) RCR+ BFDV, replicative BFDV vector. 2) RCR- non-replicative mutant, same as (1) but contains an inactivated mutant *rep* gene. 3) pTHRep vector for expression of BFDV *rep*. 4) pGL4.13, luciferase expression vector (Promega™). 5) RCR- Luc(F), non-replicative mutant luciferase hybrid. 6) RCR- Luc ΔSV40 (deleted simian vacuolating virus 40 promoter), luciferase expression by native *rep* promoter 7) RCR+ Luc(F), replicative luciferase BFDV hybrid. 8) RCR- Luc(R), reverse orientation non-replicative mutant luciferase hybrid. 9) RCR+ Luc(R), reverse orientation replicative luciferase BFDV hybrid. All vectors also contained the pUK57 simple backbone with the *E. coli* pMB1 origin of replication and an ampicillin resistance gene under the *bla* bacterial promoter (Not depicted).

2.3.1 Rolling circle replication of a partial BFDV genome repeat in HEK-293T

To determine whether the BFDV full-length genome (Figure 2.4:B) was capable of replicating in mammalian cells, HEK-293T cells were transfected with a linear partial BFDV genome repeat, designated RCR+ BFDV (Figure 2.4:A). After transfection, total DNA was extracted for RCA to enrich for circular DNA and the RCA product linearised using *Bam*HI (one enzyme site situated in BFDV genome). Analysis of the restriction enzyme digestion of the RCA product indicated the presence of two prominent DNA fragments: the transfected DNA (4.5 kb) and a 2.0 kb DNA fragment (Figure 2.4:C). The 2.0 kb DNA fragment was present at a higher intensity than the 4.5 kb fragment. This was corroborated by previous findings by our laboratory (Regnard, 2015).

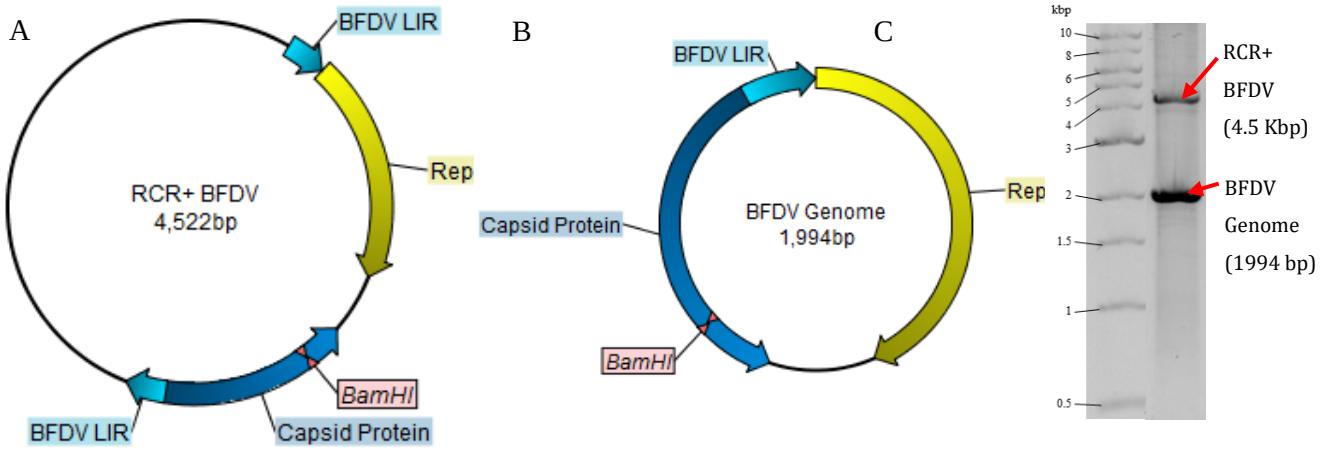

Figure 2.4: The replication of partial BFDV genome repeat transfected into mammalian cells. A) Sequence map of the RCR+ BFDV vector containing a partial genome repeat of a second LIR fragment. B) Sequence map of the full BFDV genome created by RCR. C) Agarose gel of RCA DNA digested with *Bam*HI indicating bands for the transfected plasmid (Input DNA) and the resulting RCR amplicon, which is the BFDV genome.

To confirm that the genome replication observed in the presence of the partial genome repeat was a result of RCR, the start codon for *rep* was disrupted to create a mutant *rep* that would not be expressed (Figure 2.5:A). This mutant was assessed as described above. Analysis indicated the presence of only one prominent DNA fragment, corresponding to the transfected BFDV mutant plasmid (4.5 kb); no 2.0 kb DNA fragment was present (Figure 2.5:B).

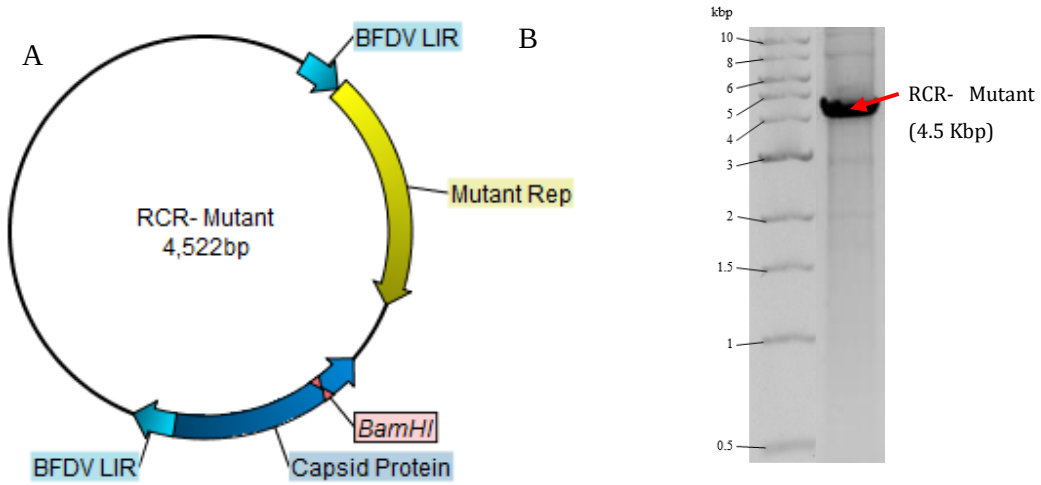

Figure 2.5: The disruption of RCR by mutation of the BFDV *rep*. A) Sequence map of the RCR- mutant partial BFDV genome repeat (4.5 kb). B) Agarose gel of RCA product treated with *Bam*HI.

Aside from the disrupted *rep* gene, the non-replicating (RCR-) mutant (Figure 2.5) is otherwise identical to the initial replicating (RCR+) RCR+ BFDV plasmid (Figure 2.4). This property served as the basis for comparative testing and characterization of RCR.

2.3.2 Transient restoration of RCR using *rep* supplied *in trans*

To establish whether RCR could be restored for the mutant plasmid by transiently adding Rep, a new mammalian expression vector (to express BFDV *rep)* was created. This was done by subcloning *rep* into a mammalian expression plasmid, developed by Tanzer *et al.*, (2011). The backbone of this vector was obtained by excising out *HIV-1C Gag* mosaic from the pTJDNA4, obtained from Tsungai Jongwe (Jongwe *et al.*, 2016). This vector was used to obtain the mammalian expression vector backbone originally developed as the pTH vector, by Tanzer et al., (2011). The functional BFDV *rep* was PCR amplified from the RCR+ BFDV vector with primers that introduced *HindIII* and *BamHI* restriction sites (Section 2.2.4), then subcloned into the vector backbone to create the pTHRep vector (Figure 2.6:B). This powerful mammalian expression vector contains the full CMV Immediate/Early promoter and enhancer sequence and an additional enhancer element taken from the porcine circovirus (PCV) designated as pCap. This enhancer element is part of the promoter sequence for the PCV Capsid gene (Boshart et al., 1985; Schmidt et al., 1990; Tanzer et al., 2011).

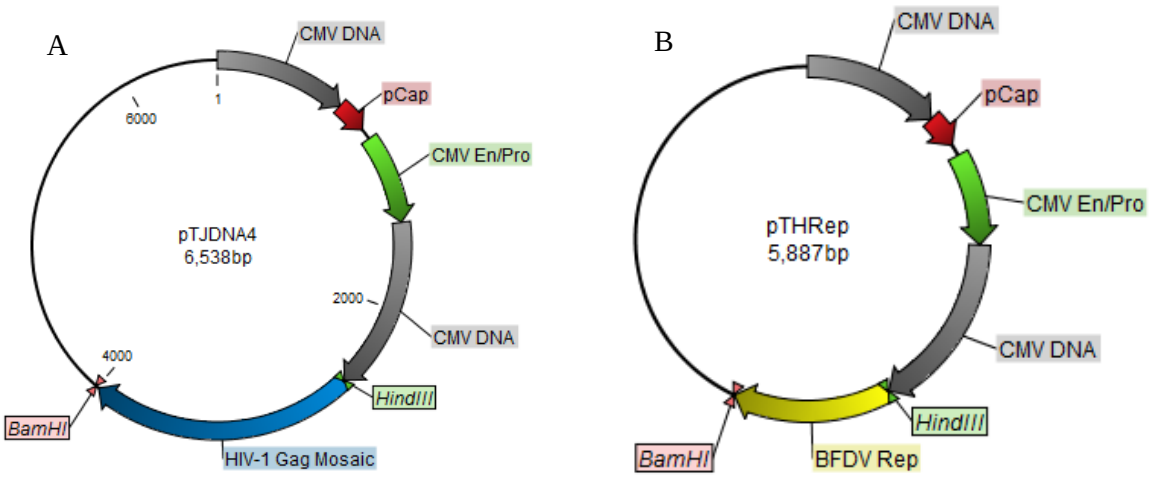

Figure 2.6: Creation of the pTHRep vector. A) pTJDNA4 vector containing a hybrid CMV promoter that includes the CMV intron and cis acting elements as well as the pCap enhancer element (Tanzer *et al.,* 2011). B) New pTHRep vector generated by subcloning the BFDV *rep* gene into the pTJDNA4 vector using *HindIII* and *BamHI* (Jongwe *et al.,* 2016).

For transient expression of Rep *in trans*, pTHRep was cotransfected with the RCR- mutant plasmid (Figure 2.7:A-B) in HEK-293T cells. This completely restored RCR, as demonstrated by the three prominent linear DNA bands after digestion with BamHI (Figure 2.7:C). These bands depict the pTHRep vector (5.9 kb), the RCR- mutant plasmid (4.5 kb) and (critically) the RCR amplicon (2.0 kb), indicating that RCR has been restored.

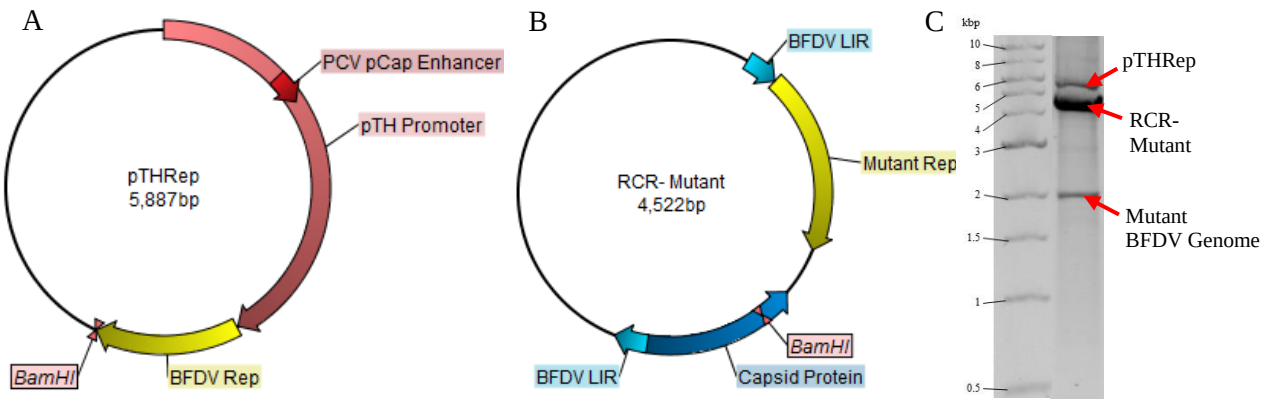

Figure 2.7 The transient restoration of RCR for the RCR- Mutant in HEK-293T cells using *rep* supplied *in trans*. Sequence maps of A) pTHRep (5.9 kb) and B) BFDV Mutant (4.5 kb) ←C) Agarose gel of *Bam*HI linearised RCA product generated from HEK-293T total DNA containing co-transfected DNA.

2.3.3 DNA sequencing to verify the observed RCR amplicon bands are the product of RCR recircularisation of the two LIR DNA sequences

To verify that the DNA bands seen with digested RCA-produced DNA were in fact the RCR amplicons predicted, a DNA sequencing experiment was run. To demonstrate that RCR could amplify foreign DNA, the experiment was performed on a vector that contained minimal native BFDV DNA. This vector's predicted RCR amplicon contained a target antigen of interest, the HIV-1C Gag mosaic gene, a copy of eGFP and two poxvirus promoters, and was flanked by two BFDV LIR sequences each 160 bp in length (Figure 2.8:A). The expected RCR amplicon product was generated *in silico* using CLC BIO Main Workbench, and was predicted to be 2724 bp in size (Figure 2.8:B).

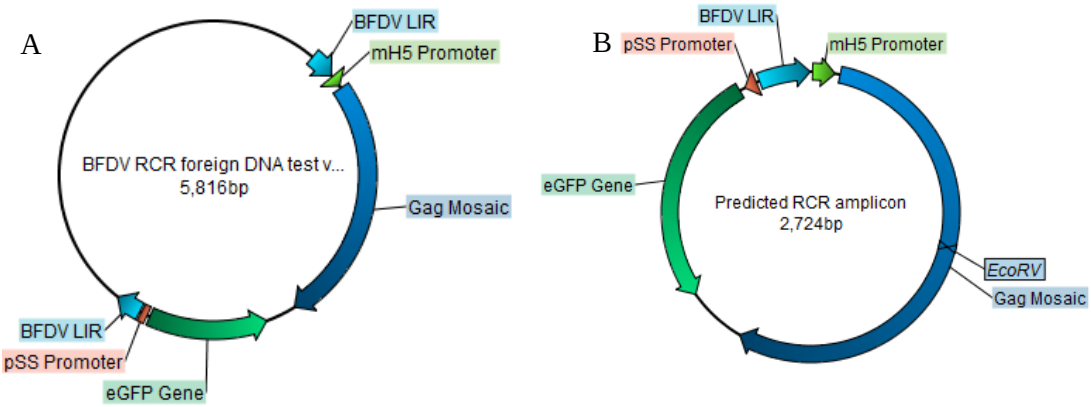

Figure 2.8. In silico prediction of amplicon generated by RCR performed on DNA foreign to BFDV. A) RCR foreign DNA Test transfection plasmid. B) *In-silico* predicted RCR amplicon expected to be generated by RCR upon transient expression of *rep* by cotransfection with pTHRep vector.

The minimal BFDV foreign DNA test vector (Figure 2.8:A) was cotransfected into HeLa S3 cells with pTHRep (Figure 2.7:A) and cells were further cultured. RCA screening was then done using *EcoRV* to obtain blunt end linearized RCA DNA. From this band at the predicted amplicon size was identified (Appendix A4). This band was then excised from the gel and subcloned into the pJet 1.2 Blunt end cloning and sequencing vector and sent for DNA sequencing. The sequencing results were then compared with the predicted amplicon sequence generated in-silico. This resulted in a 100% sequence identity match (data not shown) indicating the band extracted was the predicted amplicon and validating the methodology to verify RCR activity.

2.3.4 Luciferase expression after transient induction of RCR

To characterise the effects of RCR on gene expression, a series of luciferase expression experiments were devised. For these, an RCR-inducible luciferase expression vector was created with luciferase driven by the simian vacuolating virus 40 (SV40) promoter, in the RCR- mutant plasmid replacing most of the BFDV *rep* and *cp* genes. This vector was designated as RCR-Luc(F) (Figure 2.9:C).

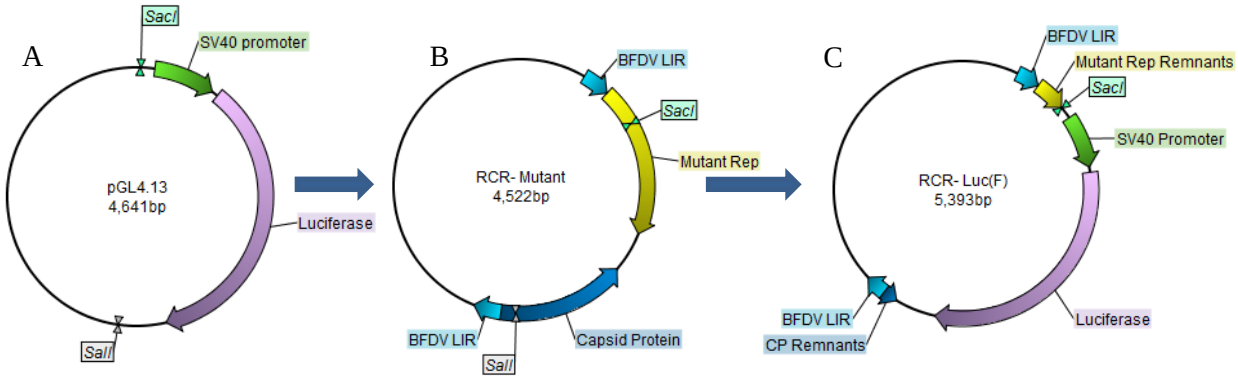

Figure 2.9: The replacement of mutant *rep* and *cp* with a luciferase expression cassette from the pGL4.13 vector. A) pGL4.13 reporter plasmid containing a luciferase expression cassette. B) The RCR- partial BFDV genome repeat mutant. C) The BFDV *rep* and *cp* replaced with the luciferase expression cassette to create RCR- Luc(F).

All subcloning was verified by multiple restriction digest analysis (data not shown) and the pGL4.13 vector (Figure 2.9:A) was used as a positive control in assays assessing variants of RCR-capable expression vectors. All self-replicating vectors were verified to produce the expected amplicons via RCA (Appendix A4,A5)

2.3.5 Expression inhibition by Rep and RCR

The RCR- Luc(F) vector was co-transfected with *rep* and luciferase activity measured by assessing relative luminescence units (RLU) (Figure 2.10). Relatively insignificant luminescence of <6000 units was seen for the duration of the experiment for the *rep* only negative control. Strong luminescence, $>10^7$ units, was detected for the pGL4.13 positive control from 18 hours post transfection (pt) and the intensity increased, reaching a maximum 90 h pt. The RCR- Luc(F) followed the same trend as the

positive control; however, when co-transfected with *rep* luminescence, readouts decreased 1000-fold for the duration of the experiment, ($p<0.01$). This experiment was performed multiple times and the results were repeatable. The presence of the predicted RCR amplicon, from RCR- Luc(F) when *rep* was added transiently, was verified by RCA (Appendix A4; Lane 15).

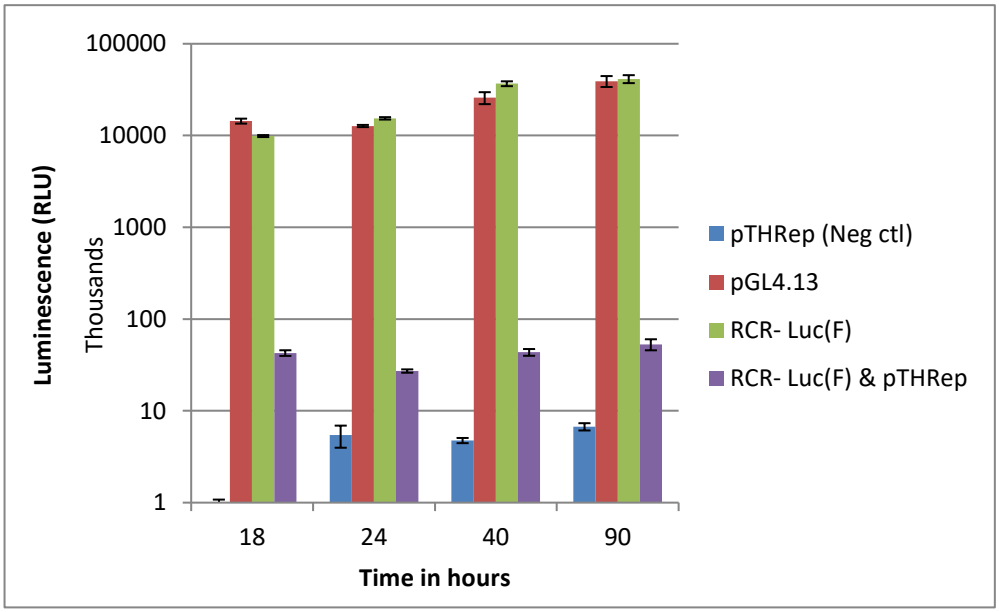

Figure 2.10: The effect of RCR on reporter gene expression. Luciferase expression measured in relative luminescence units (RLU) over time from HEK-293T transfected with: pTHRep(neg), (blue), pGL4.13 (red), RCR- Luc(F) (green) and RCR- Luc(F) and pTHRep (purple). Co-transfections performed at 1:1 ratio of DNA for each plasmid ($p<0.01$).

An experiment was devised to evaluate the apparent inhibitory effect of *rep* expression when introduced by the pTHRep vector. For this, limited transfections were set up using a total of 250 ng transfected DNA per well. This consisted of 231 ng RCR- Luc(F) (0.065 pmol) cotransfected with $1/10^{th}$, $1/50^{th}$ or $1/100^{th}$ (e.g. 0.0065; 0.0013 and 0.00065 pmol) of pTHRep. Total DNA transfected was normalized to 250 ng by adding a non-mammalian expression plasmid pUC19 (Figure 2.11). By co-transfecting a lower copy number of pTHRep with RCR- Luc(F), it was demonstrated that inhibition by *rep* is dependent on its concentration. Here I show that even the lowest co-transfection ratio of 100:1 (I.E. 0.065 pmol RCR- Luc to 0.00065 pmol pTHRep) still resulted in a highly significant ($p<0.01$) reduction in luciferase expression to ~25% as that seen in the absence of *rep* (Figure 2.11).

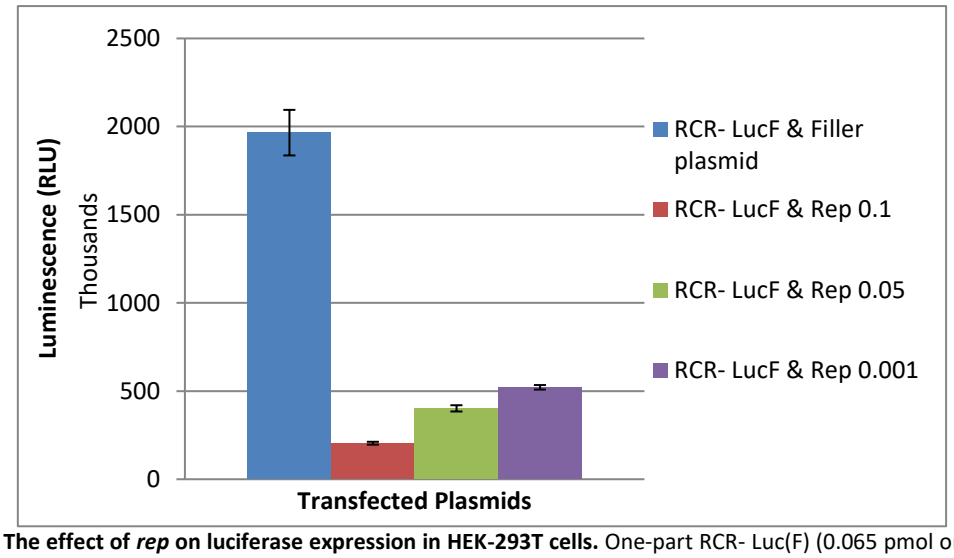

Figure 2.11: The effect of *rep* on luciferase expression in HEK-293T cells. One-part RCR- Luc(F) (0.065 pmol or 231 ng) was cotransfected with either pUC19 filler plasmid only, or with 1/10th; 1/50th and 1/100th (e.g. 0.0065; 0.0013 and 0.00065 pmol) of pTHRep. Total DNA normalized to 250 ng by adding pUC19 as required (n=6), ($p<0.01$).

To further investigate the suppression effects of Rep and whether this had any connection with the SV40 promoter, an additional control was introduced with the positive control (pGL4.13) co-transfected with pTHRep in a 1:1 ratio. No difference in luminescence was observed between this new positive control in standard positive control of only pGL4,13 vector (Figure 2.12), *(blue:orange)*. This set of experiments also indicated that the native promoter for *rep*, present in the LIR sequence, appears to act as an enhancer to the SV40 promoter. This was shown by the increased luminescence from the RCR-Luc(F) vector over that achieved by the pGL4.13 vector by ~50%, (Figure 2.12), (*red:blue*).

The relative strength of this native *rep* promoter in the LIR was also investigated independently. For this a new vector was constructed, in which the SV40 promoter was removed, creating the RCR- Luc ΔSV40 vector (Figure 2.3). In contrast to the ~50% enhancer effect demonstrated when the LIR promoter acted in combination with the SV40 promoter, removal of the SV40 promoter resulted in a dramatic drop in luminescence readout to ~3.8% of that obtained by the pGL4.13 positive control (Figure 2.12), *(green:red)* a relatively massive ~26-fold decrease. This indicated that, by itself, the promoter within the LIR region for *rep* demonstrated ~1/26th of the strength the SV40 promoter has when driving gene expression in HEK-293T cells. Combinations of the pTHRep vector with the RCR inducible vectors, namely RCR- Luc(F) and RCR- Luc ΔSV40, resulted in highly significant decreases in luminescence (Figure 2.12), *(purple & light blue)*, as was previously demonstrated (Figures 2.10-2.11). ANOVA was performed on these data were all shown to be highly significant, with p values $p<0.01$ for all the relevant luminescence data discussed.

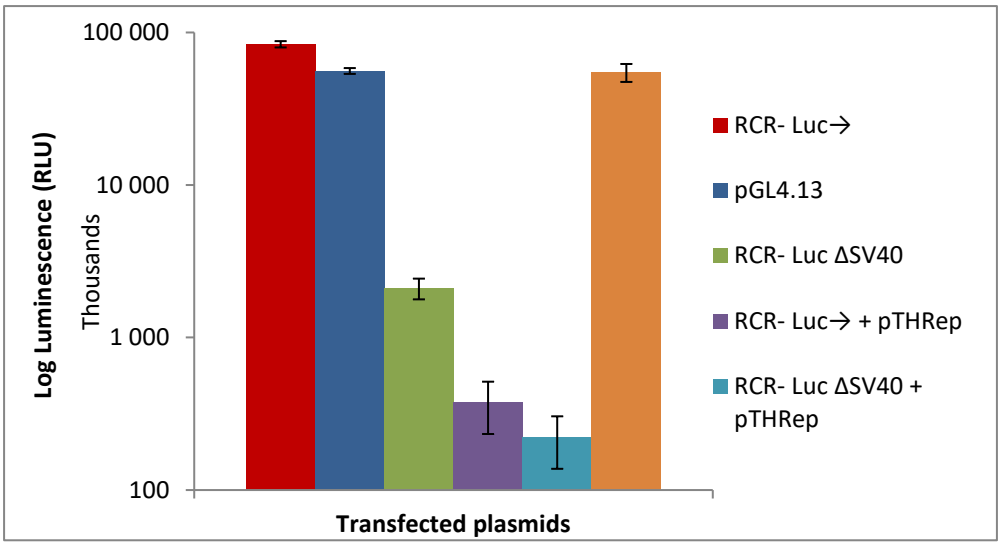

Figure 2.12: The effect of the SV40 promoter on luciferase expression with *rep* supplied in trans in HEK-293T cells. Luciferase expression driven by different combinations of the LIR and SV40 promoter elements and tested with *rep* supplied in trans by the pTHRep vector at a 1:1 ratio calculated in pmols (n=6). ANOVA ($p<0.01$), were error bars overlap difference was insignificant.

After characterizing the strength of the native *rep* promoter (Figure 2.12), the effect of RCR on luciferase expression was investigated when the *rep* gene is driven by its native promoter. To do this a fully self-contained and self-replicating (RCR+) luciferase expression vector was designed and developed (Figure 2.13). This was achieved by PCR amplifying the BFDV *LIR* and *rep* DNA sequence from the RCR+ BFDV vector (Figure 2.3:A) using primers that introduced the *NotI* and *XhoI* restriction sites. This was then subcloned into the RCR- Luc(F) vector (Figure 2.10:C) backbone after its mutant *rep* and *LIR* sequence were excised using *AscI* and *XhoI* restriction endonucleases. The subcloning used a single sticky end ligation step to add the PCR insert after it had been digesting using *XhoI*; this was followed by a blunting step to blunt the *AscI* site and a second ligation step to complete the subcloning. The new vector created was designated RCR+ Luc(F) (Figure 2.13). Its ability to self-replicate was verified by RCA screening (Appendix A4).

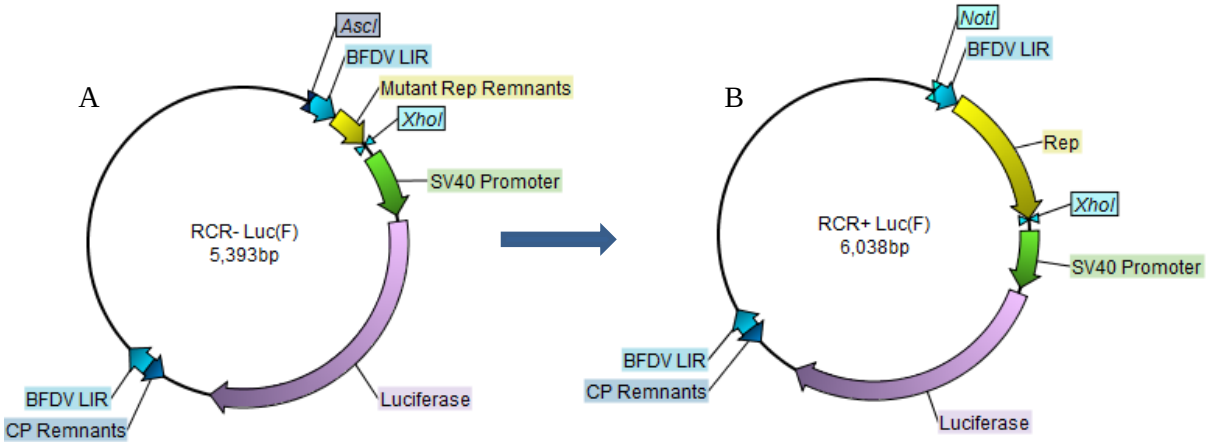

Figure 2.13: Design and development of the fully self-replicating luciferase expression vector RCR+ Luc(F). A) The mutant *LIR-rep* sequence was excised from RCR- Luc(F) with *AscI* and *XhoI* while the functional *LIR-rep* insert was PCR amplified from RCR+ BFDV using primers to introduce *NotI* and *XhoI* sites and subcloned into the backbone in a 1 sticky end 1 blunt end subcloning procedure to create RCR+ Luc(F).

Luciferase assays using this new vector, however, also resulted in lower luminescence as compared with the non-replicating RCR- Luc(F) vector (Figure 2.14). The level of inhibition was dramatically reduced, however, compared to experiments where *rep* was introduced in *trans* using the pTHRep vector to induce RCR (Figures 2.10-2.11). This result was demonstrated in three different transfectable cell lines, Hek293, HeLaS3 and Hek293T which range approximately 2 orders of magnitude in gene expression capability. The replicating RCR+ Luc(F) vector consistently produced a luminescence readout of approximately 12-18% of that obtained by the non-replicating RCR- Luc(F) vector in all cell lines tested (Figure 2.14). This represents an ~100-fold increase in luminescence as compared to that observed when introducing *rep* in trans using the pTHRep vector (Figures 2.10-2.12). These data were highly significant (P<0.01).

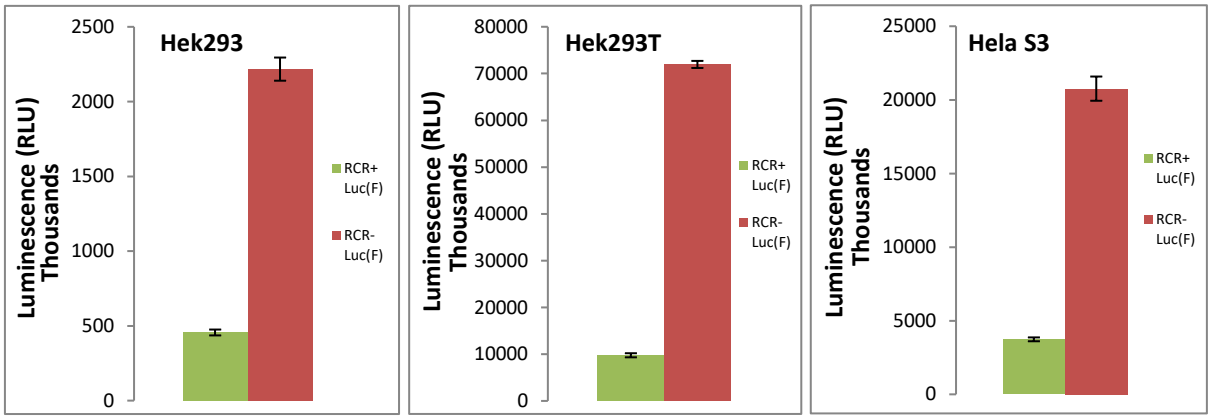

Figure 2.14: Comparisons of luciferase expression 48 h pt, by replicating (RCR+) and non-replicating (RCR-) vectors in different cell lines. The fully contained self-replicating, RCR+ Luc(F) vector, expresses less luciferase in all cell lines tested as compared with the non-replicating, RCR- Luc(F) vector (n=8), p<0.01.

2.3.6 Redesigning the RCR system for optimized expression

Despite the ~100-fold improvement in luciferase expression when *rep* was driven by its own demonstrably weaker promoter, a new vector design was developed that would place the gene of interest in place of the native viral capsid gene on the antisense strand of DNA to *rep* and in the reverse orientation to it.

To reorient *luc* a new series of subcloning experiments had to be performed. A new vector backbone was created from RCR+ BFDV vector by excising the *cp* gene using *SphI* and *BamHI* (Figure 2.15:A). The expression cassette insert was then excised from the pGL4.13 vector using *EcoRV* and *BamHI* (Figure 2.15:B). This was then ligated into the backbone in a 1 sticky end 1 blunt end subcloning procedure to create a new self-replicating vector with *luc* in reverse (R) orientation on the antisense DNA strand to *rep* (Figure 2.15:C). A non-replicating RCR- Luc(R) version was then created using a simple subcloning procedure to replace the functional *rep* with the mutant *rep* from the RCR- (data not

shown). Both vectors were then screened using restriction digests and RCA to verify RCR amplicon formation for RCR+ version and the lack thereof for RCR- version (Appendix A5).

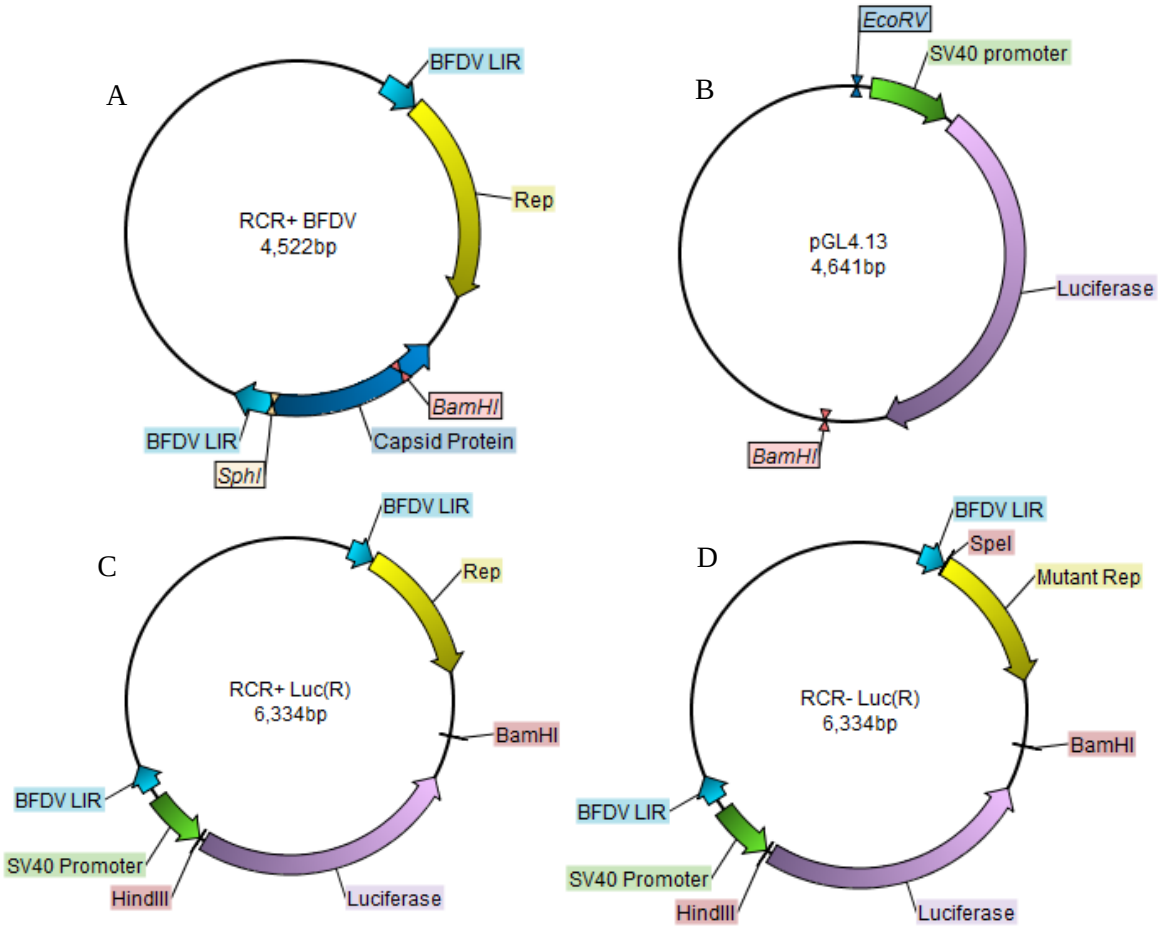

Figure 2.15: Subcloning procedure to create RCR+ Luc(R). A) A vector backbone was created from RCR+ BFDV by excising the capsid protein using *SphI* and *BamHI.* B) An expression cassette insert was created from the pGL4.13 vector using *EcoRV* and *BamHI* and subcloned into the backbone to create C) RCR+ Luc(R) vector from which the D) RCR- Luc(R) vector was made by subcloning the mutant *rep* in to replace the functional *rep*.

After verifying RCR amplicon formation using RCA, luciferase assays were conducted with the new RCR- and RCR+ Luc(R) vectors. These indicated that the inhibition effects seen previously by Rep were negated in HeLa S3 cells, but still present, albeit to a lesser degree, in HEK-293T cells (Figure 2.16).

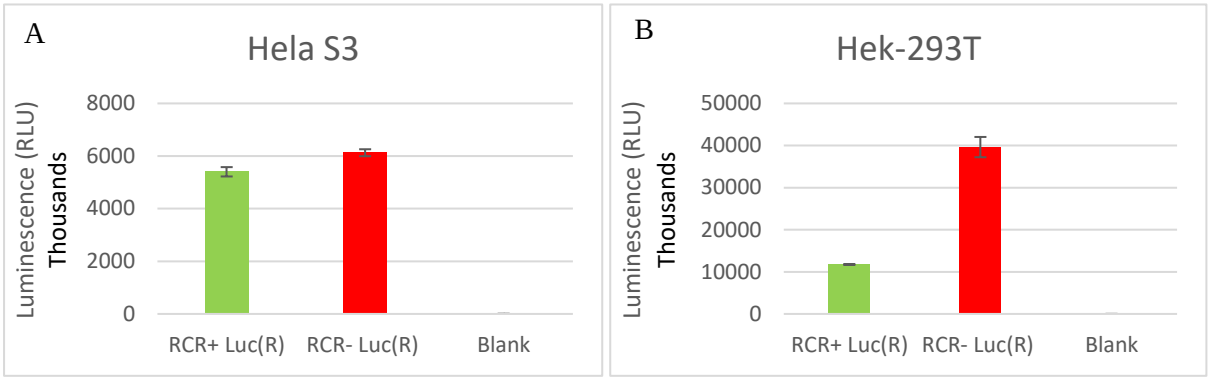

Figure 2.16: Luciferase expression from the newly developed RCR+ Luc(R) and RCR- Luc(R) vectors, 48 h pt. A) HeLa S3 cells and B) HEK-293T cells (n=6), $p<0.05$.

2.3.7 Characterizing the redesigned RCR+/- vectors expression

Further and detailed characterization of the newly developed vector design was conducted to better quantify the differences between the new replicating (RCR+ Luc(R)) and non-replicating (RCR- Luc(R)) vectors (Figure 2.15). Due to the presence of the SV40 promoter in the vector and the fact that HEK-293T cells have been genetically modified to include the SV40 large T-antigen gene in them, only HeLa S3 cells were used for further characterization as this variable could not be controlled for in HEK-293T cell quantification tests.

Expression levels of luciferase at 48 h pt in HeLa S3 cells transfected with different DNA amounts appear to follow an S-curve (Figure 2.17) as DNA concentrations increased. At 1200-1500 ng range this S-curve appears to level off, as saturation levels are reached.

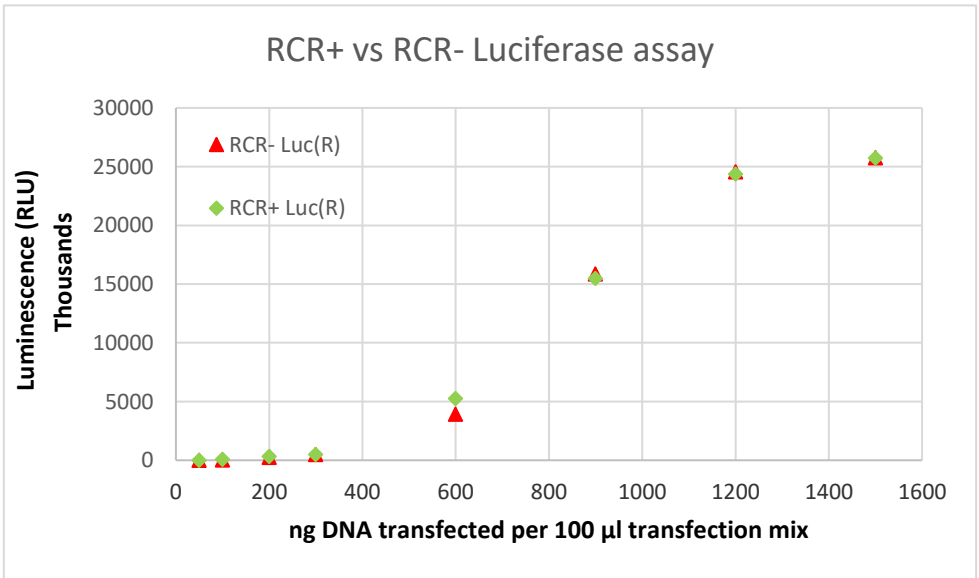

Figure 2.17: Characterization of luciferase expression by RCR+ Luc(R) and RCR- Luc(R) vectors 48 h pt in HeLa S3 cells. A) Luciferase assay testing a range of DNA transfection concentrations for the RCR+ and RCR- vectors (n=6).

To evaluate luciferase expression over a longer period, cells were transfected under standard conditions and evaluated at 48 h pt or passaged then and cultured until 96 h pt before performing luciferase assays (Figure 2.17).

At 48 h pt (Figure 2.18:A) no significant difference in overall luciferase expression is apparent between the RCR+ Luc(R) and RCR- Luc(R) vectors; however, at 96 h pt after performing 1 passage at 48 h, it becomes apparent that cells transfected with the RCR+ Luc(R) vector had lost significantly less luciferase expression than the RCR- Luc(R) samples and were expressing ~2-fold more luciferase overall ($p<0.01$) (Figure 2.18:B). In these assays one can see that the relative ratio difference in luminescence between the non-replicating vectors, namely RCR- Luc(R) and pGL4.13, remains approximately the same at the different times. This is observed as the relative difference between in the height of their bar graphs with each other, where the luminescence of RCR- Luc(R) is consistently approximately 2/3rds the height of the bar of pGL4.13 ($p<0.01$). The RCR+ Luc(R) sample, however, alters in its relative level of luminescence over time with respect to the two non-replicating (RCR-) vectors. This is indicative of a dynamic system at play that counteracts the generally decreasing trend in luminescence over time. This experiment was repeated more than three times with similar results (data not shown).

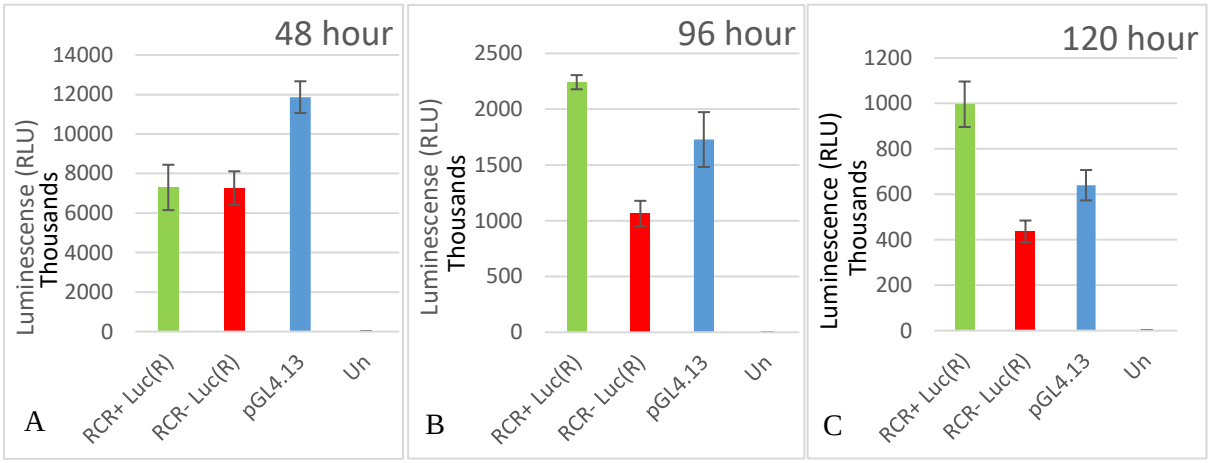

Figure 2.18: Time course of luciferase expression from the RCR+ Luc(R) and RCR- Luc(R) and the control, pGL4.13 luciferase expression vectors transfected into HeLa S3 cells. A) 48 h pt and at B) 96 h pt after 1 passage at 48 h. C) 120 h pt after 1 passage at 72 h, (Note: this sample cultured in complete media containing a lower amount, 5%, FBS (n=6), $p<0.01$.

After demonstrating and repeating the above results to verify that the improvements in heterologous gene expression were real, investigation of alternative vector designs was halted, and two additional sets of the RCR+ and RCR- vectors of the same design (depicted in Figure 2.15) were created using different genes of interest: these were eGFP and HIV-1C Gag mosaic genes, using the same subcloning procedure. These vectors were developed for further and more extensive testing and in-depth analysis

of gene expression from the new RCR DNA expression technology. Vector diagrams of these, with their alternative genes of interest, are depicted below (Figure 2.19).

Once the new RCR+ and RCR- (R) design had been finalized, two more sets of replicating RCR+ and non-replicating RCR- plasmids were created by subcloning in two new genes of interest; namely, HIV1C Gag mosaic from the pTJDNA4 vector (Figure 2.6), which already had HindIII and BamHI sites, and eGFP, which was PCR amplified from the pGEMVA (Appendix A1) vector using primers that introduce the required restrictions sites (Table 2.2.4). All vectors were screened using multiple restriction digests and RCA screening was performed to verify correct functionality and plasmid size (Appendix A5).

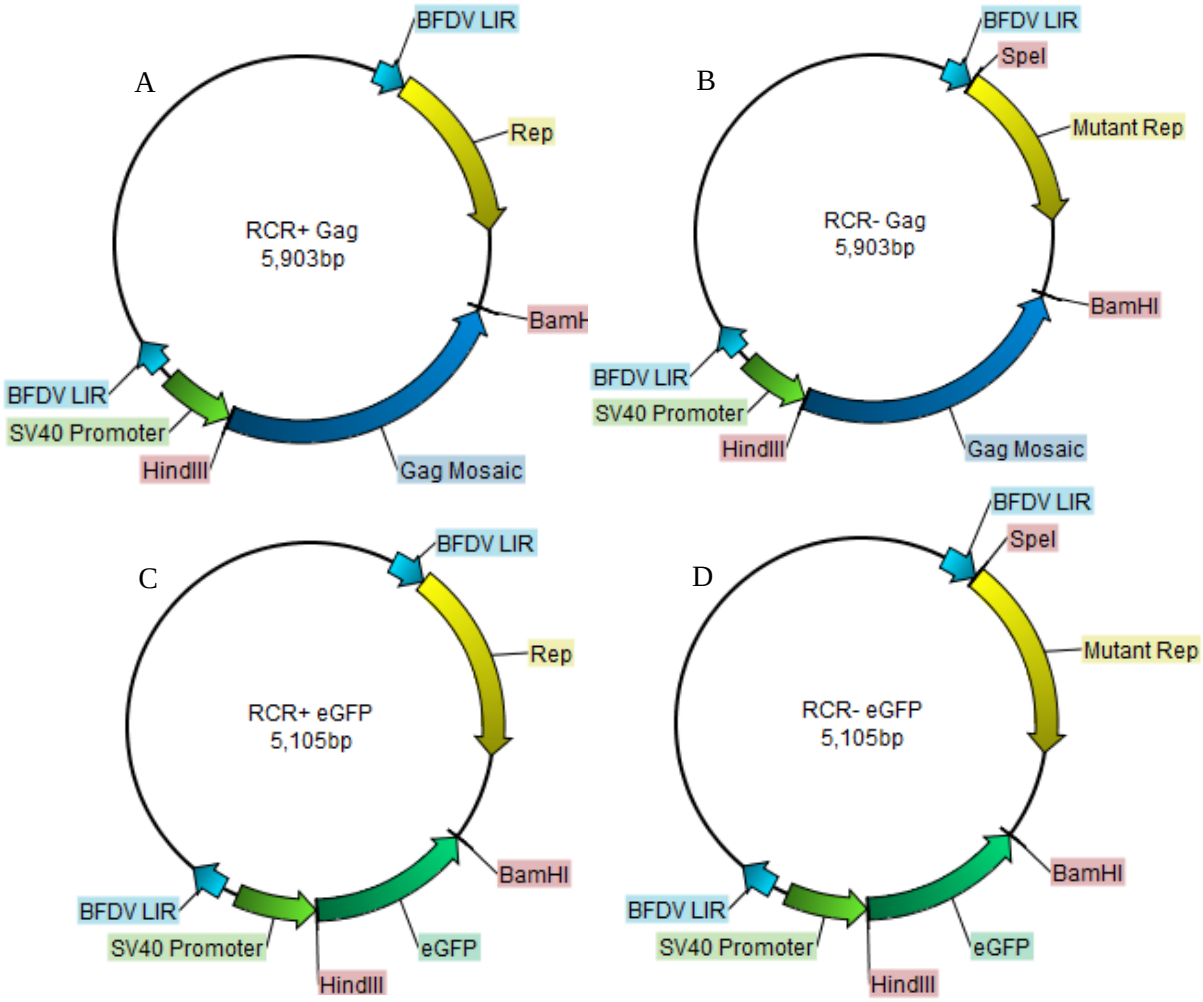

Figure 2.19: New RCR+ and RCR- expression vectors using the same design as Figure 2.14. The new vector pairs are as follows. A) RCR+ HIV-1C Gag mosaic. B) RCR- HIV-1C Gag mosaic. C) RCR+ eGFP D) RCR- eGFP.

This constituted the end of vector design and R&D phase of this project. At this stage it was already apparent that this self-replication expression technology is fascinatingly complex and has amazing potential capabilities.

2.4 Discussion

In work reported in this chapter, a series of design and development experiments were undertaken to develop, test, and verify the core research goals required for developing the RCR system from BFDV into a novel viable self-replicating DNA expression technology. This was achieved by designing, building and prototyping several different vector designs, testing their expression characteristics, and verifying RCR functionality. Optimising the critical functions required for this technology to become viable involved several complex areas of design, redesign and advanced troubleshooting. Ultimately, these experiments allowed me to develop the technology from a theoretical idea, into what appears to be a viable replicating DNA gene expression system.

A cornerstone of the research conducted here was the fact that RCR creates smaller, and therefore more easily-identifiable, amplicons from plasmids that contain two copies of the BFDV LIR genomic DNA fragment. This was originally discovered in a series of replication experiments conducted in plants on the geminivirus beet curly top virus (BCTV) (Stenger et al., 1991). The technique has since then been widely adopted and used to enhance gene expression in a variety of geminivirus-based plant expression vectors, where it has been primarily used as a tool for amplifying and producing large yields of a variety of proteins, and improving yields for plant based protein expression systems (Gutierrez, 1999; Laufs et al., 1995; Liu et al., 1999; Regnard, 2015; Regnard et al., 2010). We recently demonstrated, and reported, that the technique also appears to be applicable in mammalian cell culture for HEK-293T and HEK-293TT cells, using the BFDV genome and a partial repeat of its LIR fragment. These experiments successfully generated the full-length BFDV genome from the transfected RCR+ BFDV plasmid (Regnard et al., 2017). Similarly, an inactive version of the plasmid (RCR- BFDV) was also demonstrated to be incapable of producing RCR amplicons. These core experiments were investigated further in a variety of different cell lines (data not shown) and genomic configurations in this project to assess broader viability for vaccine applications (Figures 2.3-2.5) to confirm that the RCR system possessed the capability of amplifying entirely foreign DNA sequences that included target vaccine antigens of interest (Appendix A4). RCA analysis (to confirm RCR functionality) was performed repeatedly on every vector constructed, to ensure that this core replication functionality was active in all replicating vectors investigated.

Developing and testing the restoration of RCR in the disabled RCR- BFDV vector by the transient addition of Rep from the pTHRep vector provided an important developmental tool, which allowed me to compartmentalise the components of RCR and to investigate the potential of this technology to operate independently of the viral genome from which it is derived. In these tests, an amplicon made up of entirely foreign DNA to BFDV (excluding the two *LIR* repeat sequences) and containing target HIV-1C vaccine antigen Gag mosaic gene, was successfully induced to undergo RCR. The amplicon creation was verified by RCA analysis and DNA sequencing of the product produced. This confirmed

that the RCA-derived products seen in gels are RCR amplicons, that the RCR process can amplify foreign DNA sequences, and that it specifically does work on our target HIV-1C Gag antigen. This series of experiments also briefly investigated RCR functionality across four theoretical configurations of the genetic components being utilised. These were with the *rep* gene sequence inside and outside the amplicon and driven by its native promoter which is inside the *LIR* DNA sequence; *rep* outside the amplicon driven by the *SV40* promoter, and finally with Rep added in *trans* by expressing it using the pTHRep vector.

Initial success in developing, testing and verifying luciferase expression and RCR amplicon creation upon transient introduction of Rep for the RCR- Luc(F) vector was accompanied by arguably the biggest challenge of this project: the discovery that transient *rep* expression from the pTHRep vector resulted in massive downregulation of expression of the reporter gene *luc* (Figure 2.10).

The inhibition generated by introducing *rep* in trans was so strong, that to compare or even see the resultant level of luciferase expression on a graph, required viewing it on the log scale. The 'silver lining' associated with this observation was the discovery that the RCR- Luc(F) vector appeared to elevate luciferase expression by ~1.5-fold or 50% over that seen by its parent vector pGL4.13, a finding that was replicated several times (Figure 2.12.). This indicates that the BFDV LIR sequence can act as a gene expression enhancer when it is placed upstream of the SV40 enhancer/promoter sequence. As it is a relatively small DNA fragment (176 bp), this finding is potentially useful in a variety of possible applications. A similar finding has previously been made with regards to the PCV capsid promoter (Pcap), which has been used to enhance the expression capabilities of the already powerful CMV immediate early enhancer/promoter sequence (Tanzer et al., 2011)

After observing and testing the effect in a range of experiments, it became apparent that the inhibition was Rep concentration-dependent (Figure 2.11). Intriguingly, after some research it appears that this inhibition process is both inseparable from RCR, and is probably a form of self-regulation, necessary to maintain viral fitness by regulation of RCR. The process, which has not been thoroughly studied for BFDV but has been for its closest genetic relative PCV, involves a self-limiting function of Rep whereby the protein interacts with its own promoter to limit expression of the *rep* gene (Faurez et al., 2010, 2009; Niagro et al., 1998).

In the case of PCV, the inhibition appears to work by Rep binding to two hexamer repeats called H1/H2 that are present in the PCV *LIR* gene fragment immediately adjacent to its stem loop structure formation. Rep binding to this region has been demonstrated to be critical for both RCR and inhibition of *rep* expression (Mankertz *et al.,* 2004; Mankertz and Hillenbrand, 2002).

The inhibition process itself has been quite thoroughly investigated in the case of PCV, where it has been proposed that Rep achieves this via interaction and recruitment of specific host transcription

factors and inhibitors, some of which have been putatively identified. Evidence for this proposed mechanism of action comes from the identification of likely transcription factor binding sites located on the C-terminal of PCV Rep; these sites are thought to interact with transcription factors ZNF265, VG5Q and TDG (Adams *et al.,* 2001; Faurez *et al.,* 2009; Finsterbusch *et al.,* 2009; Steinfeldt *et al.,* 2007). The observations of luciferase inhibition by Rep when the LIR fragment is present, and the absence of inhibition by Rep with the pGL4.13 vector where the LIR is not present, suggests that a similar mechanism of inhibition is being caused by BFDV Rep.
That this this inhibition activity is present despite the location of the *luc* gene being well downstream of the LIR sequence, with the presence of the entire SV40 enhancer/promoter sequence residing in-between the LIR and *luc* sequence, provides further evidence of complex transcription inhibitor activity, in action similar to that described for PCV, is something worthy of more investigation.

A direct, and more obvious, manner in which Rep may contribute towards expression inhibition is the active process of RCR. Such inhibition is essentially a form of competitive inhibition between DNA polymerases and RNA polymerases for access to the DNA. Competitive inhibition between these two enzymes alone would not however be sufficient to account for the high magnitude of gene suppression observed both here and for PCV (Faurez et al., 2010; Finsterbusch and Mankertz, 2009; Ramsay and Tipton, 2017; Toogood, 2002). Genetic analysis done on BFDV, which I also independently verified *in silico,* indicates the presence of two octamer repeats of GGGGCACC in the BFDV LIR in the same location as the H1/H2 hexamer repeats (CGGCAG) reported for PCV. This octamer is present four times within the BFDV LIR, as is the PCV hexamer within the PCV LIR, implying similar possible functionality (Bassami et al., 1998; Finsterbusch and Mankertz, 2009).

To troubleshoot and understand the implications of this inhibition process more, some appreciation of the relative strength of the native BFDV LIR promoter for *rep* needed to be investigated. To this end, the RCR- Luc (ΔSV40) vector was created (Figure 2.3). Using this approach, I was able to test the strength of the native *rep* promoter by performing luciferase assays and comparing these directly with the SV40 promoter in the pGL4.13 vector. These experiments demonstrated that the BFDV LIR promoter is approximately 3.8% as powerful as the well-described SV40 promoter in HEK-293T cells (Figure 2.12). This knowledge, and a more evolutionary understanding of the reasons why these inhibition systems exist, helped inform future vector design decisions for this technology.

Further development and testing demonstrated a 100-fold improvement in luciferase expression from the new fully self-replicating RCR+ Luc(F) vector, where *rep* expression, driven by its native promoter, was compared with the RCR- Luc(F) vector, where Rep was introduced *in trans*. This improvement was demonstrated and verified in three mammalian cells lines tested (Figures 2.13 & 2.14). It also helped verify and confirm the high efficiency of the complex Rep-directed self-inhibition process.

Based on the newly developed understanding of the action of Rep from experimentation and its inhibitory role inside cells explored in the literature, a new set of RCR+ Luc(R) and RCR- Luc(R) expression vectors were designed and developed for testing. This time, the SV40 promoter and the gene of interest were placed on the antisense strand of DNA to *rep,* in the reverse orientation in the location of the BFDV capsid protein (Figure 2.3 & 2.15). Viral capsid proteins are typically the most expressed viral proteins for any virus, for the obvious reason that they need to encapsulate the genome. This follows the well-known mathematics of surface area to volume ratio, which when applied to viruses, becomes a relevant formula for capsid protein expression levels (Harris and Theriot, 2018). Placing the antigen of interest here helps it avoid Rep-associated inhibition mechanisms while potentially also benefiting from the native viral capsid promoter, as discussed in Appendix A.

Excluding the BFDV capsid protein raised some further considerations, as it may serve to increase RCR amplicon concentrations in cell nuclei because the BFDV Cp is believed to manage nuclear DNA export. The capsid protein may also facilitate the nuclear import of Rep (Heath et al., 2006). Without capsid protein assistance, though Rep, at a size of ~34 kDa, is still sufficiently small to actively diffuse into the nucleus via the nuclear pore complex (Bassami et al., 1998; Niagro et al., 1998). Nuclear pore complexes readily allow proteins up to 60 kDa to freely diffuse through them; in fact, proteins as large as 110 kDa have been shown to be able to diffuse into the nucleus (Wang and Brattain, 2007). That said, without assistance, Rep may become more randomly and evenly distributed in the cell throughout the cytoplasm and nucleus. This change may affect the rate RCR occurring, and thereby the speed at which gene copy numbers increase.

To investigate the expression characteristics of these new designs, luciferase assays were performed in HEK-293T cells and HeLa S3 cells. These assays indicated that the inhibition effects seen previously by Rep were virtually absent in the HeLa S3 cells, but were still present, albeit to a far lesser degree, in HEK-293T cells (Figure 2.16). This conundrum could be explained by the fact that HEK-293T cells have been genetically modified to improve transfection and gene expression in tissue culture. The modification, introduced in HEK0293T cells, was the addition of the simian vacuolating virus 40 (SV40) large T-antigen gene sequence, encoding a protein that plays a variety of roles that cause these improvements. This antigen also contains recognition and binding sites for the SV40 origin of replication, a DNA sequence present in the SV40 promoter sequence. This antigen is heavily involved in replication of the SV40 virus, and its activity, in this respect, is exploited in HEK-293T cells to enhance DNA transfection and gene expression, and to allow replication of plasmids containing the SV40 origin of replication sequence (ori) (Boshart et al., 1985; Jacobsen et al., 2009; Palmer and Rybicki, 1998; Walther and Stein, 2009).

Given that the experimental aim was the investigation of RCR, the mere possibility of having different replication system components in play was undesirable. Accordingly, all further testing of this novel self-replicating DNA expression technology was conducted in HeLa S3 cells.

More extensive and comprehensive luciferase assays, conducted with the new vectors, further reproduced and demonstrated that the inhibitory effects of Rep were not present in transfections using the new RCR+ Luc(R) vector, as compared to the RCR+ Luc(R) vector across a controlled series of transfection concentrations (Figure 2.17). This experiment was optimised to investigate the full effective transfection range and resulted in a convincing S-curve of luciferase expression activity which demonstrated a high degree of linear improvement in expression over the 300-1200 ng range for both the RCR+ and RCR- Luc(R) vectors, which then levelled out for transfections >1200 ng (Figure 2.17).

Finally, a set of transfections to test luciferase expression, from the new vectors over an extended time frame, were set up and luciferase assays run. These experiments conducted after one passage and grown to allow for evaluation at 96 h and 120 h pt, demonstrated clearly that in the long term, the RCR+ Luc(R) vector was expressing approximately double the amount of luciferase at 96 h and 120 h pt than the RCR- Luc(R) vector.

This concluded the design stage for developing this technology. With the vector design finalized, four new plasmid vectors, using the same design, were designed and developed to allow for further testing and characterizing of the developed RCR self-replicating DNA gene expression technology. These vectors included RCR+ and RCR- versions using eGFP as an alternative reporter gene and the HIV-1C Gag mosaic gene as a model T-cell antigen for vaccine immunogenicity investigation (Figure 2.19 & Appendix A5).

3. Characterization and quantification of RCR gene expression technology

3.1 Introduction

A key goal in developing this DNA expression technology was to demonstrate its potential use as an enhanced DNA vaccine vector. To achieve this objective, it was necessary to assess its performance in amplifying gene expression, ideally from low initial inoculation starting levels that could be considered partially representative of real-world DNA vaccine uptake levels *in vivo*. This is because DNA vaccines in general, and specifically in large animals or humans, are known to have inefficient delivery to target cell nuclei (Wahren and Liu, 2014; Yi et al., 2018). This low uptake and delivery to target cell nuclei presents one of the biggest challenges facing DNA vaccine research and development. Various methods are employed to compensate for this, such as using highly efficient DNA promoters and optimised delivery methods, or enhancing immunogenicity of the DNA by including a high concentration of CpG motifs on the DNA and adding various adjuvants or expressing genes that can enhance immunogenicity. None of these options have, however, proven to be particularly effective at improving the typically weak immunogenic responses obtained by DNA vaccines in large animal models and humans (Ferraro et al., 2011; Hasson et al., 2015; Li et al., 2012; Modra, 2015; Williams, 2013; Yi et al., 2018).

The ability of this new vector to replicate itself and to amplify its effects offers a real opportunity to rectify and address this crucial problem and other issues faced by DNA vaccines. It was therefore important to devise suitable tests for this technology, such as to test (in tissue culture) inefficient DNA delivery to the target cells. In contrast to the inefficient DNA delivery observed in humans and large animal models, in tissue culture, DNA uptake via transfection methods and the resulting gene expression is not problematic in most transfectable cell lines (Modra, 2015; Patil et al., 2005). In tissue culture, high efficiency transfection reagents, like X-tremeGENE™ Hp (Roche), are able to transfect plasmid DNA very effectively into the highly exposed monolayer of cells found in a cell culture plate. Efficacy seen in cell culture, however, does not translate into detectable improvements in DNA uptake for real world DNA vaccines unfortunately. For this reason, these types of transfection reagents are not used to adjuvant DNA vaccines (Dupuis et al., 2000; Rose et al., 2015; Yi et al., 2018).

To better understand the problems associated with conventional DNA vaccines, one must consider the environment in which they function. A cell maintains homeostasis and balance through a myriad of incredibly complex, not yet fully understood, ways. These include many biochemical feedback loops, chemical signalling pathways, and reactions involving a multitude of chemically active molecules, enzyme catalysts and cellular proteins and structures (Nielsen and Keasling, 2016; Yuan et al., 2016). A cell, as an active living system, uses external energy sources and fuel with a high active turnover rate

of these compounds, to stay ahead of entropy and respond to different stimuli in order to maintain this state of homeostasis and balance we call life. The ability of cellular life to maintain this balance , and the robustness in which it does this, is truly a wonder of life. The capacity of living systems to adapt and self-correct to a state of homeostatic equilibrium bears careful consideration and appreciation (Nielsen and Keasling, 2016; Richardson and Ponka, 1997; Smirnova et al., 2015).

Arguably, it is this same self-correcting nature of the biochemical systems that maintain homeostasis and grant cells broad resilience to a wide variety of adverse conditions necessary for life to exist that is the true nemesis of conventional non-replicating DNA vaccines. This is because having an inherent tolerance to entropy and cellular disruption, while maintaining a high molecular turnover rate, serves to minimise the desired immunological effects of conventional DNA vaccines (Dupuis et al., 2000; Smirnova et al., 2015). This is because a conventional DNA vaccine remains an inactive entity within a highly active intracellular world that is highly capable of maintaining and restoring itself through many kinds of adverse disrupting scenarios and conditions. This kind of resilience comes with a level of immunogenic tolerance inherent to the nature of such a system and developed through evolutionary processes that enable cellular life to exist and thrive (Chen et al., 2013; Giglia-Mari et al., 2011; Leitner et al., 2003; Pennock et al., 2013; Schluns et al., 2000). Conventional DNA vaccines, which have no positive feedback mechanisms available to them or typically any feedback systems at all – -therefore exist at the mercy of these highly active cellular systems, operating around them within the nucleus (within the confines and rules of these cellular systems, without any dynamic edge) (Pennock et al., 2013). When a conventional DNA vaccine starts to express a viral antigen, it fails to fully recapitulate the pathogenic nature of a virus. Without being active in some sense (to drive its own maintenance, survival and dominance) it would be unable to present as a true pathogenic threat, nor represent virality.

Simply transcribing a gene or antigen in the dynamic swarm of biochemical activity occurring inside a living cell, an inanimate vaccine element, like a non-replicative DNA expression vector, is vulnerable to the devastating effects of entropy within the confined environment that is a cell. As unlike a cell, which can defy its local entropy as it is supported by it host organism. The DNA expression vector has no such support and therefore no ability to maintain or protect its existence and activity. As such a small naked plasmid with a single gene and promoter stands little chance of being able to alter the equilibrium of a living cell which is actively maintained. As the cells high molecular turnover continually drives the biochemical momentum of life towards a state of health, while its own innate defence mechanisms seek to actively shut down, degrade or silence the exposed plasmid. In this sense it is unsurprising that DNA vaccines often exhibit limited effectiveness. To truly generate and maintain an elevated level of antigen expression required for a meaningful long lived and effective, T-cell immune response, DNA vaccines need to gain an edge within this complex environment. This is why animate vaccine systems, such as live attenuated vaccines are notably more successful than inanimate and synthetic vaccine technologies such as non-replicating DNA vaccines, soluble proteins or inactivated viruses (Burgers et al., 2009;

Collins et al., 2017; Cosma and Eisenlohr, 2018; Hu and Sun, 2016; Luo et al., 2016; Nordström et al., 2005; Pennock et al., 2013; Smirnova et al., 2015; Wells et al., 1997).

In this sense, a non-replicating DNA vaccine will never be as capable at stimulating an immunogenic response or sustaining an elevated level of expression as a replicating vaccine can be. Without any ability to adapt and change within an adapting and hostile environment, non-replicating DNA vectors exist at the mercy and control of the cellular system in which they reside. The replicating DNA expression technology being developed here, however, is capable of manipulating and breaking the rules that govern and maintain the order and dominance of that system, significantly disrupting its ability to maintain homeostasis. A key part of that governance is maintaining the cells' safety from the immune system, which is performed by an incredibly complex set of immune tolerance inducing mechanisms and pathways that need to be actively maintained. These systems are an integral part of the immune system and present in all complex multicellular life (Pennock et al., 2013). The RCR DNA in this scenario is more like a virus as it carries with it an innate characteristic of viral life, a viral like amplification of genomic material and gene expression. Like a virus, the RCR DNA expression system can therefore also overwhelm the delicate balance maintained by the biochemical systems within its host cell.. As such, a replicating DNA vaccine, driven by this viral replication and gene expression amplification processes, is far better suited to antagonise and stimulate the kind of immunogenic actions from the hosts innate and adaptive immune system components. This should help activate the desired T-cell type of immunity, better than a conventional DNA vaccine can.

We know from the literature that live vaccines are more highly immunogenic than inactivated ones (Burton, 2017; Gilbert, 2012; Keller-Stanislawski et al., 2014; Kollaritsch and Rendi-Wagner, 2013). This appears to be because, the better a vaccine can mimic the active nature of the disease it is designed to inoculate against (arguably for the same reasons discussed above), the bigger the cellular disruption, and stronger the immune response. It is reasonable to assume that the replicating DNA expression technology can similarly create stronger levels of more cellular disruption to generate improvements in immune responses and advance DNA vaccine research and development approaches.

While the replication of live viral vaccines is often discussed as a major safety topic in virology (Li et al., 2012), in this case it is important to point out that the replicating RCR DNA gene expression technology does not replicate in the same sense as a virus, because, unlike a virus, the vector cannot infect new cells. Without an ability to spread within the body, its replication process is better viewed as a replication-induced genetic self-suicide process, rather than a viral life cycle. Furthermore, DNA is readily destroyed in the body when it is outside a cell's nucleus (Patil et al., 2005; Sasaki and Kinjo, 2010; Wells et al., 1997; Williams, 2013; Wolff et al., 1990).

The second theoretical activity of a self-replicating DNA expression system, like the one developed, is that the process of DNA replication via RCR itself should be capable of stimulating unique

immunogenic and biochemical responses from host cells that non-replicating DNA expression systems cannot. This postulated activity is based on the possible interactions with immediate products of DNA replication, which should trigger responses from known DNA damage detection and intranuclear pathogen recognition receptors such as cGAS/STING, IFI16 and TLR9, among others (Chen et al., 2013; Diner et al., 2015; Knipe, 2015). These should, in theory, give the replicating DNA technology greater capacity to stimulate DAMPs and PAMPs, conferring adjuvant-like effects by increasing the sheer abundance of vector DNA within a cell and creating a high concentration of pathogenic DNA full of immunogenic, CpG motifs, for the PRRs to detect. As well as creating various unique intermediate ssDNA and nicked dsDNA species that develop during RCR. This includes unique stem loop structures, which are believed to also be highly immunogenic and detectable by various DNA damage and pathogen recognition receptors (Campisi, 2014; Cheung, 2015, 2012; Diner et al., 2015; Giglia-Mari et al., 2011; Illingworth and Bird, 2009; Paludan and Bowie, 2013). This, at the very least, should enhance PRR binding and increase cellular biochemical signalling in response to higher DNA presence. Furthermore, these kinds of changes are known to alter cellular metabolic processes in a manner that is associated with enhanced immunogenic response gene upregulation and innate immune response activation (Campisi, 2014; Hasson et al., 2015; Kobiyama et al., 2013a; Scheller et al., 2002). Identifying and characterising the type and magnitude of the internal cellular response generated in affected cells is a vastly complex and difficult task. To do this, affected cells were inspected in terms of their more basic characteristics, such as size, morphology, growth rate and internal cellular structures. That these changes can potentially be inspected using microscopy, offers a valuable window into identifying the occurrence of possible complex internal cellular changes, which in turn may indicate significant and highly influential changes in gene signalling patterns within affected cells (Cardis et al., 2017). Microscopy was therefore an area of high interest when performing tissue culture testing of this technology, as such changes are expected to occur during antiviral response gene activation.

The primary aims for this chapter were to test, demonstrate and characterise the expression capabilities and profile of the vector system, to determine if any observable cellular and metabolic effects were being induced, and to try to ascertain the extent of such effects. The objective was to look for evidence that the vector system was achieving any of its theoretical capabilities that could help it counteract or mitigate some of the critical issues faced by current DNA vaccines. Demonstrating an improvement in gene expression over time was therefore also an important goal, as was investigating the shape and rate of expression changes and how these correspond with any cellular changes, was also a key area of interest for experimental investigation. The use of relevant non-replicating negative controls was important, as were highly optimised transfection procedures to ensure a high degree of reproducibility. Accordingly, a non-replicating control that was essentially identical (aside from a 2 bp mutation in the start codon of *Rep)* was created and used for comparative purposes for all replicating vectors designed and developed. This ensured a high degree of consistency over all transfection experiments, as did the

use of experimentally tested and verified highly supercoiled >95% DNA, which is known to promote consistent and efficient cell transfections (Sousa et al., 2009).

After finalizing the vector designs and obtaining the highest possible quality of >95% supercoiled DNA for each of the described vectors (Appendix A), a series of detailed and sensitive characterization experiments were set up to investigate and test the characteristics and attributes of the vector system using the new reporter gene eGFP and a HIV-1C Gag mosaic "gene of interest". These experiments were designed with the aim of validating and qualifying the system's use as an enhanced vaccine candidate in animal experiments using the murine Balb/cJ animal model (Bennett and Chopra, 1993; Saade and Petrovsky, 2012).

Consideration of the data generated thus far meant that only HeLa S3 cells were selected for further detailed characterization experiments. While these cells are transfected less efficiently than HEK-293T cells, for example, they were deemed to potentially better reflect real-world DNA vaccine expression and uptake levels that might be expected *in vivo* in Balb/cJ mice. HeLa S3 cells are epithelial in origin and were derived from cancerous cervical tissue. Epithelial tissues are believed to play important immunological roles and are considered good targets for vaccine inoculations (Dupuis et al., 2000; Wolff et al., 1990). Finally, HEK-293T cells have been artificially genetically modified to incorporate the SV40 large T-antigen, a DNA helicase that binds to the viral replication origin and replication forks, and plays a variety of other roles affecting gene expression (Ahuja et al., 2005; DiMaio, 2019). For these reasons it was deemed to be highly likely to interfere with the functionality of RCR DNA replication in HEK-293T cells, when using plasmids that contain the origin of replication sequence of SV40, which is present in the SV40 enhancer/promoter used to drive expression of our gene of interest.

3.2 Materials and methods

3.2.1 Conventional Microscopy

Tissue cultured cells, transfected using fluorescent vectors were regularly inspected and imaged in tissue culture plates using a conventional (ZEISS, Germany) Axio Vert.A1 inverted microscope with 5x, 10x, 20x and 40x objective lenses, equipped with a ZEISS HBO 50 halogen lighting system and a ZEISS Axiocam ICm1 camera. When images were taken, exposure settings were adjusted so that the brightest positive sample was set to be within the camera's sensitivity range. These settings were then saved and used for all subsequent imaging to ensure that accurate and comparable image data was collected.

3.2.2 Flow cytometry and FACS

Flow cytometry with fluorescence activated cell sorting (FACS) was used to sort, count and quantify fluorescence and cellular morphology of HeLa S3. For these experiments, transfections were performed using standard transfection protocols, then centrifuged (500 x g; 5 min), resuspended in PBS and passed through a 70 µM sieve. Flow cytometry was done on a Becton Dickinson FACS Aria flow cytometer using a 100 µm nozzle and blue laser light at 488 nm for eGFP excitation. Data was collected using the BD FACS Diva software v6.0 and subsequent analysis done in FlowJo v10.5.0 under the free license for Africa. The cell populations were identified and gated on a forward scatter (FSC) vs. side scatter (SSC) dot plot, using a linear scale, in acquisition mode. The negative control was used to set photo multiplier tube (PMT) voltages as well as instrument optimization. BD Cytometer Setup and Tracking Beads were used for calibration and standardization of the instrument. GFP containing cells were analysed in the FITC channel. A threshold of 5000 on the FSC channels was set to remove sample debris. Cells that fit established criteria were sorted for further investigation. Calibration and gating parameters were captured (see Appendix C).

For flow cytometry, 50,000 cells were analysed in each experimental run and data was recorded for the metrics of SSC-A, FSC-A and eGFP fluorescence. Initial experiments were used to inform the calibration parameters for subsequent flow cytometry experiments where HeLa S3 cells transfected with RCR+ and RCR- eGFP expression plasmids were analysed at 24 h, 48 h and 96 h pt. Cell gating, selection and analysis was performed using FlowJo v10.5.0 (Appendix C).

3.2.3 Confocal microscopy of transfected HeLa S3 cells

Confocal microscopy was performed in four well chamber slides and pre-treated (5 min; 0.03% poly-L-lysine in PBS). Transfections were performed using standard protocols. At 24 h or 48 h pt the media was carefully aspirated with a 1 ml pipette. Cells were fixed (~100 µl, 4% paraformaldehyde, 5 min). Then washed three times with PBS and stained with (Hoechst 33342 (10 mg/ml); 1:5000 in PBS for 30

sec). After three more PBS washes, the well chambers were removed and ~ 20 µl Mowiol with ~20 mg/ml n-propyl gallate, with a cover slide was applied and dried overnight at room temperature (RT) then stored at 4° C until imaged, making use of a ZEISS LSM 880 with Airyscan (ZEISS, Germany) inverted confocal microscope, equipped with an argon laser, providing light at 488 nm for eGFP fluorescence and 405 nm for Hoechst stains. The system made use of a high sensitivity photomultiplier tube imager that was calibrated against the brightest positive fluorescent sample to prevent sensor overexposure. Calibrated image settings were saved and applied for all subsequent images collected, to ensure accurate and comparable data collection. Images were captured as a series of Z-stacks and merged into a maximum intensity projection. This allowed for quantification of fluorescence intensity using the ZEISS Zen Blue 2.5 software suite. Cells positive for fluorescence were identified using the merged channels image data and (independently) carefully outlined using the spline contour tool, E.g. (Figure 3.1). Thereafter, the Zen Blue software was used to calculate the mean level of eGFP fluorescence per positively-identified cell. The software also calculated the total surface area of each selected cell (Carl Zeiss Microscopy, 2015, 2013; Cruz, 2016; Gray et al., n.d.).

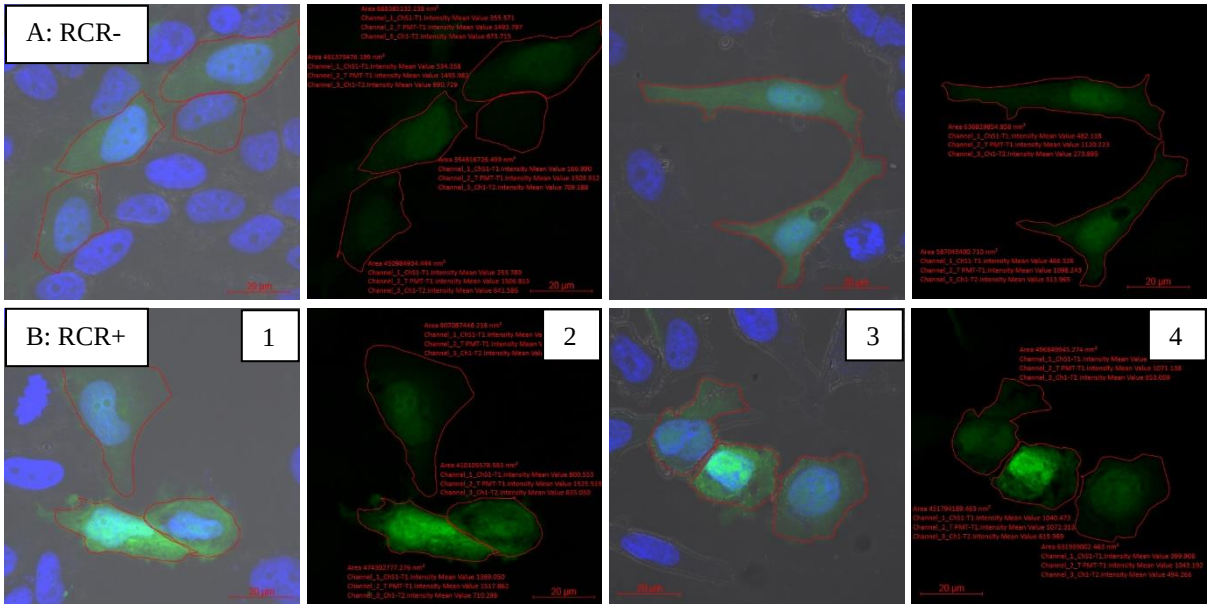

Figure 3.1: Quantification of eGFP expression in HeLa S3 cells using confocal microscopy. A) RCR- eGFP transfected cells. B) RCR+ eGFP transfected cells. Images from left to right 1) merged channels 24 h; 2) eGFP 24 h; 3) merged channels 48 h; 4) eGFP 48 h.

3.2.4 Western blot for HIV-1C Gag

Transfected cells in 6 well TC plates were lysed with 200 µl Glolysis buffer (Promega) 48-96 h pt and in the presence of protease inhibitors. Cell lysate was centrifuged at 10,000 x g for 5 min and the supernatant collected. For each lane (28 µl sample; 2 µl XT reducing agent (BioRad), 10 µl loading

dye was combined, boiled for 5 min, and loaded on an 8% or 12% sodium dodecyl sulphate polyacrylamide gel electrophoresis (SDS-PAGE) gel with 4% stacking gel and electrophoresed (200V, 45 min). Thereafter, it was transferred onto a polyvinylidene fluoride (PVDF) membrane (25V, 1 h) using transfer buffer (25 mM Tris; 190 mM glycine; 20% methanol). Blocking was performed in (2% BSA; PBS; 0.1% Tween-100, 1 h). A goat anti-human p24 (BioRad #4999-9007) at 1/1000 dilution in blocking solution was used as primary antibody, overnight, and mouse anti-goat secondary conjugated to alkaline phosphatase, 1 h were used with NBT/BCIR (BioRad) to develop the bands. Densitometry analysis of the bands was performed in image lab 5.2.1 using the same HIV-1C Gag mosaic gene expressed in MVA as a positive control, and as the reference band required for densitometry.

3.3 Results

To characterise and quantify the effects RCR has on gene expression, the newly developed RCR+ and RCR- eGFP DNA vectors were used to investigate the effects of RCR at the individual cellular level. Evaluation of overall cellular health and morphology was also investigated.

3.3.1 Investigating expression with eGFP vectors

Initial transfections, using RCR+ and RCR- vector variants containing an eGFP reporter, revealed that the replicating RCR+ vector clearly expressed more eGFP than its non-replicating RCR- counterpart. This was true at 24 h, 48 h and 96 h pt (Figure 3.2) where the overall fluorescence was notably higher for RCR+ vs RCR- transfected cells. In addition to this, there appeared to be a noticeably higher number of super bright cells in the RCR+ transfected samples, compared to the RCR- samples, particularly so at the later time points. The cell morphology of the RCR+ cells also appears to be different again particularly so for the most fluorescent cells. These appear to be slightly larger to the naked eye and were more frequently observed with rounded up cellular morphology, and diffusely distributed on the culture plate (Figure 3.2). Transfected cell count appeared mostly identical at 24 h pt but even at 48 h and certainly at 96 h pt the total number of fluorescent cells appeared to be greater for the RCR- transfections. Being less bright, this was not immediately apparent but, under higher magnification, it was easier to discern (Figure 3.2).

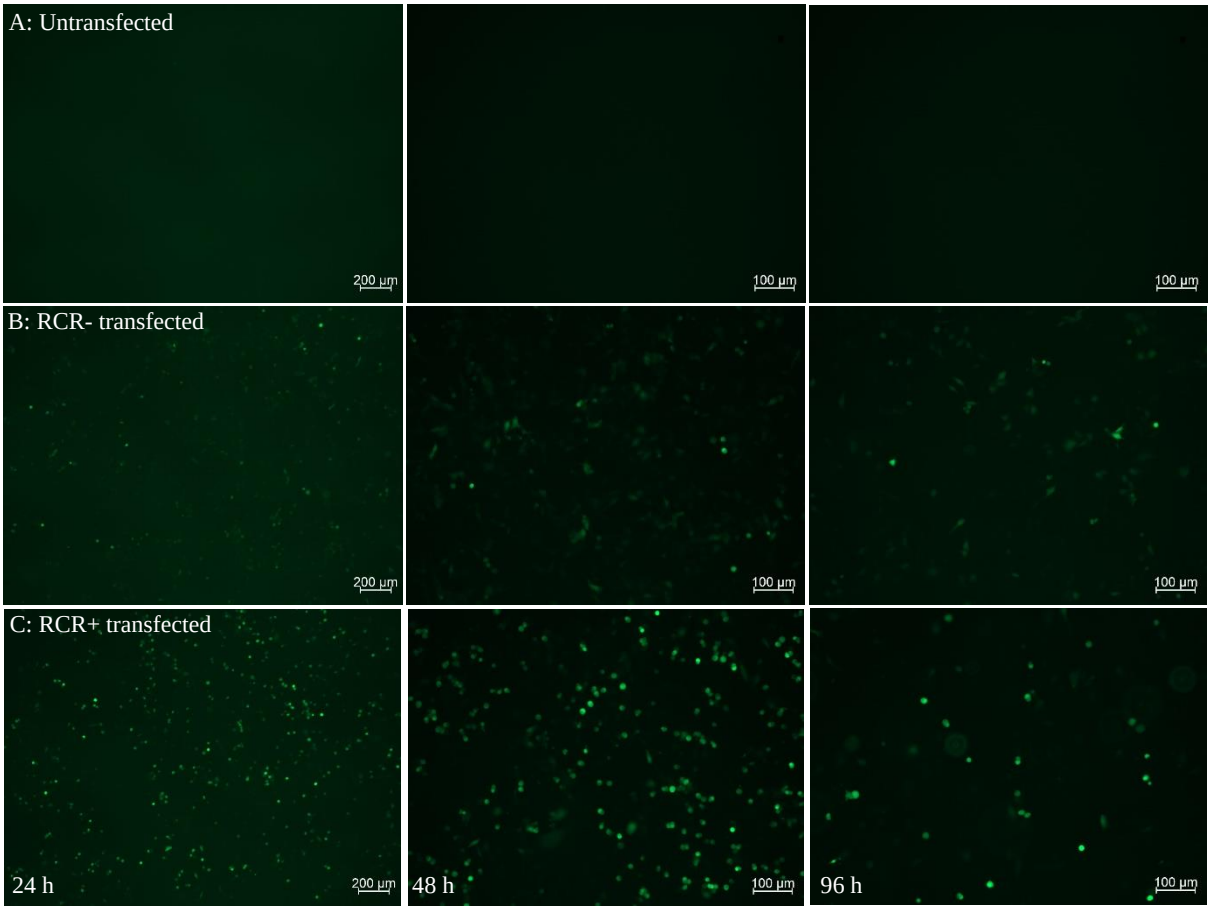

Figure 3.2: Inverted fluorescence microscopy of HeLa S3 cells taken at 24 h, 48 h and 96 h post transfection (pt). Cells were either A) untransfected, or transfected with B) RCR- eGFP, or C) RCR+ eGFP vectors.

3.3.2 Flow cytometry (FACS) of transfected HeLa S3 cells

Flow cytometry experiments were set up to evaluate the expression profile and cellular characteristics 24 h, 48 h and 96 h pt using HeLa S3 cells transfected with the RCR+ and RCR- eGFP variant expression vectors (Appendix A4).

Pseudoplots drawn from the analysis of 50,000 HeLa S3 cells are depicted in Figure 3.3. To aid analysis, the fluorescent Q2 quadrant was gated at the 500 fluorescence units mark to eliminate untransfected cells and cellular auto fluorescence. On analysing this population, it became apparent that there is very little difference between RCR+ and RCR- eGFP vectors at 24 h pt (when considering that the Q2 population represents only ~2.1% of cells analysed in both samples. It is also noted here however, that at this early time point the flow cytometry system has a limited ability to separate the eGFP signal from cellular auto fluorescence, as was evident in comparisons with the negative controls and the gates set in Figure 3.3. By 48 h, however, the fluorescent positive Q2 population of the RCR- eGFP sample represented 10.4% of the total evaluated cells, while the RCR+ eGFP sample represented only 8.8% of its population at this time (thus representing a divergence in the relative percentage of the Q2 eGFP

positive population between these samples). This divergence becomes notably more prominent at 96 h pt, where Q2 population of the RCR- eGFP sample makes up 18.3% of the total evaluated cells while the Q2 of the RCR+ eGFP sample represents just 9.5% of its total.

This divergence in the total Q2 positive population appears to be accompanied by an overall increase in cellular granularity (SSC-A) for the RCR+ eGFP sample, which also appears to correlate with eGFP fluorescence intensity. This has not been observed in the RCR- samples. It is also noted that the transfection efficiency between the RCR+ and RCR- eGFP vectors was tested (data not shown) and was highly consistent. This was as expected because these vectors are identical in both size and bp sequence, only differing by a few bp where the start codon of *rep* was mutated.

At 96 h, the Q3 population also becomes divergent between RCR+ and RCR- samples, especially relative to its corresponding Q2 population. The Q3 cell population represents cells with low cellular granularity (SSC-A) that are budding or have recently divided and are also fluorescent positive. While still a relatively small portion of the overall cells, this population appears to be three times greater for the RCR+ transfected cells at 96 h pt than the RCR- transfected cells.

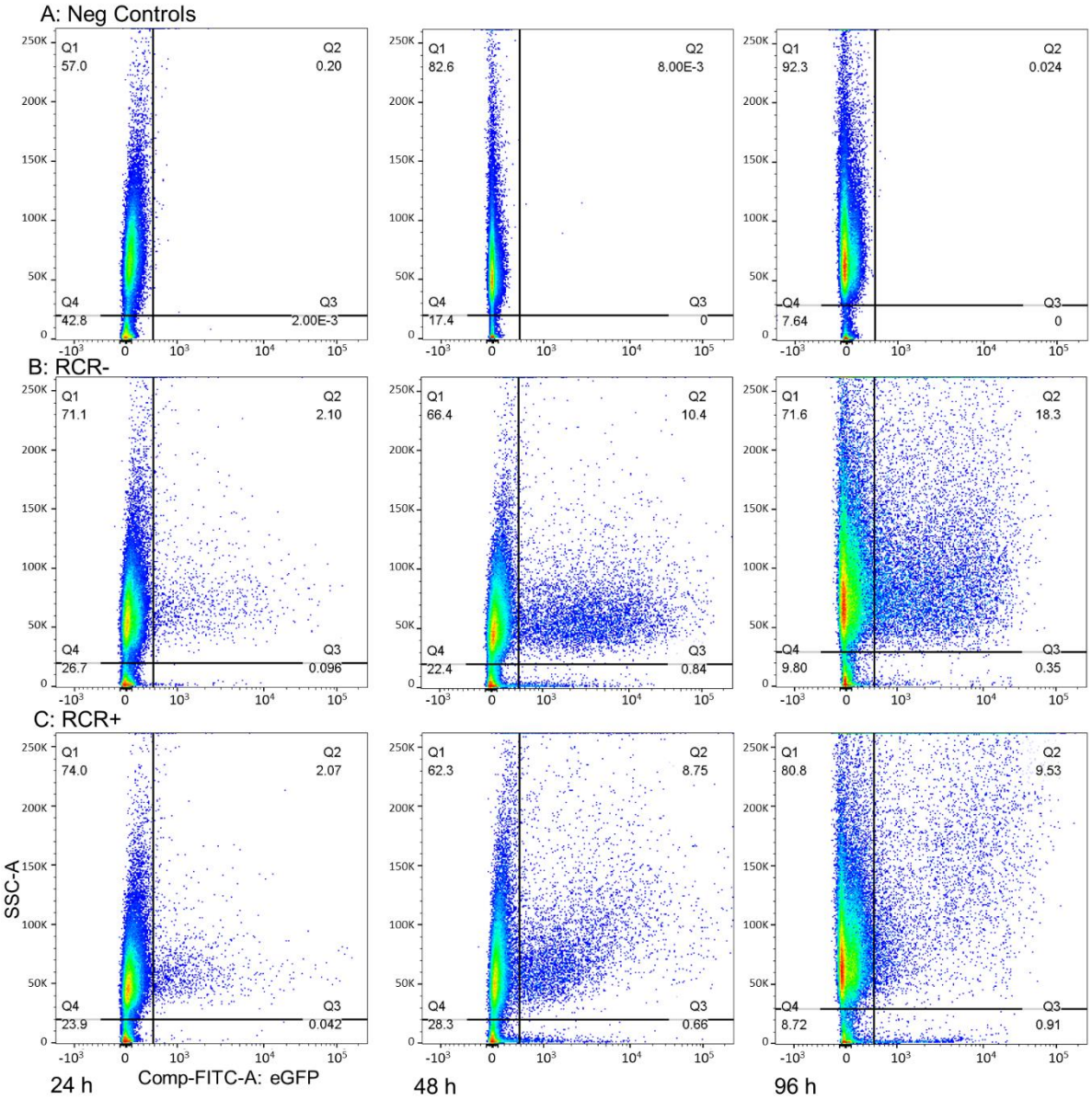

Figure 3.3: Flow cytometry data from 50,000 HeLa S3 cells depicted as Pseudoplots of side scatter area (SSC-A) versus eGFP fluorescence. (A) Negative control, (B) RCR- eGFP, (C) RCR+ eGFP samples evaluated at, 24 h, 48 h and 96 h, post transfection. Bold lines depict gating parameters with the percentage of cells in each quadrant is shown under quadrant descriptor (Q1-4).

To evaluate the nature of the differences between the RCR+ and RCR- transfected cells, data was gathered from flow cytometry for the Q2 fluorescent positive populations (Figure 3.3) and depicted as a series of sets of histograms for analysis (Figures 3.4-3.6). These data sets included (FITC-A:GFP), indicating the cellular eGFP fluorescence intensity (Figure 3.4), side scatter analysis (SSC-A), indicating the internal cellular granularity of the fluorescent positive cells (Figure 3.5) and the forward scatter analysis (FSC-A), indicating their cellular size (Figure 3.6).

At 24 h pt, the eGFP fluorescent intensity distribution of the RCR+ sample differs only slightly from that of RCR- sample. This difference is outlined in purple rectangle, where one can see the relative area

of the histogram under the curve within the outlined region, is larger for the RCR+ sample, than it is for the RCR- sample. Below 500 units of fluorescence, the cells' eGFP fluorescence was indistinguishable from cellular autofluorescence, as illustrated by the gating parameters set against the negative controls (Figure 3.3). At 48 h pt it appears that the left tail of a bell curve distribution developed for the RCR- eGFP sample (purple circle), which is not present for the RCR+ sample. By 96 h pt the distribution still looks like the right side of a bell curve for the RCR- sample, but for the RCR+ sample it appears that the distribution curve itself has become reshaped, broadening and flattening out across the fluorescent intensity range and extending its right tail. This indicates that the absolute maximum level of eGFP expression has significantly increased (more than doubling). In addition, the total number of fluorescent cells, with fluorescence levels as high or higher than, the highest levels recorded in the non-replicating equivalent eGFP expression control vector, has substantially increased in relative terms compared to the rest of the fluorescent positive cell population. This population can be loosely defined as the relative population of fluorescent cells with fluorescent intensity levels > $1x10^4$ RFU, which have been demarcated with a purple line (Figure 3.4: 96 h). This shift in population is also indicative of the vector system performing as anticipated, which is to say that cells were expected to uptake the replicating vector in concentrations essentially identical to that of the non-replicating equivalent vector. Thereafter, however, as replication occurs, this uptake distribution was expected to change, skewing to the right as RCR increased relative gene copy numbers in the nuclei of affected cells. These data appear to agree with this prediction.

When looking at the SSC-A (cellular granularity) histogram distributions of the Q2 eGFP positive populations (Figure 3.5), one can see that, for the RCR- samples, the distribution shape remains consistent from 24 h to 48 h, with an upward shift and broadening of essentially the same distribution at 96 h. For the RCR+ sample, however, it appears a rightward shift and broadening occurs earlier on, at 48 h pt. By 96 h this broadening has dramatically altered the overall shape and character of histogram distribution of cellular granularity itself. It appears to have levelled out across the SSC-A range, dropping off in a linear manner, as opposed to the exponential one seen for the RCR- samples, which follow a more normal right-tailed distribution curve for the SSC-A data. A larger proportion of the fluorescent RCR+ Q2 population is made up of cells with a cellular granularity >150,000, indicating higher level of internal complexity and probably some interesting metabolic activity. To the extreme right on all the SSC-A histograms a spike is present; this represents readings that were above the sensitivity range and were therefore off the scale. Typically, this very high granularity population is of cells undergoing cellular division. Greater prominence of high levels of SSC-A in the RCR+ samples is likely indicative of slowed-down or otherwise hindered cellular maturation and metabolism during the S-phase of the cell cycle and longer duration of time spent in this phase.

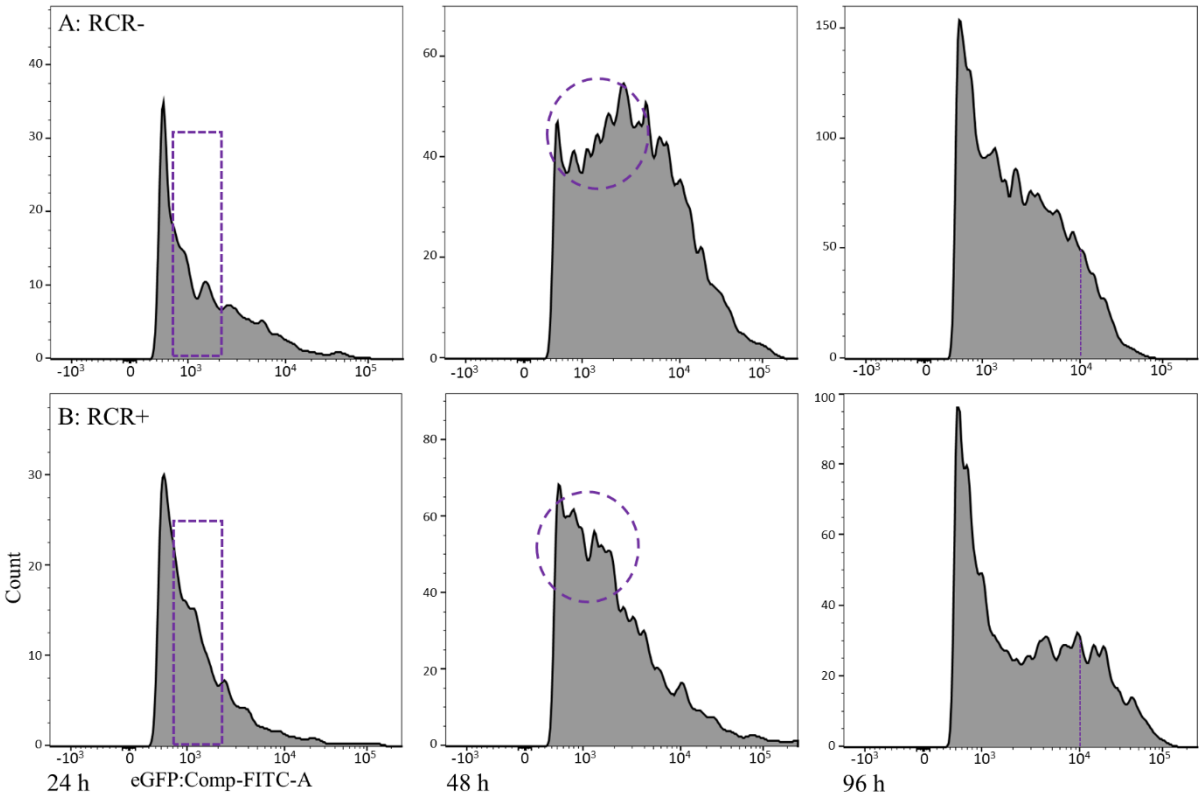

Figure 3.4: Histograms of eGFP intensity among fluorescent positive cell population (Q2). HeLa S3 cells transfected with the: A) RCR- eGFP and B) RCR+ eGFP expression vectors. Evaluated 24 h, 48 h and 96 h pt. RCR+ samples exhibit an upward shift in fluorescence <20000 units (rectangle) redefines the shape of the distribution curve at 24h, 48 h and 96h pt. By 96h pt the RCR+ sample distribution has a greater proportion of cells with fluorescence >10,000 units (line) extending the right tail of the overall distribution as compared to the RCR- sample.

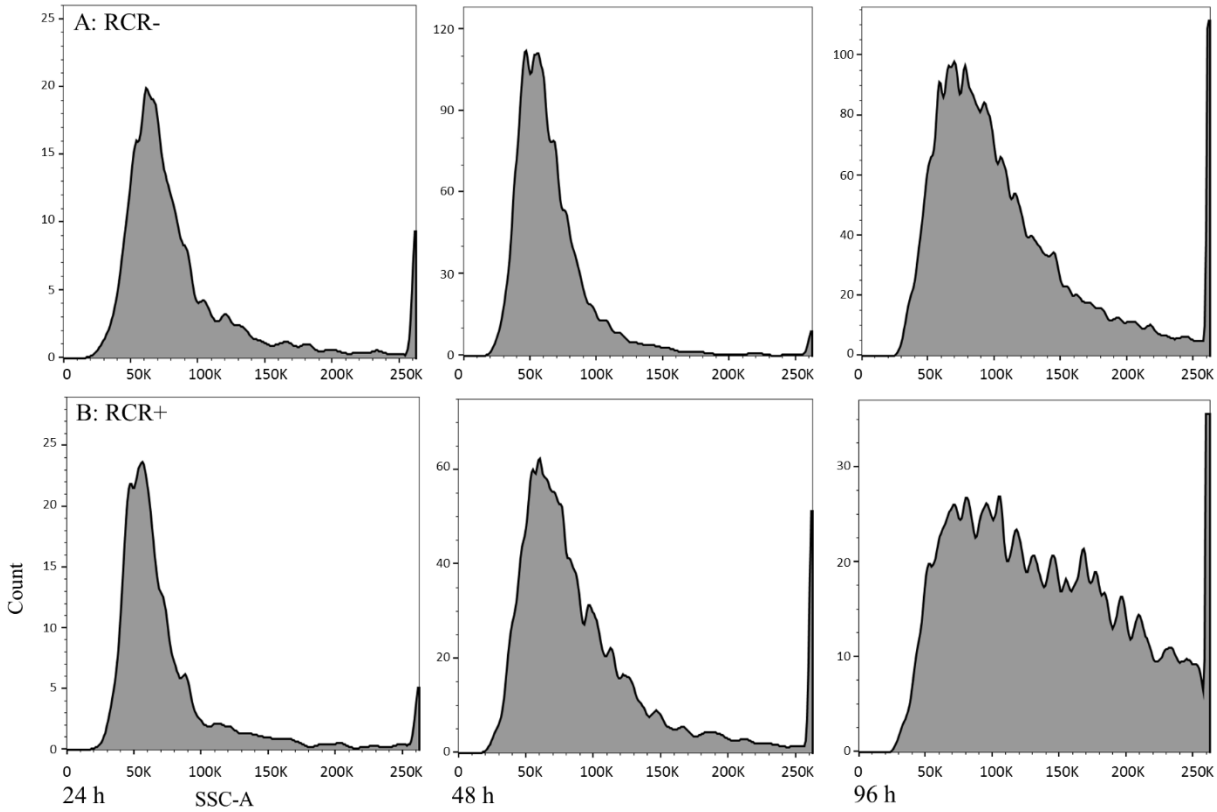

Figure 3.5: Histograms of side scatter area (SSC-A) depicting internal cellular granularity and complexity of the fluorescent positive Q2 population. Fluorescent positive HeLa S3 cells analysed 24 h, 48 h and 96 h pt as histograms depicting the SSC-A data from flow cytometry for A) RCR- eGFP; and B) RCR+ eGFP expression vectors. An increasing shift in internal cellular granularity with time pt is observed in RCR+ samples as compared to RCR- samples.

A detectable shift in the forward scatter area (FSC-A) was also seen in the RCR+ Q2 fluorescent population, as compared with the equivalent RCR- population, indicating that changes in cell size were occurring (Figure 3.6). While the change observed here was a subtler in comparison to the eGFP and SSC-A histograms, it was still significant ($p=0.024456$) at 48 h and more so at 96 h. Changes in the physical size of RCR+ transfected cells versus RCR- is a further demonstration of intriguing metabolic activity being induced in response to the replicating DNA expression technology. Early alteration in the cellular size distribution is evident at 24 h pt, where a significant change in average cellular size develops for the RCR+ eGFP sample, compared to the RCR- sample, with the peak of the distribution shifting towards the right (purple rectangles). At 48 h pt, the RCR- transfected cells appear to follow a normal distribution with a relatively small right skewed tail, whereas the RCR+ transfected population appears to be more heavily right skewed (purple rectangles). By 96 h pt, the RCR+ samples size distribution appears to be levelling out across the FSC-A range in a manner similar to that seen in the SSC-A histograms, with the median shifting towards the right (purple line). Methods of flow cytometry data analysis have been discussed in the literature (Adan et al., 2017; McLean et al., 2016; Soboleski et al., 2005; Tzur et al., 2011).

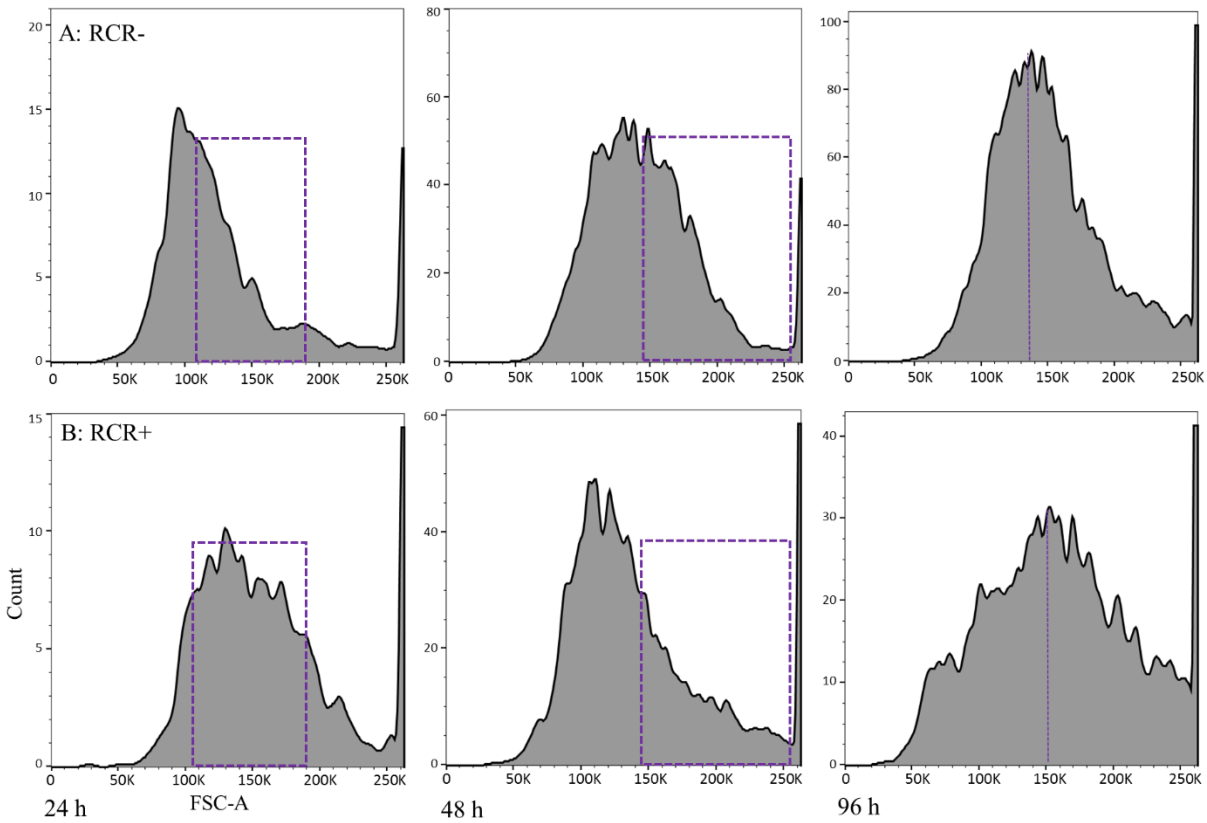

Figure 3.6: Forward scatter area (FSC-A) histograms indicating the distribution of cellular size among the transfected fluorescent Q2 population of HeLa S3 cells. Cells were transfected with A) RCR- eGFP; and B) RCR+ eGFP expression vectors and evaluated at 24 h, 48 h and 96 h pt. RCR+ transfected cells appear to have a size (FSC-A) distribution that has shifted upwards with clear change in mean cellular size seen 96h pt.

For all the above data sets, a variety of statistical metrics were also calculated for analysis and reference to aid in interpreting and understanding the nature of the differences depicted in the histograms. In addition to calculating these basic statistical metrics in FlowJo, an analysis of variance (ANOVA) was also performed between the RCR+ and RCR- samples for each data set (FSC-A, SSC-A and eGFP) at each time point recorded (24 h, 48 h and 96 h). This was used to show that these differences were significant, to demonstrate their divergent nature, and to gain information relating to the source of their statistical variances. All these statistical analyses strongly supported the divergent nature these samples demonstrated over time: at 24 h pt results were mostly similar, but by 48 h, were massively different across all three data sets, analysed with high degrees of significance. By 96 h pt, the level of significance was exponentially higher in all data sets with the highest level obtained for the eGFP data with $p= 4.42x10^{-77}$. The increasing F-scores in the different ANOVAs done over time also further confirms this trend.

3.3.3 Re-culturing of HeLa S3 cells post FACS

After collecting flow cytometry data from the transfected cells, fluorescent activated cell sorting (FACS) was set up to collect the healthiest eGFP positive population of the remaining sample for further cell culture. For this purpose, a new set of gating parameters were set to eliminate cellular debris, actively dividing cells, DNA autofluorescence and generally unhealthy cells. These parameters were set in the FACS Diva v6.1.3 software suite and are recorded in Appendix C. The abbreviated data from FACS is presented in Table 3.1.

Table 3.1: FACS performed 96 h pt on HeLa S3 cells transfected with the RCR- and RCR+ eGFP DNA expression vectors.

Sorting Parameters	**RCR- eGFP**	**RCR+ eGFP**
Total events	15,976,129	14,724,624
Left Sort	2,507,113	961,735
% Purity	79.2%	81.2%
% Sorted	**15.69%**	**6.53%**

To understand the long-term expression characteristics and survivability of the RCR- and RCR+ eGFP vectors in the HeLa S3 cells the fluorescent transfected cells were sorted using FACS and re-cultured in tissue culture for up to 11 days after their initial transfections. This included two passages after FACS. Microscopy imaging of these cells are presented in Figure 3.7.

After re-culturing, the brilliance of the eGFP fluorescence for the RCR+ eGFP transfected cells did not appear to decline by the 8 or 11 days pt, compared with the re-cultured RCR- transfected cells, which steadily lost fluorescence intensity from ~48 h pt (Figures 3.6). This was after the cells had gone through FACS and been passaged twice. Highly fluorescent cells exhibiting healthy cell morphology were still visible in the RCR+ eGFP sample after performing FACS, re-culturing them and passaging them twice over 11 days. At this point. the wild type HeLa S3 cells had outgrown and overcrowded both the RCR+ and RCR- eGFP transfected cells to a stage when further passaging was deemed futile. A pure population may well have been able to be cultured for longer; however, the growth rate of the RCR+ transfected cells was notably slower than RCR- transfected cells and much slower than wild type HeLa S3 cells. While the RCR+ transfected cells with extremely bright fluorescence did (in my estimation) exhibit more rounded morphology on average, there were still plenty more exhibiting healthy morphology throughout the experiment. In all transfections, some transfected cells do tend to round up, as do a portion of untransfected cells. The more prominent rounding up of the morphology, seen on the Day 11 images below, was due to cell confluence being reached.

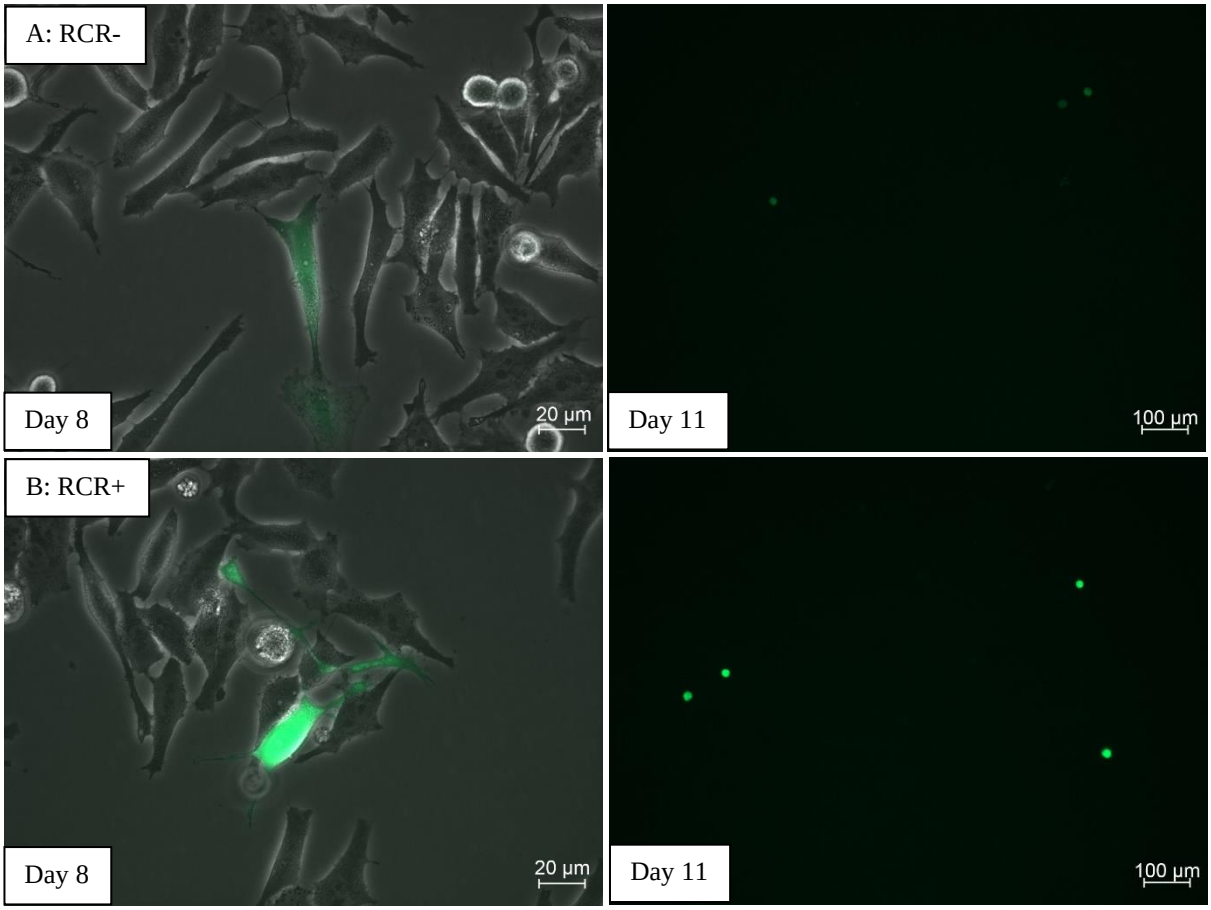

Figure 3.7: Time course evaluation of fluorescence from A) RCR- and B) RCR+ eGFP expression vectors in HeLa S3 cells. Left: Merged eGFP and transmitted light images taken at 8 days pt, at 400 x magnification, with cells still exhibiting healthy cell morphology. Right: eGFP fluorescent channel images taken at 11 days under at 100x magnification, showing most of the remaining fluorescent cells have rounded unhealthy cell morphology by this time.

3.3.4 Quantifying eGFP fluorescence with confocal microscopy

Due to the light sensitivity and separation capabilities of the confocal microscopy, this method proved to be a valuable tool for quantifying eGFP fluorescence. An example of an image of RCR+ and RCR- eGFP transfected HeLa S3 cells is presented in Figure 3.8 below in which the contours of the individual cell have been outlined for determining their total surface area and the mean fluorescent signal throughout the depth of each individual cell.

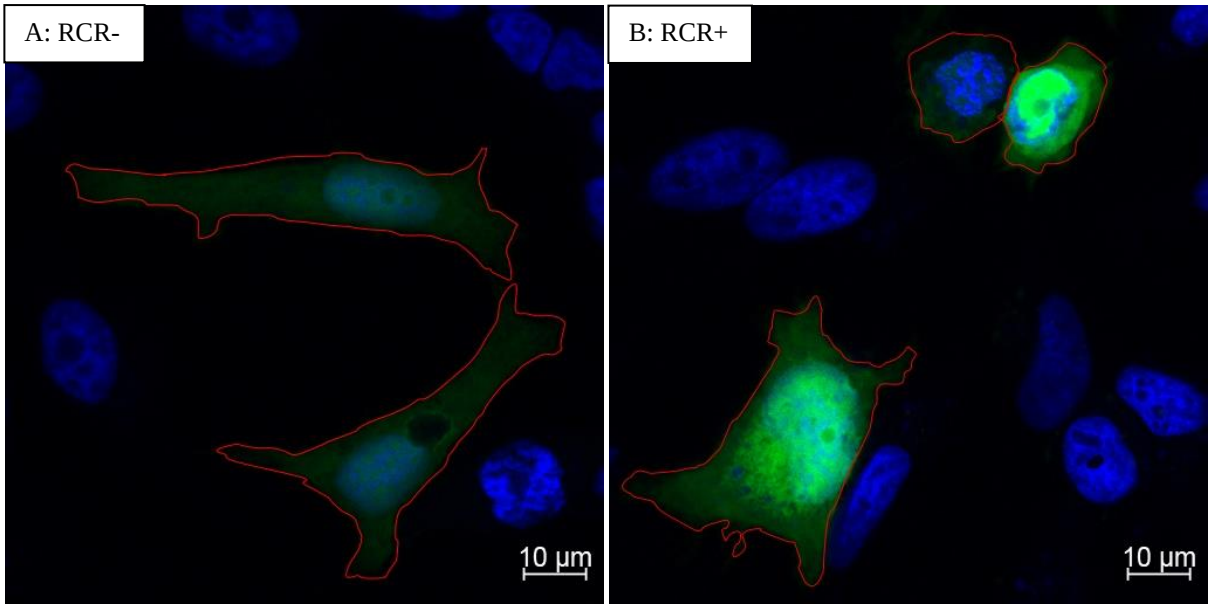

Figure 3.8: Confocal microscopy maximum intensity projection of HeLa S3 cells transfected with A) RCR- and B) RCR+ eGFP DNA expression vectors taken at 24 h pt. Spline contour mapping of fluorescent cells using Zeiss Zen Blue 3.1 software suite allowed for quantification of the significantly greater fluorescence observed in cells transfected with RCR+ eGFP vectors.

Using confocal microscopy allowed for earlier detection and quantification of the eGFP fluorescence signal which was not possible using flow cytometry. By measuring 100s of transfected cells individually for each sample, an overall histogram was constructed from maximum intensity projection contour-selected image data. This was then depicted as the relative percentage of cells analysed for each sample versus their mean fluorescence intensity over increments of 100 RFU across the range of possible fluorescent intensities detectable by the con-focal setup 24 h pt (Figure 3.9). This histogram generated, clearly depicts the upward shift in fluorescence intensities of the RCR+ eGFP samples versus the RCR- ones, and that this has occurred as early as 24 h pt. In this histogram, the eGFP fluorescent RCR- cells have over 60% of their total population exhibiting a fluorescence intensity of less than <300 units, while for the RCR+ samples, ~85% of the population has a fluorescence intensity of greater than >300 units. Furthermore, the RCR+ samples have a much greater range of possible fluorescence intensities above this point with the highest examples recording. fluorescence intensities of ~1700-1800 units. The highest RCR- samples were only ~700-800 units.

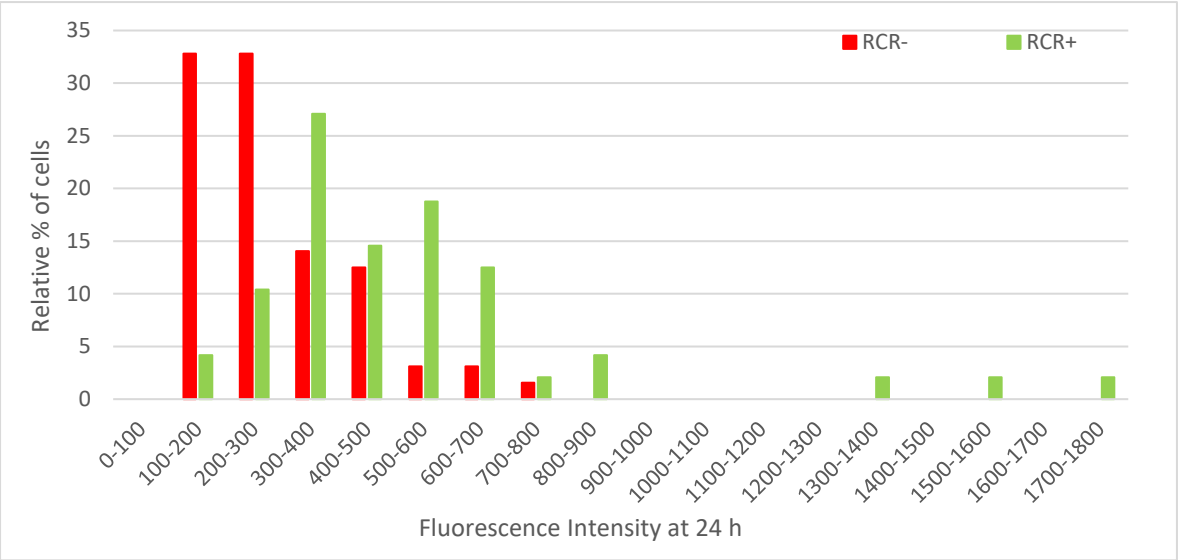

Figure 3.9: Histogram of the relative percentage of cells transfected with RCR- (red) and RCR+ (green) eGFP expression vectors and their fluorescence intensities calculated from maximum intensity projections in Zeiss Zen 3.1 graphed in 100-unit intervals of relative fluorescence units (RFU). Fluorescence in HeLa S3 cells 24 h pt ($p<0.01$)..

An overall evaluation and comparison of the fluorescence intensities and the mean average cell size, as well as a graph depicting the fluorescence intensity recorded for each cell evaluated from low to high (Figure 3.10:B). In these analyses, not only do the RCR+ samples have a higher overall mean fluorescence intensity (that is 1.8-fold greater than that of RCR- transfected cells) but they also have a higher average cell surface area that is 1.9-fold greater. Error bars depicting the 95% confidence interval indicate that the difference between the sample means was highly significant. Because this increase in overall surface area is coupled to the increase in mean fluorescence intensity, which is per unit area, this indicates that the overall increase in eGFP expression per cell is even greater, as the cells themselves have become larger. This corroborates with the flow cytometry data, when comparing the fluorescence of the measured RCR- and RCR+ transfected cells individually, arranged from lowest to highest (Figure 3.10:B). It appears that the least fluorescent cells match up more closely to each other in terms of fluorescence intensity, but the RCR+ transfected cells are still brighter. This difference then rapidly widens to a point where, when arranged from low to high, each RCR+ cell is approximately twice as bright as its RCR- transfected counterpart. This is consistent all the way up to the very brightest cells where the differences broaden further to a point when the brightest RCR+ transfected cells are more than twice as bright as the brightest RCR- cells.

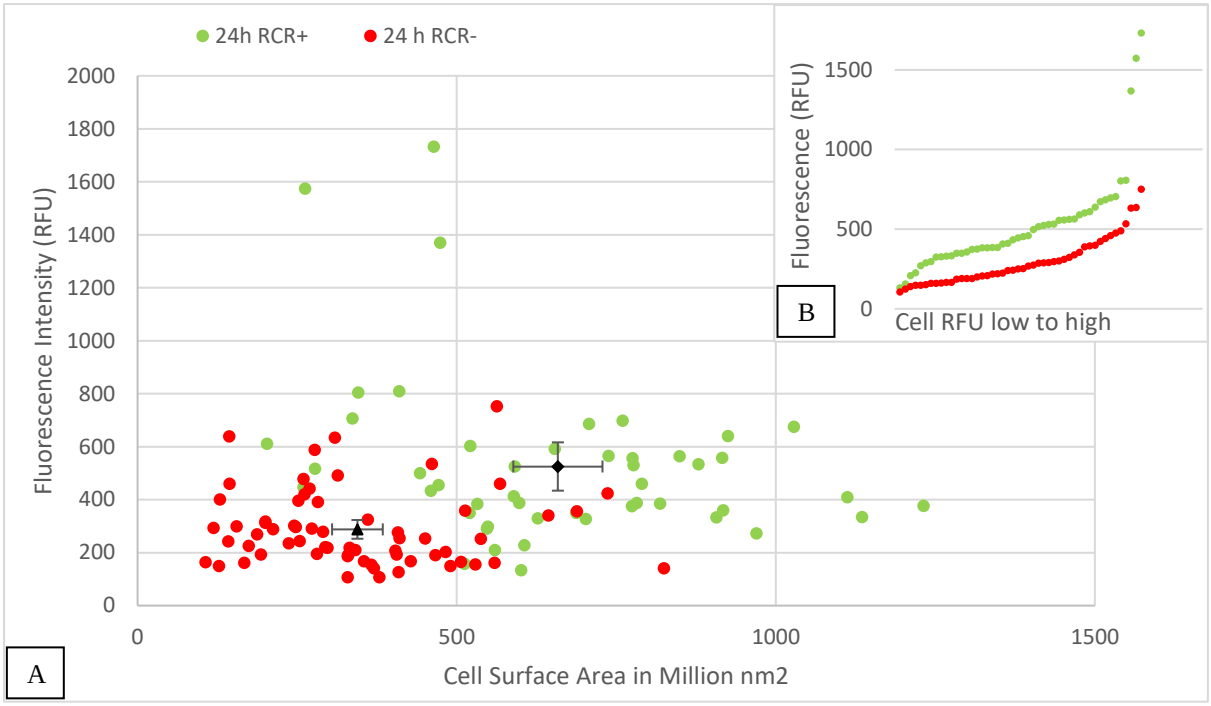

Figure 3.10: Differences in fluorescence intensity and cell size of HeLa S3 cells transfected for 24 h then imaged under confocal microscopy as quantified by confocal microscopy in terms of relative fluorescence units (RFU) with RCR- (red) and RCR+ (green) eGFP expression vectors. A) XY scatter plot of recorded cells with mean fluorescence and cell surface area points depicted showing error bars for the 95% confidence interval, ($p<0.01$). B) Individual cellular RFU from low to high.

The above analysis was repeated using different transfection durations (data not shown) and produced a highly similar result.

To more realistically investigate the effects of RCR *in situ* a new set of transfection experiments were conducted, wherein the transfection times were limited to 4 h by aspirating the media containing the transfection mix and replacing it with fresh media. This severely limited the time, and therefore amount of DNA, that was taken up by the cells, which in turn massively reduced the corresponding level of fluorescence, as was clearly evident at 96 h pt for the RCR- eGFP samples (Figure 3.11), compared with the same sample where transfections ran unabated (Figure 3.1). The weak fluorescence seen by the RCR- eGFP transfected cells in these experiments verified that the experimental aim, which was limiting *in situ* DNA availability, had been achieved. Furthermore, as had been postulated, the same procedure performed with the RCR+ eGFP vector generated high contrast image comparisons, demonstrating a highly significant improvement in eGFP expression in the RCR+ sample, compared with that in the RCR- sample (Figure 3.11).

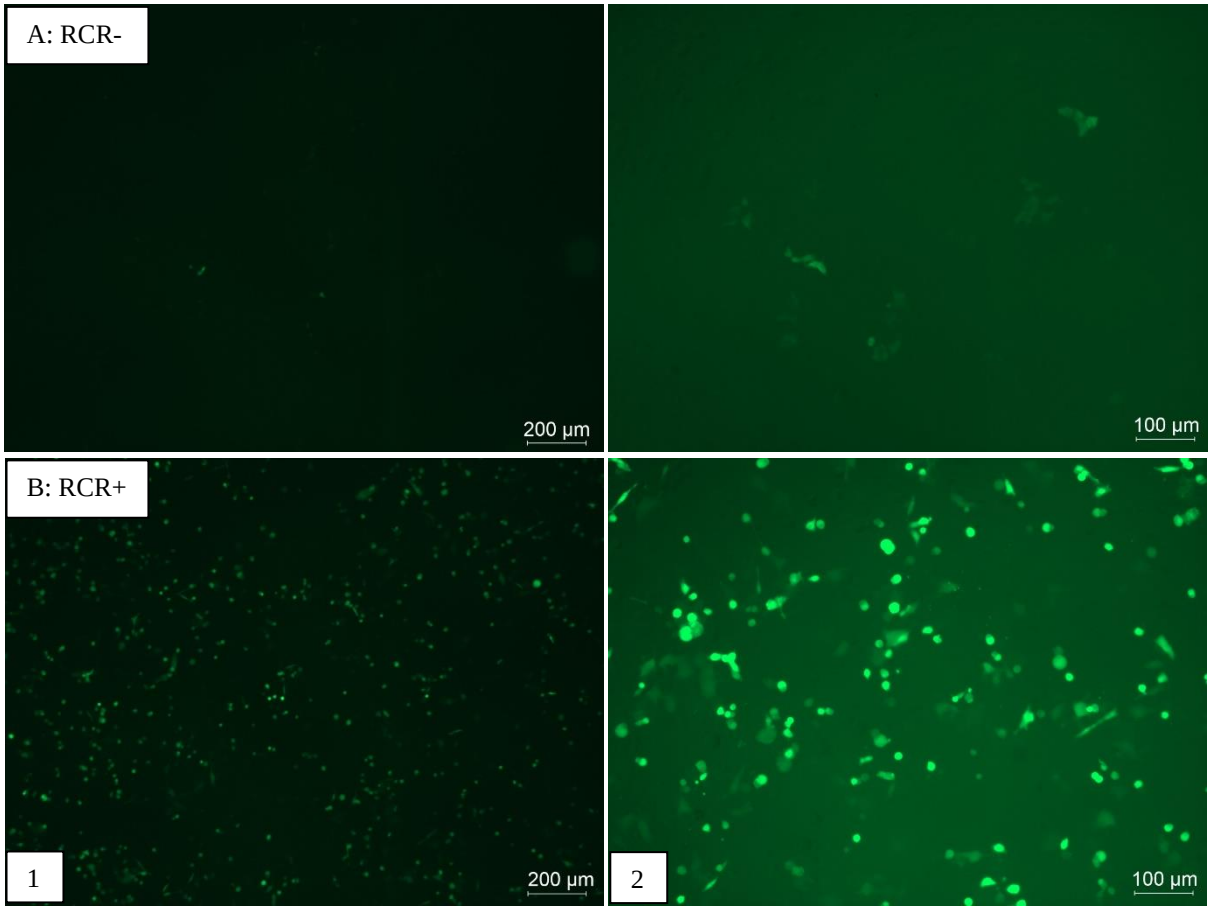

Figure 3.11: Time limited DNA transfections of HeLa S3 cells with A) RCR- and B) RCR+ eGFP expression vectors taken 96 h pt. Low DNA vaccine uptake was simulated by stopping DNA transfection after 4h. Images taken at 1) 50x and 2) 100x magnification.

To investigate how meaningful these differences between the RCR+ and RCR- samples were, and to determine the magnitude of the change compared with the previous quantifications, a repeat of the confocal microscopy quantification experiments was conducted using the new limited transfection protocol (Figure 3.11). The same analyses were performed as before: this time, when analysing the histogram produced (Figure 3.12), it appears that the RCR+ sample had a greater proportion of cells distributed with higher fluorescence intensity readouts than it did before. Indicating that the RCR+ transfected cells have shifted towards higher fluorescence intensities across whole the range of transfected cells. This created a wider range in relative fluorescence values and higher relative highs for the brightest transfected cells.

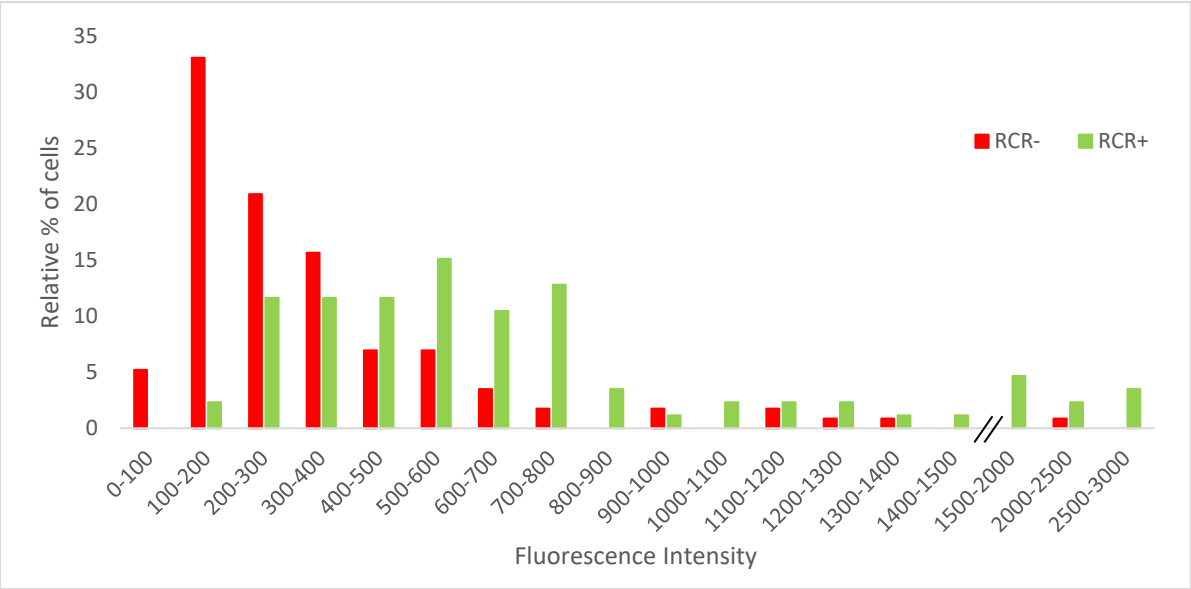

Figure 3.12: Histogram showing the relative percentage of the cell populations transfected with either RCR- (red) and RCR+ (green) eGFP expression vectors and their relative fluorescence unit (RFU) intensities at 100 RFU intervals. Fluorescence intensity was determined in ZEISS Zen blue from HeLa S3 cells that had been transfected for 4 h then cultured for 24 h ($p<0.01$).

A difference in mean relative fluorescence, indicated as black points with error bars, of 2.3 fold (Figure 3.13) is observed when comparing the RCR+ population versus the RCR- population. Indicating the relative change in effect grew by 0.5 fold, from the 1.8 fold change observed when less DNA was transfected into the cells (Figure 3.10). Similarly, changes in the mean cell surface area between the two transfection methods was also observed with a 1.84 fold change now, versus 1.91 fold before.

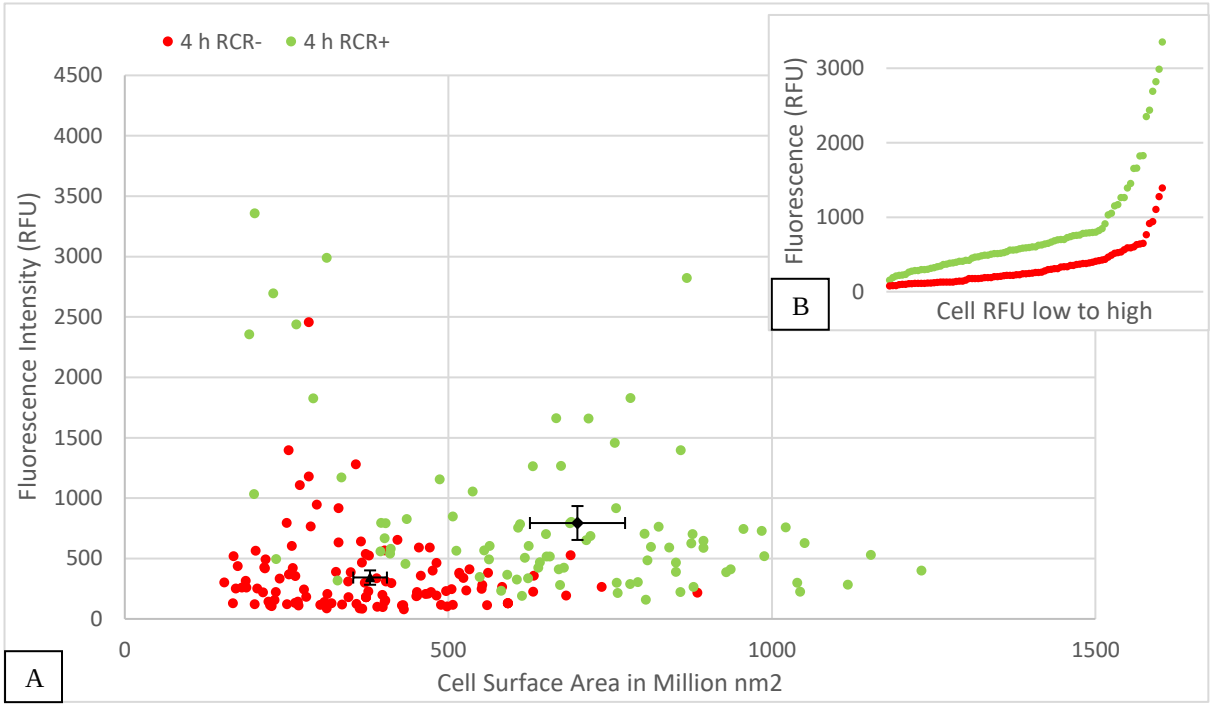

Figure 3.13: Differences in fluorescence intensity and cell size in HeLa S3 cells transfected for 4 h with RCR- (red) and RCR+ (green) eGFP expression vectors determined by confocal microscopy. A) XY scatter plot of recorded cells with mean fluorescence and cell surface area points depicted showing error bars for the 95% confidence interval ($p<0.01$). B) Individual cellular fluorescence from low to high.

This analysis suggests the RCR system has dynamic effects on gene expression and physical characteristics of affected cells. These effects are more prominent when less DNA is transfected into the cells. This suggests that the variable nature of the effect is being actively compensated for and responded to by the affected cells. Understanding the complex nature of such cellular compensation mechanisms, however, remains a mystery. The evidence gathered here however is sufficiently compelling to suggest that meaningful and significant metabolic cellular changes are occurring, and these appear to exhibit characteristics associated with known immunogenic cellular response mechanisms.

3.3.6 HIV-1C Gag mosaic expression was verified by western blot

To verify the expression of the HIV-1C Gag mosaic gene, which is a model T-cell antigen and vaccine target in our research group, western blots were performed on cells transfected with the RCR- and RCR+ Gag expression vectors. As can be seen in Figure 3.14, no band was present for the negative control lane, and a clear band at ~55 kDa was present in the MVA positive control. Bands corresponding in size to the positive control were visible for the DNA transfections. As might be expected, the most prominent and darkest bands corresponded with the highest DNA transfection amounts, while the fainter bands corresponded with the lowest DNA transfection amounts. The RCR+ sample however had darker band at its lowest transfection concentration, compared with the RCR- transfected with the same DNA amount. Interestingly, this scenario was reversed at the highest transfection levels, with the RCR- sample having a darker band than the RCR+ sample, while at the 0.5 µg DNA transfection level it appears that the RCR+ sample also has a darker band. A similar result to the one depicted below was also obtained for western blots performed in HEK-293T cells (data not shown).

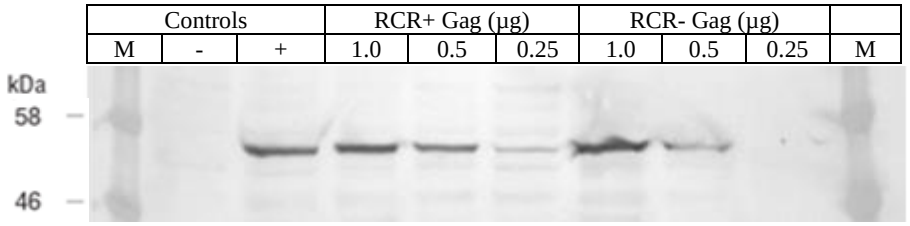

Figure 3.14 HIV p-24 western blot of HIV-1C Gag mosaic expressed by MVA in Hek293T cells (+ Ctl) and the RCR- and RCR+ gene expression vectors in HeLa S3 cells 48 h pt. Cells were transfected with either 1.0 µg, 0.5 µg or 0.25 µg of DNA per well of the RCR- and RCR+ Gag expression vectors.

Densitometry analysis from the above western blot analysis was used to provide a rough estimate of relative level HIV-1C Gag expression from the different DNA transfection concentrations for each vector. For this analysis Gag from the MVA positive control expressed in HEK-293T cells was used as the reference sample of comparison. The results of this analysis are depicted in Figure 3.15. This

analysis indicated that at the lowest transfection levels the RCR+ expression technology has the greatest amplification effect, while using high transfection concentrations resulted in lower levels of expression (Figure 3.15).

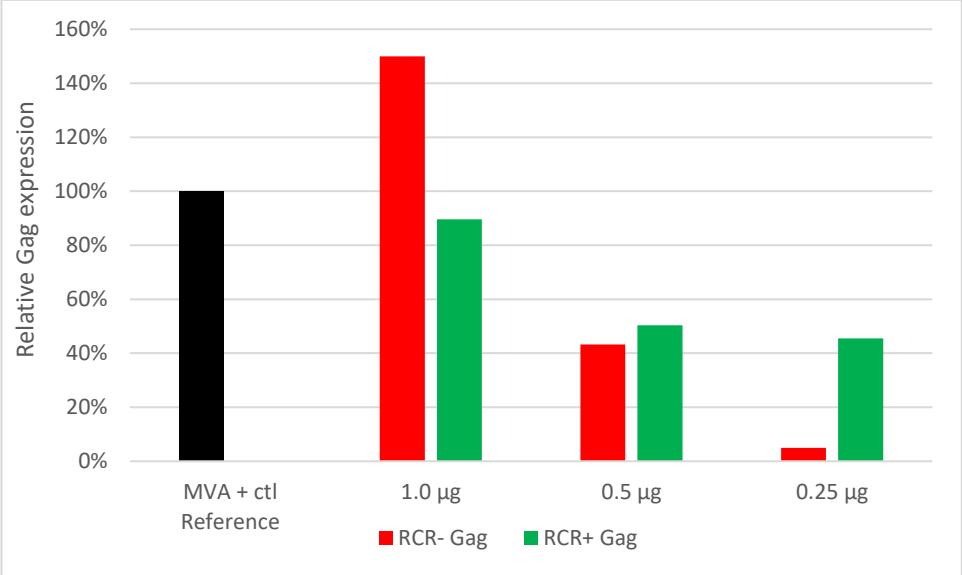

Figure 3.15: Densitometry analysis of HIV-1C Gag expression by RCR- (red) and RCR+ (green) Gag expression vectors in HeLa S3 cells relative to an MVA positive control expressed in HEK-293T cells. HeLa S3 cells were transfected with either 1.0 µg, 0.5 µg or 0.25 µg of either the RCR- or RCR+ HIV-1C Gag mosaic DNA expression vectors. Western blots with densitometry analysis were performed on samples from cells harvested 48 h pt.

3.4 Discussion

3.4.1 Microscopy

My first transfections using RCR+ and RCR- eGFP expression vectors clearly demonstrated that the RCR+ vector expressed more eGFP per cell than the RCR- eGFP control (Figure 3.2). Interestingly, upon closer inspection there appeared to be numerically more fluorescent cells in the RCR- samples. This observation was corroborated with more prominent and clear observations at later times, such as 96 h pt. At these later time points, e.g. 48 h and 96 h, the RCR+ samples also appeared to have noticeably brighter fluorescence on average than the RCR- samples and a higher number of exceptionally bright fluorescent cells, which also appeared to exhibit altered cell size and morphology (Figures 3.10, 3.13).

Collectively, these observations demonstrate that the RCR DNA expression technology is dynamic in nature and one that is somewhat 'intuitive' (being capable of inducing these fundamental cellular changes in structure and metabolism while maintaining elevated expression levels without killing the afflicted cells for an extended duration of time) (Figure 3.7). Such dynamic cellular effects are coupled with a dynamic gene of interest expression profile, whereby it appears that even cells that start with the weakest or lowest levels of eGFP expression over time, come to match and exceed the highest levels obtained from non-replicating RCR- samples. This essentially confirms a capability that was postulated and, as has now been demonstrated, can only be attributed to the effects of RCR.

In transfections with the RCR- eGFP vector, some highly fluorescent cells are also present at around 48 h pt. These often also typically exhibit rounder larger cell morphology and appear to simply be the most heavily transfected cells. However, for RCR- eGFP vectors, by 96 h pt most of those cells have disappeared or dimmed down with the overall fluorescence intensity steadily decreasing among the non-replicating vector transfected cells. This is similar to what is reported in the literature on DNA transfections with GFP (Kirsch et al., 2003; Soboleski et al., 2005). While at these later times the opposite of this is true for the replicating RCR+ eGFP samples, which increase in brightness with time. This was further demonstrated and corroborated in long term expression evaluations using extended growth times aided by FACS (Figure 3.7).

The viral nature of these observed expression activities is arguably a better representative of a viral infection and its gene expression profile. This places the RCR DNA expression technology in a better state of gene expression, to more realistically stimulate the complex biochemical antiviral cellular machinery, pathogen recognition receptors, and DNA damage sensing cellular systems that collectively initiate the desired molecular responses (collectively referred to as the PAMPs and DAMPs) (Giglia-Mari et al., 2011; Kumar et al., 2011; Li and Chen, 2018).

3.4.1 Flow Cytometry

Results from flow cytometry analysis provided answers to several core experimental questions; by having a very high sample size, it was possible to construct detailed histograms of eGFP expression from the fluorescent data and to evaluate internal cellular complexity and granularity from side scatter analysis (SSC-A). Flow cytometry also helped detect and quantify more subtle changes, such as alterations in average cell size from forward scatter analysis (FSC-A), (Adan et al., 2017; Cardis et al., 2017; Soboleski et al., 2005; Tzur et al., 2011). These data helped determine important aspects of cellular health and metabolic growth rates being affected by the deployment of the developed replicating DNA expression system. Analysis of size shifts and interpretation of flow cytometry data sets is discussed by (Adan et al., 2017; McLean et al., 2016; Soboleski et al., 2005; Tzur et al., 2011)

Data gathered from these experiments, demonstrated that powerful and dynamic changes occurred within cells transfected with the replicating RCR+ eGFP vector, and that these were not present in cells transfected with the non-replicating RCR- eGFP vector. Furthermore, these changes appear to have magnified over time for all three cellular characteristics recorded in flow cytometry, namely: (eGFP fluorescence, SSC-A and FSC-A). Statistical evaluation using a one-way ANOVA analyses was performed on each of the three datasets to determine the degree to which they differed and how this changed with time. This analysis helped track the divergent nature of the differences caused by the replicating vectors effects. Due to the high similarity of the RCR+ and RCR- vectors the early ANOVA analysis, at 24 h post transfection, indicated that no significant differences were initially detectable in all three flow cytometry data sets between the RCR+ and RCR- samples at 24 h. This is best demonstrated by their calculated p-values for each comparison: eGFP: $p=0.83$; SSC-A $p=0.85$ and FSC-A $p=0.90$ indicating, in all metrics, that the fluorescent populations of the two samples were mostly similar at this time. The relative ratio of fluorescent cells to non-fluorescent cells was also identical between RCR+ and RCR- samples at approximately 2.1%. It is noted that this low percentage does not reflect transfection efficiency because, at this stage, only a small percentage of the most highly transfected cells have expressed sufficient eGFP to be detectable In other words, at this time, the flow cytometry equipment used had a limited ability to separate low levels of eGFP fluorescence from background autofluorescence. Nevertheless 2.1% of the 50,000 cells analysed were differentiable at the 24 h pt. This still represents over 1000 individual cells, which was more than sufficient for an ANOVA analysis. Being representative of the most transfected cells, this population has the potential to initiate RCR at this early stage, due to rapid early expression of Rep, but also has potentially the least headroom for RCR to demonstrate improvements in expression by increasing copy number (which is presumed to be already high for this particular cell population) (Faurez et al., 2010; Sousa et al., 2009).

The divergent nature of the RCR+ and RCR- samples is demonstrated by a massive change in the level of significance between them as determined by one-way ANOVA calculations at 24 h and 48 h pt across

all three metrics recorded. At 24 h pt, none of these were significantly different between RCR- and RCR+ sample but by 48 h pt all of them were. At 48 h pt, ANOVA performed on eGFP fluorescence data indicated that the RCR+ and RCR- populations were highly different with a high level of significance of $p=3.5 \times 10^{-7}$ and, by 96 h pt, this became $p = 4.42 \times 10^{-77}$. These levels of statistical significance are somewhat ridiculous and beg the question as to why they are so significant. As it turns out, the reason comes down to the nature of the assumptions from which the statistical model is based. An ANOVA is a parametric statistical model which bases its comparison on the assumption that the populations being compared follow some form of a normal type of distribution and their statistical errors are also distributed normally (Kim, 2017). We also know that DNA transfections, in general, do follow a lognormal distribution (McLean et al., 2016). That makes this core assumption true when comparing DNA transfections using the same concentration, size and copy number, and that are controlled as is the case here. If comparing non-replicating plasmids, this assumption also remains true over time. However, we are not comparing two non-replicating plasmids here, but rather one non-replicating plasmid with one replicating plasmid. Herein lies the answer to the extremity of the obtained p-values. While the DNA transfection of the replicating plasmid almost certainly starts out as a lognormal distribution among the cells that take it in (as in the non-replicating plasmid), over time (as RCR occurs) this fundamental core assumption of the ANOVA statistical model breaks down. As far as I could determine, there is no suitable statistical model that can account for this fundamental change in the nature of the RCR vector. An ANOVA appears to still be the best possible comparison in this case, as all the initial assumptions of the model remain true and this fundamental change in nature by the RCR+ vector can be anticipated to do what has essentially been observed here: break the model. In this sense, the excessive level of statistical significance obtained, that increases with time but is not present at all in the beginning, is in fact what should be expected from active RCR. This because we are expecting the RCR+ system to replicate and induce alterations in cellular gene expression at a fundamental level, while simultaneously altering the initial starting DNA concentration distribution within affected cell nuclei. This makes a core assumption of the ANOVA statistical model, initially true, then later false and more so over time (Kim, 2017; Stoline, 1981; Wilcox and Wilcox, 2010). It is expected that this functionality will break the model and, as a result, divergent and highly improbable p-values should be obtained. Anything less might be taken as a sign that the core functionality of DNA replication was not functioning. Other statistical models were considered; nevertheless, a one way ANOVA was still deemed to be the best suited statistical model for comparing these two DNA expression vectors (Kim, 2017).

The ANOVA p-values also statistically demonstrate that the expression profile of RCR+ samples changes over time in a manner that is fundamentally different from the RCR- samples. The relative increase in p-value significance from 24 to 48 and to 96 h pt demonstrates (in a purely mathematical way) the compounding nature of the amplification process and the effects it has (Cohen, 2011; Kim,

2017). These numbers also effectively demonstrate the effectiveness of the RCR amplification process to enact powerful and compounding intracellular change. We see this visually in the histograms too where the shape of the distribution curves, particularly for eGFP fluorescence and SSC-A, mutate over time becoming stretched and flattening out.

The conclusions from ANOVA for the eGFP histogram data are effectively further corroborated by the ANOVAs performed on the SSC-A and FSC-A data too. For the SSC-A at 24 h pt, p=0.85 this became p=0.0013 by 48 h pt and p=1.11 $x10^{-6}$ by 96 h pt. The same compounding divergent trend was confirmed for the FSC-A data set as well: where, at 24 h pt, ANOVA on the FSC-A produced an insignificant p = 0.90, which became significant at 48 h pt with p = 0.024 and which grew exponentially to p = 0.0005 by 96 h pt. Additional more basic statistical metrics (calculated in FlowJo) further outline the nature of the described change, detailing how the skewness of the histogram distributions changes over time and how the co-efficient of variances and standard deviations increase more for the RCR+ samples over time. These data are available in Appendix B.

Of the cellular changes tracked in flow cytometry, the significant changes in internal cellular granularity for the RCR+ samples are of interest. This kind of change is known to be caused by increased concentrations of internal subcellular elements such as granzymes, lysosomes and DNA itself (Cardis et al., 2017). During cellular division, cellular granularity naturally increases when cells undergo DNA replication in the S-phase of their life cycle (before cell division) (Pollard et al., 2017). It has been shown that this is also when RCR is most active, primarily because of the oversupply of DNA polymerase and other DNA replication machinery, associated with cellular S-phase (Pollard et al., 2017). It is also here where the RCR process is thought to exert the greatest impact on the subcellular life cycle of affected cells. Taking advantage of the internal cellular changes that occur during this time, and ultimately hindering the progression of normal S-phase (Cheung, 2012; Laufs et al., 1995; Palmer and Rybicki, 1998). This understanding of RCR and Reps functionality (reported in the literature) is supported by our experimental observations made during flow cytometry tests During these tests, increased cellular fluorescence was found to correlate with increased cellular granularity and increased cell size as well as delayed (or hindered) cell division, resulting in an increase in the relative proportion of cells exhibiting high cellular granularity (Figures 3.3-3.6). In the above circumstances, it is possible to observe a situation in which eGFP fluorescence intensity effectively tracks and correlates well with cellular granularity.

This provides a powerful indicator that RCR is affecting internal cellular metabolic processes, creating changes that are not present in the non-replicating RCR- transfected samples. Such fundamental changes have a high probability of affecting almost everything about the afflicted cells and, at the very least, represent a powerful disruption of cellular state and homeostasis. These observations are in line with our understanding of Reps function and the RCR process described in the literature (Cheung, 2015,

2012; Gutierrez, 1999). In such instances, one expects to see the impact of RCR on the cell to become more strenuous and dominant for the host cell as the viral system takes over and repurposes available internal cellular resources to express its encoded genes in a manner that arguably mimics the disease progression of the virus from which it was derived (Amery-Gale et al., 2017; Regnard et al., 2017).

The compounding eGFP expression and cellular effects of RCR generate a similarly growing, divergent set of increasingly statistically significant p-values from ANOVA calculations. This was observed for eGFP fluorescence, internal complexity/granularity and cell size. These are accompanied by a similar observation of divergence between the samples, in terms of the total number of fluorescent cells and therefore cellular growth rates and metabolism. Both samples start out with ~2.1% fluorescent positive cells out of the total flow cytometry evaluated population at 24 h pt. This begins to diverge at 48 h pt where the relevant RCR- samples population becomes 10.4% and is only 8.8% for the RCR+ sample. By 96 h pt, this difference grows with the fluorescent positive RCR- sample representing 18.3% of the total evaluated cells, and the RCR+ sample only representing 9.5% of the total cells (Figure 3.3). This is direct evidence of cellular metabolic slow down or death, and is a clear indication that the RCR+ expression technology is causing cellular strain and inducing an internal metabolic cellular response (Nielsen and Keasling, 2016). Deciphering the true nature of this metabolic slow-down however, is decidedly more difficult and complex than discovering its existence. Literature on the various known forms of programmed cell death and cellular defences would suggest that one possible explanation might be the induction of a form of necrotic cell death and possibly even a specific from known as immunogenic cell death (ICD). This would be an ideal outcome for a vaccine but it is, however, also a difficult and complex outcome to prove (Galluzzi et al., 2016; Kepp et al., 2014; Smirnova et al., 2015; Wenzel et al., 2012). Various other explanations, such as cellular senescence or other forms of programmed cell death, could be adopted to explain these observations. For various reasons, these are however considered less likely, given the observations that have been made here. If apoptosis was occurring, for example, it would be easily seen in high magnification microscopy among the fluorescent cells, but this is not the case. Similarly, cellular senescence would be expected to halt cell division of the affected cells, but this also was not the case, since it was observed to continue to occur for extended periods of time, which suggests that progression through the cellular life cycle was not halted, but rather just disrupted or slowed down (Campisi, 2014).

It is worth keeping in mind that these observations are occurring within HeLa S3 cells, a known cancerous cell line (Masters, 2002; Smirnova et al., 2015). As such, demonstrating an ability to hinder cell growth and slow cellular metabolism in these cells, with a possibility of also increasing cellular defence mechanism activation, is worth consideration. There may be various useful applications of this technology in cancer research and vaccines, where this type of capability is sought after (McNeel et al., 2012; Wahren and Liu, 2014).

As previously discussed, DNA replication via RCR may present as DNA damage to the cell. This is due to the linear ssDNA and nicked dsDNA intermediate forms that occur during RCR, all of which have specific DNA damage-sensing mechanisms (Campisi, 2014; Cheung, 2015, 2012; Diner et al., 2015; Giglia-Mari et al., 2011; Li and Chen, 2018). DNA damage-monitoring biochemical pathways are known to be responsible for inducing the activation of DNA repair machinery as well as cellular senescence and apoptosis. It is only logical to assume that active RCR may be stimulating these biochemical pathways via several known (and possibly other postulated) PRRs (Diner et al., 2016, 2015; Giglia-Mari et al., 2011). The outcome of such stimulation itself is virtually impossible to guess as this would be dependent on a variety of highly dynamic cellular factors such as cellular health, nutrient availability, metabolic state, and inter-cellular chemokine signalling, among others (Li et al., 2012; Saade and Petrovsky, 2012; Takeda and Akira, 2015). In the long term though, such stimulation becomes less and less likely to go unnoticed by the cell, and therefore more likely to stimulate an immunogenic response (Diner et al., 2016, 2015).

At the subcellular biochemical level, the complexity of the possible signalling interactions within the known likely metabolic pathways that can cause the types of observations we are seeing, is incredibly difficult to understand and interpret. However, at the cell systems level of analysis, we do not need to necessarily understand the precise combination of gene responses and activations responsible for the observed cellular changes. At this stage it is only possible to make an educated guess concerning the probable nature, and likely direction, in which those changes are driving the cellular response. In this case, we also have a wealth of information from the available literature and studies on these overall cellular molecular patterns, how they manifest in observable traits, and the nature of their underlying molecular causes (Kepp et al., 2014; Kumar et al., 2011; Smirnova et al., 2015; Takeda and Akira, 2015). We also have a good idea of which PRR's and PAMPs the RCR expression technology should target, such as viral DNA sensors like IFI16 and TLR9, and the nuclear DNA damage and homeostasis monitoring systems responsible for detecting nicked and broken DNA species which are produced as intermediary DNA species during the process of RCR (Campisi, 2014; Diner et al., 2015; Giglia-Mari et al., 2011; Kumar et al., 2011). There is good reason to believe these combined stimuli should prove to be more capable of breaking known innate immune tolerance mechanisms, to enhance the cellular immunogenic response (Luo et al., 2016; Makkouk and Weiner, 2015). Literature on the DAMPs and PAMPs indicates that their activation in many ways appears to manifest in cellular observations that correlate well with our observations of RCR+ transfected cells (Campisi, 2014; Diner et al., 2015; Gilbert, 2012; Kumar et al., 2011). For example, metabolic slow down (as seen in response to RCR+ vectors) is a hallmark signature of PAMPs and DAMPs and forms a fundamental component of the cellular immunogenic response mechanisms. Internal cellular reorganization, arguably, suggested here by the detection of increased internal cellular granularity, may also play a role in such processes

(Galluzzi et al., 2016; Kumar et al., 2011; McMichael and Koff, 2014; Nielsen and Keasling, 2016; Smirnova et al., 2015).

The inordinate complexity of the internal cellular processes involved however, makes proving the activation of particular immunogenic PAMPs (such as ICD or upregulation of the type I interferon response) a difficult task experimentally, although results discussed in the literature suggests that this is the most probable outcome (Diner et al., 2015; Paludan and Bowie, 2013). In other words, it represents a possible hypothesis that can be put forward, given our knowledge of the likely cellular PAMPs and PRRs involved. What we appear to be observing seems to correlate very well with what can be expected from the activation of immunogenic PAMPs that are known to enhance the generation of T-cell immunogenicity and are associated with viral and pathogenic infection (Belshe et al., 1998; Brice et al., 2007; Galluzzi et al., 2016; Hofer, 2014; Latz et al., 2004; Scheller et al., 2002; Smirnova et al., 2015; Yuan et al., 2016). Further experimental work is, however, required to test this claim and there exists a variety of experimental methods and ways in which this can be done. These include gene arrays, proteomics and a variety of immunogenicity studies. There are also some specific cellular assays that can be undertaken, to look directly for the induction of ICD in a TC environment (Kepp et al., 2014).

In terms of understanding the raw changes in fluorescence demonstrated, several biological drivers of gene expression must be taken into consideration. The direct observation of the overall increase in the proportion of cells exhibiting a relatively high fluorescence from 10,000−100,000 + RFU for the RCR+ sample, and extremely high fluorescence levels (up to ~150,000 RFU at 96 h) deserves specific discussion. This observation demonstrates unequivocally that the internal localised concentrations of the gene of interest eGFP within these cells is higher (on average) per cell and can reach levels that are approximately double those seen from the most fluorescent RCR- transfected cells. Overall, it appears that an upward shift in the fluorescence from each cell has occurred throughout the fluorescent-positive population. Literature would suggest that this type of action should improve immunogenicity (Hovav et al., 2007; Rathinam and Fitzgerald, 2011). However, these fluorescent observations alone do not cover the scope of the overall observations made. When interpreting this evidence, additional consideration must also be given to results indicating that overall internal eGFP expression has roughly doubled, while cellular metabolism and growth rate appear to have decreased by approximately half, and cell size has increased. This suggests that the true amplification relative to cellular metabolism a kind of ‘per capita’ expression *per se,* which is meaningfully larger than the fluorescent data alone indicates. It is perhaps unwise to infer too much from this counter correlation between fluorescence, metabolism and increased cell size, particularly since an important factor in this evaluation remains completely unknown, which is the internal rate at which cellular protein degradation is occurring. This important factor could have increased or decreased in response to the replicating vector. That said, if the observed cellular metabolic slowdown is caused by an immunogenic type of response, as we suspect

it is. We also know, from the literature, that this kind of cellular response is typically accompanied by an overall increase in internal cellular protein degradation processes, which are an integral part of such immunogenic responses. Indeed, increased protein degradation is an integral part of increasing antigen presentation via the MHC Class I mechanisms (Altenburg et al., 2016; Geldmacher et al., 2007; Kumar et al., 2011). If this is the case, the true magnitude of the relative level of localised gene expression amplification caused by RCR would be arguably significantly higher than the level we are currently observing. If that is the case, the overall increase in cellular eGFP expression per cell represents the 'triumph' of the viral RCR process, taking over internal cellular resources while battling the internal cellular response and defence mechanisms designed to hinder and halt viral cellular takeover. Whether this apparent viral-like 'victory' over the cell by the RCR DNA expression technology translates into enhanced immunogenicity is yet to be determined.

An alternative, and more benign, explanation is simply that the increased eGFP expression might be accounted for by the metabolic slowdown through the simple accumulation of eGFP. This simpler explanation is both logical and valid and arguably better suits the test of Ockham's razor. Available scientific literature on how the innate cellular defence mechanisms work. Taken in combination with the available literature on an array of PRRs that are capable of recognising intracellular pathogenic DNA. Suggests that the explanation given above is more likely (Altenburg et al., 2016; Cocchi et al., 1995; Guo, 2014; Hu and Sun, 2016; Makkouk and Weiner, 2015; Material et al., 2013; Nielsen and Keasling, 2016; Paludan and Bowie, 2013; Pickering and Davies, 2012; Wells et al., 1997). No other explanation for the metabolic decrease observed appear to adequately explain the observed accumulation of eGFP.

3.4.2 Re-culturing HeLa S3 cells

After performing FACS, the sorted fluorescent cells were successfully cultured for up to 11 days pt through multiple passages (Figure 3.7). In these experiments, the RCR+ transfected cells remained highly fluorescent over the full duration of continued cell culture while the RCR- transfected cells faded in brightness over time and cell division. This indicates that RCR can boost and maintain elevated expression levels across multiple cell divisions and cellular passage. This is something non-replicating expression systems are not capable of (Kirsch et al., 2003). The RCR+ cells were observed to grow and divide, but they did so at a noticeably slower rate. This made culturing them past 11 days pt impractical, due to the rapid overgrowth of wild type cells during this time and loss of ~75% of the fluorescent cells in each passage.

These re-culturing experiments demonstrated some core capabilities of this technology. First, that it could elevate local cell expression levels and sustain these elevated levels over time and through cell divisions. Secondly, during the passage of time, all cells from all relative levels of transfection appeared to elevate expression to what may be best described as a relative cellular upper limit. This upper limit

appears to be at least twice as high as the level of fluorescence obtained from the brightest non-replicating RCR- eGFP transfected cells (Figures 3.2 & 3.7). This directly demonstrates some of the core postulated capabilities of this technology. Mainly, the ability to elevate localised gene expression levels and the ability to stabilise it off and sustain it at some elevated level. These experiments also demonstrated that these cells maintained the ability to survive and progress through cell division in this state for the extended period of up to 11 days, as tested. Due to the obvious and visible effects of slowed cellular metabolism, evaluation beyond 11days was not possible in tissue culture (because of the faster outgrowth of untransfected HeLa S3 cells which could not be eliminated by FACS). It is therefore difficult to evaluate the rate of the compounding amplification effect created by the RCR cycle. The validity of a comparison to living animal tissue cells must also be questioned in this case, as live animal cells generally have notably different metabolic characteristics and rates of growth, in comparison to the rapidly growing HeLa S3 cells used in tissue culture. It would be fair to assume that the progression rate and amplification curve from the RCR expression system developed would likely be somewhat slower in a live animal model than what was observed in cell culture (Masters, 2002; Wen et al., 2014). That said, the disease progression rate of PBFD, which is fairly slow (taking months to progress through stages), might be a good place from which to start estimations (Amery-Gale et al., 2017; Pass and Perry, 1984; Regnard et al., 2015). The rate at which the RCR progresses and compounds its effects in animals is something that should be investigated and an important factor for vaccine immunogenicity experimental design. Quite extensive animal experimentation over various time scales is required to determine this.

3.4.3 Confocal Microscopy

Results from these experiments independently corroborated most of the findings made from flow cytometry. The ability of the superior optics and light filters from confocal microscopy allowed for the use of this technique to better detect and resolve true eGFP fluorescence from cellular autofluorescence earlier on. This led to more accurate quantification and determination of the effects of RCR on eGFP expression at 24 h pt. From these experiments attempts were made to detect changes in the rate of eGFP expression between cells transfected with minimal amounts of DNA vs amounts. In doing so I was able to demonstrate a dynamic effect size from RCR expression amplification whereby the starting amount of DNA was linked to the strength of the gene amplification obtained. This was demonstrably larger when starting from lower concentrations, as had been speculated based on current understanding of RCR and Rep (Cheung, 2015, 2012). This was observed as a large increase in the relative number of cells exhibiting fluorescence from 300-700 RFU range and from a relative decrease in the proportion of cells from the 0-300 RFU range. The data gathered from confocal microscopy also supported the proposed idea that each portion of the transfection distribution curve migrates upward, as would be expected from RCR changing the copy number and DNA concentration of the DNA received from transfection −a process that results in a rightward shift the normal distribution obtained from a standard

DNA transfection along the fluorescence intensity axis (Figure 3.9). This is precisely what we appear to be seeing in the histograms generated from confocal eGFP quantification (Figures 3.9 & 3.12). When each measured cell was ordered from lowest to highest fluorescence intensity and then graphed (Figure 3.10:B), one can see this shift appear as the separation between the RCR+ and RCR- sample over the whole range of all the measured cells, with the RCR+ cells exhibiting roughly twice the fluorescence as that of their RCR- counterparts.

Graphing the measured cells against each other in an x-y scatter plot allows for changes in their relative cell size or surface area and fluorescence to be seen together. From this analysis it is apparent that, as their physical cell size increased, so too did their relative fluorescent levels. Interestingly though, it can be noted that the very brightest examples were at the lowest end of the size range (Figure 3.10:A). These examples represent newly-divided cells, which suggests that the greatest relative level of expression occurs after cell division. This observation supports the idea that RCR occurs mostly during cellular S-phase and that this phase of cell growth is delayed. We see that, for the RCR+ eGFP transfected cells, a trend in an overall increase in cell size (x-axis) is accompanied by an overall increase of cellular fluorescence (y-axis) for cells above 500 million nm^2 (medium to large cells), with the largest RCR+ examples being notably bigger than the largest RCR- examples. Below 500 million nm^2 we see that the smallest RCR+ cells also exhibit the brightest fluorescence. This can be explained by RCR occurring predominantly during cellular S-phase. This results in inhibiting the speed at which cellular S-phase occurs and is an idea supported by the literature on RCR (Cheung, 2012; Laufs et al., 1995; Palmer and Rybicki, 1998). Given this explanation, one would expect a relative proportional increase in the number of cells existing in a state of S-Phase or entering the state from G-phase, i.e. cell states which directly correlate with cell size (which concurs with what we observed). Furthermore, hindrance of the progression through this life cycle phase should logically result in these cells growing to a larger overall cell size at the end of S-phase. This, in turn, should also translate into larger cell sizes for the divided cells, following the completion of cell division. These newly-divided cells, having just undergone a phase of RCR, would have the greatest concentration of RCR amplicons expressing eGFP and therefore should also have the highest levels of fluorescence. Experimentally, this is precisely what we observed (Figures 3.10:A & 3.13:A).

To measure the dynamic effect size of RCR gene expression amplification relative to DNA concentration, two different transfection methods were used to obtain different starting DNA transfection concentrations. By comparing a time-limited transfection that was stopped after 4 h with an unlimited transfection (which was not stopped) and measuring fluorescence using confocal at 24 h pt, it was possible to compare the effects of RCR on gene expression, when starting with a lower or higher DNA concentration and copy number. Here the relative difference in starting concentration is effectively demonstrated by the RCR- eGFP sample control and by comparing the fluorescence obtained using the different transfection techniques. After carrying out this procedure, it became

obvious that the 4 h transfection was clearly far dimmer at the 24 h pt than when DNA transfection time was unlimited (Figures 3.2B vs 3.11A).

By recording and evaluating the fluorescence of as many fluorescent cells as possible and recording the change between the RCR_ and RCR+ samples for each transfection technique (Figures 3.9 & 3.10) and (Figures 3.12 & 3.13), it was possible to determine (and quantify) the relative effect that RCR amplification was having on gene expression for each transfection method. These data showed that the RCR+ vector elevated the mean fluorescence over that of the RCR- vector by 2.32-fold at 24 h pt, when using the 4 h time-limited transfections, and by only 1.83-fold when using an unlimited transfection time. This represents a dynamic difference in effect size of ~27% and provides strong evidence that RCR is demonstrably a dynamic amplification process that appears to exert a relatively greater effect size when starting from lower DNA transfection concentrations. This supports the idea that Rep is exerting its speculated, and previously discussed, self-limiting capabilities to limit runaway RCR from occurring. The mechanics of how this is thought to be done was discussed previously and is supported by literature (Cheung, 2015, 2012; Gutierrez, 1999). This effectively demonstrates that effects of RCR are more prominent at lower starting concentrations and that the postulated self-limiting capabilities, that are arguably crucial for the technology to reach a highly elevated yet sustainable upper expression limit inside a cell, appear to be in effect, and quantifiable when comparing these different transfection methods for obtaining different DNA starting concentrations. It should be possible to map out the full amplification curve and define it in biochemical terms. The nature and the shape of this complex amplification and inhibition curve are currently unknown, but would be useful to define.

These data also support the idea that RCR could have the ability to start from very low initial levels and steadily increase until this level is reached. The cellular RCR gene expression ‘glass ceiling’ that (presumably) if crossed, would result in cell death and burnout. This capacity of RCR is arguably an evolutionary requirement for effective chronic virality. In this manner, the RCR DNA expression technology is arguably able to recapitulate the cellular state of chronic viral infection. Without the ability to spread this state to more cells other than by cell division (which is demonstrably significantly reduced) these cells are, at best, in only a semi-stable state that ultimately could hardly go unnoticed by the immune system, given what we know about the biochemistry of this state and the manner by which the immune system seeks out these types of unhealthy cells (Cheung, 2015; Hu and Sun, 2016; Janeway and Medzhitov, 2002; Kumar et al., 2011; Material et al., 2013; Paludan and Bowie, 2013; Takeda and Akira, 2015; Wenzel et al., 2012; Yuan et al., 2016).

Interestingly, cell morphology also appeared to be somewhat healthier in experiments using lower DNA transfection levels. This can be expected as over-transfection with DNA is known to be cytotoxic in cell culture (Luo and Saltzman, 2000).

These data suggest that the developed RCR DNA expression technology could be promising in terms of improving real-world DNA vaccine efficiencies (taking note that one of the biggest problems for DNA vaccines, especially in humans and large animals, is their low and inefficient DNA uptake into host cell nuclei). The reasons for this are well documented, with rapid DNA loss and degradation occurring after patient inoculation (Kutzler and Weiner, 2008; Li *et al.*, 2012). Typically for DNA vaccines, only a very small amount is ever able to make it into target cell nuclei. That small amount, however, is capable of generating an important and highly sought-after type of immunogenic effect, known as T-cell immunogenicity (Cole *et al.,* 2015). These low-level DNA transfections therefore better represent real-world vaccinations and the observations made here, where RCR+ vectors demonstrably exert stronger amplification effects at lower starting levels, meaning that one of the fundamental problems with inefficient delivery can be arguably mitigated by this technology. Furthermore, it has been previously demonstrated that the decreased gene expression from DNA expression vectors known as promoter 'switch off'. Such a scenario can be regarded as a process mediated by the immune system and a problem for conventional DNA vaccines, both of which can be counteracted by replicating of the genes creating gene redundancy and mitigating immune suppression effects while amplifying (not decreasing) expression (Wells et al., 1997). This viral characteristic, conferred by RCR DNA expression technology, serves to directly combat the various immune tolerance mechanisms that are causing gene silencing and that plague conventional DNA vaccines. These immune tolerance barriers must be overcome to elicit the powerful T-cell responses and immunogenicity required from a T-cell vaccine (Galluzzi et al., 2016; Gilbert, 2012; Hu and Sun, 2016; Luo et al., 2016; Makkouk and Weiner, 2015; Vermaelen, 2019) .

These data demonstrate the effects of elevated localised eGFP expression in conjunction with the observed metabolic changes and alterations in cell size (Figures 3.7-3.13). These results add to, and corroborate, the previously-discussed flow cytometry data and further support the idea that internal cellular structural reorganization is occurring. As discussed before, this should translate to improved cellular immunogenicity (Brice et al., 2007; Burgers et al., 2009; Dupuis et al., 2000; Galluzzi et al., 2016; Kepp et al., 2014). The viral origin and nature demonstrated by the RCR process indicates that this technology is well suited for the induction of a strong Type I interferon immunogenic response (Chen et al., 2013; Cheung, 2015; Diner et al., 2015; Galluzzi et al., 2016; Kepp et al., 2014; Kumar et al., 2011). Investigating whether the highly immunogenic process, known as immunogenic regulated cell death (ICD), being induced is of high interest experimentally. Investigating this possibility can be done by performing an initial panel of three basic experiments that can be done in TC. These experiments test for the externalization of calreticulin on the outer cell membranes and the excretion of ATP and High Mobility Group Box 1 protein (HMGB1) into cellular media. These are three hallmark signatures of ICD and immunogenic signalling to the immune system. The 'gold standard' for detecting ICD, however, would require an additional animal experiment, whereby a cancerous mouse cell line is

induced to be in an ICD state and then injected into a mouse. If no cancer develops after a few months the unaltered cancer is then injected into the same mouse, a process that gives the mouse the cancer. In this experiment, ICD is proven to have been successfully induced by nothing less than the effective clearance and cure of cancer (Galluzzi et al., 2018, 2016; Kepp et al., 2014). This technology needs to be investigated in this manner to see whether it has this capability. The rapid manner in which this technology can be adapted, by swapping out genes and promoters and combining multiple amplicons, means that one could relatively easily, cheaply and rapidly adapt it to work against virtually any disease or type of cancer. This could make it a powerful research and vaccine development tool.

3.4.4 HIV-1C Gag mosaic western blot and densitometry

Western blot analysis and tissue culture RCA analysis of the RCR- and RCR+ HIV-1C Gag mosaic expression vectors demonstrated that the RCR+ sample was capable of replicating in mammalian cells and that both could express the HIV-1C Gag mosaic antigen interest. The densitometry analysis indicated that similar alterations in gene expression, observed for eGFP and Luciferase, were also occurring for the antigen. This verified that RCR+ and RCR- Gag vectors were working and could therefore be used experimentally for animal testing in Balb/cJ mice. No further quantification of Gag expression was done because luciferase and eGFP were far better reporter genes and therefore expression quantification, done using these, was more accurate and cheaper to perform. Nevertheless, the western blot experiment was important in demonstrating that the technology was functional, using a different gene of interest.

3.5 Conclusions

In conclusion, I was able to successfully test and demonstrate various aspects of the theorised capabilities of the developed technology. This demonstrated that the RCR DNA expression technology developed could create a strong and dynamic amplification of heterologous gene expression. This was accompanied by the observation of an interesting set of morphological and metabolic cellular changes that were induced in affected host cells. These changes hint at a complex and shifting set of genetic responses being activated within affected host cells that were not present in cells transfected with non-replicating equivalent DNA expression vector controls. The experimental evidence also indicates that the expression technology developed can create a meaningful and sustained amplification effect on heterologous gene expression that is compounded over time. The ability to compound improvements over time is something that is completely novel for this technology, in comparison with other DNA expression vectors, and something that is expected to be highly beneficial for generating T-cell immunogenicity. As postulated, it appears that the compounding effects of this technology take hold at the lowest possible transfection levels, tested where they demonstrate the strongest effect. This amplification process then appears to compound until cellular resource depletion and/or Rep self-

limitation effects come into play. It appears though, that at this upper limit, a severe level of cellular strain is observed, suggesting that this limit is possibly close to the theoretically sustainable limit of the host cell. It is also clearly higher than what is obtainable by increasing DNA transfection levels when using the non-replicating RCR- expression vectors. This makes sense, as increasing DNA transfection inevitably increases cellular toxicity from the transfection reagent and also results in increased levels of cytoplasmic DNA (Modra, 2015; Roche, 2014). This ultimately means that DNA transfection cannot be used to reach the upper expression limitations of an individual cell. It appears that the developed RCR DNA expression technology is able to reach far higher levels of heterologous gene expression per cell, which should translate into better immunogenicity (Gilbert, 2012; Williams, 2013).

This evidence has many implications that require further investigation. To achieve further verification and validation of the viability of this technology, it was deemed necessary to continue basic research experimentation using it within a live animal model for *in-situ* analysis. For this research, the Balb/cJ mouse strain was selected as an ideal model as it provides a good experimental model to evaluate this through intramuscular injection of the plasmid constructs to evaluate eGFP expression and T-cell immunogenicity. It has been previously used within our research group, from which knowledge about working with this animal model could be utilised. A murine animal model was also used for eGFP expression experiments in skeletal muscle tissues in a key research paper from which we derived suitable experimental protocols and techniques (Liadaki et al., 2007). This allowed us to use a similar protocol to analyse heterologous eGFP expression, using the developed expression technology *in-situ* and to compare it, to quantify differences *in-vivo* in a live animal model.

Characterising the RCR-amplified DNA expression system, for use as a vaccine development technology, revealed a complex and dynamic amplification process at work that can increase heterologous gene expression in a dynamic manner over time. As this process occurs, it is accompanied by several observable metabolic and structural changes in the host cells operates. These changes manifest primarily as a dramatic reduction in cellular growth rate, estimated as being ~50% slower after 96 h, and a detectable increase of the internal cellular complexity and granularity as well as physical cell size (Figures 3.2-3.6). These fundamental changes are believed to reflect deeper internal alterations responsible for causing the observed cellular metabolic changes. Activating such types of intracellular host response mechanisms was a primary goal of this technology (in addition to improving localised gene of interest or antigen expression levels). Data gathered from expression and cellular analysis indicates that these research goals have being achieved. Direct improvement in the relative localised level of gene-of-interest expression appears to be around ~100%, but of far greater importance was the improvement in relative individual cellular gene expression levels, which appeared to compound with time to eventually approach what appears to be a local cellular maximum. The unfixed fluid ability to compound gene expression gains over time and sustain a highly elevated level of heterologous gene expression from a very low starting point (Figures 3.9-3.13), represents a new DNA vaccine capability

hitherto unrealised in this research field (Kobiyama et al., 2013a; Rangarajan, 2014). This serves as a direct demonstration of this technology's potential to enhance DNA vaccines by increasing local relative levels of antigen concentrations, which should in turn increase immunogenic responses by increasing immune exposure to target antigens, and help break immunotolerance mechanisms (Brice et al., 2007; Collins et al., 2017; Knudsen et al., 2015; Makkouk and Weiner, 2015; Nolz and Harty, 2011; Pennock et al., 2013; Vermaelen, 2019; Wells et al., 1997).

Heterologous gene expression from conventional, non-replicating DNA expression vectors is known to steadily fade after maximal expression levels have been reached (Kirsch et al., 2003). Here I have demonstrated that the RCR+ DNA expression vector is capable of achieving the opposite, with expression increasing over time towards a relative cellular maximum, which in turn also appears to be roughly double that seen from the brightest non-replicating RCR- samples (Figures 3.2 & 3.7).

This vector technology is fundamentally different to the self-replicating RNA vaccine expression systems which are deployed from a DNA vaccine vector. This gene expression technology was developed from a self-replicating RNA replication cycle derived from the RNA replication system of a ssRNA+ Alphavirus. While this system is good at generating T-cell responses (Knudsen et al., 2015; Leitner et al., 2003; Lundstrom, 2016; Schell et al., 2015), our technology is significantly different in that it is the DNA that replicates, and it does so within the host cell nucleus. This gives it unique characteristics and potentially higher long-term stability than replicating RNA-based expression systems (Sasaki and Kinjo, 2010). As a replicating DNA expression technology, our vector system has unique abilities to specifically stimulate particular DNA and nuclear-related PRRs and to initiate PAMP associated with nuclear viral infection and replication. This fundamental difference in operational location should result in a different type of cellular immunogenic response, or at least one that is directed differently from the internal cellular antiviral immunogenic response perspective (Hasson et al., 2015; Kobiyama et al., 2013a, 2013b; Yi et al., 2018). It is possible that these two systems could even be hybridised, with a replicating DNA vector generating a replicating RNA vector – but this remains to be investigated by others.

One of the primary goals in developing this technology was determining its potential to trigger strong internal cellular responses, which should ideally also be highly immunogenic in nature. The observed cellular effects, in response to the introduction of the replicating DNA expression vector, demonstrate that at some level this is happening (although determining the extent of exactly how immunogenic the induced responses are, has yet to be determined). The mere observation of these metabolic and structural changes occurring in cell culture is enough to confirm that the cellular impact of this technology, and the internal metabolic response induced by it, is more profound than what we observe from the non-replicating DNA expression vectors. Observing such cellular effects can be highly informative with respect to the internal cellular state and probable genetic response (Elmore, 2007). Truly decoding the

complexity these observations and their precise nature, however, requires a lot more extensive experimentation.

As complicated as these internal cellular responses are, at this stage it is already clear from the experimental work done here that this technology has demonstrated a novel type of gene expression capability and, critically, the ability to induce strong, cell-altering, internal responses. This ability in and of itself is of high potential value in the prophylactic and therapeutic vaccine fields, and represents a new form of possible metabolic engineering (Nielsen and Keasling, 2016). As has been demonstrated, the RCR technology can simultaneously act to amplify multiple amplicons. It is therefore possible to apply this technology as a research tool to amplify and express a variety of combinations of genes to combined synergistic effect. Such an ability to broadly amplify expression from an array of heterologous genes is an exciting prospect (Faurez et al., 2010; Regnard et al., 2017; Yin et al., 2015). For this reason, I believe that this technology may have a variety of important applications.

Some caution should be exercised, however, with regards to the virus from which this expression system was derived. BFDV is a simple virus consisting of only two genes with a ~2 kbp genome. This virus, like all viruses, and particularly chronically-infecting viruses, has an evolutionary requirement of evading immunogenicity (Gilbert, 2012; Koonin et al., 2015; Virgin et al., 2009). The manner in which it achieves this functionality is not yet fully understood; however, there is evidence that at least some of this functionality is conferred by actions performed by the Rep protein itself, and perhaps the process of RCR (Allan et al., 2012; Amery-Gale et al., 2017; Bonne et al., 2019; Fort et al., 2010; Huang et al., 2016). It would be prudent for further investigation in terms of immunogenicity, as effects conferred by Rep could be detrimental or beneficial to the goals of enhanced DNA amplification and immunogenicity, depending on the mechanism, magnitude and nature of the effects. Similarly, learning about any immune evasion mechanism due to Rep would be helpful in rational vaccine design decision making, as this knowledge can be capitalised upon to improve the chances of obtaining certain desired immunogenic effects (McMichael and Koff, 2014; Nielsen and Keasling, 2016). For example, there exists a vast body of literature relating to engineering genetic responses and overcoming immune tolerances. The complex nature of the internal and external cellular and immune signalling pathways responsible however, makes the notion of directing and controlling these systems far from trivial. Yet it is not improbable that this could be achieved, and various strategies to do so are considered in the literature (Leitner et al., 2003; Luo et al., 2016; Makkouk and Weiner, 2015; Rathinam and Fitzgerald, 2011). Breaking immunotolerance most likely requires a combination of multiple strong forms of immunogenic stimuli, and is arguably a major reason why the generation of this type of immunity has been so elusive and difficult to effectively achieve. An issue that is broadly discussed, and one that conventional DNA vaccines or even inactivated viral vaccines are known to struggle with, is sustaining a meaningful level of stimulation for long enough for the response to not only activate but also evolve and mature into the kind of T-cell response that is long lived, specific and powerful enough to transcend

into the kind of immunogenicity that can be generated from live vaccines (Bolhassani and Yazdi, 2009; Brice et al., 2007; Buchbinder et al., 2008; Burgers et al., 2009; Cole et al., 2015; Cosma and Eisenlohr, 2018; Diner et al., 2015; Galluzzi et al., 2016; Gilbert, 2012; Hokey and Weiner, 2006; Kepp et al., 2014; Kobiyama et al., 2013a; Kutzler and Weiner, 2008; Leitner et al., 2003; Li et al., 2012; Ljungberg and Liljestrom, 2015; Marino et al., 2011; McNeel et al., 2012; Nielsen and Keasling, 2016; Nordström et al., 2005; Rodriguez et al., 2002; Schell et al., 2015; Stephenson and Barouch, 2013; Wahren and Liu, 2014).

4. Testing RCR expression and antiviral response in Balb/cJ mice

4.1 Introduction

The experiments reported in this Chapter had several research goals in mind. The first was to determine the longevity of foreign gene expression within a live animal model. The second was to evaluate the changes in overall expression within the animal model, and to compare this with what had been observed in tissue culture, while looking for correlations that could indicate RCR amplification was working and was causing changes in eGFP expression, compared to controls. One of the more difficult aspects to assess was the rate of RCR and the change this makes in relation to time. In tissue culture (Chapter 3) I determined that the RCR process proceeds through a somewhat stable and steady increase in gene expression per cell which eventually takes virtually all transfected cells towards an extremely high level of gene expression, at which point the cellular health and stability of the cells is compromised. In order to test the DNA expression technology in an animal model, therefore, two pilot animal experiments were designed to be run in Balb/cJ mice. These experiments investigated two key areas of interest. The first pilot study looked at differences in eGFP expression between the RCR+ and RCR- eGFP vectors and a third group which combined the RCR+ eGFP vector with the pTHRep vector, in a co-inoculation regiment designed to evaluate the effect of bolstering overall Rep expression. The idea of this experiment was to assess the overall expression of eGFP in the inoculated mice muscle tissue one-month post inoculation, to determine if processes observed in tissue-cultured cells were also occurring within the mouse muscle tissue. Evaluating RCR+ and RCR- vectors allowed me to look for changes in overall expression; including a 3rd pilot group with RCR+ eGFP, boosted with additional pTHRep, expressing Rep under a powerful promoter which allowed me to test whether the rate of RCR can be increased transiently by the expression of extra Rep within the live animal model.

High quality T-cell immunogenicity is one of the more complex and elusive forms of immunity to generate, research has shown that when it comes to T-cell immunogenicity, the quality and magnitude of a T-cell response do not always correlate (Panagioti et al., 2018). There are many reasons for this but, simply put, the inordinate level of complexity of the intracellular biochemical immune signalling pathways, and the complex combination of immunogenic stimuli that require activation, is difficult to replicate with an inanimate and ultimately artificial immunological threat such as a vaccine (Vermaelen, 2019). To investigate the extent RCR technology can induce a differential antiviral gene response, a RT^2 profiler antiviral response gene array from Qiagen was used to evaluate differences in a selection of 84 important antiviral response genes. Based on our knowledge of RCR and the PRRs that RCR amplicons could stimulate, assessing the antiviral and DNA damage response genes would be a logical

target set of genes that may become differentially activated by a self-replicating plasmid (using RCR technology) in comparison to non-replicating DNA vaccines. As the antiviral response gene array also includes some DNA response genes, it was the logical choice to start with; however, while a larger set of genes and multiple arrays would be ideal, for the purposes of this pilot experiment (to identify differential gene expression), the antiviral response gene array was sufficient (Diner et al., 2015; Illingworth and Bird, 2009; Knipe, 2015).

As part of the effort to determine the immunogenicity of the candidate vaccine, a pilot immunogenicity experiment, to evaluate the interferon gamma response generated from the HIV-1C Gag mosaic RCR+ and RCR- vaccine variants, was designed. This pilot experiment was designed to maximise the ability to differentiate advantages that might be gained from RCR technology, and was set up as a dual inoculation regiment using low inoculation concentrations. This was to demonstrate the possible capacity that RCR expression technology might have in terms of reducing dosage requirements of DNA vaccines.

4.2 Materials and Methods

Animal research ethics approval was obtained from the UCT Health Sciences Animal Ethics Committee (AEC) in accordance with the Faculty of Health Sciences rules and regulations (AEC approval # 017/016).

4.2.1 Animal husbandry, welfare and care of Balb/cJ mice

Animal research experiments used female Balb/cJ (Jaxson Labs; USA) mice, bred as strain UCT4 at the specific pathogen free (SPF) level 2 animal breeding facility at UCT. After 8-10 weeks they were transferred to the UCT Research Animal Facility (RAF) where they remained for the duration of the study. Here the mice were housed, fed and monitored by the trained and certified RAF staff using the specialised facilities and equipment within the facility according to their standard operating procedure (SOP). All inoculations and procedures were performed on the animals by an experienced animal technologist.

4.2.2 Handling and inoculations

Mice were kept in groups of three and acclimatised to their environment for one week before inoculations were performed. Each mouse received a single 50 µl inoculation in the anterior tibialis muscle of the right hind limb on Day 0. The inoculations for the groups are outlined in Table 4.2.2.

Table 4.2.2. Inoculation dosages for murine eGFP quantification

Mouse Group	DNA included in inoculum			Total volume
	RCR+ eGFP	RCR- eGFP	pTHRep	
Group 1	50 µg	-	-	50 µl
Group 2	-	50 µg	-	50 µl
Group 3	50 µg	-	10 µg	50 µl
Neg Control	-	-	10 µg	50 µl

4.2.2 Animal euthanasia procedure and tissue harvesting

The mice were euthanised by exsanguination under general anaesthesia with ketamine/xylazine (200 µl per 20 g mouse) administered via intraperitoneal injection. Pedal reflex was used to determine depth of anaesthesia. If insufficient after 20 minutes, an additional ½ dose of ketamine/xylazine was administered. No pedal withdrawal after stimulation indicated that the depth of anaesthesia was sufficient for cardiac puncture and exsanguination. Animals were placed in dorsal recumbency, and a 26G needle was inserted adjacent the xiphoid cartilage and into the heart. A maximum of 1.8 mL of blood was collected and stored at 4 °C (Diehl *et al.*, 2001). Exsanguination lasted between 1-3 minutes and therefore no warming, ocular lubrication or any other protocol while under anaesthesia was required. Death was confirmed by cervical dislocation of the neck. Thereafter their spleens and the anterior tibialis muscle of the inoculation site were harvested, placed in RPMI media, and put on ice.

4.2.3 Muscle tissue preparation and sectioning

To preserve eGFP expression a published protocol (Liadaki *et al.*, 2007) was used. The harvested anterior tibialis muscle was fixed in 4% paraformaldehyde in PBS at 4°C overnight and then saturated in sterile 20% sucrose in PBS (0.22 µm filtered), for 4-24 h. The sample was then embedded in Frozen Section Compound (FSC) 22 (Leica, Germany) and frozen at -80°C until sectioning.

Sectioning was performed on a CM 1850 cryostat (Leica) where two 10 µM and two 20 µM cross sections were made for each muscle tissue at a depth of ¼ and ½ way through the muscle tissue. Longitudinal sections were also made for each sample, ½ way through the tissue collecting two 10 µM and two 20 µM (as before). Slides were treated with a drop of Mowiol containing ~10 mg per ml n-propyl gallate as an antifade reagent. Cover slips were added, and samples allowed to dry overnight at RT, and stored at 4°C until confocal microscopy.

4.2.4 Confocal microscopy of muscle sections

A ZEISS LSM 880 Airyscan confocal microscope was used to quantify eGFP fluorescence in sectioned mouse muscle samples using a similar method as described previously in (Section 3.2.3.). However, this time image capturing was done as a series of z-stacks run in tile scans of up to 8x8 images and merged into a single giant z-stack image file for the full muscle cross section. This was transformed

into a maximum intensity projection for fluorescence quantification in the manner previously described (Section 3.2.3). This was only done for muscle cross sections where individual muscle fibre bundles could be identified and selected. Data was then tabulated and analysed in MS Excel. All images taken were done so using identical exposure and capture settings calibrated to the brightest fluorescence found in the sample to prevent the possibility of overexposure. Positive fluorescence was identified as those muscle fibre bundles exhibiting fluorescence readouts at least 2σ higher than the average background autofluorescence level recorded for the negative control. Data was normalised by quantifying the relative background fluorescence of untransfected muscle fibre bundles for each sample and subtracting this from the average positive muscle fibre bundles readout to determine the fluorescence attributable to eGFP as the true readout.

For longitudinally sectioned samples, an entirely different method of data analysis and quantification was employed. This was done using ImageJ Fiji, public software suite, (Open Source, Github) to calculate the mean integrated density of eGFP fluorescence over the entire longitudinal sectioned Z-stack tile scan. A cut-off threshold of 2σ from the mean of the negative control was used to eliminate background and autofluorescence and this was applied to all images. This method was completely unbiased in nature and no normalization was used (Collins, 2007; Cruz, 2016; Gray et al., n.d.). This raw data was graphed for comparison with the analysis performed on the muscle cross sections.

4.2.5 Antiviral Response RT² Profiler PCR Array

To identify any unique alterations in gene expression, 84 key antiviral response genes were evaluated using Human Antiviral Response RT² Profiler PCR Arrays (Qiagen, USA). In this experiment, DNA transfections were carefully controlled so that the same amount of total DNA was transfected in each sample using the exact same amount of transfection reagent. To achieve this, pUC19 was used as a filler plasmid and as a non-expressing DNA transfection negative control. The RCR+ and RCR- Gag expression vectors, as well as the pTHRep and RCR+ eGFP vectors, were evaluated for their induction of antiviral response genes in comparison to the pUC19 plasmid (as the negative control). Plasmids were transfected into HeLa S3 cells seeded at ~20% confluency in six well plates that were then grown to ~70% confluency (~48 h) before transfections were performed using standard transfection protocols. Each experimental plasmid was added in a 5:1 ratio with 5 sample plasmid DNA to 1 part pUC19 filler plasmid or 1 part pTHRep used to boost RCR, with a negative control that used only a pUC19 plasmid. Cells were cultured under standard conditions for 48 h, after which RNA was extracted using RNEasy Plus mini kit (Qiagen). RT^2 profiler array analysis was performed by the centre for proteomic and genomic research (CPGR, RSA) who also did quality control testing on the RNA samples before the arrays were run on an ABI QuantStudio 12K Flex qPCR (Invitrogen, USA). Data analysis was performed in MS Excel with the use of a template document developed specifically for RT^2 profiler array and provided by Qiagen through their website. A cut-off threshold was set at 1.5 fold change in

gene expression for positive identification of relevant alteration in gene expression. This level was chosen to aid in the identification of altered gene expression profiles because FACS had identified that HeLa S3 transfections were ~20% efficient. This meant the true change in gene expression per cell should be ~5 times higher than that reported by the RT^2 profiler array, which justified using the lower threshold. Furthermore, in terms of data normalization of the array, one of the best methods is to normalize RNA array data against, is to make use of a carefully selected set of housekeeping genes that are stably expressed in all cells (Jacobsen et al., 2009). The Qiagen gene arrays uses this method with five selected housekeeping genes for its arrays, to ensure high quality and accurate data normalization. Because this method of normalization was used, it also helped justify the reduction of the cut-off threshold from the standard 2.0 to 1.5fold change. The data normalization is performed automatically when analysing the Qiagen MS Excel template for analysis of the array data. Analysis was done per manufacturer instructions, and all gene expression changes were recoded with relevant level of significance of each finding above the threshold (available in Appendix D).

Because these arrays work by benchmarking sample data against the control data, by normalizing the data with five known housekeeping genes, it becomes possible to run additional cross comparisons between data sets individually as well as against the negative control. This allows for additional semi-independent analyses of the array data to be made. They remain semi-independent because the sample data remains the same. Two of these additional analyses were done to provide additional supporting evidence and possibly identify new unique alterations in gene expression not detected by the primary comparisons. In the primary comparison all samples tested were evaluated against a pUC19 negative control. This was the perfect baseline negative control because the pUC19 vector is essentially the non-expressing backbone of all the other DNA vectors used. It contains the same core DNA sequence as all the plasmids tested with none of the mammalian expression genetics. Primary analyses with pUC19 used the same concentrations of DNA and transfection reagent. These components are known to be capable of influencing gene responses, which made pUC19 an ideal primary control. However, in terms of comparing RCR+ and RCR- vectors, pUC19 was not the ideal control. Here the use of additional cross comparisons between the RCR+ and RCR- vectors helped generate more usable data from the gene arrays. The first direct comparison was the RCR+ vs RCR- Gag vectors. This presented the ideal control data set for evaluating the effects of RCR while still controlling for any independent effects from Gag expression. Cross sample analysis was also performed with the combined RCR+ and pTHRep sample versus the RCR- Gag sample datasets. In this way differences detected in one analysis of sample datasets can be cross examined and ideally corroborated with the additional cross comparisons to strengthen overall findings. It is therefore important to keep in mind which samples are being compared and which sample was used as the reference control when discussing the array results.

4.3 Results

4.3.2 Evaluation of eGFP expression in Balb/cJ mice

Confocal microscopy was used to quantify eGFP expression in mouse muscle cross sections. Tissue sections of negative control mouse samples indicated a uniform level of eGFP fluorescence from all muscle fibre bundles as expected. This was recorded and used to define the cut-off threshold for positive fluorescence detection. The fluorescence of the RCR+ eGFP transfected muscle samples and that of the RCR+ eGFP and pTHRep boosted sample both exhibited brighter eGFP fluorescence than the RCR- eGFP samples 28 days post inoculation. The presence of a few exceptionally bright muscle fibre bundles was noted only in the RCR+ eGFP with pTHRep boosted samples (Figures 4.1 and 4.2).

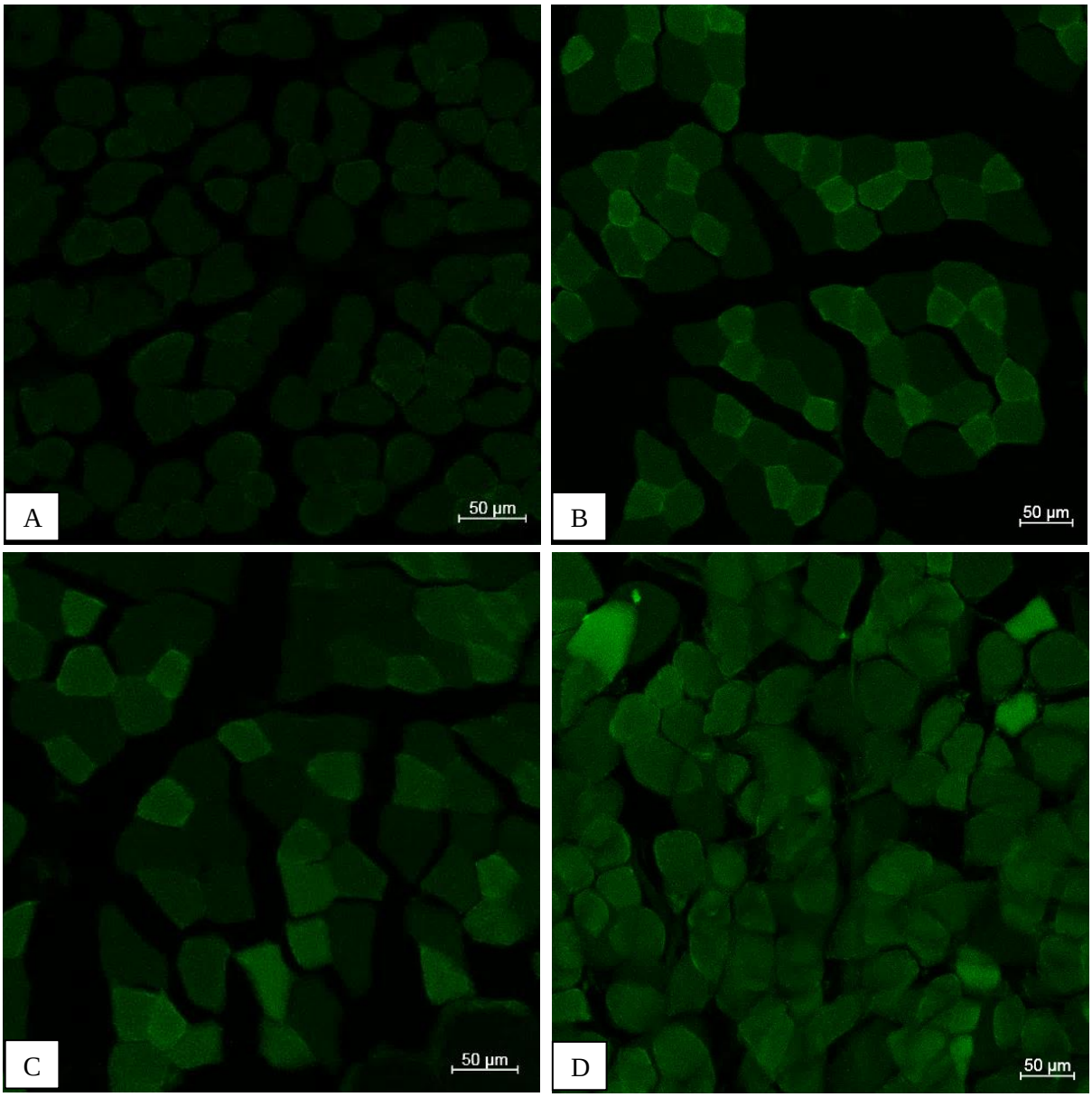

Figure 4.1 Cross section examples of the anterior tibialis muscle of Balb/cJ mice in green channel for eGFP. Inoculated with: A) pTHRep only (Neg control), B) RCR- eGFP, C) RCR+ eGFP and D) RCR+ eGFP and pTHRep.

The ability to see differences in eGFP fluorescence with the naked eye is limited; it is clearer when the green (eGFP) and blue (nucleus) channels are combined. With the blue DAPI channel visible the multinucleate nature of skeletal muscle is depicted clearly (Figure 4.2).

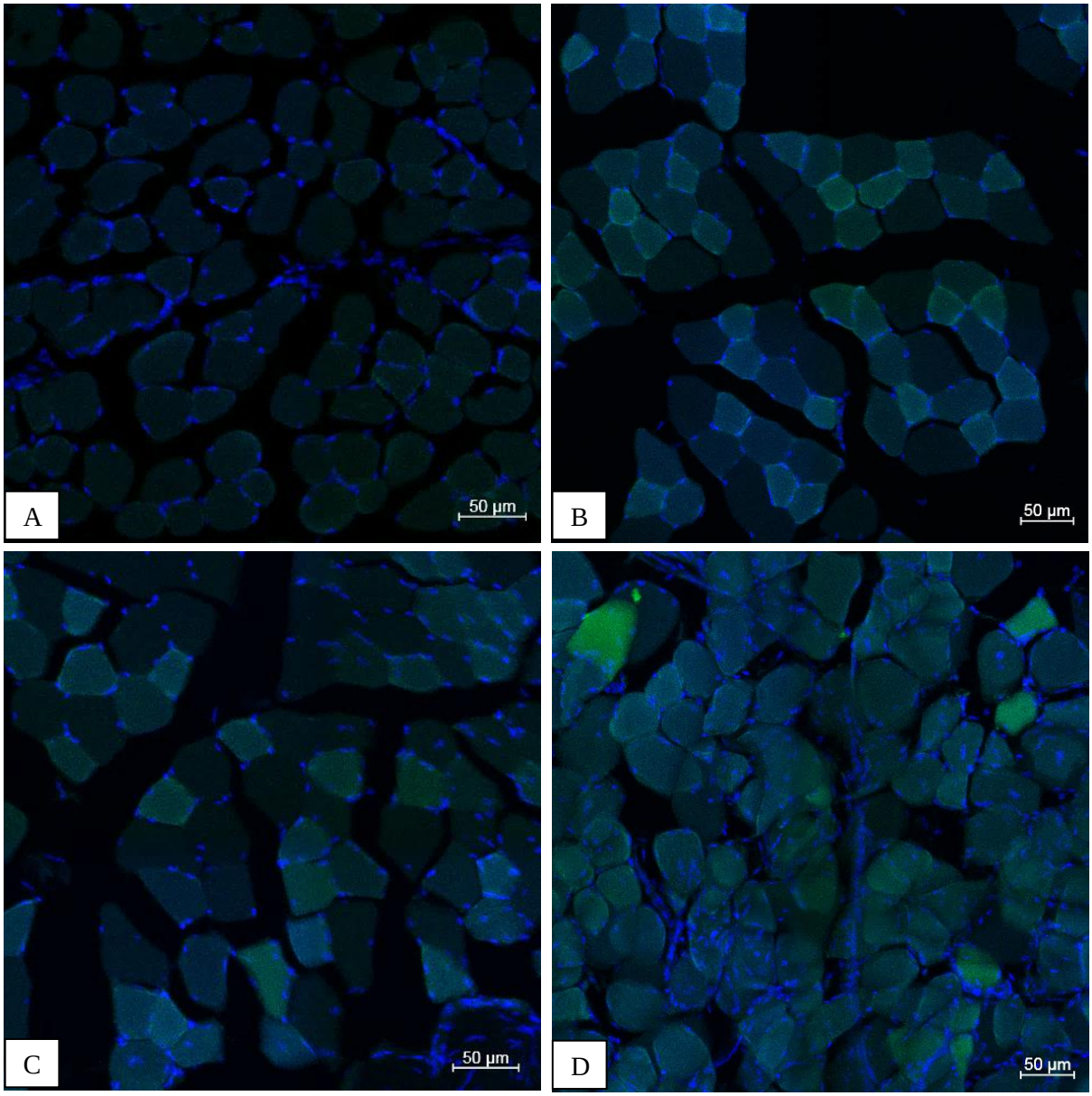

Figure 4.2 Cross section examples of the anterior tibialis muscle of Balb/cJ mice in green for eGFP and blue for cellular nuclei. Inoculated with: A) pTHRep only (Neg control), B) RCR- eGFP, C) RCR+ eGFP and D) RCR+ eGFP and pTHRep.

To capture as much image data as possible from each anterior tibialis muscle cross section, tile scan images of up to 8x8 Z-stack captures were taken and merged together. These images gave a great overview over the whole muscle cross section: these merged images are depicted in Figure 4.3. Overall it was evident that for the RCR- samples there was noticeably more fluorescence, but this exhibited in uniform in nature. In contrast to that the RCR+ vector inoculated samples clearly exhibited greater variance in fluorescence brightness between individual muscle fibre bundles (Figure 4.3).

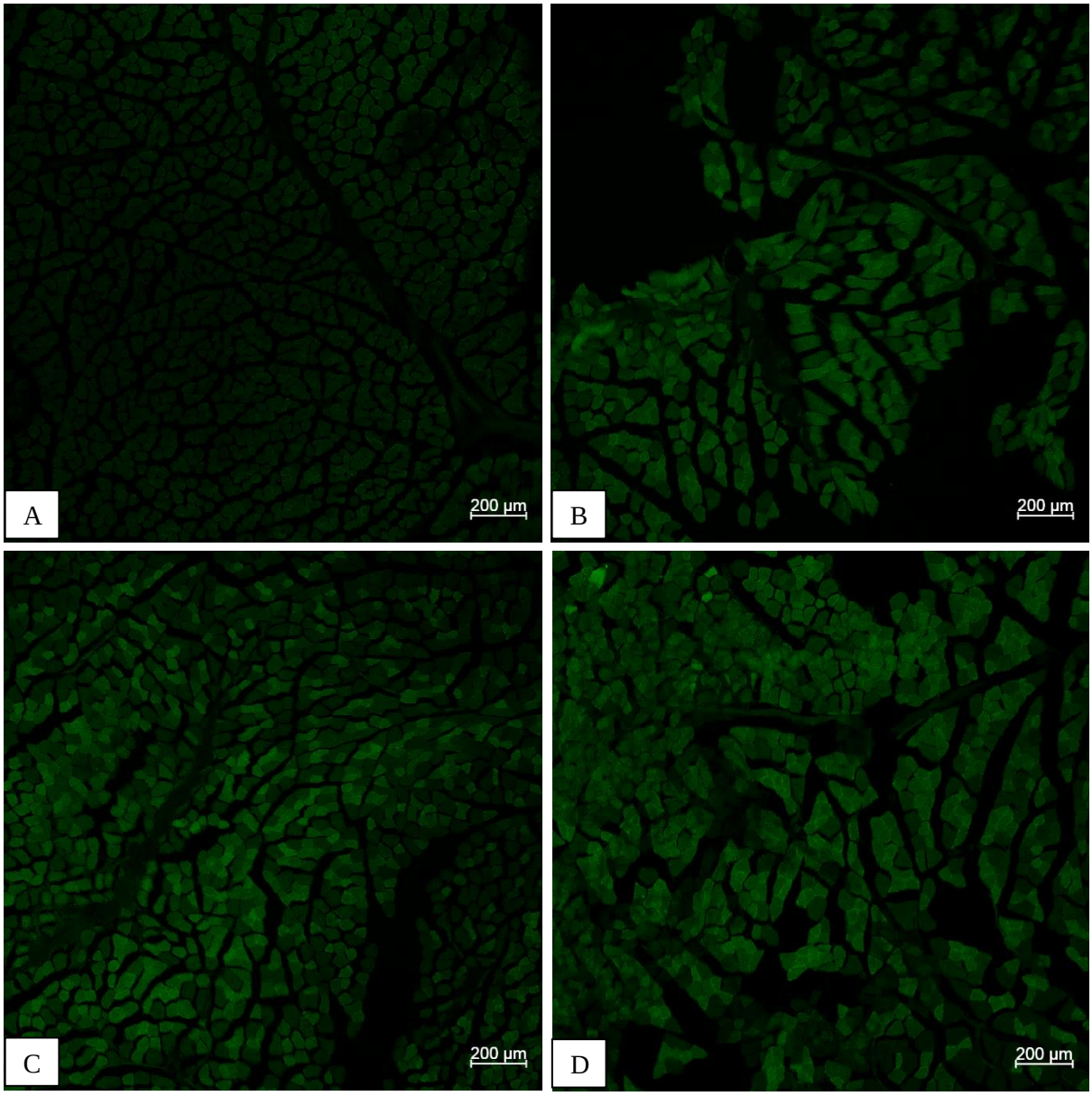

Figure 4.3 Merged tile scan images cross sections of anterior tibialis muscle of Balb/cJ mice showing the green capture data. Inoculated with: A) pTHRep only (Neg control), B) RCR- eGFP, C) RCR+ eGFP and D) RCR+ eGFP and pTHRep.

To quantify gene expression in the mouse muscle tissues, confocal microscopy was used to evaluate the relative mean eGFP fluorescence of individual muscle fibre bundles from the different inoculation groups of mice (Figure 4.4). The mean fluorescence of the brightest 100 muscle fibre bundles was recorded from each mouse muscle tissue sample and normalized by subtracting the mean background/autofluorescence signal to determine a true signal. These data were then depicted as a relative percentage change and their significance was calculated by ANOVA using ($p=0.5$). A minimum signal cut-off value was also set as two standard deviations ($2\ \sigma$) of the negative control this was 20%. This analysis indicated that the RCR- eGFP sample had a mean eGFP fluorescence level in affected muscle fibre bundles that was 129 +/-5% brighter than the background/autofluorescence level. Tissue

inoculated with RCR+ eGFP vectors were ~170% brighter than negative/background levels, and tissues inoculated with both RCR+ eGFP and pTHRep were ~217% above background levels (Figure 4.4). The standard error of the mean fluorescence from between the three tissue samples from each mouse was calculated for Figure 4.4 to be +/- 6% for the RCR- sample +/- 16% for the RCR+ sample and ~+/- 23% for the RCR+ eGFP and pTHRep sample. An ANOVA was also performed for all 300 readings made (100 per sample) which indicated the differences in means were highly significant (p>0.99). Changing variance and fluorescence range between samples was also observed warranting further statistical investigation.

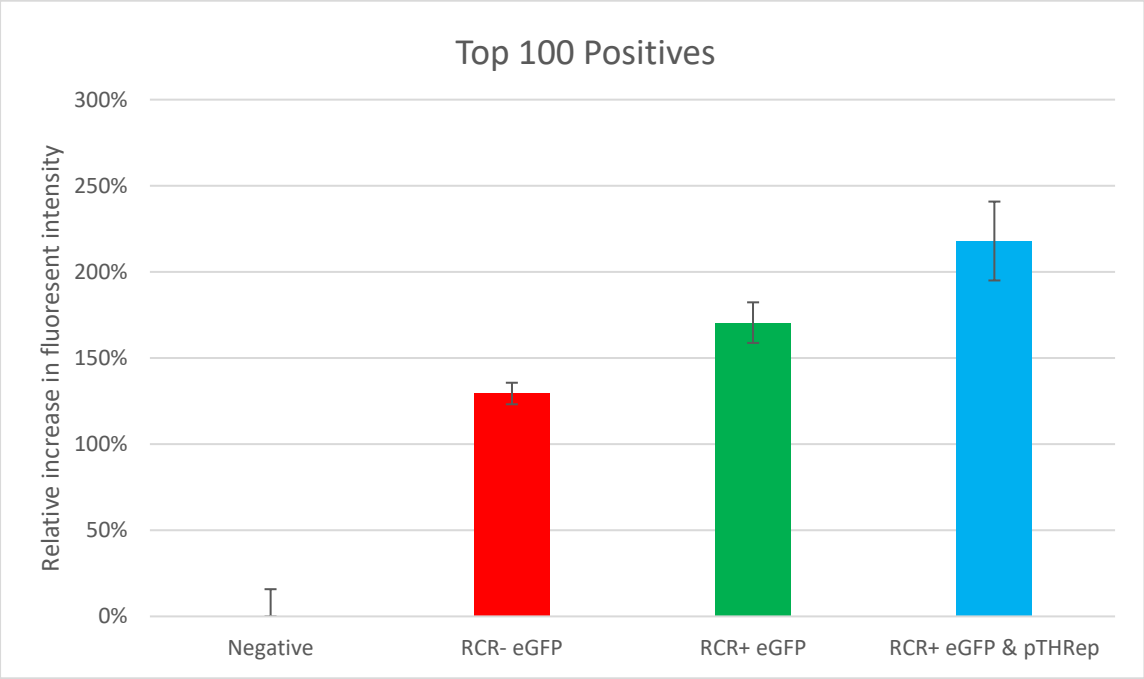

Figure 4.4 Relative change in fluorescence intensity in muscle fibre bundles of Balb/cJ mice. The mice were inoculated with 50 µg either RCR+ or RCR- eGFP expression plasmid and 10 µg pTHRep plasmid as indicated in 50 µl sterile PBS. Negative control was inoculated with PBS only. (Error bars = standard error of 3 sample mean & Neg control = 2σ).

Descriptive statistics were generated from the data analysis which revealed several interesting characteristics to the data that are of interest and not visible in the graphical analysis of the mean fluorescence shown in Figure 4.4. These statistics are tabulated below in Table 4.1. Several informative figures stand out. The 99% confidence interval for the mean from 300 recorded fluorescent fibre bundles, (100 per sample) increases across the samples with increasing fluorescence ranging from 3 to 6% (p=0.99), indicating that the differences in mean eGFP fluorescence are highly significant. The variance goes from ~0.05 for RCR- to 0.10 for RCR+ and 0.18 for RCR+ & pTHRep samples indicating the RCR technology increasing the variance of the eGFP expression distribution. This is corroborated by a similar upward shift in the standard deviations and range statistics which is particularly altered in the RCR+ & pTHRep sample. The RCR- sample is more heavily positively skewed than the samples

containing RCR+ vectors, indicating the lower frequency of highly fluorescent muscle fibre bundles. This is corroborated by the medians which shift upward for the RCR+ and RCR+ & pTHRep samples. The standard error in table 4.1 is calculated from 300 readings 100 per mouse tissue sample while in the graph it is calculated from the 3 averages of those 100 readouts. It is important to recognise that this variance observed experimentally and, in the statistics, is in line with our expectations for the RCR expression technology, which by nature should be producing increases in variance and fluorescence range.

Table 4.1: Descriptive statistics of the eGFP fluorescence readouts in mouse muscle tissues

Descriptive statistic	RCR- eGFP	RCR+ eGFP	RCR+ & pTHRep
Mean	1.294032	1.705453	2.179297
Standard Error (300 read)	0.013241	0.018735	0.024444
Median	1.247412	1.630581	2.161605
Standard Deviation	0.229348	0.324495	0.423382
Sample Variance	0.052601	0.105297	0.179252
Skewness	1.693743	1.035241	1.030763
Range	1.6272	1.733269	3.022745
Minimum	0.979584	1.220332	1.480126
Maximum	2.606784	2.9536	4.502871
Sum	388.2097	511.636	653.7891
Confidence Level(99.0%)	0.034327	0.048567	0.063368

It was noted that in the RCR+ eGFP and pTHRep samples there were a few muscle fibre bundles that exhibited extremely high levels of variance above the background with notably brighter levels of eGFP expression (Figure 4.5). To demonstrate this, the relative change in the mean eGFP fluorescence for the brightest muscle fibre bundle was recorded independently to be ~450% (red) (Table 4.1: maximum) above the background/negative control level. Only samples that had been inoculated with both the RCR+ eGFP and pTHRep vectors exhibited such high extremes in fluorescent levels. These bright outliers account for the increased margin of error overall for the RCR+ eGFP and RCR+ eGFP with pTHRep samples. In addition to this, some tiny localised hotspots within muscle fibre bundles were also identified to have extremely elevated eGFP fluorescence levels. The brightest one of these had a recorded fluorescence level that was ~650% (Figure 4.5: yellow arrow) higher than the background/negative reference level, which is >5 fold higher than the RCR mean and >2 fold higher than the RCR- maximum recorded level. Highly fluorescence fibre bundles and localised extremes like these were only seen in samples inoculated with RCR+ vectors. In addition to this, it appeared that, on average, transfections using RCR+ vectors appeared to have a higher count of fibre bundles that could be definitively identified as being positively transfected by having mean fluorescence levels of at least 2σ above the background/negative fluorescence mean.

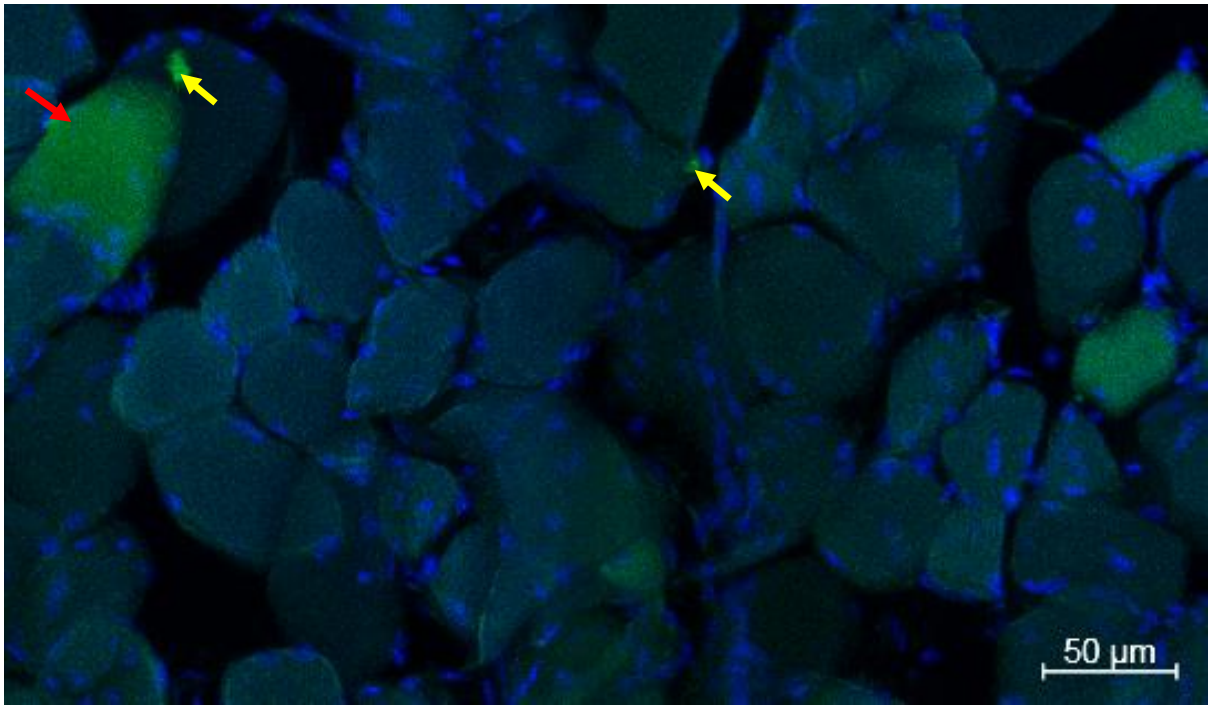

Figure 4.5 Hyper expression of eGFP in Balb/cJ mice muscle fibre bundles inoculated with RCR+ eGFP and pTHRep vectors. The muscle fibre bundle (red) exhibited eGFP fluorescence ~450% elevated over negative control autofluorescence levels. While the identified hotspot (yellow) had ~650% brighter fluorescence. Blue fluorescence is from Hoechst-stained nuclei surrounding the multinucleate muscle fibre bundles.

In addition to the cross-sectioning analysis, the mouse muscle tissues were also sectioned longitudinally (Figure 4.6). As with cross sections, confocal microscopy was used to quantify fluorescent image data of the longitudinal muscle tissue sections. Low background fluorescence was detected from the negative control as before and used to establish a cut-off threshold. Tissue samples inoculated with the RCR- eGFP vector had visibly more eGFP fluorescence than the negative control. While tissue samples inoculated with RCR+ eGFP vectors also had notably brighter fluorescence than that of RCR- eGFP inoculated samples (Figure 4.6). Fluorescence from tissue samples inoculated with both the RCR+ eGFP and pTHRep vectors could not be readily differentiated from the RCR+ eGFP samples. In general, it was harder to evaluate fluorescence from the longitudinal muscle sections; however, it appeared that the RCR+ eGFP and pTHRep samples did have a few instances of notably higher eGFP fluorescence in select muscle fibre bundles (Figure 4.6: red arrow).

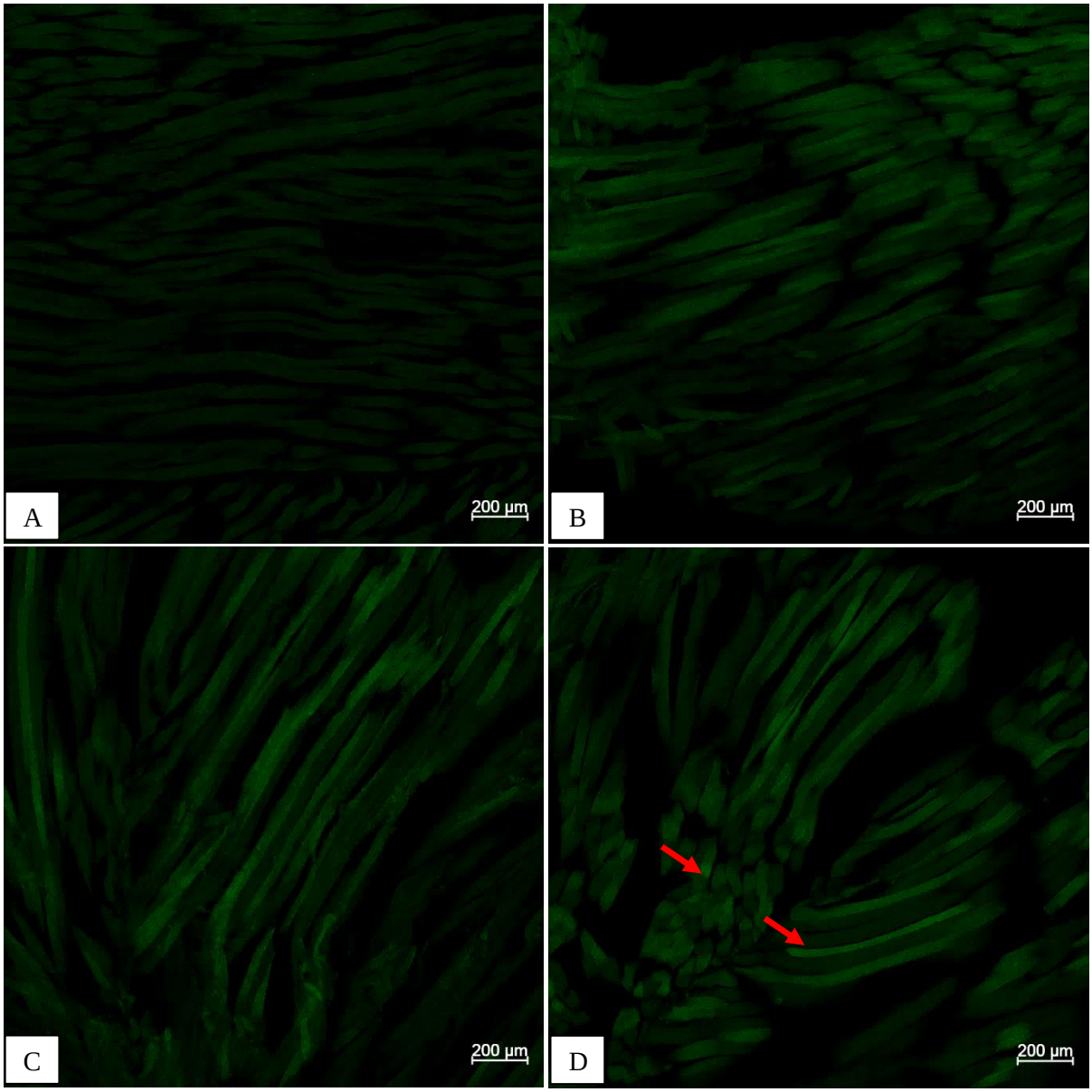

Figure 4.6. Longitudinal sectioning examples of the anterior tibialis muscle of Balb/cJ mice. Inoculated with: A) pTHRep only (Neg control), B) RCR- eGFP, C) RCR+ eGFP and D) RCR+ eGFP and pTHRep, (n=3).

Identifying differences in eGFP expression using only green channel image data was challenging; however, merging the blue channel or transmitted light channels assisted in visual inspection to spot differences in brightness (Figure 4.7: red arrows).

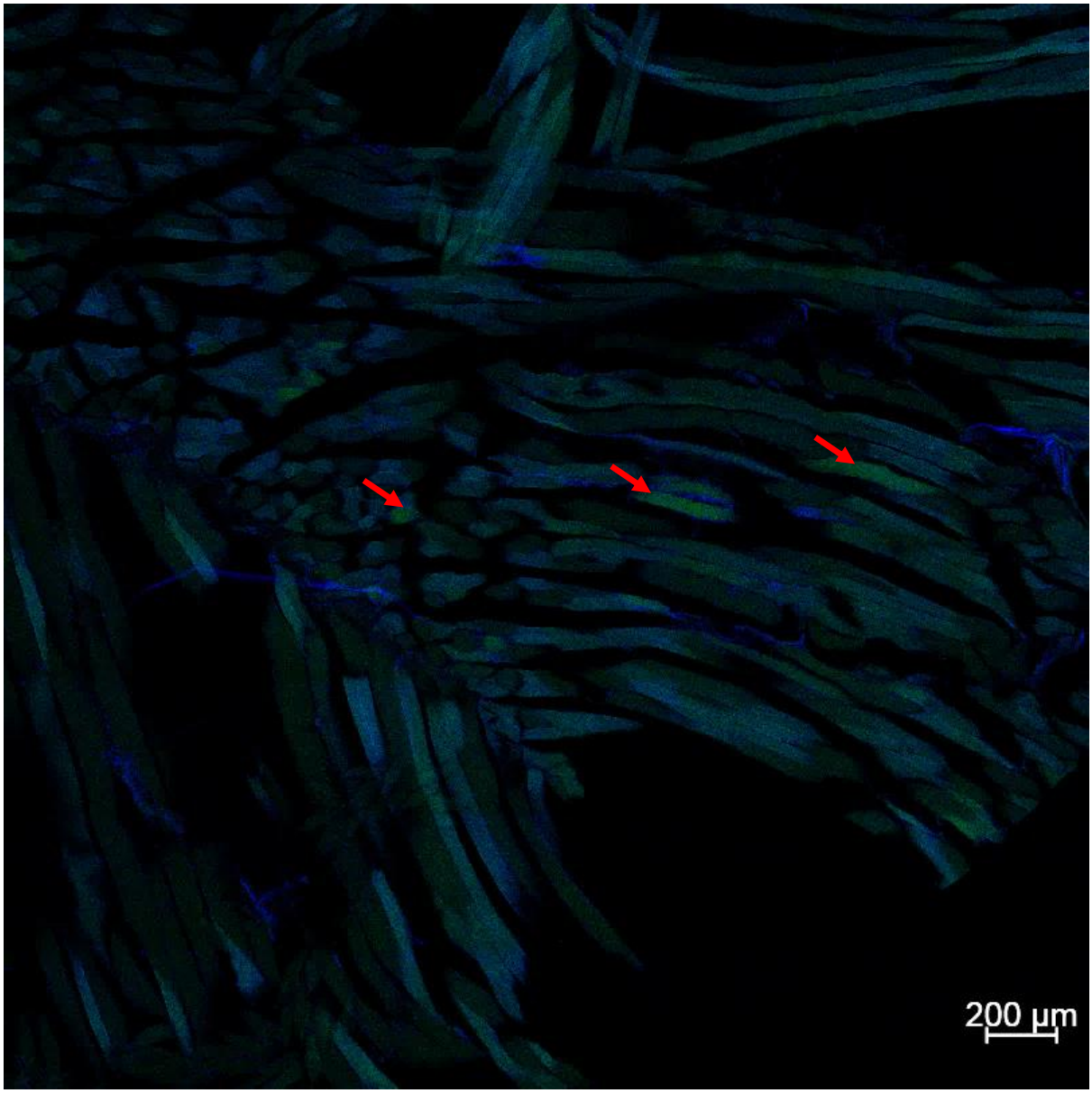

Figure 4.7. Longitudinal section of the anterior tibialis muscle of Balb/cJ mice. Inoculated with RCR+ eGFP and pTHRep.

Analysis of eGFP fluorescence from longitudinal muscle sections was challenging; accordingly, an entirely different image thresholding method of analysis and quantification was used to calculate the mean integrated density of the eGFP fluorescence across the Z-stacked tile-scan and graphed (Figure 4.8). This different type of analysis generally corroborated well with the previous analysis done on muscle cross sections, indicating an increase in the mean eGFP fluorescence signal across the whole tile scan image for the RCR+ eGFP samples compared to the RCR- eGFP samples. It also indicated the RCR+ eGFP and pTHRep samples had greater variance and a higher estimated mean compared to the RCR+ eGFP samples alone, due to the more crude nature of this type of analysis, with a single readout across the whole image tile scan as well as lacking the ability of normalizing the data. This produced greater margins of error (Figure 4.8).

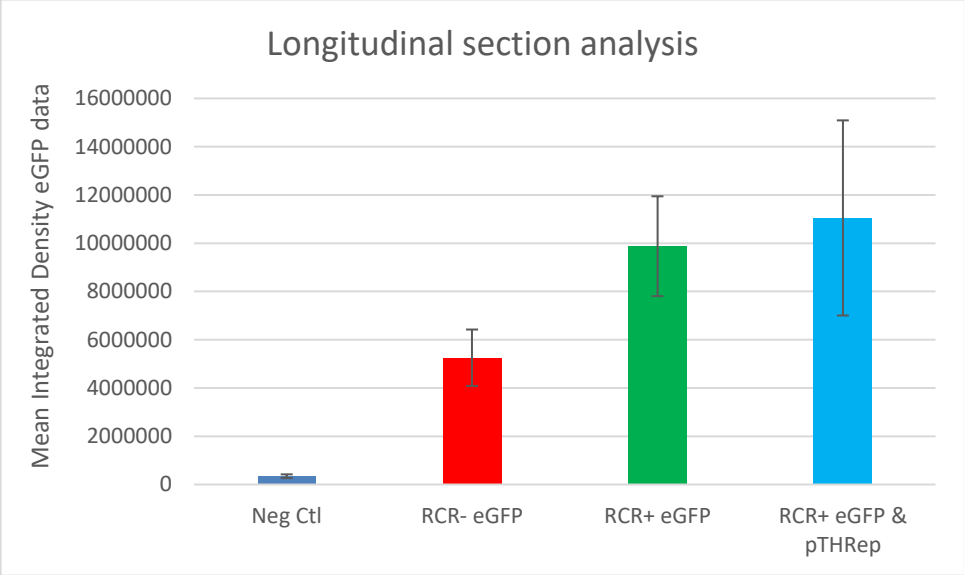

Figure 4.8 Relative change in eGFP fluorescence in longitudinal sections of the anterior tibialis muscle of Balb/cJ mice. The mean integrated density of the green fluorescent channel image data from maximum intensity projections after thresholding values below 2σ of that of the negative control sample (n=3) error bars = standard error.

4.3.3 Evaluation of Antiviral response genes by RT^2 profiler array

The pilot RT^2 profiler gene array identified 9 potential unique antiviral response genes as having evidence of being upregulated by the transfection of the test gene expression vectors, compared to the pUC19 negative control (Figure 4.9). Several differences in gene expression profile were identified when comparing the RCR+ and RCR- Gag expression vectors. Notably, the RCR+ Gag vector appears to prominently increase the expression levels of Interleukin 12B, (IL12B), Caspase Recruitment Domain Family Member 9, (CARD9) and (to a lesser extent) increase C-X-C Motif Chemokine Ligand 11, (CXCL11) and C-C Motif Chemokine Ligand 5, (CCL5). In comparison, the non-replicating RCR- Gag vector only increased CARD9 expression among those mentioned. It also upregulated expression of Mediterranean fever, aka pyrin innate immunity regulator (MEFV), which was not altered by the RCR+ Gag vector.

The controls inoculated with only pTHRep, which expresses Rep at high levels, induced several unique gene expression alterations compared with the pUC19 negative control, which expresses no genes. Under these high Rep expression conditions, CARD9 was the most upregulated of all the upregulated genes. This vector also induced detectable increases in CCL5 expression as well as MEFV, DExH-box helicase 58 (DHX58) and Interferon Regulatory Factor 5 (IRF5). When pTHRep was coupled with RCR+ Gag vector, to boost RCR, the same genes were upregulated except for MEFV, which did not appear to be upregulated. This coupled reaction also uniquely appeared to upregulate MX Dynamin Like GTPase 1 (MX1).

The alternative replicating test vector (RCR+ eGFP vector) showed evidence of upregulation of IRF5, as well as increased CARD9, CCL5, DHX58 and C-X-C Motif Chemokine Ligand 8 (CXCL8) expression levels.

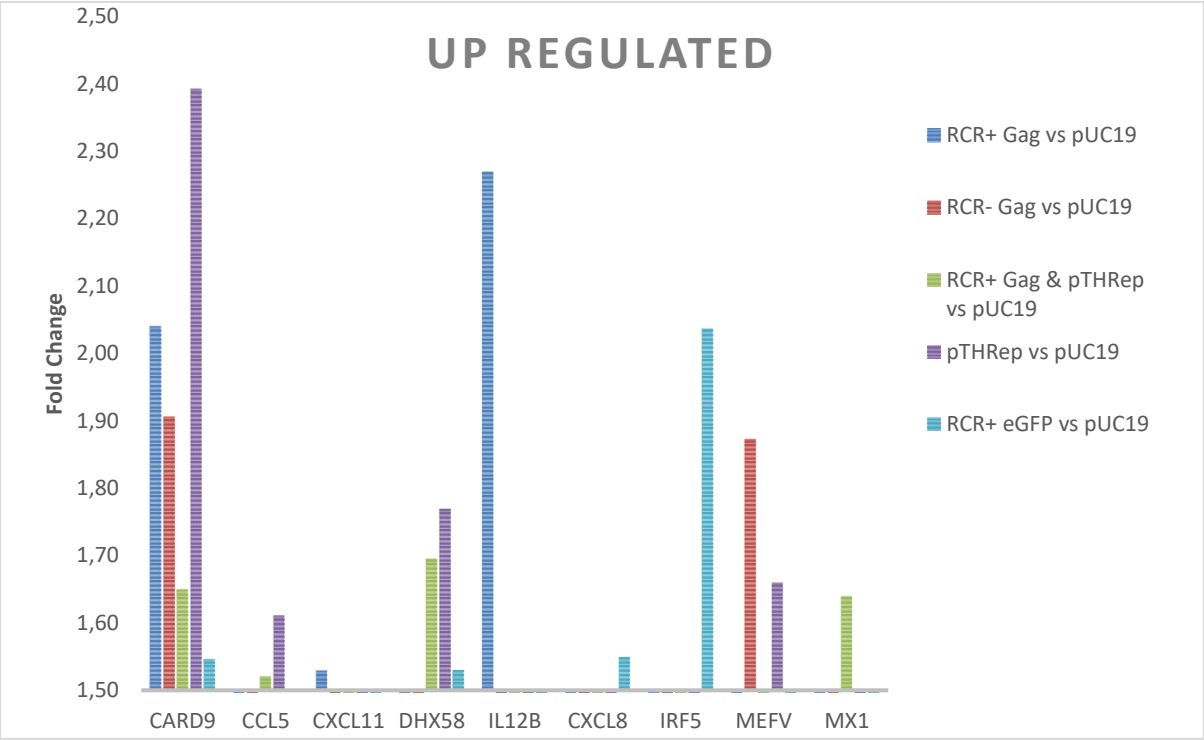

Figure 4.9. Upregulated antiviral response genes in HeLa S3 cells transfected with DNA expression vectors as compared to transfections using pUC19 DNA as the negative control standard. The legend on the right indicates the sample data gathered and how it compares to the negative control used, the pUC19 plasmid.

Four downregulated antiviral response genes were also identified (Figure 4.10). Of these, the downregulation of CASP10 in response to the pTHRep vector stood out prominently as the most downregulated gene, with a ~3.6-fold decrease in expression. This finding also had the highest level of statistical significance in the array experiments ($p=0.0068$). This was also observed in the combined RCR+ Gag and pTHRep sample at a lower magnitude of -1.8 fold, ($p=0.09$). All fold changes and their respective p-values are available in Appendix D. The only other gene identified as been possibly downregulated was Interferon Beta 1 (IFNB1), but this was likely to be a false positive due to its weak p-value ($p=0.43$). The p-values of MX1 and CXCL8 were sufficiently high enough to indicate the lack of evidence that their expression had been altered (they were likely to be false positives).

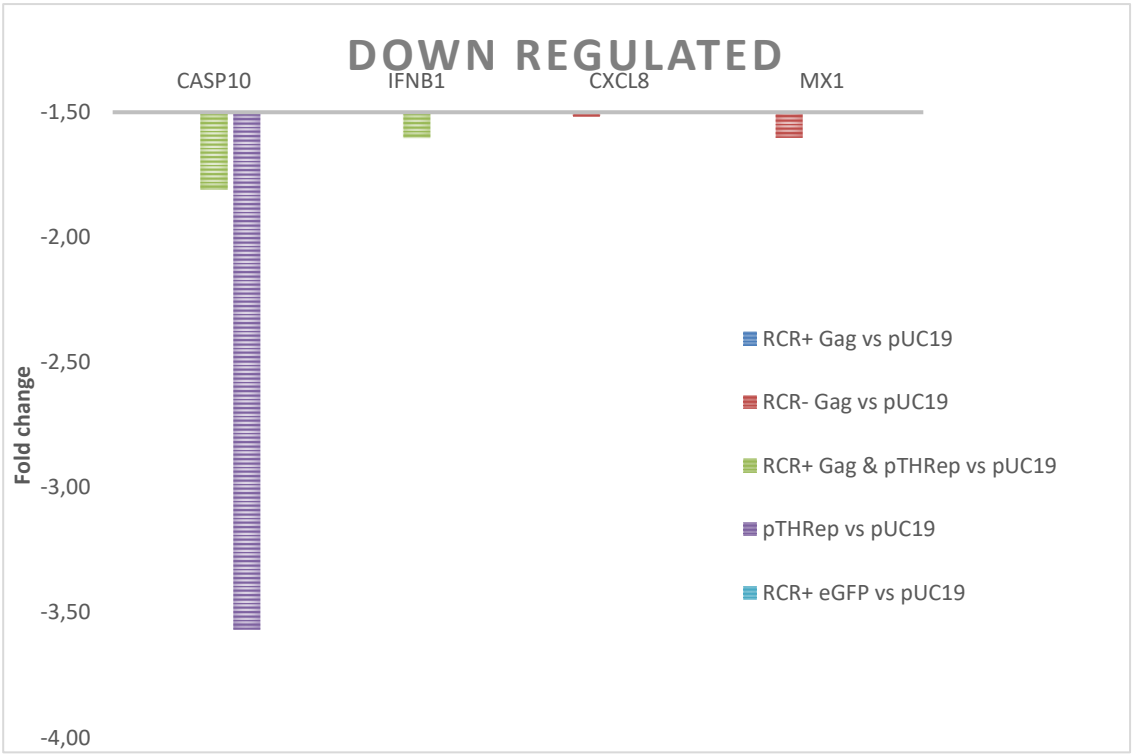

Figure 4.10 Downregulated antiviral response genes in HeLa S3 cells transfected with DNA expression vectors as compared to transfections using pUC19 DNA as the negative control standard.

Due to the nature of this type of analysis, where the up- and down-regulated genes are benchmarked against a negative sample, which for the above analysis was pUC19, it was possible to perform three additional cross analyses using the same data. As these analyses are based on the same data set, they are not independent measurements. They do however complement the findings and help identify other genes whose expression is specifically altered by RCR: in direct comparisons between the RCR+ Gag with and without pTHRep versus the RCR- Gag vector; and another where the RCR+ eGFP vector were used as alternative reference vectors. These analyses lent some supporting evidence to previous findings and helped identify new potentially affected genes (Figure 4.11). Fold change data and p-values are available in Appendix D.

In the primary direct comparative analysis four upregulated genes were identified for the RCR+ Gag sample, as compared to the RCR- Gag sample: these were CCL5, CXCL11, IL12B and MX1. This analysis corroborates the initial analysis, while comparison of the RCR+ Gag with pTHRep versus RCR- Gag identified five genes as having evidence of been up-regulated; namely, CCL5, DHX58, CXCL8, MX1 and 2'-5'-oligoadenylate synthetase 2 (OAS2) (Figure 4.11). The CCL5 finding corroborates other independent readings with the RCR+ Gag vector, and the primary analysis complemented these findings with relatively good p-values for this experiment (Appendix D) while DHX58 and CXCL8 had poor p-values and therefore a high probability of been false positives. The MX1 finding corroborates the primary analysis and showed upregulation in two of the cross sample analyses using alternative reference samples. While p-values of these samples are relatively weak, the fact that this comes up from three analyses reinforces this finding as being probably true. OAS2 on the

other hand is also likely to be a false positive, with a weak p-value and no corroborating readings in cross analyses.

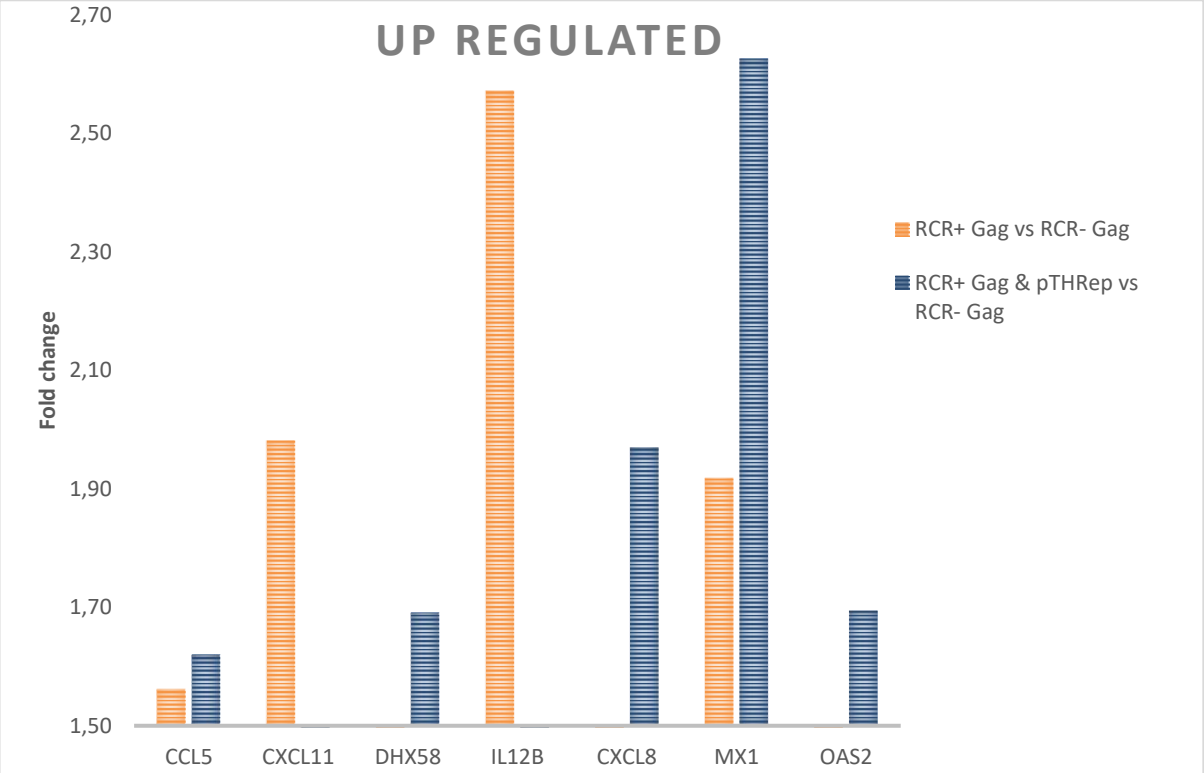

Figure 4.11 Upregulated antiviral response genes in HeLa S3 cells transfected with DNA expression vectors and using RCR- Gag and RCR+ eGFP vectors for comparative negative standards.

The downregulated genes of the same comparison were graphed separately (Figure 4.12). In this case the primary analysis indicated IL1B and MEFV being down regulated in RCR+ Gag as directly compared with the RCR- Gag vector. When pTHRep was added, CASP10 was downregulated, corroborating the previous finding with reference to Rep. The downregulation of MEFV when RCR- Gag is reference echoes the initial finding where it was upregulated in comparison with pUC19. The switch in sign here is because the RCR- Gag vector was now the reference plasmid.

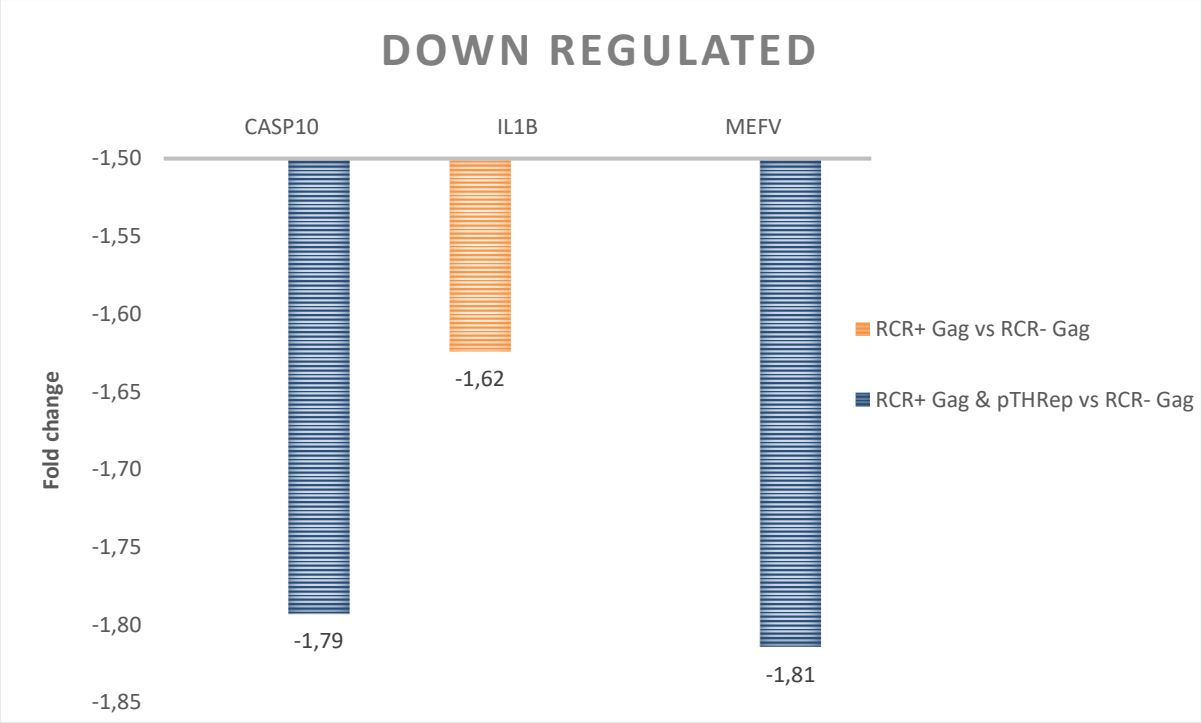

Figure 4.12 Downregulated antiviral response genes in HeLa S3 cells transfected with DNA expression vectors and using RCR- Gag and RCR+ eGFP vectors for comparative negative standards.

4.4 Discussion

4.4.1 Evaluating eGFP expression in Balb/cJ mice

The primary research goal for the work reported in this Chapter was determining whether the replicating DNA expression vector could increase heterologous gene expression *in vivo* in a live animal model. The results obtained (Figures 4.1-4.8) indicate that the self-replicating RCR+ vectors did result in overall higher eGFP expression in muscle fibre bundles by a significant margin ($p<0.01$). The addition of Rep transiently by co-inoculation of pTHRep also appears to have had a significant boosting effect on mean eGFP expression ($P<0.01$) in the muscle fibre bundles. In addition to boosting the mean expression of eGFP, use of the self-replicating vector appears to have approximately doubled the size of the range of expression values recorded, compared to controls. This is evident from the descriptive statistics (Table 4.1) where the range, variance and standard deviation of the fluorescent fibre bundles increases from the RCR- vector to the RCR+ vectors and further increases with the addition of pTHRep in the inoculum. The high standard deviation is attributed to a high range of possible fluorescent readouts, and the approximate doubling in the standard deviation range and variance (from RCR- eGFP to the RCR+ with pTHRep) is evidence of how RCR altered the gene expression profile of the affected muscle fibre bundles. This is less evident in the graph of Figure 4.4 but is quite apparent in visual inspection (Figure 4.1-4.3), where highly fluorescent individual muscle fibre bundles contrast noticeably with the less fluorescent fibre bundles, particularly in the RCR+ eGFP with pTHRep samples (Figure 4.1-4.3). In data capturing it was also evident that, in the RCR+ and RCR+ with pTHRep

samples, more examples of positively fluorescent muscle fibre bundles were present overall, while 100 positive muscle fibre bundle readings were made for each muscle tissue sample collected from the nine sample mice and one control in this experiment. It would have easily been possible to identify 200+ for the RCR+ eGFP with pTHRep samples but would have been difficult to identify more than roughly 150 examples from the RCR- EGFP vector above the 2σ positive identification cut-off. This indicates that muscle fibre bundles which took up RCR+ eGFP vector at low amounts, at levels that are typically insufficient to produce a positive fluorescence signal 28 days post inoculation using the RCR- eGFP vector, were detectable when using the RCR+ eGFP vector and the RCR+ eGFP with pTHRep vectors.

This observed effect is best explained by use of an RCR+ vector increasing the gene copy numbers of eGFP. The amount of DNA inoculated into each mouse was carefully measured and controlled for, and the animal technician conducting inoculations was highly trained with many years of experience in performing intramuscular inoculations in mice. The likelihood of human error in delivering inaccurate dosages is therefore low. Furthermore, human error cannot account for the huge difference in eGFP expression range increases in variance and standard deviation as well as alteration in the skewness of the eGFP distribution data statistics recorded (Table 4.1). Collectively, these statistics indicate that the difference between the RCR- and the Rep boosted RCR+ eGFP vectors was an overall doubling in total fluorescence or sum of samples as well as the variance and range and the maximum recorded readings. Furthermore, this does not include the observation that there appeared to be more fluorescent muscle fibre bundles overall in the RCR+ with pTHRep sample. The most fluorescent muscle fibre bundles also had localised eGFP ‘hot spots’ with extremely high fluorescence more than twice as bright as the brightest muscle fibre identified in the RCR- inoculated samples (Figure 4.5). Furthermore, human error cannot rationally account for these localised ‘hot spot’ observations. These observations are therefore taken as meaningful and powerful evidence that the RCR technology is performing as anticipated and desired in the Balb/cJ animal model.

The methodology used to quantify eGFP fluorescence in mouse muscle tissues does have some notable limitations. The mice have to be euthanised and the tissue samples prepared in a series of labour-intensive steps. Once sections have been created, they must be viewed, and microscopy image data captured as soon as possible because fluorescence of the same fades over time, despite best efforts to minimise this with antifade reagents. There is a far superior method, using luciferase expression within the skin tissues of live mice, where this can be monitored daily in live animals and does not require animal euthanasia to make a reading (Petkov et al., 2018). This method was considered but the necessary equipment was unavailable at our facility. A follow up experiment to quantify the expression over a 3-6 month period in muscle and skin tissue (using this method) is recommended as a follow up to this pilot study. Evidence gathered from such a study would ascertain whether the RCR technology would be capable of establishing a stronger presence and copy number with higher expression over a greater time period, or by boosting the rate of RCR by transient introduction of Rep. In such tests, it would be

advisable to also test for its utility by tracking luminescence from RCR- Luciferase inoculated mice before and after pTHRep is inoculated at the same inoculation site.

The above observations also provide evidence that the RCR expression technology has a variable rate of induction that can be accelerated by greater presence of Rep, demonstrated here by the addition of Rep on the PTHRep vector which utilises a far more powerful and broadly-used CMV promoter to boost Rep expression and ensure high concentrations. This demonstrates that in this system there exists an ability to alter and engineer the rate of RCR *in vivo* by controlling Rep concentration to alter the rate of RCR and therefore expression levels of the gene of interest as a result of increased gene copy numbers (Cheung, 2015).

The evaluation and quantification of the altered eGFP expression profiles between the RCR+ and RCR- vectors was corroborated by an additional different type of analysis performed on the longitudinal muscle sections, using a technique that is not prone to selection bias (Figures 4.6-4.8). Corroboration between the two analysis and fluorescence quantification methods used, one more precise and accurate, and one less prone to bias (Abramoff et al., 2004; Bankhead, 2016; Carl Zeiss Microscopy, 2015, 2013; Cruz, 2016; Gagniuc and Ionescu-Tirgoviste, 2012; Gray et al., n.d.). Such analysis strengthens the validity of this result and also verifies that the analysis was done appropriately.

The gene expression profile that this RCR+ DNA expression technology appears to follow can be likened to a viral life cycle. In many ways it is, in fact, a viral life cycle or rather a distillation of the replication process of one. It appears to start out like any normal DNA expression vector initially, or exactly like its near identical twin non-replicating vector RCR- eGFP vector. Then it begins to slowly and steadily alter itself and its associated gene expression, amplifying it as it steadily begins to take over local resources as it simultaneously magnifies its ability to do so by increasing its copy number. Over the period of a month this accumulated increase is detectable and manifests as a notable increase in eGFP expression in affected muscle fibre bundles. Like a virus, the replication process appears to ramp up over time under the control of Rep, which we know directs the RCR process (Cheung, 2015). In time it appears that eGFP expression begins to reach a state of excess or hyper-over-expression that is not seen in RCR- vectors and develops more slowly if pTHRep is not added to boost Rep concentrations (Figures 4.1-4.5). This progression of increasing eGFP expression in many ways' mimics, or recapitulates, the progression of real virus gene expression and its life cycle. Unlike a real virus, however, the RCR+ DNA expression technology consists only of naked DNA and is devoid of any mechanism of truly propagating to new target cells. The fundamental lack of this basic requirement for viral life and propagation to future cells, and a critical concern in vaccine design safety, represents a considerable strength of this technology and is arguably a far better safety mechanism than the limited host range that prevents viral propagation of attenuated vaccines, for example.

Verifying this theory, however, requires further extensive and intensive cell culture experimentation and analysis. It is fair to say, though, that the preliminary evidence gathered thus far in these pilot studies is promising and the technology, as developed, is ready to progress to further testing.

Concurrent with the eGFP animal study presented here, an investigation into immunogenicity was also conducted using HIV-1C Gag mosaic as an antigen. This pilot study used the self-replicating vaccine vector to deliver limited low dosage (10 µg) inoculations and tested for improvements in immunogenicity. This study successfully demonstrated that the RCR+ and RCR- Gag vectors were generating T-cell immunogenicity. Comparative analysis was however inconclusive, due to low responses, most likely as a result of the low dosages given and contamination in at least one of the samples, as indicated by inconsistencies in the controls (results not shown). Nevertheless, the successful eGFP experiments in mice, and the results obtained from the Gag immunogenicity study, have greatly helped inform how a future, more comprehensive, immunogenicity study could be set up to thoroughly investigate this technology. From those inconclusive results a longitudinal immunogenicity study using standard inoculation dosages is justified and recommended.

Based on the evidence presented here from the eGFP animal study, using dosages of 50 µg and 1-month post inoculation evaluation, it is likely that the above-mentioned immunogenicity study was flawed with respect to the decision to utilise the lowest possible dosage in inoculations. These low levels probably limited the availability of Rep with its weak native promoter (previously discussed) to a level where RCR does not readily occur. While dosage reduction benefits may yet be realised from this technology, these would be best determined in a future series of more extensive experiments that include the use of different promoter(s). The immunogenicity pilot study was at least successful in identifying lower limits of dosage ranges and times for testing. Determining the extent of immunogenicity differences between the RCR+ and RCR- Gag expression vectors in a long-form experiment should therefore become one of the primary future experimental research goals.

In addition to this research into possible mechanisms of action and PRRs that RCR may induce indicate that in future immunogenicity studies, additional targets such as IFNα/β, IL-1α/β, IL-2, IL-10, IL-12 and TNF-α could be used to better identify the extent to which antiviral responses are being activated, and which parts of the immune response are been altered (Georg and Sander, 2019; Janeway and Medzhitov, 2002; Li and Chen, 2018; Saez-Cirion et al., 2016). Various dosage and vector combinations should also be assessed to determine the full range of effects and activity of this dynamical replication system. Additional genes of interest can also be added to the expression technology so that antibody responses may also be assessed (Dalod et al., 2002; Georg and Sander, 2019; Moore et al., 2001).

The evidence and understanding gained from the eGFP animal pilot study and tissue culture work indicate that the RCR process and its effects on gene expression take time to amplify and accrue. This

occurs relatively rapidly in fast growing tissue culture cells but may occur much more slowly in live animal cells. Furthermore, because the promoter for Rep is weak and its expression relies on positive feedback loop created by RCR, this would imply that at low levels the amplification process is slow to start but exponential at the end. This is of course complicated by the self-inhibiting activity of Rep on its own promoter, which serves to ensure RCR is maintained at levels that are optimal to the native virus from which the technology originates. To fully understand this system in tissue culture and as a vaccine, extensive optimisation experiments must be conducted. Evidence gathered thus far on the dosages used would imply that this optimum may lie after the 1-month time point analysed. It is worth considering that the progression of PBFD in psittacine birds occurs over 3-12 months (Pass and Perry, 1985, 1984; Regnard et al., 2015). It is reasonable that this technology should be evaluated over a similar time period.

Determining how fast RCR can ramp up, and the effects it has as it does a longitudinal immunogenicity study with multiple evaluation points, would be ideal to properly to map out these effects. The observation that introducing Rep in trans boosts eGFP expression, supports the idea that the rate of RCR and Rep expression is crucial in determining these effects. Because this process is dynamic in nature (as is cell growth in tissue culture), determining these effects may be difficult and require extensive testing and evaluation at multiple time points in animals to determine.

Hypothetically, at some level a multivariate enzyme kinetics and saturation equation theoretically controls this process: balancing cellular health, homeostasis and growth state, with DNA polymerase availability, Rep concentration, and RCR amplicon copy number. As a process from viral origins this balancing act forms a part of the viral life cycle. That said, the complex nature of this balance and how it forms between these mechanisms and other factors, such immune responses are completely unknown and worthy of future research. From the experimental evidence gathered thus far however, it appears that the balance RCR does establish inside its host cells is not static in nature. Rather it appears to progress and develop over time in what is best described as a viral-like fashion. Such a scenario was observed in tissue culture and is evident in the mouse muscle fibre tissues; both exhibited examples of excessive extremes that were not present in non-replicating RCR- samples.

Without delving into the complex intricacies of such mechanisms, it is apparent that the system is driven by the positive feedback and expression loop created by Rep and RCR. It may therefore be hypothetically possible to use the RCR feedback loop to adjust and control the expression of a target gene of interest. Traditionally a process controlled by adjusting promoter strength, if it is possible to control copy numbers by periodically introducing Rep to increase them via RCR until a target level is achieved. It would, at least in theory, be possible to use this technology to try to fine-control expression levels of a target, gene of interest under conditions where Rep expression can be controlled.

4.4.2 Evaluation of antiviral response genes

To gather evidence indicating that RCR technology may induce differences in antiviral gene responses, a pilot study using an 84 gene RT^2 profiler antiviral response gene array (Qiagen) was used to specifically look for evidence of differences in antiviral response gene activation between the RCR+ and RCR- vectors as well as responses induced by the pTHRep vector.

Interpreting the results from these arrays presented certain analysis challenges as only one of the findings had a high statistical significance level with a ($p=0.006$) while several findings were borderline ($p<0.1$) and others offered weak evidence ($p<0.2$). It is important to interpret these findings in context that this experiment was conducted where the evidence gathered from flow cytometry and tissue culture experiments has already unequivocally shown that metabolic and physical changes in cellular structure are being induced in response to active RCR. In this sense, the pilot array was run to primarily test the conditions under which it was run and to gather further supporting evidence of differences in antiviral response gene activation. Only three arrays per sample were run for this pilot study, under ideal conditions. In these assays 6 to 12 replicates are run, to obtain results with high statistical significance.

When evaluating results from RNA profiler arrays, it is worth discussing how these arrays work and what can and should not be interpreted from mRNA quantification methods. Indeed, research papers that explore important issues around misinterpretation and over interpretation of mRNA array results have been written (Jacobsen et al., 2009). These considerations were kept in mind when running this array, however, as the primary research goal for this pilot experiment was for it to provide supporting evidence for the metabolic and physiological changes observed in tissue culture, con-focal microscopy and flow cytometry experiments. It is important to point out that the findings made by the array results are taken in the greater context of what those experiments have shown.

Evaluating the up-regulated genes, it appears that CARD9 is the only gene upregulated in all samples as compared with the pUC19 negative control (Figure 4.9). CARD9 acts as a key adaptor mediating signal transduction from the PRRs and acts as a mediator of cellular apoptosis and a positive regulator of NF-κB activation; it is also a key transcription factor for both innate and adaptive immunity (Bertin et al., 2000; Sparwasser et al., 2006). Interestingly, while it appears to be upregulated in all the samples, it appears to be less so when pTHRep is added to the RCR+ Gag and the least upregulated for the RCR+ eGFP sample. These samples may be the most replicative ones because in RCA analysis they produce the strongest RCR amplicon bands (Appendix A).

CCL5 is a gene involved in recruitment of leukocytes to inflammatory sites as well as the activation and proliferation of NK cells and a natural HIV-suppressive factor (Secchi et al., 2018). It has been shown to be secreted by various immune cell types and specifically by activated CD8+ T cells (Cocchi et al., 1995; Zapata et al., 2016). It appears to be noticeably upregulated in all RCR+ samples as well

as in the pTHRep sample but not so for the non-replicative RCR- Gag sample (Figure 4.9). This links Rep and possibly RCR itself with an increased likelihood of immune cell recruitment and NK cell proliferation. This finding was repeated in all four primary sample analyses and seen again in the cross analysis between the RCR+ and RCR- samples. These duplications increase the validity of the result despite its relatively poor p-value.

Both CXCL11 and IL12B are associated with the recruitment of immune cells such as T-cells, NK and macrophages and both influence the development of a Th1 type immune response (Flier et al., 2001; Teng et al., 2015; Tokunaga et al., 2018). They appear to be uniquely upregulated by the RCR+ Gag vector alone and not corroborated by the combined RCR+ Gag and pTHRep sample (Figure 4.9). This would suggest that this effect is due to the unique combination and balance of Rep and Gag provided by the RCR+ Gag sample and that, as more Rep is expressed, it disappears. It is possible that the cotransfection of pTHRep, which expresses vastly more Rep than the native LIR promoter and which we now know induces CASP10 suppression (Figure 4.10). It may therefore be responsible for this anomalous result and lack of correlation between RCR+ Gag and, as observed where RCR+ Gag is combined with pTHRep, is due to effects caused by stronger Rep expression. The effect appears to be powerful and, if true, would suggest that as Rep concentration increases, it may cause the corresponding cellular gene response to shift.

Interestingly, another gene DHX58 also appears to have been up regulated for RCR+ samples that contained higher dosages of pTHRep and therefore Rep expression (Figure 4.9). This finding seemingly correlates with Rep concentration with the pTHRep vector alone causing the highest increase, followed by the RCR+ Gag and pTHRep sample which was transfected with a lower amount of pTHRep than the pTHRep only sample. This is followed by the RCR+ eGFP vector which was the smallest vector in size, with the smallest-sized amplicon. This, it was thought, may have made it a more efficient self-replicating RCR vector. A notion supported by the observation that it consistently produced some of the most prominent amplicon bands in RCA verification gels (Appendix A1). Increased RCR replication efficiency would imply that it would also have higher Rep concentration, as expression would ramp up from RCR faster for the smaller and easier-to-produce amplicons. Alternatively, eGFP may simply be a less toxic protein compared to Gag which could account for a greater cellular tolerance to RCR+ eGFP vector and explain its better apparent replication in RCA gels.

DHX58 is a part of innate antiviral immune regulation response and is known to act as a regulator of DDX58/RIG-I and IFIH1/MDA5 mediated antiviral signalling. It can have both negative and positive regulatory functions and it may therefore be difficult to characterise its functionality. It is known to be involved as a part of the innate immune response to various RNA viruses and DNA viruses (including poxviruses). The DHX58 protein binds directly to both ssRNA and dsRNA, with a higher affinity for dsRNA. It directly links into viral DNA and RNA sensing mechanisms PRRs and associated PAMPs

(Komuro and Horvath, 2006; Yoneyama et al., 2005). This indicates that Rep and RCR appear to be directly interacting with the systems of the intracellular innate immunity and triggering PAMPs to a higher degree than non-replicating vectors and vectors that do not express Rep. This result did not have highly desirable p-values but was consistent across multiple samples, which lends further credence to the idea that Rep itself, and the associated RCR activity, functions to enhance the activation of PAMPs, potentially also creating adjuvant-like effects, compared to non-replicating DNA vectors. Repeat experiments using improved techniques a higher number of samples, repeats, and additional controls, should be conducted to properly verify these findings. As a pilot study however, these findings were consistent across the relevant samples, indicating it is unlikely that they are anomalous in nature.

The RCR+ eGFP sample appeared to be upregulating CXCL8 a gene which promotes chemotaxis and is a primary cytokine involved in recruiting neutrophils to the site of an infection. It is known to be one of the most potent chemoattractant molecules and is an important stimulant of the innate immune response (Oliveira et al., 2019). Similarly, IRF5 was also shown to have relatively strong upregulation by the RCR+ eGFP vector compared to pUC19. In this case however it is difficult to say whether these results are real or not, due to weak p-values. This regulatory factor is proinflammatory in nature and has been linked directly to the Toll like receptor stimulation (Ren et al., 2014). Ideally, additional controls, higher sample repeats, and a direct comparison between RCR+ and RCR- eGFP vectors, would help to confirm the validity of this finding. As this sample was added as a control itself in this pilot study, it did not have the additional controls it required to cross-compare its findings in the manner done for the RCR+ Gag samples that could corroborate findings made on it. Nevertheless, these findings are intriguing and worthy of further investigation.

The only gene to be upregulated by the non-replicating vectors RCR- Gag and pTHRep and not the replicating RCR+ vectors, was *MEFV*. This gene is associated with Familial Mediterranean fever (FMF), a recessive disorder characterized by episodes of fever and neutrophil-mediated serosal membrane inflammation (Centola et al., 2000). The *MEFV* gene creates a protein called pyrin which is associated with keeping inflammation processes under control, as a gene that regulates and mediates inflammation (Shahbaznejad et al., 2018). It is very interesting that only the non-replicating RCR- vectors demonstrated evidence of *MEFV* upregulation, when replicating RCR+ vectors did not. This implies that mediation of the inflammation response by *MEFV* is not occurring when RCR replication is occurring, implying greater cellular inflammation response to RCR+ vectors and DNA replication process. In the non-replicating DNA vectors, inflammation regulation by *MEFV* does occur, at least by the 48 h evaluation time. This suggests that RCR+ vectors are more inflammatory than RCR- vectors, and that antiviral cellular responses to inoculated DNA may possibly have begun to be mitigated as early as 48 hours. The p-values of this result were relatively good. *MEFV*, a gene involved in the prevention of immune overactivation and inflammation, here demonstrates evidence of upregulation and, therefore, active suppression of inflammation for non-replicating vectors that is not present in

replicating vectors. This result complements the idea that RCR technology presents as a viable pathogen to inoculated cells and the non-replicating normal DNA expression systems do not (Georg and Sander, 2019).

The direct comparison between RCR+ and RCR- Gag vectors served as an important control and test for detection of differences between RCR+ and RCR- vectors (Figure 4.11). This was the most well controlled evaluation to detect direct effects caused by RCR. In this evaluation CCL5, CXCL11, IL12B, MX1 appear to have notably altered expression profiles. CCL5, is a member of the CC subfamily and functions as a chemoattractant for eosinophils, blood monocytes and memory T helper cells. It has been shown to elicit the release of histamine from basophils and activate eosinophils such as NK cells and is one of the major HIV-suppressive factors produced by CD8+ cells. It is a natural ligand to the chemokine receptor chemokine (C-C motif) receptor 5 (CCR5), and it suppresses in vitro replication of R5 strains of HIV-1, which use CCR5 as a coreceptor. This finding was duplicated in all the replicating RCR+ vectors and also appears to be present in samples expressing Rep. This indicates that it may be induced by the presence of Rep and possibly enhanced by replicating DNA.

The MX1 gene appears to follow a similar pattern but, unlike CCL5, its expression is not altered by the presence of Rep at all. It is therefore the only gene that has been identified, in multiple cross analyses, to be upregulated in response to RCR. This gene is responsible for encoding guanosine triphosphate (GTP)-metabolizing protein, a protein known to be responsible for antagonizing viral replication of several different RNA and DNA viruses. Interestingly, recent research done specifically on the ATPase and GTPase activity of BFDV Rep, has outlined the ability of this protein to perform these functions. Indeed, ATPase and GTPase activity is in fact a cellular requirement for replicating DNA viruses, which need hydrolyse and free dNTPs required for replication. It logically can also be seen as an immunogenic stimuli (Huang et al., 2016). Here we see the upregulation of MX1 specifically to DNA replication as a prominent part of the cellular antiviral response and this type of stimulation does not occur in response to non-replicative DNA vaccines. The ability of MX1 to target and restrict a broad range of viral replication processes is associated with its similar structure to the GTPase family of enzymes. Its antiviral replication effects have been demonstrated in several case studies, such as in thogoto virus (THOV) where it prevents viral replication by inhibiting the nuclear import of viral nucleocapsids (Verhelst et al., 2012). In La Crosse virus (LACV), replication inhibition was demonstrated by the sequestration of viral nucleoprotein into perinuclear complexes, preventing genome amplification, budding, and egress (Kochs et al., 2002). In influenza A virus (IAV) it has been linked to replication inhibition associated with decreased, or delaying, nuclear pore synthesis and the blocking of endocytic traffic, preventing virus particles entering the nucleus (Verhelst et al., 2012). It is also associated with increased endoplasmic reticulum stress-mediated cell death after influenza infection. Induction of this gene in response to replicating RCR+ vectors, as well as its apparent bolstering by the addition of pTHRep and the absence of altered gene expression in the non-replicating RCR- vectors, pUC19 and

pTHRep vectors, is strong evidence that unique antiviral gene responses are being induced by the RCR DNA replication process itself. MX1 is a gene that is also induced by type I and type II interferons and a part of the interferon response pathways. This directly implicates the RCR, DNA replication process itself with the enhanced activation of the type I and II interferon response pathways (Verhelst et al., 2012). These findings support the idea that RCR appears to be generating unique antiviral responses that suggest that RCR+ vectors should promote stronger immunogenic responses than equivalent inanimate and non-replicating RCR- DNA vectors.

4.4.3 Caspase-10 suppression by Rep

The most significant result from the array was the finding that Caspase 10, (CASP10) is massively downregulated 3.57-fold by Rep ($p=0.0068$), (Figure 4.10). Detecting fold decreases of such a magnitude and significance is more meaningful and informative than a similar magnitude detection of a fold increase (Jacobsen et al., 2009). This finding becomes more interesting when one considers that the transfection efficiency shown for HeLa S3 cells was ~20%, which heavily biases the array toward being able to detect gene upregulation of expression over down regulation. My recorded transfection efficiencies were in line with the up to 25% transfection efficiency that has been reported elsewhere as, a highly efficient HeLa cell transfection (Fukumoto et al., 2010). At face value, this downregulation result appears to be problematic, as it implies the effect is induced in untransfected cells as a fold decrease of the reported magnitude and significance cannot logically be achieved from a transfected population of only 20%.

It is unlikely that Rep could generate extracellular signalling to suppress CASP10 expression in neighbouring cells. As this contradicts conventional immunogenic cellular signalling dogma as well as our canonical understanding of CASP10. As CASP10 activity is known to typically be induced by extracellular signalling, not suppressed (Banos-Lara and Méndez, 2010). So, what is going on? The only viable and logical explanation is that foreign plasmid DNA induces CASP10 upregulation. This makes sense, as the negative control included the pUC19 plasmid DNA in it, a non-gene expressing DNA-only control. Therefore, any effect induced by plasmid DNA itself, is not detectable in these tests which did not include an untransfected control, arguable a mistake given these data. This effect is detected here however only because Rep appears to be capable of supressing CASP10 thereby counteracting the upregulation generated by the presence of foreign DNA from transfection. This explanation agrees with the literature on innate intracellular defence mechanisms such as the AIM2 inflammasome are known to recognise intracellular cytosolic, pathogenic DNA and initiate an apoptotic response (Lugrin and Martinon, 2018; Wenzel et al., 2012). These mechanisms effectively act as a limiting factor relating to how much DNA can be transfected in cell tissue culture before apoptosis occurs (noting that this effect, is commonly observed when too much DNA is transfected in cell culture) (Isaacs, 2004; Roche, 2014).

The observed reduction in CASP10 expression therefore no longer needs to be explained in relation to the 80% of untransfected cells, as would be the case for other potential explanations. Its detection by the array indicates Rep expression counteracts the induction effect transfected plasmid DNA has on CASP10. This action by Rep has a clear and logical evolutionary connection. Viral survival and competitiveness would clearly benefit from the suppression of cellular apoptosis in infected cells. Prevention of innate apoptotic antiviral cellular responses is a common problem faced by practically all viruses and invading pathogens, and various mechanisms pathogens use to avoid this outcome have been described (Kumar et al., 2011; Parham, 2014). Indeed mechanisms capable of apoptosis induction have been identified and discussed as potential targets for broad spectrum antiviral drug development, and several such drugs exist (Hanauske-Abel et al., 2013). The suppression of CASP10 by Rep, therefore, appears to be a viral defence mechanism against the innate apoptotic defence pathway (Fan et al., 2005; Wang et al., 2001).

Caspase 10 is a particularly important member of the cysteine-aspartic acid protease (caspase) family, a group of enzymes that require proteolytic processing for them to become active. The caspases are known for their own sequential activation in a process known as the cascade of caspases, which plays a central role in the execution-phase of cellular apoptosis (Fan et al., 2005; Wang et al., 2001). Mutations in CASP10 have been associated with type IIA autoimmune lymphoproliferative syndrome, non-Hodgkin lymphoma, and gastric cancer. CASP10 is believed to function as a primary initiator and activator of the cascade of caspases. It is responsible for the direct activation of caspases 3 and 7 and the protein itself is processed by caspase 8. Coincidentally caspase 8 is associated with mediating the switching between cellular necrosis and apoptosis via the receptor-interacting serine-threonine kinases (RIP) which initiate programmed cellular necrosis (Galluzzi et al., 2018, 2009). Furthermore, it is known that when herpesvirus DNA is detected in the nucleus by IFI16, this stimulates the creation of cytokines while cGAS (which also detects viral nuclear DNA) has been shown to initiate apoptosis via STING (Diner et al., 2016). CASP10 along with the cFLIP mechanism are believed to be responsible for co-ordinately regulating the CD95L-mediated signalling which influences cell death or survival outcomes. This links inhibition by Rep of CASP10 to cellular necrosis observed in PBFD and its associated cytokine storm causing inflammation (Horn et al., 2017; Ritchie, 2013; Ritchie et al., 1989). Indeed the apoptotic cascade of caspases, when it occurs, is predominantly an anti-inflammatory process in nature, while necrosis is very much pro-inflammatory (Scheller et al., 2002).

This explanation corroborates with the way in which PBFD presents which is the development of acquired immunodeficiency syndrome (AIDS) induced by chronic inflammation and cellular necrosis (Pass and Perry, 1985, 1984; Ritchie et al., 1989). Chronic inflammation is well-documented to cause immunosuppression via over-production of cytokines driven by NF-κB immune regulation mechanisms (Kanterman et al., 2012). NF-κB is also directly involved in B- and T- cell activation and is known to help regulate immune responses to infection and inflammation (Zhang et al., 2017). NF-κB activation

is also believed to promote cell survival, and cytokine production and is also linked to the RIG-1 mediated antiviral signalling cascade (Kim et al., 2017). The activity of these systems however, is highly complex and can depend on overall cellular health and state (Galluzzi et al., 2009; Lin et al., 2014; Zhang et al., 2017).

It would seem then, that the BFDV appears to have repurposed the known inhibitory capabilities of its Rep to possibly prevent apoptosis and favour cellular necrosis in infected host cells, which is seen in PBFD. This theory is worth investigating further as it could have many implications if true.

Necrosis begins with a process known as oncosis, which involves cellular swelling and ends in karyolysis of the nucleus (Galluzzi et al., 2016; Li and Chen, 2018). It is worth noting that morphologically similar observations were made in RCR+ transfected cells. One of the most notable forms of necrosis described is known as immunogenic cell death (ICD), which is of particular interest due to the extremely efficient generation of T-cell immunity when it occurs (Elmore, 2007; Galluzzi et al., 2016; Kepp et al., 2014). ICD is accompanied by several documented cellular markers, such as the externalisation of calreticulin and the excretion of large amounts of ATP and High Mobility Group Box 1 (HMGB-1) into the extracellular matrix, and a Type I interferon response pathway activation. However, detection of these markers is still not considered sufficient evidence to prove the induction of ICD. Conversely for ICD, the demise of only a few cells infected by an invading pathogen can trigger a robust antigen-specific immune response. When this happens, not only does ICD direct a successful immune response, clearing the invading pathogens, but it also results in the establishment of long-term immunological memory (Kempen et al., 2015). Several chemotherapeutics are known stimulators of ICD, although more effective ones are been searched for. Given the evidence gathered thus far the effects of RCR+ vectors in transfected cells. It is worth investigating if this technology may be used induce ICD wither on its own or in combination with other adjuvants and drugs (Carmona-Gutierrez et al., 2018; Galluzzi et al., 2016, 2009).

Induction of ICD could potentially become a potent mechanism as a cancer therapeutic and vaccine and mechanisms of inducing are actively been sought out in this field of research (Galluzzi et al., 2016).

This also has direct relevance to designing potential treatments of PBFD. If the above theory is true apoptotic inducing drugs such as Mitomycin C, ciclopirox or deferiprone could conceivably be used as therapeutics to treat PBFD (Hanauske-Abel et al., 2013).

4.5 Conclusions

One of the goals of running the array experiment was to show whether an immunogenic trend could be identified among key antiviral response genes in response to the replicating RCR+ Gag vector that was not present in the RCR- Gag vector, and any unique effects caused by Rep and the process of RCR.

In this context, use of the array was successful: while the p-values of a lot of the results achieved could be better, these experiments did provide supporting evidence of a trend of increased antiviral response gene activation and possibly some suppression in response to RCR and Rep too, for which effects were observed in cell culture and flow cytometry. The secondary objective related to testing the methodology used here, and identifying whether these arrays were suitable for this line of research. i.e. whether it would be possible to generate sufficiently strong evidence and data to properly investigate the cellular metabolic and physiological observations and phenomena observed. The array demonstrated this potential does exist but also revealed that further optimisations in the methodology used would be highly beneficial and help reduce future costs. Follow up studies are recommended to validate these findings.

As for the eGFP expression in mice, these experiments provided evidence that the RCR technology is functional in a live murine animal model, and capable of increasing eGFP expression in this setting. It also demonstrated that the addition of Rep *in trans* could be used to enhance this process with definitive effect. Furthermore, it demonstrated localised extremities in eGFP expression within particular muscle fibre bundles and localised 'hot spots'. This evidence supports the idea that the technology can be used in dynamic and flexible ways, to amplify gene expression in targeted locations. An example might be using cell-specific promoters for Rep and a gene of interest that would allow the technology to selectively target specific cells for expression amplification of a targeted gene. Such an approach would thereby avoid problems associated with high levels of expression of the gene of interest in non-target cells (that would be difficult to avoid when powerful broad-spectrum promoters such as CMV, or SV40 are used). It may also allow for specific, yet relatively weak, promoters to be used in scenarios where they may be ineffective before RCR, but are effective once a high enough copy number is created by RCR. Follow up research here is also recommended possibly using luciferase as a reporter gene for whole animal assessment of gene expression using advanced expression characterization methods (Petkov et al., 2018).

5 Final discussion and conclusions

5.1 Final thoughts and discussion

Working on the self-amplifying DNA virus-based gene expression system described in this thesis has been a long and confusing journey of discovery. The truly difficult aspect has been coming to terms with and interpreting dynamic results and appreciating the multipurpose nature of this system. BFDV appears to be a simple virus, with just two basic genes in a genome <2 kbp in size. This necessitates that the virus develops multiple functionalities and uses for its proteins, a process quite common for viral proteins. The extent to which BFDV achieves this, and more specifically, how multifunctional its Rep is, is truly astounding. Its capabilities are what serve as the basis of this technology.

The multiple functionalities of Rep and the process of RCR which it is responsible for initiating and directing, arguably represent the very essence of the concept of "virality". Rep is responsible for both hijacking the host's cellular resources and redirecting them effectively towards viral replication and proliferation. The ability to inhibit its expression as its own concentration increases, forms an essential part of its evolutionary fitness and therefore the essence of virality. This is multifaceted as for optimal proliferation to occur, at some point further production of Rep is no longer required. As Rep does not exit the host cell, making excess represents a waste of resources and at this point the ability to maximise host cellular resources for viral proliferation represents a clear option in terms of evolutionary fitness. This means maximising viral capsid expression, while Rep-driven RCR maintains a steady production of viral genomes (Cheung, 2012; Finsterbusch and Mankertz, 2009). Rep has a multiplicity of functions; the essence of virality relates to the ability to actively thwart and overcome the innate antiviral cellular defences. This is necessary for the virus to be able to fully co-opt the resources available in the cell and to replicate and propagate. This task appears to be executed by Rep as well. As a DNA-binding protein, and one associated with its own inhibition, it is well suited to become repurposed for this role. The ability to adapt to recognise and inhibit other cellular gene targets that may benefit the virus in their absence, is a strong evolutionary driving force on such viral proteins. From results shown in this thesis, there is perhaps no better target for Rep to apply this dual role to than Caspase 10, as preventing its expression stops apoptosis. Downstream targets of CASP10 cannot stop this process, as once the cascade of caspases begin, they also initiate positive feedback loops, that all but ensure the process completes (Elmore, 2007; Galluzzi et al., 2009; Horn et al., 2017; Scheller et al., 2002; Yuan et al., 2016). This was an unlooked for, but novel finding, and one which will probably inform work on other DNA viruses with small genomes.

The above observations a proverbial trifecta of virality, consisting of pathogenic DNA replication, massive gene overexpression and metabolic cellular takeover by suppression of the primary immediate

antiviral response, to create a viral-like dominance over the cellular metabolic and biochemical processes of life. This take-over is necessary to maintain high levels of viral gene expression while the host cell is drained of resources with viral efficiency. Achieving these goals serves as a primary signal to the immune system that the host cell has lost its initial battle against an invading pathogen, such as a virus. These signal to the cell that the pathogen is viable and that a more powerful and capable immunological response, such as a T-cell response, must be initiated for this pathogen to be defeated. Inanimate vaccines which are not capable of mimicking these effects, are typically less T-cell immunogenic, while live vaccines that are detected as being viable and which generate these types of effects are significantly more immunogenic, particularly with regards to the highly sought after T-cell immunity (Georg and Sander, 2019).

While the RCR gene expression technology is not a live virus vector, it partially mimics the cellular effects generated by one. These differences manifest themselves observably and can be detected by confocal microscopy, in flow cytometry and in FACS observations as well as being observed in changes in gene expression. These include the activation of antiviral response genes and the suppression of others in a manner similar to real viral infections. Specifically, in tissue culture, the expression system is able to elevate eGFP expression in individual cells to levels more than twice as what can be achieved on a per-cell basis, by non-replicating RCR- vectors. This demonstrates an important virus-like capability, which is to hijack a cell and manipulate it into tolerating gene expression conditions that a healthy cell would not, and does not, tolerate. In DNA transfections this is observed as a maximum amount of DNA that may be transfected. If this is exceeded in tissue culture transfections, the result is cellular apoptosis by mechanisms that have been well described (Diner et al., 2016; Lugrin and Martinon, 2018; Wenzel et al., 2012). The ability to exceed this tolerance level and thwart innate cellular signalling to undergo apoptosis is evident in experiments with the self-amplifying vector technology. This ability also represents a clear way in which immunological tolerance is broken and one which may need to be broken for the full activation and initiation of the next immunological defence signalling cascade required for the activation and development of T-cell immunity. Preventing cellular apoptosis is a key part of this as this also ensures the longer exposure required for T-cell 'training', and generates inflammation via cellular necrosis, which in turn is associated with the mechanisms that promote and enhance T-cell activation and differentiation (Georg and Sander, 2019; Kobiyama et al., 2013b; Lugrin and Martinon, 2018; Paludan and Bowie, 2013; Rose et al., 2015).

All the evidence presented in this thesis so far suggests that this technology is viable, and it has the potential to be leveraged to rapidly develop powerful targeted and capable T-cell immunity-generating DNA vaccines. A variety of other possible therapeutic applications may also exist, such as targeted gene activation and expression, gene therapy and improving gene expression yields for difficult-to-express targets. Further experimentation to explore these capabilities and possibilities is warranted.

In conclusion, this research has resulted in several novel findings in relation to the feasibility and utility of adapting the BFDV RCR process for use as a novel replicating DNA gene expression system and vaccine development technology. The first fundamental finding that was tested extensively was the ability to replicate, and synthesise distinct unique circular DNA amplicons that could only be assembled by the process of RCR in mammalian cell culture without the full BFDV genome. This process was tested with various genes of interest and demonstrated to work regardless of the gene sequence being amplified by RCR. Thus, proving that the system can be used to amplify virtually any gene of interest for increased gene expression. The native Rep promoter was also shown to be capable of acting as an enhancer to the SV40 promoter and the native Capsid promoter, which lies within the Rep gene sequence, was shown to be active in mammalian cells and was quantified using luciferase as having a relative gene expression strength of approximately 3.8% of the SV40 promoter when tested within Hek293T cells. The amplification process itself is not straightforward however and the evidence gathered indicates that it is a dynamic process of amplification with dynamic cellular effects on the host cell. This therefore becomes a multivariate problem with processes such as gene expression increasing while cellular metabolism appears to be decreasing. Overall, the net effect on gene expression appears to generate at least a two-fold increase in the expression of a target gene of interest per cell and altered cellular effects, despite the apparent decrease in cellular metabolic rate which implies increased cellular catalysis. All these factors should be considered together when considering this technology. Finally, preliminary evidence suggests that Rep, the protein responsible for initiating RCR, may be actively suppressing innate antiviral response mechanisms responsible for activation of the expression of Caspase 10. This has wide reaching implications in terms of antiviral signalling processes and indicates that the technology is both stimulating the activation of antiviral response genes and actively performing viral defence actions against the innate cellular response. These findings correlate well with observations of cellular necrosis observed in PBFD and offer a potential biochemical explanation as to their primary cause. The ability of actively suppress gene expression is not a novel finding for Rep, which was known to suppress its own expression. This finding however is novel in that this is a new gene that appears to also be actively suppressed by Rep. It is possible that it could have a broader array of genes that it is able to directly or even indirectly suppress. As a known DNA binding protein of viral origin, this kind of capability by Rep is not unexpected. These capabilities appear to extend from tissue culture into live murine model. While this research is still at a relatively basic level, there does appear to be real potential for adopting it further for a variety of possible medical applications, particularly the generation of cellular immunity.

5.2 Recommended future work

Several possible future experiments, that could immediately follow up on the research reported here, were identified. These are outlined below.

Testing and confirming whether RCR technology can induce ICD

A set of follow-up experiments are recommended for determining if the highly immunogenic form of cell death (ICD) can be induced by this self-replicating vector system. This form of cell death is characterised by a known set of DAMPs, leakage of DNA into the cellular cytoplasm, cellular surface exposure of calreticulin and extracellular excretion of ATP as well as the degradation and externalization of nuclear high mobility group Box 1 protein HMGB1. Initial tests to look for this could give an indication as to whether this process might be occurring. However, these DAMPs alone cannot fully confirm and verify that ICD is indeed occurring. To do that, another murine experiment (considered the 'gold standard' for detecting ICD) is required. This experiment may be conducted by selecting a suitable cancerous mouse cell line which can be grown and transfected with the RCR expression technology in tissue culture. Transfected sample cells are then inoculated into live mice which are monitored for tumour development, with untransfected cells of the same type used as positive cancer controls. If, after a period of time, the mice inoculated with the RCR+ vector transfected tumour cells have not developed cancer, while the controls have, this could be considered as a partial success. If that is the case, the same mice could be later inoculated with the unaltered tumour cell line and monitored for the development of tumours. If they fail to develop tumours from the initially-altered cell line and then recover from a cancer-inducing inoculation of the same unaltered cell line, this would be considered as proof that the vector is capable of inducing the immunogenic process known as ICD.

Further investigation of unique gene upregulation and alteration patterns

The array experiment conducted here was a pilot study. Further investigation, using more controls, a higher number of replicates, and testing in cells that transfect with greater efficiencies, is recommended to decode the unique gene activations and responses being triggered by this vector system. There are many arrays that can be assessed and experiments to assess changes in gene regulation and the observed cellular effects. Array follow-up experiments could investigate innate and adaptive immune responses, inflammatory response genes, cell death pathways, apoptosis, cytokine signalling and receptor production, cellular metabolism and surface markers, as well as a larger set of known antiviral response genes. Ultimately, these arrays could also be run on cells harvested from live mice to determine gene responses in the context of a living animal model. These kinds of experiments could help to unravel the full scope of precisely how the cells are responding to the introduction of this technology. These experiments could be extensive or just focus on a few select areas of cellular biochemistry and gene response. If necessary, such studies could also be extended to include proteomics.

Cellular immunogenicity

Immunogenicity experiments were conducted but were mostly inconclusive. Initial analysis indicated that inoculations with small DNA dosages in mice would have the greatest potential to demonstrate dramatic improvements. However, due to low dosages, the response was weak, and differences were difficult to gauge. Furthermore, the dosage may have been too low and weak for RCR to be able to initiate and develop a strong effect in the limited duration of the study. For this reason, and based on the eGFP mouse experiment which used higher inoculation dosages and was able to demonstrate a recordable change in eGFP expression, it is recommended that a follow-up ELISpot experiment be conducted using the higher DNA inoculation dosages, and to carry out a long term evaluation of the interferon gamma and IL-2 response generated after six to nine months post-inoculation. Given the results generated thus far and our knowledge around BFDV disease progression, this time frame would probably be better suited to detect the immunogenic effects generated by RCR. Additional controls and combinations of inoculum should also be investigated, to guarantee coverage of all possible angles with regards to different levels of Rep expression and durations for RCR.

In addition to evaluating T-cell responses, antibody response should also be investigated by combining the RCR technology with an easy-to-assess antigen such as the influenza HA protein.

Further expression characterization in mice

Initially, the eGFP vaccine experiment in mice was meant to be a live and continuous quantification of expression, using luciferase as the reported gene to fully map out the changes of gene expression generated by RCR technology over time. This experiment was not conducted because, at the time, the apparatus to perform the live animal imaging for luminescence was not available. This scenario has changed, and given the results obtained from the eGFP expression experiment in mouse muscle tissues, performing this more advanced, and essentially better-suited, quantification experiment should be a top priority. Intradermal and intramuscular inoculations could be performed (over an extended period of time) to investigate the full gene of interest expression profile in the mice, and to fully characterise the expression profile created by this vector technology. Detailed protocols on how these live DNA immunization experiments should be conducted are available (Petkov et al., 2018).

Hypothesised therapeutic treatment for BFDV

During the course of this PhD, a mechanism by which BFDV prevents cellular apoptosis and promotes cellular necrosis was identified. Massive inflammation, excessive immune activation and cellular necrosis are the most lethal aspects of PBFD in diseased birds (Pass and Perry, 1985, 1984; Ritchie, 2013), and the evidence gathered here suggests that this is achieved and encouraged by the thwarting of natural apoptosis. A basic study to test the effects of both topical and ingested delivery of therapeutic

dosages of known apoptosis-inducing drugs as a hypothetical treatment for diseased birds is worth investigating. For diseased psittacine birds, the survival rate is very low and the disease has been described as mostly lethal (Hakimuddin et al., 2016; Pass and Perry, 1984; Ritchie, 2013). As these drugs are already FDA approved and in use medically in humans, obtaining them for an animal study should be relatively affordable and easy. As the proposed treatment is therapeutic in nature, animal ethical considerations are easily made as new birds need not be infected with a deadly disease. The hypothetical treatment can simply be administered by parrot breeders to their already-diseased birds and their outcomes recorded. (As these birds typically have poor outcomes due to their existing infections, and they are of high value, ethically and financially there are good reasons to conduct such an investigation.

Possible mechanism by which Rep increases cellular tolerance to pathogenic DNA

This possibility is easily tested: The Rep-expressing vector is already constructed and available, and transfections in tissue culture using a range of DNA transfection amounts, that include lethal dosages of DNA, can be established in a series of transfection experiments. Once established, co-transfection experiments with pTHRep can be performed to determine whether the introduction of Rep at various concentrations increases cell survivability and gene expression in cells with Rep versus cells without Rep. If this test proves to be valid, tests with toxic proteins can also be conducted to determine if expressing Rep increases cell survivability when toxic proteins are been expressed.

Multiple RCR amplicon amplifications

Experiments using multiple RCR-inducible plasmids, each expressing a different gene of interest, could be combined with the transient introduction of Rep to initiate RCR to amplify multiple gene targets. It is also worth altering the strength of Rep expression by testing Rep with various promoters, including cell-specific promoters that might be used to further refine applications of this technology.

Investigate Rep inhibition targets

Bioinformatics approaches can be used to find and identify other possible Rep binding sites. This information can then be used to help identify other possible promoters and genes that might also be inhibited by Rep. Follow-up experiments can be conducted to verify these findings and to quantify the strength and type of inhibition created by Rep.

Appendices

Appendix A – RCR amplicon tests and RCA screening gels

Once the RCR amplicons were verified, three additional vectors were created to test and verify functional RCR from vectors employing three separate design configurations for this technology with regards to the *rep* gene. This included *rep* inside and outside the amplicon being driven by its native *LIR* promoter and a third configuration with rep being driven by the SV40 promoter (Figure A1).

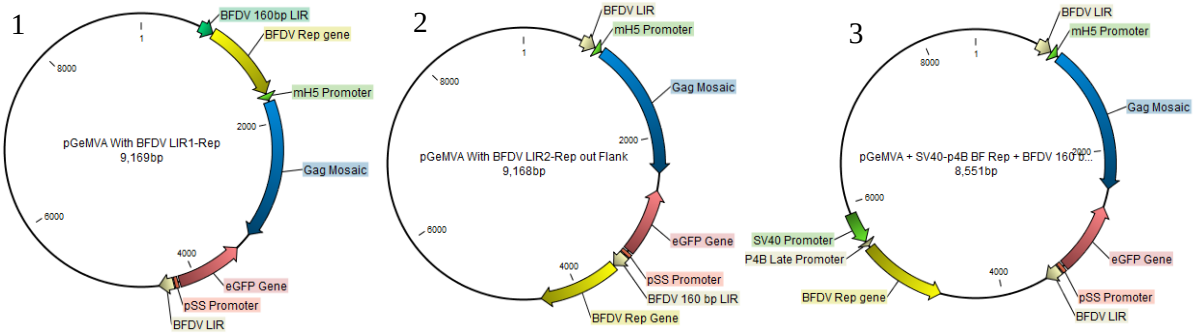

Figure A1: Three self-replicating variants of the RCR technology. 1) *Rep* driven by the native *LIR* promoter and inside the predicted amplicon. 2) *Rep* driven by the second *LIR* fragments promoter and residing outside the predicted amplicon 3) *Rep* driven by the poxviral P4B late promoter combined with the *SV40* promoter and residing outside the amplicon.

Serendipitously transfections in HeLa S3 cells with these plasmids demonstrated RCR through an indirect activation of the BFDV Capsid Promoter for driving eGFP which resides inside the rep sequence (Figure A1). This experiment demonstrated that an addition of the *SV40* promoter is not required to use this technology and the activation of RCR can be used to simultaneously activate gene expression from an input plasmid (Figure B2). RCR was verified for all plasmids via RCA analysis.

When *rep* is upstream of eGFP, the native BFDV Capsid promoter within *rep* drives eGFP expression (Figure A1:2). When *rep* is not present upstream of eGFP, as in (Figure A1:3), no eGFP expression occurs. Finally, when *rep* lies within the amplicon (Figure A1:1), as RCR occurs the *rep* sequence is repositioned to be immediately upstream of eGFP in the created amplicon, resulting in active eGFP expression. This demonstrates a possibility of using this technology to activate gene expression in a variety of complex ways, with a variety of potential medical uses.

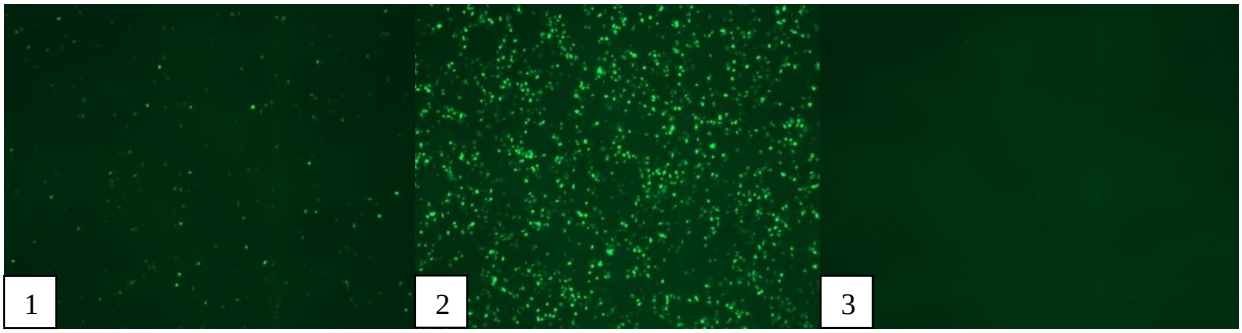

Figure A2: Plasmids of Figure A1 transfected into HeLa S3 cells and imaged 48 h pt. 1) *Rep* within the *LIR* flanks; 2) Rep outside the *LIR* flanks upstream of eGFP and 3) *Rep* outside flanks within a different region of the plasmid being driven by the *SV40* promoter.

The native BFDV Capsid promoter within the BFDV *rep* gene sequence is in the same locality as the PCV Capsid promoter. In the case of PCV, its promoter has been demonstrated to exhibit expression enhancing activity when placed upstream of the CMV Enhancer/promoter sequence (Tanzer *et al.*, 2011). After demonstration of the activity of the BFDV Capsid promoter, a bioinformatics investigation was undertaken to putatively map and identify the core promoter region within the BFDV *rep* sequence and compare it to the PCV one. This was done using an online neural network promoter prediction algorithm Version 2.2 available at http://www.fruitfly.org/seq_tools/promoter.html (Reese, 2001, 2000). CpG islands were also evaluated across this sequence using the method developed by Gardiner-Garden and Frommer (1987) http://www.bioinformatics.org/sms2/cpg_islands.html. This tool identified the entire antisense strand from the LIR through Rep positively as a CpG island. (Note: CpG islands are characterised a sequence range where the Observed vs expected CG value is greater than 0.6 over a region with a GC content over 50% for a sequence at least 200 bp in length. For the sequence depicted in Figure A3 this classification was true with the Observed vs Expected for different sub-sections ranging from 0.6 to 1.4 and been well over 1 across the core promoter region identified.)

On the antisense DNA strand of *rep* and its adjacent *LIR* fragment, no less than 14 identified promoter elements are present over this 1027 bp fragment of DNA. This also confirms that the BFDV LIR can function as a bi-directional promoter as it contains its own CAAT box flanked by two GC boxes, to create a transcription initiation site.

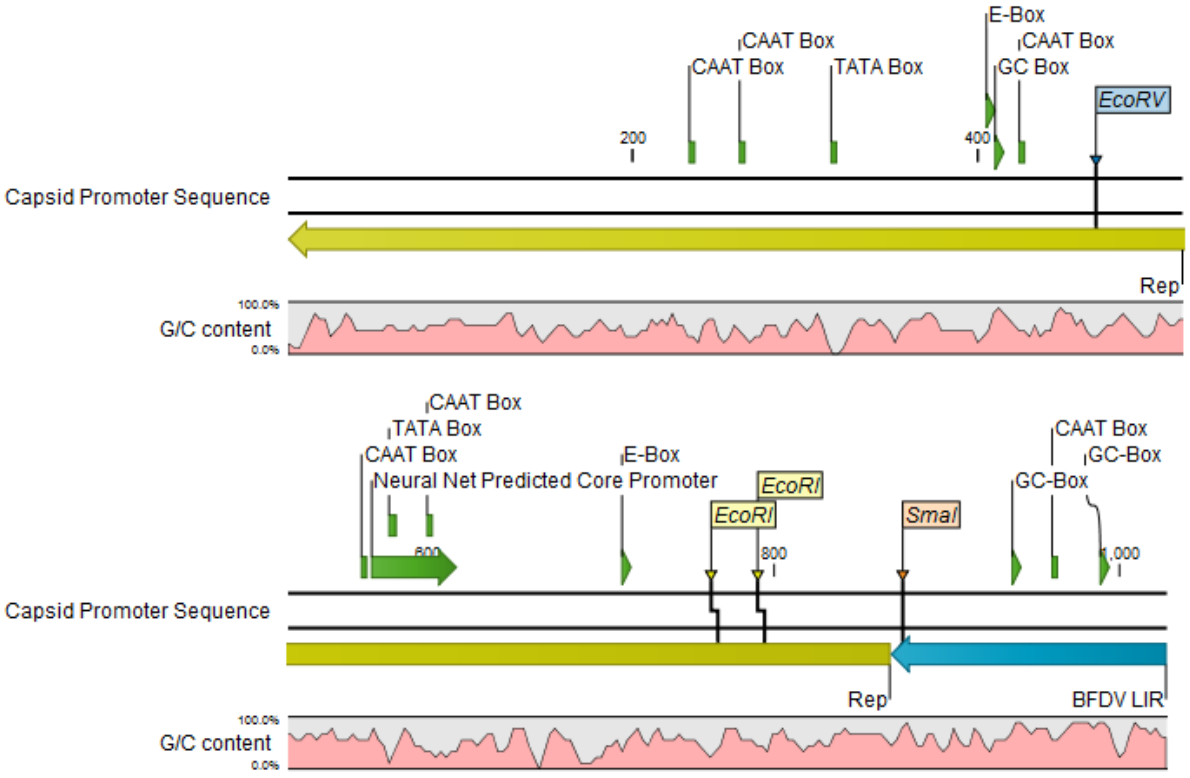

Figure A3: Neural net promoter prediction over the antisense strand of the BFDV *LIR-Rep* DNA sequence.

Verifying RCR via RCA was performed on a variety of plasmid constructs (Figure A4). For all transfected plasmids, CLCBio Main Workbench was used to predict the size of their amplicon band and these were then verified via RCA analysis. Predicted band sizes are as follows: Lane 1: 1994 BFDV RCR+ positive control; Lane 2: 3506 bp; Lane 3: 3592 bp; Lane 4&5: 2724 bp. Lanes 7-10 all contained plasmids capable of expressing BFDV Rep and were co-transfected with the BFDV Mutant plasmid to look for its amplicon. For Lanes 7-9 this band is present, indicating that the self-replicating plasmids were all expressing *rep*. Note: in Lane 7, two amplicons are identifiable. For Lane 10, however, the band is not present and possibly indicates a bad co-transfection as this sample does produce a replicon band by itself, albeit a weak one (Lane 6&19). Lanes 12-19 represent repeats of these same transfections using the pTHRep plasmid to transiently restore RCR for Lanes 13-15. All lanes (14-19) appear to have amplicon bands visible at the predicted sizes for their respective plasmids. It is noted the larger the amplicon produced, the fainter the band usually appeared, with the amplicon band for Lane 17 being the faintest.

These experiments have implications far beyond the scope of this PhD. They indicate that advanced manipulation of this technology is possible and there is potential to make highly sophisticated RCR plasmid constructs, capable of creating multiple amplicons to work in concert with different genes to generate an ever more complex and diverse range of effects.

Lane	1	2	3	4	5	6	7	8	9	10	11	12	13	14	15	16	17	18	19
DNA Ladder	+										+								
BFDV RCR+		+										+							
pTHRep 1:10 ratio													+	+	+				
BFDV Mutant							+	+	+	+			+						
S10 5.8 Kbp														+					
RCR- Luc(F)															+				
RCR+ Luc(F)			+				+									+			
S10 LIR1 Rep				+				+									+		
S10 LIR2 Rep					+				+									+	
S10 SV40 Rep						+				+									+

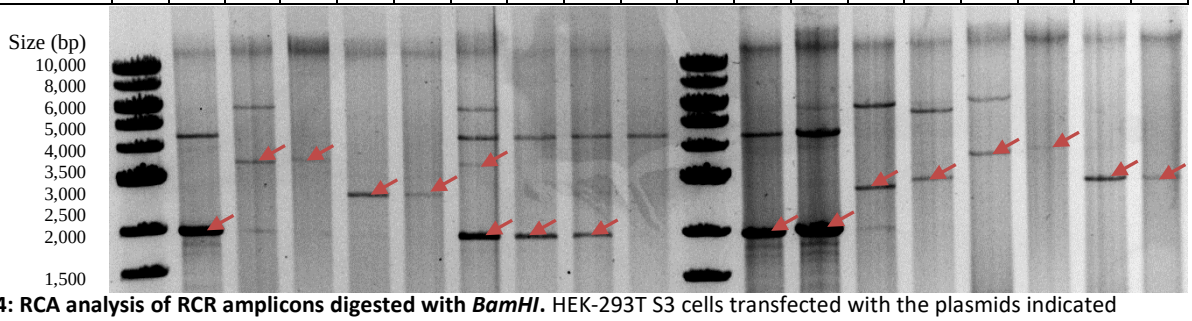

Figure A4: RCA analysis of RCR amplicons digested with *BamHI*. HEK-293T S3 cells transfected with the plasmids indicated in the table above.

Verification of RCR via RCA analysis was performed for the final RCR+ vector designs and their RCR- equivalent constructs and is shown in Figure A5.

Plasmids / Lane#	1	2	3	4	5	6	7	8	9	10
DNA Ladder	+									
RCR+ Luc(R)		+								
RCR- Luc(R)			+							
RCR+ Gag				+						
RCR- Gag					+					
RCR+ eGFP						+				
RCR- eGFP							+			
BFDV RCR+								+		
BFDV Mutant									+	
BFDV Mut + Rep										+

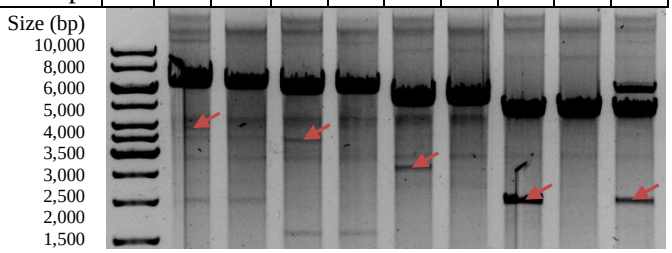

Figure A5: RCA verification of RCR amplicons for final vector constructs. *BamHI* digests of RCA DNA with predicted amplicon bands: Luciferase (3806 bp), Gag (3375 bp), eGFP (2577 bp) and the BFDV genome (1994 bp) bands are present for all the RCR+ self-replicating plasmids at their predicted locations (indicated in red) and not present in their RCR- non replicating equivalent plasmids containing the mutant Rep gene.

Appendix B – Flow Cytometry analysis using *FlowJo*

For statistical analysis, key statistical metrics were calculated in *FlowJo* and tabulated in Table B1 below. These metrics were used to evaluate and compare each of the distributions plotted and help explain and define the differences described above for these plots. Where possible, these metrics were applied to relative statistical formulae to define the population distributions and their differences. Towards this end ANOVA, the co-efficient of variance, standard deviation, mean, and medians for each histogram, were calculated and tabulated in Table B1 below.

Table B1: Statistical analyses performed on flow cytometry data for Q2 populations (Figure 3.3) of eGFP fluorescent cells at 24 h, 48 h and 96 h pt with additional analysis of the Q3 population at 96 h pt.

Population/Time Sample Statistic*	Q2/24h RCR- eGFP	Q2/24h RCR+ eGFP	Q2/48h RCR- eGFP	Q2/48h RCR+ eGFP	Q2/96h RCR- eGFP	Q2/96h RCR+ eGFP	Q3/96h RCR- eGFP	Q3/96h RCR+ eGFP
% Total Population	2.10%	2.07%	10.40%	8.75%	18.30%	9.53%	0.35%	0.91%
% +ve Population	-	-	92.5%	93.0%	98.10%	91.30%	1.90%	8.70%
CV: eGFP	253%	361%	191%	321%	153%	178%	147%	129%
CV: FSC-A	38.1%	30.8%	28.0%	36.5%	32.2%	36.0%	87.1%	85.7%
CV: SSC-A	57.7%	60.9%	50.6%	57.2%	52.0%	46.2%	109%	138%
GeoMean: eGFP	1512	1301	3125	1993	2219	2715	1736	1686
GeoMean: FSC-A	121463	151318	140934	135505	154179	158028	28121	18313
GeoMean: SSC-A	79090	67720	62244	83015	98564	135828	4758	2264
Mean: eGFP	3476	3219	7235	5865	4348	7956	3439	2653
Mean: FSC-A	129355	158623	146468	144279	162192	170534	41710	24595
Mean: SSC-A	89251	76478	67976	94568	111168	153766	9501	4157
Median: eGFP	1091	992	2888	1582	1946	2185	1283	1448
Median: FSC-A	115136	150528	141568	130368	149824	166080	28800	16832
Median: SSC-A	71872	61184	59456	77440	94464	145024	4160	1984
Robust CV: eGFP	178%	111%	176%	166%	181%	323%	246%	117%
Robust CV: FSC-A	37.5%	32.2%	27.1%	40.6%	38.9%	46.6%	208%	166%
Robust CV: SSC-A	48.8%	43.8%	36.9%	53.2%	56.0%	63.6%	523%	255%
SD: eGFP	8785	11625	13786	18803	6640	14200	5072	3417
SD: FSC-A	49233	48802	41059	52591	52157	61472	36328	21082
SD: SSC-A	51494	46607	34396	54078	57831	71059	10343	5747
Robust SD: eGFP	1943	1096	5092	2629	3518	7047	3157	1694
Robust SD: FSC-A	43232	48544	38400	52928	58208	77312	59968	27904
Robust SD: SSC-A	35072	26784	21920	41216	52864	92224	21760	5056
Skewness: eGFP	0.81	0.57	0.95	0.68	1.09	1.22	1.28	1.06
Skewness: FSC-A	0.87	0.50	0.36	0.79	0.71	0.22	1.07	1.10
Skewness: SSC-A	1.01	0.98	0.74	0.95	0.87	0.37	1.55	1.13

***Statistical formula definitions adapted from the FlowJo documentation: Mean = The arithmetic mean; Median = Relative value of the 50th percentile (The median is a more robust estimator of the central tendency of a population). GeoMean = The geometric mean. Can be a more applicable metric for a log-normal distribution and is always less than or equal to the arithmetic mean. SD = The Standard Deviation is a measure of the spread of the dataset. Robust Standard Deviation – If neither the scale values for the 84.13 percentile or 15.87 percentile of events is off-scale, then the robust standard deviation is equal to ((intensity for 84.13 percentile of events minus the median intensity) + (median intensity minus the intensity for 15.87 percentile of events)) / 2. The robust standard deviation is not as skewed by outlying values as the Standard Deviation. CV – Normalized Standard Deviation (CV = StdDev/Mean). Robust CV – Equals 100 * 1/2(Intensity [at 84.13 percentile] – Intensity [at 15.87 percentile]) / Median. The robust CV is not as skewed by outlying values as the CV. Skewness is defined as [3*(Mean – Median)/SD].**

To analyse the statistical significance and variance of the differences between the different samples for each dataset generated from flow cytometry, an ANOVA was performed in MS Excel for each dataset

at each time point collected. These results are presented in Table B2: eGFP; Table B3: SSC-A and Table B4: FSC-A below.

Table B2: Single factor ANOVA of eGFP dataset

Data Summary for eGFP ANOVA

Groups	*Sum*	*Average*	*Variance*
24 h RCR-	1050	0.256348	0.462719
24 h RCR+	1037	0.253174	0.469465
48 h RCR-	5179	1.264404	2.953517
48 h RCR+	4376	1.068359	3.10546
96 h RCR-	8956	2.186523	9.700487
96 h RCR+	4647	1.134521	3.150886

ANOVA

Source of Variation	*SS*	*df*	*MS*	*F*	*P-value*	*F crit*
24 h						
Between Groups	0.02063	1	0.02063	0.044261	**0.833373**	3.842594
Within Groups	3817.294	8190	0.466092			
Total	3817.314	8191				
48 h						
Between Groups	78.71204	1	78.71204	25.98196	**3.52E-07**	3.842594
Within Groups	24811.51	8190	3.029488			
Total	24890.22	8191				
96 h						
Between Groups	2266.538	1	2266.538	352.7309	**4.42E-77**	3.842594
Within Groups	52626.37	8190	6.425687			
Total	54892.91	8191				

Table B3: Single factor ANOVA of SSC-A dataset

Data Summary for SSC-A ANOVA

Groups	*Sum*	*Average*	*Variance*
24 h RCR-	1050	0.256347	0.685918
24 h RCR+	1037	0.253173	0.534910
48 h RCR-	5179	1.264404	5.932759
48 h RCR+	4376	1.068359	9.243189
96 h RCR-	8956	2.186523	56.5542
96 h RCR+	4647	1.134521	134.1760

SSC-A ANOVA

24 h

Source of Variation	*SS*	*df*	*MS*	*F*	*P-value*	*F crit*
Between Groups	0.02063	1	0.02063	0.033797	**0.854145**	3.842594
Within Groups	4999.294	8190	0.610414			
Total	4999.314	8191				
48 h						
Between Groups	78.71204	1	78.71204	10.37326	**0.001284**	3.842594
Within Groups	62145.51	8190	7.587974			
Total	62224.22	8191				
96 h						
Between Groups	2266.538	1	2266.538	23.76695	**1.11E-06**	3.842594
Within Groups	781040.4	8190	95.36513			
Total	783307	8191				

Table B4: Single factor ANOVA of FSC-A dataset

Data Summary for FSC-A ANOVA

Groups	*Sum*	*Average*	*Variance*
24 h RCR-	1050	0.256348	0.881767
24 h RCR+	1037	0.253174	1.92148
48 h RCR-	5179	1.264404	7.083919
48 h RCR+	4376	1.068359	24.00363
96 h RCR-	8956	2.186523	246.668
96 h RCR+	4647	1.134521	127.5475

FSC-A ANOVA

24 h

Source of Variation	*SS*	*df*	*MS*	*F*	*P-value*	*F crit*
Between Groups	0.02063	1	0.02063	0.014719	**0.90344**	3.842594
Within Groups	11479.29	8190	1.401623			
Total	11479.31	8191				
48 h						
Between Groups	78.71204	1	78.71204	5.063895	**0.024456**	3.842594
Within Groups	127303.5	8190	15.54377			
Total						
96 h						
Between Groups	2266.538	1	2266.538	12.11355	**0.000503**	3.842594
Within Groups	1532412	8190	187.1077			
Total	1534679	8191				

Appendix C – FACS gating parameters and RAW data

The gating parameters and data analysis used for FACS was captured in the FACS Diva 6.1.3 software suite and is depicted below for the FACS experiment which was performed 96 h pt.

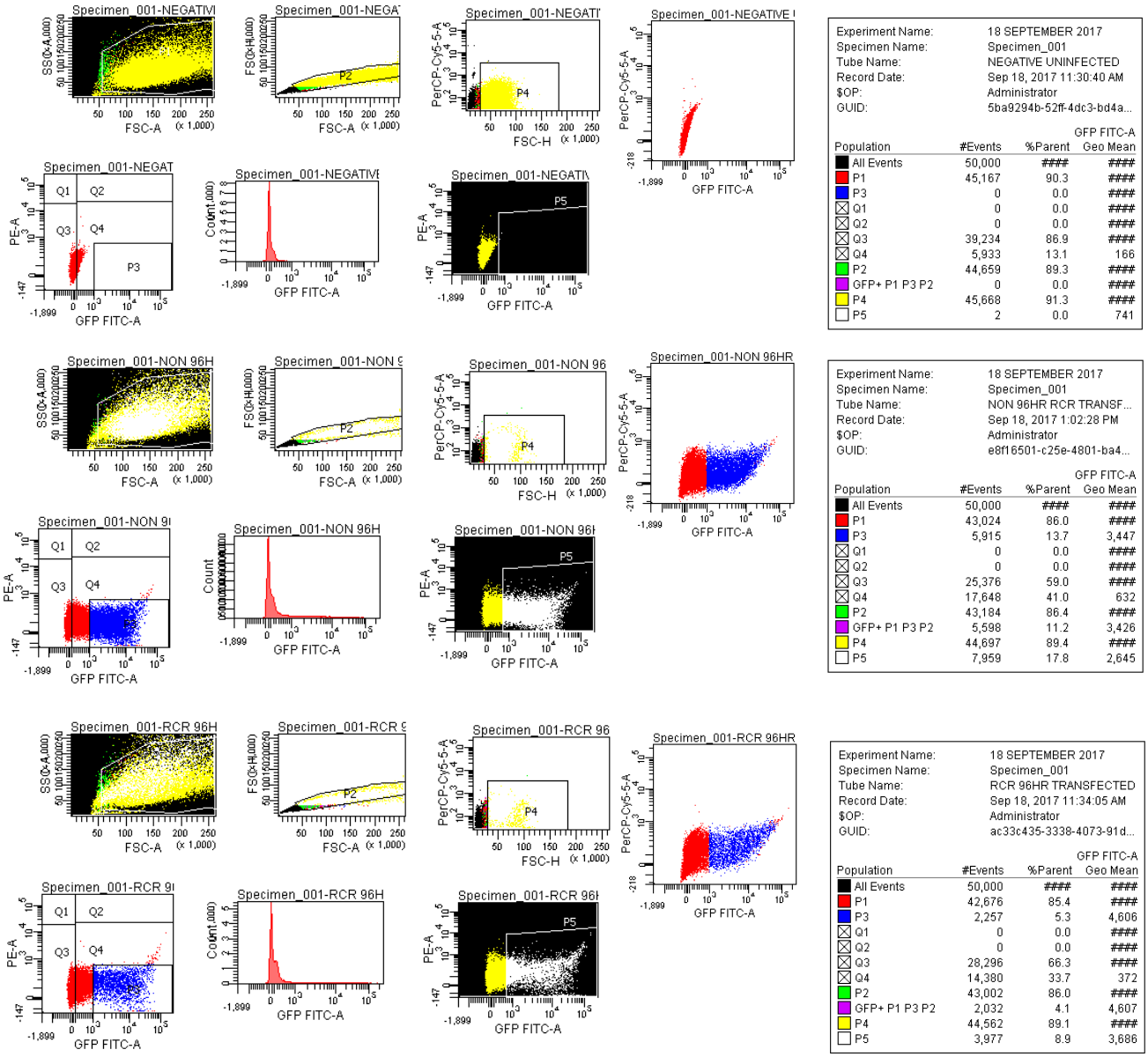

Figure C1: Screen captures from FACS Diva 6.1.3 after setting gating criteria for FACS on (Top) Negative control; (Middle) RCR- eGFP and (Bottom) RCR+ eGFP transfected HeLa S3 cells 96 h pt. P5 depicts what became the final sorted fraction, note the low fluorescent cut-off of P5 was approximately 1000.

Appendix D – RT2 Profiler array data

After running the array genes up- or down-regulated with a fold change of 1.4 or higher were selected and tabulated together for the different analyses performed. The calculated p-values for each gene were also recorded. These are presented in table D1 below.

Table D1: RT² profiler array data for genes exhibiting a fold change of >1.4 or <-1.4

Genes	RCR+ Gag vs pUC19	RCR- Gag vs pUC19	RCR+ Gag & pTHRep vs pUC19	pTHRep vs pUC19	RCR+ eGFP vs pUC19	RCR+ Gag vs RCR- Gag	RCR+ Gag & pTHRep vs RCR- Gag	RCR+ Gag vs RCR+ eGFP
Symbol	**Fold Up- or Down-Regulation**	**Fold Up- or Down-Regulation**	**Fold Up- or Down-Regulation**	**Fold Up- or Down-Regulation**	**Fold Up- or Down-Regulation**	**Fold Up- or Down-Regulation**	**Fold Up- or Down-Regulation**	**Fold Up- or Down-Regulation**
CARD9	**2.04**	1.91	1.65	**2.39**	1.55	1.07	-1.16	1.32
p-value	0.074220	0.065251	0.356754	0.128369	0.376802	0.566140	0.876159	0.629633
CASP10	1.16	-1.01	-1.81	**-3.57**	-1.06	1.17	-1.79	1.22
p-value	0.544523	0.811075	0.093632	**0.006829**	0.882316	0.650374	0.291565	0.620134
CCL3	1.40	-1.07	1.19	1.11	1.22	1.49	1.27	1.15
p-value	0.490069	0.820528	0.644582	0.800992	0.593863	0.452720	0.478589	0.614695
CCL5	1.47	-1.07	1.52	1.61	1.50	1.56	1.62	-1.02
p-value	0.468925	0.821844	0.221470	0.420507	0.433111	0.439089	0.128207	0.840355
CXCL10	1.35	1.06	1.38	1.00	-1.06	1.28	1.31	1.43
p-value	0.581921	0.864075	0.839843	0.751363	0.727972	0.663072	0.965989	0.478067
CXCL11	1.53	-1.30	-1.31	-1.35	-1.23	1.98	-1.01	1.87
p-value	0.414967	0.414927	0.454419	0.421743	0.601780	0.135774	0.936704	0.205393
DHX58	1.40	1.00	1.70	1.77	1.53	1.40	1.69	-1.09
p-value	0.559857	0.937806	0.364335	0.273067	0.453401	0.609955	0.441578	0.965908
FOS	-1.17	1.16	-1.24	-1.06	-1.29	-1.35	-1.43	1.11
p-value	0.670185	0.612568	0.613406	0.994217	0.380892	0.436292	0.408515	0.692700
IFNA1	1.22	1.19	1.19	-1.00	-1.23	1.02	-1.01	1.50
p-value	0.513011	0.551919	0.567007	0.889269	0.732658	0.957304	0.912438	0.393983
IFNA2	1.27	1.41	-1.04	1.34	1.04	-1.11	-1.47	1.22
p-value	0.959275	0.723067	0.735513	0.668490	0.895607	0.700218	0.462322	0.799928
IFNB1	-1.28	-1.14	-1.60	-1.01	-1.07	-1.12	-1.41	-1.20
p-value	0.559592	0.718394	0.434774	0.746215	0.663890	0.561467	0.505923	0.688195
IL12A	1.20	1.28	1.14	-1.47	1.17	-1.06	-1.11	1.03
p-value	0.795501	0.659291	0.807776	0.616268	0.808495	0.693208	0.863820	0.983665
IL12B	**2.27**	-1.13	-1.25	1.28	1.01	**2.57**	-1.10	**2.24**
p-value	0.408661	0.602278	0.538109	0.939663	0.655321	0.387496	0.755364	0.390607
IL1B	-1.20	1.36	-1.03	1.22	1.09	-1.62	-1.39	-1.30
p-value	0.964714	0.624012	0.976266	0.606535	0.910744	0.637383	0.608787	0.889895
IL6	-1.08	1.21	1.42	1.42	1.38	-1.31	1.17	-1.49
p-value	0.989133	0.600927	0.392116	0.389090	0.422790	0.642685	0.626510	0.442004

Table D1: Continued

Genes	RCR+ Gag vs pUC19	RCR- Gag vs pUC19	RCR+ Gag & pTHRep vs pUC19	pTHRep vs pUC19	RCR+ eGFP vs pUC19	RCR+ Gag vs RCR- Gag	RCR+ Gag & pTHRep vs RCR- Gag	RCR+ Gag vs RCR+ eGFP
Symbol	**Fold Up- or Down-Regulation**	**Fold Up- or Down-Regulation**	**Fold Up- or Down-Regulation**	**Fold Up- or Down-Regulation**	**Fold Up- or Down-Regulation**	**Fold Up- or Down-Regulation**	**Fold Up- or Down-Regulation**	**Fold Up- or Down-Regulation**
CXCL8	-1.38	-1.52	1.30	1.41	1.55	1.10	1.97	**-2.14**
p-value	0.933581	0.949516	0.544384	0.470093	0.463495	0.992453	0.665176	0.488460
IRF5	1.23	1.42	1.35	1.49	**2.04**	-1.16	-1.05	-1.66
p-value	0.887872	0.854734	0.985418	0.786453	0.560523	0.702143	0.811404	0.444994
IRF7	-1.22	1.15	-1.15	-1.19	1.11	-1.40	-1.32	-1.36
p-value	0.444486	0.752673	0.607915	0.764769	0.853632	0.211279	0.343213	0.155312
MEFV	1.26	1.87	1.03	1.66	1.23	-1.49	-1.81	1.03
p-value	0.535454	0.169301	0.927424	0.193958	0.514833	0.469278	0.177904	0.878367
MX1	1.20	-1.60	1.64	1.04	1.06	1.92	**2.63**	1.13
p-value	0.481402	0.947090	0.115320	0.681613	0.641684	0.593868	0.303498	0.970167
OAS2	-1.18	-1.49	1.13	-1.26	-1.15	1.26	1.69	-1.03
p-value	0.793331	0.422778	0.934349	0.533229	0.672862	0.542488	0.262679	0.887585
PSTPIP1	-1.05	-1.07	1.15	-1.47	-1.22	1.01	1.23	1.16
p-value	0.857953	0.811896	0.894543	0.376682	0.545405	0.721778	0.862298	0.550014
RELA	1.03	1.02	1.03	1.42	1.04	1.01	1.01	-1.01
p-value	0.476173	0.759997	0.497528	0.362045	0.334730	0.842481	0.860965	0.796890
TNF	1.36	-1.06	1.15	1.24	1.22	1.44	1.22	1.11
p-value	0.474266	0.825657	0.724145	0.572759	0.588458	0.400649	0.531196	0.734359

List of references

Abramoff, M.D., Magalhães, P.J., Ram, S.J., 2004. Image Processing with ImageJ. Biophotonics Int. 11, 36–42.

Adams, D.J., Van Der Weyden, L., Mayeda, A., Stamm, S., Morris, B.J., Rasko, J.E.J., 2001. ZNF265 - A novel spliceosomal protein able to induce alternative splicing. J. Cell Biol. 154, 25–32. https://doi.org/10.1083/jcb.200010059

Adan, A., Alizada, G., Kiraz, Y., Baran, Y., Nalbant, A., 2017. Flow cytometry: basic principles and applications. Crit. Rev. Biotechnol. 37, 163–176. https://doi.org/10.3109/07388551.2015.1128876

Afzali, A.M., Müntefering, T., Wiendl, H., Meuth, S.G., Ruck, T., 2018. Skeletal muscle cells actively shape (auto)immune responses. Autoimmun. Rev. 17, 518–529. https://doi.org/10.1016/j.autrev.2017.12.005

Ahuja, D., Sáenz-Robles, M.T., Pipas, J.M., 2005. SV40 large T antigen targets multiple cellular pathways to elicit cellular transformation. Oncogene 24, 7729–7745. https://doi.org/10.1038/sj.onc.1209046

Aiewsakun, P., Katzourakis, A., 2017. Marine origin of retroviruses in the early Palaeozoic Era. Nat. Commun. 8, 1–12. https://doi.org/10.1038/ncomms13954

Allan, G., Krakowka, S., Ellis, J., Charreyre, C., 2012. Discovery and evolving history of two genetically related but phenotypically different viruses, porcine circoviruses 1 and 2. Virus Res. 164, 4–9. https://doi.org/10.1016/j.virusres.2011.09.013

Altenburg, A.F., van de Sandt, C.E., van Trierum, S.E., De Gruyter, H.L.M., van Run, P.R.W.A., Fouchier, R.A.M., Roose, K., Saelens, X., Volz, A., Sutter, G., de Vries, R.D., Rimmelzwaan, G.F., 2016. Increased Protein Degradation Improves Influenza Virus Nucleoprotein-Specific CD8 + T Cell Activation In Vitro but Not in C57BL/6 Mice. J. Virol. 90, 10209–10219. https://doi.org/10.1128/JVI.01633-16

Amery-Gale, J., Marenda, M.S., Owens, J., Eden, P.A., Browning, G.F., Devlin, J.M., 2017. A high prevalence of beak and feather disease virus in non-psittacine Australian birds. J. Med. Microbiol. 66, 1005–1013. https://doi.org/10.1099/jmm.0.000516

Angell, T.E., Lechner, M.G., Jang, J.K., LoPresti, J.S., Epstein, A.L., 2014. MHC Class I Loss Is a Frequent Mechanism of Immune Escape in Papillary Thyroid Cancer That Is Reversed by Interferon and Selumetinib Treatment In Vitro. Clin. Cancer Res. 20, 6034–6044. https://doi.org/10.1158/1078-0432.CCR-14-0879

Arellano, B., Graber, D.J., Sentman, C.L., 2016. Regulatory T cell-based therapies for autoimmunity. Discov. Med. 22, 73–80.

Babkin, I. V., Babkina, I.N., 2015. The origin of the variola virus. Viruses 7, 1100–1112. https://doi.org/10.3390/v7031100

Badylak, S.F., 2019. Extracellular matrix and the immune system: friends or foes. Nat. Rev. Urol. https://doi.org/10.1038/s41585-019-0196-0

Bai, H., Lester, G.M.S., Petishnok, L.C., Dean, D.A., 2017. Cytoplasmic transport and nuclear import of plasmid DNA. Biosci. Rep. 37, BSR20160616. https://doi.org/10.1042/bsr20160616

Bankhead, P., 2016. Analyzing fluorescence microscopy images with ImageJ Analyzing fluorescence microscopy images with ImageJ. Belfast.

Banos-Lara, M. del R., Méndez, E., 2010. Role of individual caspases induced by astrovirus on the processing of its structural protein and its release from the cell through a non-lytic mechanism. Virology 401, 322–332. https://doi.org/10.1016/j.virol.2010.02.028

Bassami, M.R., Berryman, D., Wilcox, G.E., Raidal, S.R., 1998. Psittacine beak and feather disease virus nucleotide sequence analysis and its relationship to porcine circovirus, plant circoviruses, and chicken anaemia virus. Virology 249, 453–9. https://doi.org/10.1006/viro.1998.9324

Bednarski, J.J., Sleckman, B.P., 2019. At the intersection of DNA damage and immune responses. Nat. Rev. Immunol. https://doi.org/10.1038/s41577-019-0135-6

Behrens, E.M., Koretzky, G.A., 2017. Review: Cytokine Storm Syndrome: Looking Toward the Precision Medicine Era. Arthritis Rheumatol. 69, 1135–1143. https://doi.org/10.1002/art.40071

Belshe, R., Gorse, G., Mulligan, M., 1998. Induction of immune responses to HIV-1 by canarypox virus (ALVAC) HIV-1 and gp120 SF-2 recombinant vaccines in uninfected volunteers. Aids 82500,

2407–2415.
Bennett, P.M., Chopra, I. a N., 1993. Molecular Basis of. Society 37, 153–158. https://doi.org/10.1126/science.1234340
Benoit, N., 2010. Venom, antivenom and immunity [WWW Document]. URL http://www.normanbenoit.com/Venom, Antivenom and Immunity.pdf (accessed 4.18.19).
Berger, A., 2000. Science commentary : Th1 and Th2 responses : what are they ? Bmj 12, 424.
Bertani, G., 2004. Lysogeny at mid-twentieth century:P1, P2, and other experimental systems. J Bacteriol 186, 595–600. https://doi.org/10.1128/JB.186.3.595-600.2004
Bertin, J., Guo, Y., Wang, L., Srinivasula, S.M., Jacobson, M.D., Poyet, J., Merriam, S., Du, M., Dyer, M.J.S., Robison, K.E., Distefano, P.S., Alnemri, E.S., 2000. CARD9 Is a Novel Caspase Recruitment Domain-containing Protein That Interacts With BCL10 / CLAP and Activates NF- B *. J. Biol. Chem. 275, 41082–41086. https://doi.org/10.1074/jbc.C000726200
Blagoveshchenskaya, A.D., Thomas, L., Feliciangeli, S.F., Hung, C.H., Thomas, G., 2002. HIV-1 Nef downregulates MHC-I by a PACS-1- and PI3K-regulated ARF6 endocytic pathway. Cell 111, 853–866. https://doi.org/10.1016/S0092-8674(02)01162-5
Bolhassani, A., Yazdi, S.R., 2009. DNA immunization as an efficient strategy for vaccination. Avicenna J. Med. Biotechnol. 1, 71–88.
Bonne, N., Shearer, P., Sharp, M., Clark, P., Raidal, S., 2019. Assessment of recombinant beak and feather disease virus capsid protein as a vaccine for psittacine beak and feather disease 640–647. https://doi.org/10.1099/vir.0.006932-0
Boshart, M., Weber, F., Jahn, G., Dorsch-Hler, K., Fleckenstein, B., Schaffner, W., 1985. A very strong enhancer is located upstream of an immediate early gene of human cytomegalovirus. Cell 41, 521–530. https://doi.org/10.1016/S0092-8674(85)80025-8
Bourgeois-Daigneault, M.-C., Roy, D., Aitken, A., El Sayes, N., Martin, N., Varrette, O., Falls, T., St-Germain, L., Pelin, A., Lichty, B., Stojdl, D., Ungerechts, G., Diallo, J.-S., Bell, J., 2018. Neo-Adjuvant Oncolytic Virotherapy Prior to Surgery Sensitizes Triple- Negative Breast Cancer to Immune Checkpoint Therapy. Sci. Transl. Med. 1641, 1–12.
Boylston, A., 2012. The origins of inoculation 309–313.
Brice, G.T., Dobaño, C., Sedegah, M., Stefaniak, M., Graber, N.L., Campo, J.J., Carucci, D.J., Doolan, D.L., 2007. Extended immunization intervals enhance the immunogenicity and protective efficacy of plasmid DNA vaccines. Microbes Infect. 9, 1439–1446. https://doi.org/10.1016/j.micinf.2007.07.009
Buchbinder, S.P., Mehrotra, D. V., Duerr, A., Fitzgerald, D.W., Mogg, R., Li, D., Gilbert, P.B., Lama, J.R., Marmor, M., del Rio, C., McElrath, M.J., Casimiro, D.R., Gottesdiener, K.M., Chodakewitz, J.A., Corey, L., Robertson, M.N., 2008. Efficacy assessment of a cell-mediated immunity HIV-1 vaccine (the Step Study): a double-blind, randomised, placebo-controlled, test-of-concept trial. Lancet 372, 1881–1893. https://doi.org/10.1016/S0140-6736(08)61591-3
Burcelin, R., 2017. Microbiote intestinal et dialogue immunitaire au cours de la maladie métabolique. Biol. Aujourdhui. 211, 1–18. https://doi.org/10.1051/jbio/2017008
Burgers, W. a, Chege, G.K., Müller, T.L., van Harmelen, J.H., Khoury, G., Shephard, E.G., Gray, C.M., Williamson, C., Williamson, A.-L., 2009. Broad, high-magnitude and multifunctional CD4+ and CD8+ T-cell responses elicited by a DNA and modified vaccinia Ankara vaccine containing human immunodeficiency virus type 1 subtype C genes in baboons. J. Gen. Virol. 90, 468–80. https://doi.org/10.1099/vir.0.004614-0
Burton, D.R., 2017. What Are the Most Powerful Immunogen Design Vaccine Strategies? Reverse Vaccinology 2.0 Shows Great Promise. Cold Spring Harb. Perspect. Biol. 9, a030262. https://doi.org/10.1101/cshperspect.a030262
Campisi, J., 2014. Aging, Cellular Senescence, and Canc. Annu Rev Physiol 685–705. https://doi.org/10.1146/annurev-physiol-030212-183653.Aging
Carboni, V., Maaliki, C., Alyami, M., Alsaiari, S., Khashab, N., 2019. Synthetic Vehicles for Encapsulation and Delivery of CRISPR/Cas9 Gene Editing Machinery. Adv. Ther. 2, 1800085. https://doi.org/10.1002/adtp.201800085
Cardis, M.A., Ni, J., Bhawan, J., 2017. Granular cell differentiation : A review of the published work. J. Dermatol. 44, 251–258. https://doi.org/10.1111/1346-8138.13758
Carl Zeiss Microscopy, 2015. Zen2 Software Guide: The Tiles & Positions Module.

Carl Zeiss Microscopy, 2013. ZEN Blue – Exploring the Image Analysis Module.
Carmona-Gutierrez, D., Bauer, M.A., Zimmermann, A., Aguilera, A., Austriaco, N., Ayscough, K., Balzan, R., Bar-Nun, S., Barrientos, A., Belenky, P., Blondel, M., Braun, R.J., Breitenbach, M., Burhans, W.C., Buettner, S., Cavalieri, D., Chang, M., Cooper, K.F., Côrte-Real, M., Costa, V., Cullin, C., Dawes, I., Dengjel, J., Dickman, M.B., Eisenberg, T., Fahrenkrog, B., Fasel, N., Froehlich, K.-U., Gargouri, A., Giannattasio, S., Goffrini, P., Gourlay, C.W., Grant, C.M., Greenwood, M.T., Guaragnella, N., Heger, T., Heinisch, J., Herker, E., Herrmann, J.M., Hofer, S., Jiménez-Ruiz, A., Jungwirth, H., Kainz, K., Kontoyiannis, D.P., Ludovico, P., Manon, S., Martegani, E., Mazzoni, C., Megeney, L.A., Meisinger, C., Nielsen, J., Nystroem, T., Osiewacz, H.D., Outeiro, T.F., Park, H.-O., Pendl, T., Petranovic, D., Picot, S., Polčic, P., Powers, T., Ramsdale, M., Rinnerthaler, M., Rockenfeller, P., Ruckenstuhl, C., Schaffrath, R., Segovia, M., Severin, F.F., Sharon, A., Sigrist, S.J., Sommer-Ruck, C., Sousa, M.J., Thevelein, J.M., Thevissen, K., Titorenko, V., Toledano, M.B., Tuite, M., Voegtle, F.-N., Westermann, B., Winderickx, J., Wissing, S., Woelfl, S., Zhang, Z.J., Zhao, R.Y., Zhou, B., Galluzzi, L., Kroemer, G., Madeo, F., 2018. Guidelines and recommendations on yeast cell death nomenclature. Microb. Cell 5, 4–31. https://doi.org/10.15698/mic2018.01.607
Centola, M., Wood, G., Frucht, D.M., Galon, J., Aringer, M., Farrell, C., Kingma, D.W., Horwitz, M.E., Mansfield, E., Holland, S.M., Shea, J.J.O., Rosenberg, H.F., Malech, H.L., Kastner, D.L., 2000. The gene for familial Mediterranean fever , MEFV , is expressed in early leukocyte development and is regulated in response to inflammatory mediators 95, 3223–3231.
Chen, C., Itakura, E., Nelson, G.M., Sheng, M., Laurent, P., Fenk, L.A., Butcher, R.A., Hegde, R.S., Bono, M. De, 2017. Europe PMC Funders Group IL-17 is a neuromodulator of Caenorhabditis elegans ' sensory responses. Nature 542, 43–48. https://doi.org/10.1038/nature20818.
Chen, S., Cheng, A., Wang, M., 2013. Innate sensing of viruses by pattern recognition receptors in birds. Vet. Res. 44, 1. https://doi.org/10.1186/1297-9716-44-82
Cheung, A.K., 2015. Specific functions of the Rep and Rep' proteins of porcine circovirus during copy-release and rolling-circle DNA replication. Virology 481, 43–50. https://doi.org/10.1016/j.virol.2015.01.004
Cheung, A.K., 2012. Porcine circovirus: Transcription and DNA replication. Virus Res. 164, 46–53. https://doi.org/10.1016/j.virusres.2011.10.012
Clegg, C.H., Rininger, J.A., Baldwin, S.L., 2013. Clinical vaccine development for H5N1 influenza. Expert Rev. Vaccines 12, 767–777. https://doi.org/10.1586/14760584.2013.811178.Clinical
Cocchi, F., Devico, A.L., Garzino-demo, A., Arya, S.K., Gallo, R.C., Lussot, P., 1995. Identification of RANTES, MIP-1α, and MIP-1β as the Major HIV-Suppressive Factors Produced by CD8+ T Cells. Science (80-.). 270, 1811–1815. https://doi.org/10.1126/science.270.5243.1811
Cohen, H.W., 2011. P values: Use and misuse in medical literature. Am. J. Hypertens. 24, 18–23. https://doi.org/10.1038/ajh.2010.205
Cole, G., McCaffrey, J., Ali, A.A., McCarthy, H.O., 2015. DNA vaccination for prostate cancer: Key concepts and considerations. Cancer Nanotechnol. 6. https://doi.org/10.1186/s12645-015-0010-5
Collings, A., Pitkänen, Jukka, Strengell, M., Tähtinen, M., Pitkänen, Jaakko, Lagerstedt, A., Hakkarainen, K., Ovod, V., Sutter, G., Ustav, M., Ustav, E., Männik, A., Ranki, A., Peterson, P., Krohn, K., 1999. Humoral and cellular immune responses to HIV-1 Nef in mice DNA-immunised with non-replicating or self-replicating expression vectors. Vaccine 18, 460–467. https://doi.org/10.1016/S0264-410X(99)00245-5
Collins, N., Hochheiser, K., Carbone, F.R., Gebhardt, T., 2017. Sustained accumulation of antigen-presenting cells after infection promotes local T-cell immunity. Immunol. Cell Biol. 95, 878–883. https://doi.org/10.1038/icb.2017.60
Collins, T.J., 2007. ImageJ for microscopy 43. https://doi.org/10.2144/000112517
Cortés, A., Muñoz-Antoli, C., Esteban, J.G., Toledo, R., 2017. Th2 and Th1 Responses: Clear and Hidden Sides of Immunity Against Intestinal Helminths. Trends Parasitol. 33, 678–693. https://doi.org/10.1016/j.pt.2017.05.004
Cosma, G., Eisenlohr, L., 2018. CD8 + T-cell responses in vaccination : reconsidering targets and function in the context of chronic antigen stimulation [version 1 ; referees : 2 approved] Referee Status : 7, 1–8. https://doi.org/10.12688/f1000research.14115.1
Costa-Mattioli, M., Sonenberg, N., 2008. RAPping production of type I interferon in pDCs through

mTOR. Nat. Immunol. 9, 1097–1099. https://doi.org/10.1038/ni1008-1097
Crowther, R.A., Berriman, J.A., Curran, W.L., Allan, G.M., Todd, D., 2003. Comparison of the Structures of Three Circoviruses: Chicken Anemia Virus, Porcine Circovirus Type 2, and Beak and Feather Disease Virus. J. Virol. 77, 13036–13041. https://doi.org/10.1128/JVI.77.24.13036-13041.2003
Cruz, J.M. Dela, 2016. Basic Image Analysis with ImageJ, Institute of Biotechnology.
Dalod, M., Salazar-Mather, T.P., Malmgaard, L., Lewis, C., Asselin-Paturel, C., Brière, F., Trinchieri, G., Biron, C. a, 2002. Interferon alpha/beta and interleukin 12 responses to viral infections: pathways regulating dendritic cell cytokine expression in vivo. J. Exp. Med. 195, 517–28.
Dauphin, G., Zientara, S., 2007. West Nile virus: Recent trends in diagnosis and vaccine development. Vaccine 25, 5563–5576. https://doi.org/10.1016/j.vaccine.2006.12.005
Deeks, S.G., Overbaugh, J., Phillips, A., Buchbinder, S., 2015. HIV infection. Nat. Rev. Dis. Prim. 1. https://doi.org/10.1038/nrdp.2015.35
Dell'Oste, V., Caneparo, V., de Andrea, M., Gariglio, M., Landolfo, S., 2013. IFI16 Autoantibodies, Third Edit. ed, Autoantibodies: Third Edition. Elsevier. https://doi.org/10.1016/B978-0-444-56378-1.00040-X
Diehl, K.-H., Hull, R., Morton, D., Pfister, R., Rabemampianina, Y., Smith, D., Vidal, J.-M., Van De Vorstenbosch, C., 2001. A Good Practice Guide to the Administration of Substances and Removal of Blood, Including Routes and Volumes GOOD PRACTICE GUIDE FOR ADMINISTRATION OF SUBSTANCES. J. Appl. Toxicol. J. Appl. Toxicol 21, 15–23. https://doi.org/10.1002/jat.727
DiMaio, D., 2019. Small size, big impact: how studies of small DNA tumour viruses revolutionized biology. Philos. Trans. R. Soc. B Biol. Sci. 374, 20180300. https://doi.org/10.1098/rstb.2018.0300
Diner, B.A., Lum, K.K., Cristea, I.M., 2015. The emerging role of nuclear viral DNA sensors. J. Biol. Chem. 290, 26412–26421. https://doi.org/10.1074/jbc.R115.652289
Diner, B.A., Lum, K.K., Toettcher, J.E., Cristea, I.M., 2016. Viral DNA Sensors IFI16 and Cyclic GMP-AMP Synthase Possess Distinct Functions in Regulating Viral Gene Expression, Immune Defenses, and Apoptotic Responses during Herpesvirus Infection. MBio 7, 1–15. https://doi.org/10.1128/mBio.01553-16
Dupuis, M., Denis-Mize, K., Woo, C., Goldbeck, C., Selby, M.J., Chen, M., Otten, G.R., Ulmer, J.B., Donnelly, J.J., Ott, G., McDonald, D.M., 2000. Distribution of DNA Vaccines Determines Their Immunogenicity After Intramuscular Injection in Mice. J. Immunol. 165, 2850–2858. https://doi.org/10.4049/jimmunol.165.5.2850
Ebina, H., Misawa, N., Kanemura, Y., Koyanagi, Y., 2013. Harnessing the CRISPR/Cas9 system to disrupt latent HIV-1 provirus. Sci. Rep. 3, 2510. https://doi.org/10.1038/srep02510
Elmore, S., 2007. Apoptosis: a review of programmed cell death. Toxicol. Pathol. 35, 495–516. https://doi.org/https://doi.org/10.1016/j.addr.2019.02.003
Englund, P., Lindroos, E., Nennesmo, I., Klareskog, L., Lundberg, I.E., 2001. Skeletal muscle fibers express major histocompatibility complex class II antigens independently of inflammatory infiltrates in inflammatory myopathies. Am. J. Pathol. 159, 1263–1273. https://doi.org/10.1016/S0002-9440(10)62513-8
Esparza, J., Nitsche, A., Damaso, C.R., 2018. Beyond the myths: Novel findings for old paradigms in the history of the smallpox vaccine. PLoS Pathog. 14, 1–6. https://doi.org/10.1371/journal.ppat.1007082
Fan, T., Han, L., Cong, R., Liang, J., 2005. Caspase Family Proteases and Apoptosis Molecular Properties of Caspases 37, 719–727. https://doi.org/10.1111/j.1745-7270.2005.00108.x
Faurez, F., Dory, D., Grasland, B., Jestin, A., 2009. Replication of porcine circoviruses. Virol. J. 6, 60. https://doi.org/10.1186/1743-422X-6-60
Faurez, F., Dory, D., Henry, A., Bougeard, S., Jestin, A., 2010. Replication efficiency of rolling-circle replicon-based plasmids derived from porcine circovirus 2 in eukaryotic cells. J. Virol. Methods 165, 27–35. https://doi.org/10.1016/j.jviromet.2009.12.013
Feins, S., Kong, W., Williams, E.F., Milone, M.C., Fraietta, J.A., 2019. An introduction to chimeric antigen receptor (CAR) T-cell immunotherapy for human cancer. Am. J. Hematol. 94, S3–S9. https://doi.org/10.1002/ajh.25418
Fellay, J., Shianna, K. V., Ge, D., Colombo, S., Ledergerber, B., Weale, M., Zhang, K., Gumbs, C., Castagna, A., Cossarizza, A., Cozzi-Lepri, A., De Luca, A., Easterbrook, P., Francioli, P., Mallal,

S., Martinez-Picado, J., Miro, J.M., Obel, N., Smith, J.P., Wyniger, J., Descombes, P., Antonarakis, S.E., Letvin, N.L., McMichael, A.J., Haynes, B.F., Telenti, A., Goldstein, D.B., 2007. A whole-genome association study of major determinants for host control of HIV-1. Science (80-.). 317, 944–947. https://doi.org/10.1126/science.1143767

Ferraro, B., Morrow, M.P., Hutnick, N.A., Shin, T.H., Lucke, C.E., Weiner, D.B., 2011. Clinical Applications of DNA Vaccines : Current Progress 53. https://doi.org/10.1093/cid/cir334

Finsterbusch, T., Mankertz, A., 2009. Porcine circoviruses—Small but powerful. Virus Res. 143, 177–183. https://doi.org/10.1016/j.virusres.2009.02.009

Finsterbusch, T., Steinfeldt, T., Doberstein, K., Rödner, C., Mankertz, A., 2009. Interaction of the replication proteins and the capsid protein of porcine circovirus type 1 and 2 with host proteins. Virology 386, 122–131. https://doi.org/10.1016/j.virol.2008.12.039

Fitzgerald, D.W., Janes, H., Robertson, M., Coombs, R., Frank, I., Gilbert, P., Loufty, M., Mehrotra, D., Duerr, A., 2011. An Ad5-vectored HIV-1 vaccine elicits cell-mediated immunity but does not affect disease progression in HIV-1-infected male subjects: Results from a randomized placebo-controlled trial (The step study). J. Infect. Dis. 203, 765–772. https://doi.org/10.1093/infdis/jiq114

Flier, J., Boorsma, D.M., Beek, P.J. Van, Nieboer, C., Stoof, T.J., Willemze, R., Tensen, C.P., 2001. Differential expression of CXCR3 targeting chemokines CXCL10 , CXCL9 , and CXCL11 in different types of skin inflammation 398–405.

Fort, M., Fernandes, L.T., Nofrarias, M., Díaz, I., Sibila, M., Pujols, J., Mateu, E., Segalés, J., 2009. Development of cell-mediated immunity to porcine circovirus type 2 (PCV2) in caesarean-derived, colostrum-deprived piglets. Vet. Immunol. Immunopathol. 129, 101–107. https://doi.org/10.1016/j.vetimm.2008.12.024

Fort, M., Sibila, M., Nofrarías, M., Pérez-Martín, E., Olvera, A., Mateu, E., Segalés, J., 2010. Porcine circovirus type 2 (PCV2) Cap and Rep proteins are involved in the development of cell-mediated immunity upon PCV2 infection. Vet. Immunol. Immunopathol. 137, 226–234. https://doi.org/10.1016/j.vetimm.2010.05.013

Fukumoto, Y., Obata, Y., Ishibashi, K., Tamura, N., Kikuchi, I., Aoyama, K., Hattori, Y., Tsuda, K., Nakayama, Y., Yamaguchi, N., 2010. Cost-effective gene transfection by DNA compaction at pH 4.0 using acidified, long shelf-life polyethylenimine. Cytotechnology 62, 73–82. https://doi.org/10.1007/s10616-010-9259-z

Gagniuc, P., Ionescu-Tirgoviste, C., 2012. Eukaryotic genomes may exhibit up to 10 generic classes of gene promoters. BMC Genomics 13, 512. https://doi.org/10.1186/1471-2164-13-512

Galluzzi, L., Buqué, A., Kepp, O., Zitvogel, L., Kroemer, G., 2016. Immunogenic cell death in cancer and infectious disease. Nat. Publ. Gr. 17, 97–111. https://doi.org/10.1038/nri.2016.107

Galluzzi, L., Kepp, O., Kroemer, G., 2009. RIP Kinases Initiate Programmed Necrosis. J. Mol. Cell Biol. 8–10. https://doi.org/10.1093/jmcb/mjp007

Galluzzi, L., Vitale, I., Aaronson, S.A., Abrams, J.M., Adam, D., Agostinis, P., Alnemri, E.S., Altucci, L., Amelio, I., Andrews, D.W., Annicchiarico-Petruzzelli, M., Antonov, A. V., Arama, E., Baehrecke, E.H., Barlev, N.A., Bazan, N.G., Bernassola, F., Bertrand, M.J.M., Bianchi, K., Blagosklonny, M. V., Blomgren, K., Borner, C., Boya, P., Brenner, C., Campanella, M., Candi, E., Carmona-Gutierrez, D., Cecconi, F., Chan, F.K.-M., Chandel, N.S., Cheng, E.H., Chipuk, J.E., Cidlowski, J.A., Ciechanover, A., Cohen, G.M., Conrad, M., Cubillos-Ruiz, J.R., Czabotar, P.E., D'Angiolella, V., Dawson, T.M., Dawson, V.L., De Laurenzi, V., De Maria, R., Debatin, K.-M., DeBerardinis, R.J., Deshmukh, M., Di Daniele, N., Di Virgilio, F., Dixit, V.M., Dixon, S.J., Duckett, C.S., Dynlacht, B.D., El-Deiry, W.S., Elrod, J.W., Fimia, G.M., Fulda, S., García-Sáez, A.J., Garg, A.D., Garrido, C., Gavathiotis, E., Golstein, P., Gottlieb, E., Green, D.R., Greene, L.A., Gronemeyer, H., Gross, A., Hajnoczky, G., Hardwick, J.M., Harris, I.S., Hengartner, M.O., Hetz, C., Ichijo, H., Jäättelä, M., Joseph, B., Jost, P.J., Juin, P.P., Kaiser, W.J., Karin, M., Kaufmann, T., Kepp, O., Kimchi, A., Kitsis, R.N., Klionsky, D.J., Knight, R.A., Kumar, S., Lee, S.W., Lemasters, J.J., Levine, B., Linkermann, A., Lipton, S.A., Lockshin, R.A., López-Otín, C., Lowe, S.W., Luedde, T., Lugli, E., MacFarlane, M., Madeo, F., Malewicz, M., Malorni, W., Manic, G., Marine, J.-C., Martin, S.J., Martinou, J.-C., Medema, J.P., Mehlen, P., Meier, P., Melino, S., Miao, E.A., Molkentin, J.D., Moll, U.M., Muñoz-Pinedo, C., Nagata, S., Nuñez, G., Oberst, A., Oren, M., Overholtzer, M., Pagano, M., Panaretakis, T., Pasparakis, M., Penninger, J.M., Pereira, D.M., Pervaiz, S., Peter, M.E., Piacentini, M., Pinton, P., Prehn, J.H.M.,

Puthalakath, H., Rabinovich, G.A., Rehm, M., Rizzuto, R., Rodrigues, C.M.P., Rubinsztein, D.C., Rudel, T., Ryan, K.M., Sayan, E., Scorrano, L., Shao, F., Shi, Y., Silke, J., Simon, H.-U., Sistigu, A., Stockwell, B.R., Strasser, A., Szabadkai, G., Tait, S.W.G., Tang, D., Tavernarakis, N., Thorburn, A., Tsujimoto, Y., Turk, B., Vanden Berghe, T., Vandenabeele, P., Vander Heiden, M.G., Villunger, A., Virgin, H.W., Vousden, K.H., Vucic, D., Wagner, E.F., Walczak, H., Wallach, D., Wang, Y., Wells, J.A., Wood, W., Yuan, J., Zakeri, Z., Zhivotovsky, B., Zitvogel, L., Melino, G., Kroemer, G., 2018. Molecular mechanisms of cell death: recommendations of the Nomenclature Committee on Cell Death 2018. Cell Death Differ. https://doi.org/10.1038/s41418-017-0012-4

Garber, D. a, O'Mara, L. a, Gangadhara, S., McQuoid, M., Zhang, X., Zheng, R., Gill, K., Verma, M., Yu, T., Johnson, B., Li, B., Derdeyn, C. a, Ibegbu, C., Altman, J.D., Hunter, E., Feinberg, M.B., 2012. Deletion of specific immune-modulatory genes from modified vaccinia virus Ankara-based HIV vaccines engenders improved immunogenicity in rhesus macaques. J. Virol. 86, 12605–15. https://doi.org/10.1128/JVI.00246-12

Gardiner-Garden, M., Frommer, M., 1987. CpG Islands in vertebrate genomes. J. Mol. Biol. 196, 261–282. https://doi.org/10.1016/0022-2836(87)90689-9

Geldmacher, C., Currier, J.R., Herrmann, E., Haule, A., Kuta, E., McCutchan, F., Njovu, L., Geis, S., Hoffmann, O., Maboko, L., Williamson, C., Birx, D., Meyerhans, A., Cox, J., Hoelscher, M., 2007. CD8 T-cell recognition of multiple epitopes within specific Gag regions is associated with maintenance of a low steady-state viremia in human immunodeficiency virus type 1-seropositive patients. J. Virol. 81, 2440–8. https://doi.org/10.1128/JVI.01847-06

Georg, P., Sander, L.E., 2019. Innate sensors that regulate vaccine responses. Curr. Opin. Immunol. 59, 31–41. https://doi.org/10.1016/j.coi.2019.02.006

Gibbs, M.J., Weiller, G.F., 1999. Evidence that a plant virus switched hosts to infect a vertebrate and then recombined with a vertebrate-infecting virus. Proc. Natl. Acad. Sci. 96, 8022–8027. https://doi.org/10.1073/pnas.96.14.8022

Giglia-Mari, G., Zotter, A., Vermeulen, W., 2011. DNA damage response. Cold Spring Harb. Perspect. Biol. 3, 1–19. https://doi.org/10.1101/cshperspect.a000745

Gilbert, S.C., 2012. T-cell-inducing vaccines - what's the future. Immunology 135, 19–26. https://doi.org/10.1111/j.1365-2567.2011.03517.x

Gray, Q., Across, L., Image, E., Object, S., n.d. Basic Intensity Quantification with ImageJ 1–5.

Gross, C.P., Sepkowitz, K.A., 1998. The myth of the medical breakthrough: Smallpox, vaccination, and Jenner reconsidered. Int. J. Infect. Dis. 3, 54–60. https://doi.org/10.1016/S1201-9712(98)90096-0

Gross, S., Catez, F., Masumoto, H., Lomonte, P., 2012. Centromere Architecture Breakdown Induced by the Viral E3 Ubiquitin Ligase ICP0 Protein of Herpes Simplex Virus Type 1. PLoS One 7, 1–13. https://doi.org/10.1371/journal.pone.0044227

Gulce-Iz, S., Saglam-Metiner, P., 2019. Current State of the Art in DNA Vaccine Delivery and Molecular Adjuvants: Bcl-xL Anti-Apoptotic Protein as a Molecular Adjuvant, in: Immune Response Activation and Immunomodulation. https://doi.org/10.5772/intechopen.82203

Guo, J., 2014. Transcription: the epicenter of gene expression. J. Zhejiang Univ. Sci. B 15, 409–411. https://doi.org/10.1631/jzus.B1400113

Gutierrez, C., 1999. Geminivirus DNA replication [J]. Cell. Mol. Life Sci. 56, 313–29. https://doi.org/10.1007/s000180050433

Hajam, I.A., Dar, P.A., Shahnawaz, I., Jaume, J.C., Lee, J.H., 2017. Bacterial flagellin-a potent immunomodulatory agent. Exp. Mol. Med. 49, 1–15. https://doi.org/10.1038/emm.2017.125

Hakimuddin, F., Abidi, F., Jafer, O., Li, C., Wernery, U., Hebel, C., Khazanehdari, K., 2016. Incidence and detection of beak and feather disease virus in psittacine birds in the UAE. Biomol. Detect. Quantif. 6, 27–32. https://doi.org/10.1016/j.bdq.2015.10.001

Hanauske-Abel, H.M., Saxena, D., Palumbo, P.E., Hanauske, A.R., Luchessi, A.D., Cambiaghi, T.D., Hoque, M., Spino, M., Gandolfi, D.D.A., Heller, D.S., Singh, S., Park, M.H., Cracchiolo, B.M., Tricta, F., Connelly, J., Popowicz, A.M., Cone, R. a., Holland, B., Pe'ery, T., Mathews, M.B., 2013. Drug-Induced Reactivation of Apoptosis Abrogates HIV-1 Infection. PLoS One 8. https://doi.org/10.1371/journal.pone.0074414

Hároníková, L., Coufal, J., Kejnovská, I., Jagelská, E.B., Fojta, M., Dvoøáková, P., Muller, P.,

Vojtesek, B., Brázda, V., 2016. IFI16 preferentially binds to DNA with quadruplex structure and enhances DNA quadruplex formation. PLoS One 11, 1–19. https://doi.org/10.1371/journal.pone.0157156
Harris, L.K., Theriot, J.A., 2018. Surface Area to Volume Ratio: A Natural Variable for Bacterial Morphogenesis. Trends Microbiol. 26, 815–832. https://doi.org/10.1016/j.tim.2018.04.008
Hasson, S.S.A.A., Al-Busaidi, J.K.Z., Sallam, T.A., 2015. The past, current and future trends in DNA vaccine immunisations. Asian Pac. J. Trop. Biomed. 5, 344–353. https://doi.org/10.1016/S2221-1691(15)30366-X
Hayward, A., 2017. Origin of the retroviruses: when, where, and how? Curr. Opin. Virol. 25, 23–27. https://doi.org/10.1016/j.coviro.2017.06.006
Heath, L., Williamson, A.-L., Rybicki, E.P., 2006. The capsid protein of beak and feather disease virus binds to the viral DNA and is responsible for transporting the replication-associated protein into the nucleus. J. Virol. 80, 7219–7225. https://doi.org/10.1128/JVI.02559-05
Heyraud-Nitschke, F., Schumacher, S., Laufs, J., Schaefer, S., Schell, J., Gronenborn, B., 1995. Determination of the origin cleavage and joining domain of geminivirus Rep proteins. Nucleic Acids Res. 23, 910–916. https://doi.org/10.1093/nar/23.6.910
Hobernik, D., Bros, M., 2018. DNA Vaccines—How Far From Clinical Use? Int. J. Mol. Sci. 19, 3605. https://doi.org/10.3390/ijms19113605
Hofer, U., 2014. Viral pathogenesis: HIV-1 adds fuel to the fire. Nat. Rev. Microbiol. 12, 74–5. https://doi.org/10.1038/nrmicro3201
Hokey, D.A., Weiner, D.B., 2006. DNA vaccines for HIV : challenges and opportunities 267–279. https://doi.org/10.1007/s00281-006-0046-z
Hongo, K., Kazama, S., Tsuno, N.H., Ishihara, S., Sunami, E., Kitayama, J., Watanabe, T., 2015. Immunohistochemical detection of high-mobility group box 1 correlates with resistance of preoperative chemoradiotherapy for lower rectal cancer: A retrospective study. World J. Surg. Oncol. 13, 1–7. https://doi.org/10.1186/1477-7819-13-7
Horn, S., Hughes, M.A., Schilling, R., Sprick, M.R., Macfarlane, M., Leverkus, M., Horn, S., Hughes, M.A., Schilling, R., Sticht, C., Tenev, T., Ploesser, M., 2017. Caspase-10 Negatively Regulates Caspase-8- Mediated Cell Death , Switching the Response to CD95L in Favor of NF- k B Activation and Cell Survival Article Caspase-10 Negatively Regulates Caspase-8-Mediated Cell Death , Switching the Response to CD95L in Fa. CellReports 19, 785–797. https://doi.org/10.1016/j.celrep.2017.04.010
Hovav, A.-H., Panas, M.W., Rahman, S., Sircar, P., Gillard, G., Cayabyab, M.J., Letvin, N.L., 2007. Duration of Antigen Expression In Vivo following DNA Immunization Modifies the Magnitude, Contraction, and Secondary Responses of CD8+ T Lymphocytes. J. Immunol. 179, 6725–6733. https://doi.org/10.4049/jimmunol.179.10.6725
Hsu, D.C., O'Connell, R.J., 2017. Progress in HIV vaccine development. Hum. Vaccines Immunother. 13, 1018–1030. https://doi.org/10.1080/21645515.2016.1276138
Hu, H., Sun, S.C., 2016. Ubiquitin signaling in immune responses. Cell Res. 26, 457–483. https://doi.org/10.1038/cr.2016.40
Hu, J., Bounds, C.E., Budgeon, L.R., Cladel, N.M., 2016. DNA Vaccines Delivered By Microneedle and Tattoo Gun Induce Protective Immune Responses to Hla-A2 . 1 Restricted CRPV E1 and HPV16e7 Epitopes in HLA-A2 . 1 Transgenic Rabbits. SM Vaccines Vaccin. J. 2, 1–8.
Huang, S.W., Liu, H.P., Chen, J.K., Shien, Y.W., Wong, M.L., Wang, C.Y., 2016. Dual ATPase and GTPase activity of the replication-associated protein (Rep) of beak and feather disease virus. Virus Res. 213, 149–161. https://doi.org/10.1016/j.virusres.2015.12.001
Illingworth, R.S., Bird, A.P., 2009. CpG islands - "A rough guide." FEBS Lett. 583, 1713–1720. https://doi.org/10.1016/j.febslet.2009.04.012
Imai, M., Watanabe, T., Hatta, M., Das, S.C., Ozawa, M., Shinya, K., Zhong, G., Hanson, A., Katsura, H., Watanabe, S., Li, C., Kawakami, E., Yamada, S., Kiso, M., Suzuki, Y., Maher, E.A., Neumann, G., Kawaoka, Y., 2012. Experimental adaptation of an influenza H5 HA confers respiratory droplet transmission to a reassortant H5 HA/H1N1 virus in ferrets. Nature 486, 420–428. https://doi.org/10.1038/nature10831
Isaacs, S.N., 2004. Vaccinia Virus and Poxvirology Methods and Protocols, in: Methods in Molecular Biology. p. 402.

Jacobsen, L.B., Calvin, S.A., Lobenhofer, E.K., 2009. Transcriptional effects of transfection: The potential for misinterpretation of gene expression data generated from transiently transfected cells. Biotechniques 47, 617–624. https://doi.org/10.2144/000113132

Jacobson, L.S., Lima, H., Goldberg, M.F., Gocheva, V., Tsiperson, V., Sutterwala, F.S., Joyce, J.A., Gapp, B. V., Blomen, V.A., Chandran, K., Brummelkamp, T.R., Diaz-Griffero, F., Brojatsch, J., 2013. Cathepsin-mediated necrosis controls the adaptive immune response by Th2 (T helper type 2)-associated adjuvants. J. Biol. Chem. 288, 7481–7491. https://doi.org/10.1074/jbc.M112.400655

Janeway, C. a, Medzhitov, R., 2002. Innate immune recognition. Annu. Rev. Immunol. 20, 197–216. https://doi.org/10.1146/annurev.immunol.20.083001.084359

Jia, X., Mclaren, P.J., Kadie, C.M., Carlson, J.M., Heckerman, D., De, P.I.W., Sullivan, J., Gonzalez, E., Davies, L., Camargo, A., Moore, J.M., Gupta, S., Crenshaw, A., Burtt, N.P., Guiducci, C., Cutrell, E., Rosenberg, R., Moss, K.L., Lemay, P., Leary, J.O., Schaefer, T., Verma, P., Toth, I., Block, B., Rothchild, A., Lian, J., Proudfoot, J., Alvino, D.M.L., Vine, S., Addo, M.M., Allen, T.M., Altfeld, M., Henn, M.R., Gall, S. Le, Streeck, H., Walker, B.D., Clinical, A., Group, T., 2011. The Major Genetic Determinants of HIV-1 Control Affect HLA Class I Peptide Presentation. Science 330, 1551–1557. https://doi.org/10.1126/science.1195271.The

Jiang, Q., Zhao, S., Liu, J., Song, L., Wang, Z.G., Ding, B., 2019. Rationally designed DNA-based nanocarriers. Adv. Drug Deliv. Rev. https://doi.org/10.1016/j.addr.2019.02.003

Kane, B.A., Bryant, K.J., McNeil, H.P., Tedla, N.T., 2014. Termination of immune activation: An essential component of healthy host immune responses. J. Innate Immun. 6, 727–738. https://doi.org/10.1159/000363449

Kanterman, J., Sade-feldman, M., Baniyash, M., 2012. New insights into chronic inflammation-induced immunosuppression. Semin. Cancer Biol. 22, 307–318. https://doi.org/10.1016/j.semcancer.2012.02.008

Karrer, U., Sierro, S., Wagner, M., Oxenius, A., Hengel, H., Koszinowski, U.H., Phillips, R.E., Klenerman, P., 2003. Memory Inflation: Continuous Accumulation of Antiviral CD8 + T Cells Over Time . J. Immunol. 170, 2022–2029. https://doi.org/10.4049/jimmunol.170.4.2022

Karrer, U., Wagner, M., Sierro, S., Oxenius, A., Hengel, H., Dumrese, T., Freigang, S., Koszinowski, U.H., Phillips, R.E., Klenerman, P., 2004. Expansion of Protective CD8+ T-Cell Responses Driven by Recombinant Cytomegaloviruses. J. Virol. 78, 2255–2264. https://doi.org/10.1128/jvi.78.5.2255-2264.2004

Keller-Stanislawski, B., Englund, J.A., Kang, G., Mangtani, P., Neuzil, K., Nohynek, H., Pless, R., Lambach, P., Zuber, P., 2014. Safety of immunization during pregnancy: A review of the evidence of selected inactivated and live attenuated vaccines. Vaccine 32, 7057–7064. https://doi.org/10.1016/j.vaccine.2014.09.052

Kempen, T.S. Van, Wenink, M.H., Leijten, E.F.A., Radstake, T.R.D.J., 2015. Perception of self : distinguishing autoimmunity from autoinflammation. Nat. Rev. Rheumatol. 1–10. https://doi.org/10.1038/nrrheum.2015.60

Kepp, O., Senovilla, L., Vitale, I., 2014. Consensus guidelines for the detection of immunogenic cell death. … 1–19. https://doi.org/10.4161/21624011.2014.955691

Kim, Jae-hoon, Park, M., Nikapitiya, C., Kim, T., Uddin, B., Lee, H., Kim, E., Ma, J.Y., Jung, J.U., Kim, Joong, Lee, J., 2017. FAS-associated factor-1 positively regulates type I interferon response to RNA virus infection by targeting NLRX1 1–26.

Kim, T.K., 2017. Understanding one-way anova using conceptual figures. Korean J. Anesthesiol. 70, 22–26. https://doi.org/10.4097/kjae.2017.70.1.22

Kipnis, J., 2018. Immune system : The " seventh sense ." J. Exp. Med. 1–2. https://doi.org/10.1084/jem.20172295

Kirsch, P., Hafner, M., Zentgraf, H., Schilling, L., 2003. Time Course of Fluorescence Intensity and Protein Expression in HeLa Cells Stably Transfected with hrGFP. Mol. Cells 15, 341–348.

Knipe, D.M., 2015. Nuclear sensing of viral DNA, epigenetic regulation of herpes simplex virus infection, and innate immunity. Virology 479–480, 153–159. https://doi.org/10.1016/j.virol.2015.02.009

Knudsen, M.L., Ljungberg, K., Tatoud, R., Weber, J., Esteban, M., Liljestr??m, P., 2015. Alphavirus replicon DNA expressing HIV antigens is an excellent prime for boosting with recombinant

Modified Vaccinia Ankara (MVA) or with HIV gp140 protein antigen. PLoS One 10, 1–17. https://doi.org/10.1371/journal.pone.0117042
Kobie, J.J., Zheng, B., Bryk, P., Barnes, M., Ritchlin, C.T., Tabechian, D.A., Anandarajah, A.P., Looney, R.J., Thiele, R.G., Anolik, J.H., Coca, A., Wei, C., Rosenberg, A.F., Feng, C., Treanor, J.J., Lee, F.E.H., Sanz, I., 2011. Decreased influenza-specific B cell responses in rheumatoid arthritis patients treated with anti-tumor necrosis factor. Arthritis Res. Ther. 13, R209. https://doi.org/10.1186/ar3542
Kobiyama, K., Jounai, N., Aoshi, T., Tozuka, M., Takeshita, F., Coban, C., Ishii, K., 2013a. Innate Immune Signaling by, Genetic Adjuvants for, DNA Vaccination. Vaccines 1, 278–292. https://doi.org/10.3390/vaccines1030278
Kobiyama, K., Jounai, N., Aoshi, T., Tozuka, M., Takeshita, F., Coban, C., Ishii, K., 2013b. Innate Immune Signaling by, Genetic Adjuvants for, DNA Vaccination. Vaccines 1, 278–292. https://doi.org/10.3390/vaccines1030278
Kochs, G., Janzen, C., Hohenberg, H., Haller, O., 2002. Antivirally active MxA protein sequesters La Crosse virus nucleocapsid protein into perinuclear complexes. PNAS 99. https://doi.org/doi㽵10.1073㽵pnas.052430399
Kollaritsch, H., Rendi-Wagner, P., 2013. 9 - Principles of Immunization, in: Keystone, J.S., Freedman, D.O., Kozarsky, P.E., Connor, B.A., Nothdurft, H.D.B.T.-T.M. (Third E. (Eds.), Travel Medicine (Third Edition). Saunders, London, pp. 67–76. https://doi.org/https://doi.org/10.1016/B978-1-4557-1076-8.00009-0
Komuro, A., Horvath, C.M., 2006. RNA- and Virus-Independent Inhibition of Antiviral Signaling by RNA Helicase LGP2. J. Virol. 80, 12332–12342. https://doi.org/10.4049/jimmunol.175.5.2851
Koonin, E. V., Dolja, V. V., Krupovic, M., 2015. Origins and evolution of viruses of eukaryotes: The ultimate modularity. Virology 479–480, 2–25. https://doi.org/10.1016/j.virol.2015.02.039
Kumar, H., Kawai, T., Akira, S., 2011. Pathogen recognition by the innate immune system. Int. Rev. Immunol. 30, 16–34. https://doi.org/10.3109/08830185.2010.529976
Kuroda, E., 2018. Unravelling how adjuvants work, and what their roles are in vaccination and allergy. Impact 2018, 44–46. https://doi.org/10.21820/23987073.2018.3.44
Kutzler, M.A., Weiner, D.B., 2008. DNA vaccines: ready for prime time? Nat. Rev. Genet. 9, 776–788. https://doi.org/10.1038/nrg2432
Latz, E., Schoenemeyer, A., Visintin, A., Fitzgerald, K.A., Monks, B.G., Knetter, C.F., Lien, E., Nilsen, N.J., Espevik, T., Golenbock, D.T., 2004. TLR9 signals after translocating from the ER to CpG DNA in the lysosome. Nat. Immunol. 5, 190–198. https://doi.org/10.1038/ni1028
Laufs, J., Jupin, I., David, C., Schumacher, S., Heyraud-Nitschke, F., Gronenborn, B., 1995. Geminivirus replication: Genetic and biochemical characterization of rep protein function, a review. Biochimie 77, 765–773. https://doi.org/10.1016/0300-9084(96)88194-6
Lawson, R.., 2004. Science in the Ancient World: An Encyclopedia (History of Science). ABC-CLIO.
Lee, Y.K., Mazmanian, S.K., 2010. Has the microbiota played a critical role in the evolution of the adaptive immune system? Science 330, 1768–73. https://doi.org/10.1126/science.1195568
Leitner, W.W., Hwang, L.N., Deveer, M.J., Zhou, A., Robert, H., Williams, B.R.G., Dubensky, T.W., Ying, H., Nicholas, P., Silverman, R.H., Williams, B.R.G., Dubensky, T.W., Ying, H., Restifo, N.P., 2003. Alphavirus-based DNA vaccine breaks immunological tolerance by activating innate antiviral pathways. Nat. Med. 9, 33–39. https://doi.org/10.1038/nmxx
Li, L., Petrovsky, N., Li, L., Petrovsky, N., 2016. Molecular mechanisms for enhanced DNA vaccine immunogenicity. Expert Rev. Vaccines 0584, 0–17. https://doi.org/10.1586/14760584.2016.1124762
Li, L., Saade, F., Petrovsky, N., 2012. The future of human DNA vaccines. J. Biotechnol. 162, 171–182. https://doi.org/10.1016/j.jbiotec.2012.08.012
Li, T., Chen, Z.J., 2018. The cGAS–cGAMP–STING pathway connects DNA damage to inflammation, senescence, and cancer. J. Exp. Med. jem.20180139. https://doi.org/10.1084/jem.20180139
Liadaki, K., Luth, E.S., Kunkel, L.M., 2007. Benchmarks Co-detection of GFP and dystrophin in skeletal muscle tissue sections. Biotechniques 42, 699–700. https://doi.org/10.2144/000112494
Lin, Z., Guo, Z., Xu, Y., Zhao, X., 2014. Identification of a secondary promoter of CASP8 and its related transcription factor PURα 57–66. https://doi.org/10.3892/ijo.2014.2436

Liu, L., Pinner, M.S., Davies, J.W., Stanley, J., 1999. Adaptation of the geminivirus bean yellow dwarf virus to dicotyledonous hosts involves both virion-sense and complementary-sense genes. J. Gen. Virol. 80, 501–506.
Liu, L., Zhong, Q., Tian, T., Dubin, K., Athale, S.K., Kupper, T.S., 2010. Epidermal injury and infection during poxvirus immunization is crucial for the generation of highly protective T cell-mediated immunity. Nat. Med. 16, 224–227. https://doi.org/10.1038/nm.2078
Ljungberg, K., Liljestrom, P., 2015. Self-replicating alphavirus RNA vaccines. Expert Rev. Vaccines 14, 177–194. https://doi.org/10.1586/14760584.2015.965690
Louveau, A., Smirnov, I., Keyes, T.J., Eccles, J.D., Rouhani, S.J., Peske, J.D., Derecki, N.C., Castle, D., Mandell, J.W., Lee, K.S., Harris, T.H., Kipnis, J., 2015. Structural and functional features of central nervous system lymphatic vessels. Nature 523, 337–341. https://doi.org/10.1038/nature14432
Lugrin, J., Martinon, F., 2018. The AIM2 inflammasome: Sensor of pathogens and cellular perturbations. Immunol. Rev. 281, 99–114. https://doi.org/10.1111/imr.12618
Lundstrom, K., 2016. Replicon RNA Viral Vectors as Vaccines. Vaccines 4, 39. https://doi.org/10.3390/vaccines4040039
Luo, D., Saltzman, W.M., 2000. Synthetic DNA delivery systems. Nat. Biotechnol. 18, 33.
Luo, X., Miller, S.D., Shea, L.D., 2016. Immune Tolerance for Autoimmune Disease and Cell Transplantation. Annu. Rev. Biomed. Eng. 18, 181–205. https://doi.org/10.1146/annurev-bioeng-110315-020137
Maeto, C., Rodríguez, A.M., Holgado, M.P., Falivene, J., Gherardi, M.M., 2014. Novel mucosal DNA-MVA HIVVaccination in which DNA-IL-12 plus cholera toxin B subunit (CTB) cooperates to enhance cellular systemic and mucosal genital tract immunity. PLoS One 9. https://doi.org/10.1371/journal.pone.0107524
Magiorkinis, G., Katzourakis, A., Lagiou, P., 2017. Roles of Endogenous Retroviruses in Early Life Events. Trends Microbiol. 25, 876–877. https://doi.org/10.1016/j.tim.2017.09.002
Makkouk, A., Weiner, G.J., 2015. Cancer Immunotherapy and Breaking Immune Tolerance: New Approaches to an Old Challenge. Cancer Res. 75, 5–10. https://doi.org/10.1158/0008-5472.CAN-14-2538
Mankertz, A., Çaliskan, R., Hattermann, K., Hillenbrand, B., Kurzendoerfer, P., Mueller, B., Schmitt, C., Steinfeldt, T., Finsterbusch, T., 2004. Molecular biology of Porcine circovirus: Analyses of gene expression and viral replication. Vet. Microbiol. 98, 81–88. https://doi.org/10.1016/j.vetmic.2003.10.014
Mankertz, A., Hillenbrand, B., 2002. Analysis of transcription of Porcine circovirus type 1. J. Gen. Virol. 83, 2743–2751. https://doi.org/10.1099/0022-1317-83-11-2743
Marino, M., Scuderi, F., Provenzano, C., Bartoccioni, E., 2011. Skeletal muscle cells: From local inflammatory response to active immunity. Gene Ther. 18, 109–116. https://doi.org/10.1038/gt.2010.124
Marrack, P., Mckee, A.S., Munks, M.W., 2009. Towards an outstanding of the adjuvant action of aluminium. Nat. Rev. Immunol. 9, 287–293.
Marrack, P., Scott-Browne, J., MacLeod, M.K.L., 2010. Terminating the immune response. Immunol. Rev. 236, 5–10. https://doi.org/10.1111/j.1600-065x.2010.00928.x
Masoomi Dezfooli, S., Gutierrez-Maddox, N., Alfaro, A., Seyfoddin, A., 2018. Encapsulation for delivering bioactives in aquaculture. Rev. Aquac. 1–30. https://doi.org/10.1111/raq.12250
Masters, J.R., 2002. HeLa cells 50 years on: the good, the bad and the ugly. Nat. Rev. Cancer 2, 315. https://doi.org/10.1038/nrc774
Material, S.O., Web, S., Press, H., York, N., Nw, A., 2013. Cyclic GMP-AMP Is an Endogenous Second Messenger in Innate Immune Signaling by Cytosolic DNA. Science (80-.). 339, 826–830. https://doi.org/10.1126/science.1229963
Maul, G.G., 1998. Nuclear domain 10, the site of DNA virus transcription and replication. BioEssays 20, 660–667. https://doi.org/10.1002/(SICI)1521-1878(199808)20:8<660::AID-BIES9>3.0.CO;2-M
McKee, A.S., Burchill, M.A., Munks, M.W., Jin, L., Kappler, J.W., Friedman, R.S., Jacobelli, J., Marrack, P., 2013. Host DNA released in response to aluminum adjuvant enhances MHC class II-mediated antigen presentation and prolongs CD4 T-cell interactions with dendritic cells. Proc.

Natl. Acad. Sci. 110, E1122–E1131. https://doi.org/10.1073/pnas.1300392110
McLean, P.F., Smolke, C.D., Salit, M., 2016. Characterizing the Non-Normal Distribution of Flow Cytometry Measurements from Transiently Expressed Constructs in Mammalian Cells. bioRxiv 1–15. https://doi.org/10.1101/057950
McMichael, A.J., Koff, W.C., 2014. Vaccines that stimulate T cell immunity to HIV-1: the next step. Nat. Immunol. 15, 319–22. https://doi.org/10.1038/ni.2844
McNeel, D.G., Becker, J.T., Johnson, L.E., Olson, B.M., 2012. DNA Vaccines for Prostate Cancer. Curr. Cancer Ther. Rev. 8, 254–263. https://doi.org/10.2174/157339412804143113
Merriam-Webster, 2019. immune system [WWW Document]. Merriam-Webster online. URL https://www.merriam-webster.com/dictionary/immune system
Mestas, J., Hughes, C.C.W., 2004. Of Mice and Not Men: Differences between Mouse and Human Immunology. J. Immunol. 172, 2731–2738. https://doi.org/10.4049/jimmunol.172.5.2731
Miliotou, A.N., Papadopoulou, L.C., 2018. CAR T-cell Therapy: A New Era in Cancer Immunotherapy. Curr. Pharm. Biotechnol. 19, 5–18. https://doi.org/10.2174/1389201019666180418095526
Modra, K., 2015. Polycation-mediated gene delivery : Challenges and considerations for the process of plasmid DNA transfection 489–498. https://doi.org/10.1002/elsc.201400043
Moelling, K., Broecker, F., 2019. Viruses and Evolution – Viruses First? A Personal Perspective. Front. Microbiol. 10, 1–13. https://doi.org/10.3389/fmicb.2019.00523
Moore, K.W., de Waal Malefyt, R., Coffman, R.L., O'Garra, A., 2001. Interleukin-10 and the interleukin-10 receptor. Annu. Rev. Immunol. 19, 683–765. https://doi.org/10.1146/annurev.immunol.19.1.683
Morita, M., Gravel, S.P., Hulea, L., Larsson, O., Pollak, M., St-Pierre, J., Topisirovic, I., 2015. MTOR coordinates protein synthesis, mitochondrial activity. Cell Cycle 14, 473–480. https://doi.org/10.4161/15384101.2014.991572
Mortimer, E., Hitzeroth, I., Buys, A., Mbewana, S., Rybicki, E., 2013. An H5N1 influenza DNA vaccine for South Africa. S. Afr. J. Sci. 109, 1–4. https://doi.org/10.1590/sajs.2013/20120053
Motwani, M., Pesiridis, S., Fitzgerald, K.A., 2019. DNA sensing by the cGAS–STING pathway in health and disease. Nat. Rev. Genet. https://doi.org/10.1038/s41576-019-0151-1
National Institutes of Health, 2002. Variolation [WWW Document]. U.S Natl. Libr. Med.
Nchinda, G., Kuroiwa, J., Oks, M., Trumpfheller, C., Park, C.G., Huang, Y., Hannaman, D., Schlesinger, S.J., Mizenina, O., Nussenzweig, M.C., Überla, K., Steinman, R.M., 2008. The efficacy of DNA vaccination is enhanced in mice by targeting the encoded protein to dendritic cells. J. Clin. Invest. 118, 1427–1436. https://doi.org/10.1172/JCI34224
Niagro, F.D., Forsthoefel, A.N., Lawther, R.P., Kamalanathan, L., Ritchie, B.W., Latimer, K.S., Lukert, P.D., 1998. Beak and feather disease virus and porcine circovirus genomes: Intermediates between the geminiviruses and plant circoviruses. Arch. Virol. 143, 1723–1744. https://doi.org/10.1007/s007050050412
Nielsen, J., Keasling, J.D., 2016. Engineering Cellular Metabolism. Cell 164, 1185–1197. https://doi.org/10.1016/j.cell.2016.02.004
Nishimoto, T., 2004. Upstream and downstream of GTPase. Biol. Chem. 381, 397–405. https://doi.org/10.1515/BC.2000.052
Nolz, J.C., Harty, J.T., 2011. Strategies and implications for prime-boost vaccination to generate memory CD8 T cells. Adv. Exp. Med. Biol., Advances in Experimental Medicine and Biology 780, 69–83. https://doi.org/10.1007/978-1-4419-5632-3_7
Nordström, E.K.L., Forsell, M.N., Barnfield, C., Bonin, E., Hanke, T., Sunström, M., Karlsson, G.B., Liljeström, P., 2005. Enhanced immunogenicity using an alphavirus replicon DNA vaccine against human immunodeficiency virus type 1. J. Gen. Virol. 86, 349–354. https://doi.org/10.1099/vir.0.80481-0
Noyce, R.S., Lederman, S., Evans, D.H., 2018. Construction of an infectious horsepox virus vaccine from chemically synthesized DNA fragments. PLoS One 13, e0188453. https://doi.org/10.1371/journal.pone.0188453
Oliveira, S. De, Reyes-aldasoro, C.C., Renshaw, S.A., Mulero, V., Calado, Â., 2019. Cxcl8 (IL-8) Mediates Neutrophil Recruitment and Behavior in the Zebrafish Inflammatory Response 8. https://doi.org/10.4049/jimmunol.1203266
Palmer, K.E., Rybicki, E.P., 1998. The Molecular Biology of Mastreviruses. Adv. Virus Res. 50, 183–

234. https://doi.org/0065-3527198
Paludan, S., Bowie, A., 2013. Immune Sensing of DNA. Immunity 38, 870–880. https://doi.org/10.1016/j.immuni.2013.05.004
Panagioti, E., Klenerman, P., Lee, L.N., van der Burg, S.H., Arens, R., 2018. Features of effective T cell-inducing vaccines against chronic viral infections. Front. Immunol. 9, 1–11. https://doi.org/10.3389/fimmu.2018.00276
Pantaleo, G., Koup, R. a, 2004. Correlates of immune protection in HIV-1 infection: what we know, what we don't know, what we should know. Nat. Med. 10, 806–10. https://doi.org/10.1038/nm0804-806
Parham, P., 2014. The Immune System. Garland Science.
Pass, D.., Perry, R.., 1985. Psittacine Beak and Feather Disease - an update. Aust. Vet. Pract. 15, 55–60.
Pass, D.A., Perry, R.A., 1984. The pathology of psittacine beak and feather disease. Aust. Vet. J. 61, 69–74. https://doi.org/10.1111/j.1751-0813.1984.tb15520.x
Patil, S.D., Rhodes, D.G., Burgess, D.J., 2005. DNA-based Therapeutics and DNA Delivery Systems : A Comprehensive Review. AAPS J. 7.
Pead, P.J., 2006. Benjamin Jesty: the first vaccinator revealed. Lancet 368, 2202. https://doi.org/10.1016/S0140-6736(06)69878-4
Penaloza-MacMaster, P., Barber, D.L., Wherry, E.J., Provine, N.M., Teigler, J.E., Parenteau, L., Blackmore, S., Borducchi, E.N., Larocca, R.A., Yates, K.B., Shen, H., Haining, W.N., Sommerstein, R., Pinschewer, D.D., Ahmed, R., Barouch, D.H., 2015. Vaccine-elicited CD4 t cells induce immunopathology after chronic lcmv infection. Science (80-.). 347, 278–282. https://doi.org/10.1126/science.aaa2148
Pennock, N.D., White, J.T., Cross, E.W., Cheney, E.E., Tamburini, B.A., Kedl, R.M., 2013. T cell responses: naive to memory and everything in between. AJP Adv. Physiol. Educ. 37, 273–283. https://doi.org/10.1152/advan.00066.2013
Petkov, S., Starodubova, E., Latanova, A., Kilpeläinen, A., Latyshev, O., Svirskis, S., Wahren, B., Chiodi, F., Gordeychuk, I., Isaguliants, M., 2018. DNA immunization site determines the level of gene expression and the magnitude, but not the type of the induced immune response. PLoS One 13, 1–22. https://doi.org/10.1371/journal.pone.0197902
Pickering, A.M., Davies, K.J.A., 2012. Degradation of damaged proteins: The main function of the 20S proteasome. Prog. Mol. Biol. Transl. Sci. 109, 227–248. https://doi.org/10.1016/B978-0-12-397863-9.00006-7
Pokorna, D., Rubio, I., Müller, M., 2008. DNA-vaccination via tattooing induces stronger humoral and cellular immune responses than intramuscular delivery supported by molecular adjuvants. Genet. Vaccines Ther. 6, 1–8. https://doi.org/10.1186/1479-0556-6-4
Pollara, J., Hart, L., Brewer, F., Pickeral, J., Packard, B., James, A., Komoriya, A., Ochsenbauer, C., Kappes, J.C., Roederer, M., Weinhold, K.J., Tomaras, G.D., Haynes, B.F., David, C., 2013. ADCC-mediating antibody responses 79, 603–612. https://doi.org/10.1002/cyto.a.21084.High
Pollard, T.D., Earnshaw, W.C., Lippincott-Schwartz, J., Johnson, G.T.B.T.-C.B. (Third E. (Eds.), 2017. Chapter 42 - S Phase and DNA Replication, in: Cell Biology (Third Edition). Elsevier, pp. 727–741. https://doi.org/https://doi.org/10.1016/B978-0-323-34126-4.00042-6
Pomié, C., Blasco-Baque, V., Klopp, P., Nicolas, S., Waget, A., Loubières, P., Azalbert, V., Puel, A., Lopez, F., Dray, C., Valet, P., Lelouvier, B., Servant, F., Courtney, M., Amar, J., Burcelin, R., Garidou, L., 2016. Triggering the adaptive immune system with commensal gut bacteria protects against insulin resistance and dysglycemia. Mol. Metab. 5, 392–403. https://doi.org/10.1016/j.molmet.2016.03.004
Ramsay, R.R., Tipton, K.F., 2017. Assessment of Enzyme Inhibition : A Review with Examples from the Development of Monoamine Oxidase and Cholinesterase Inhibitory Drugs. Molecules 22, 1–46. https://doi.org/10.3390/molecules22071192
Rangarajan, P.N., 2014. DNA Vaccines, Methods in Molecular Biology. Springer New York, New York, NY. https://doi.org/10.1007/978-1-4939-0410-5
Rathinam, V.A.K., Fitzgerald, K.A., 2011. Innate immune sensing of DNA viruses. Virology 411, 153–162. https://doi.org/10.1016/j.virol.2011.02.003
Reese, M.G., 2001. Application of a time-delay neural network to promoter annotation in the

Drosophila melanogaster genome. Comput. Chem. 26, 51–56. https://doi.org/10.1016/S0097-8485(01)00099-7
Reese, M.G., 2000. Computational prediction of gene structure and regulation in the genome of Drosophila melanogaster.
Regnard, G.L., 2015. Development of a potential challenge model and plant-produced vaccine candidate for beak and feather disease virus. Univ. Cape T. University of Cape Town.
Regnard, G.L., Boyes, R.S., Martin, R.O., Hitzeroth, I.I., Rybicki, E.P., 2015. Beak and feather disease viruses circulating in Cape parrots (Poicepahlus robustus) in South Africa. Arch. Virol. 160, 47–54. https://doi.org/10.1007/s00705-014-2226-9
Regnard, G.L., de Moor, W.R.J., Hitzeroth, I.I., Williamson, A.L., Rybicki, E.P., 2017. Xenogenic rolling-circle replication of a synthetic beak and feather disease virus genomic clone in 293TT mammalian cells and Nicotiana benthamiana. J. Gen. Virol. 98, 2329–2338. https://doi.org/10.1099/jgv.0.000915
Regnard, G.L., Halley-Stott, R.P., Tanzer, F.L., Hitzeroth, I.I., Rybicki, E.P., 2010. High level protein expression in plants through the use of a novel autonomously replicating geminivirus shuttle vector. Plant Biotechnol. J. 8, 38–46. https://doi.org/10.1111/j.1467-7652.2009.00462.x
Ren, J., Chen, X., Chen, Z.J., 2014. IKK β is an IRF5 kinase that instigates inflammation 2014. https://doi.org/10.1073/pnas.1418516111
Revington, G.N., Sunter, G., Bisaro, D.M., 1989. DNA sequences essential for replication of the B genome component of tomato golden mosaic virus. Plant Cell 1, 985–992. https://doi.org/10.1105/tpc.1.10.985
Richard, M., Herfst, S., Van Den Brand, J.M.A., De Meulder, D., Lexmond, P., Bestebroer, T.M., Fouchier, R.A.M., 2017. Mutations Driving Airborne Transmission of A/H5N1 Virus in Mammals Cause Substantial Attenuation in Chickens only when combined. Sci. Rep. 7, 1–13. https://doi.org/10.1038/s41598-017-07000-6
Richardson, D.R., Ponka, P., 1997. The molecular mechanisms of the metabolism and transport of iron in normal and neoplastic cells. Biochim. Biophys. Acta 1331, 1–40.
Richmond, J.M., Harris, J.E., 2014. Immunology and skin in health and disease. Cold Spring Harb. Perspect. Med. 4, 1–20. https://doi.org/10.1101/cshperspect.a015339
Ritchie, B.W., 2013. Psittacine beak and feather disease fact sheet. Infect. Dis. Comm. Man.
Ritchie, B.W., Niagro, F.D., Lukert, P.D., Steffens, W.L., Latimer, K.S., 1989. Characterization of a new virus from cockatoos with psittacine beak and feather disease. Virology 171, 83–88. https://doi.org/10.1016/0042-6822(89)90513-8
Rivera-Molina, Y.A., 2013. Nuclear domain 10 of the viral aspect. World J. Virol. 2, 110. https://doi.org/10.5501/wjv.v2.i3.110
Robino, P., Grego, E., Rossi, G., Bert, E., Tramuta, C., Stella, M.C., Bertoni, P., Nebbia, P., 2014. Molecular analysis and associated pathology of beak and feather disease virus isolated in Italy from young Congo African grey parrots (Psittacus erithacus) with an “atypical peracute form” of the disease. Avian Pathol. 43, 333–344. https://doi.org/10.1080/03079457.2014.934660
Roche, 2014. X-tremeGENE HP DNA Transfection Reagent [WWW Document]. Roche.
Rodriguez, F., Harkins, S., Slifka, M.K., Whitton, J.L., 2002. Immunodominance in Virus-Induced CD8 + T-Cell Responses Is Dramatically Modified by DNA Immunization and Is Regulated by Gamma Interferon Immunodominance in Virus-Induced CD8 ♂ T-Cell Responses Is Dramatically Modified by DNA Immunization and Is Regulated 76, 4251–4259. https://doi.org/10.1128/JVI.76.9.4251
Rong, N., Zhou, H., Liu, R., Wang, Y., Fan, Z., 2018. Ultrasound and microbubble mediated plasmid DNA uptake: A fast, global and multi-mechanisms involved process. J. Control. Release 273, 40–50. https://doi.org/10.1016/j.jconrel.2018.01.014
Rose, A.H., Hoffmann, F.W., Hara, J.H., Urschitz, J., Moisyadi, S., Hoffmann, P.R., Bertino, P., 2015. Adjuvants may reduce in vivo transfection levels for DNA vaccination in mice leading to reduced antigen-specific CD8+ T cell responses. Hum. Vaccin. Immunother. 11, 2305–2311. https://doi.org/http://dx.doi.org/10.1080/21645515.2015.1047567
Saade, F., Petrovsky, N., 2012. Technologies for enhanced efficacy of DNA vaccines. Expert Rev. Vaccines 11, 189–209. https://doi.org/10.1586/erv.11.188
Saez-Cirion, A., Manel, N., Berghman, L.R., 2016. Immune Responses to Retroviruses. Annu. Rev.

Immunol. 95, 2216–2218. https://doi.org/10.1146/annurev-immunol-051116-052155
Sánchez-Sampedro, L., Perdiguero, B., Mejías-Pérez, E., García-Arriaza, J., Di Pilato, M., Esteban, M., 2015. The evolution of poxvirus vaccines. Viruses 7, 1726–1803. https://doi.org/10.3390/v7041726
Sasaki, A., Kinjo, M., 2010. Monitoring intracellular degradation of exogenous DNA using diffusion properties. J. Control. Release 143, 104–111. https://doi.org/10.1016/j.jconrel.2009.12.013
Schell, J.B., Bahl, K., Folta-stogniew, E., Rose, N., Buonocore, L., Marx, P.A., Gambhira, R., Rose, J.K., 2015. Antigenic requirement for Gag in a vaccine that protects against high-dose mucosal challenge with simian immunodeficiency virus. Virology 476, 405–412. https://doi.org/http://dx.doi.org/10.1016/j.virol.2014.12.027
Scheller, C., Sopper, S., Ehrhardt, C., Flory, E., Koutsilieri, E., Ludwig, S., Meulen, V., Jassoy, C., 2002. Caspase inhibitors induce a switch from apoptotic to proinflammatory signaling in CD95-stimulated T lymphocytes. Eur. J. Immunol. 32, 2471–2480.
Schluns, K.S., Kieper, W.C., Jameson, S.C., Lefrançois, L., 2000. Interleukin-7 mediates the homeostasis of naïve and memory CD8 T cells in vivo. Nat. Immunol. 1, 426–32. https://doi.org/10.1038/80868
Schmidt, E. V, Christoph, G., Zeller, R., Leder, P., 1990. The cytomegalovirus enhancer: a pan-active control element in transgenic mice. Mol. Cell. Biol. 10, 4406–11. https://doi.org/10.1128/MCB.10.8.4406.Updated
Secchi, M., Grampa, V., Vangelista, L., 2018. Rational CCL5 mutagenesis integration in a lactobacilli platform generates extremely potent HIV-1 blockers. Sci. Rep. 1–13. https://doi.org/10.1038/s41598-018-20300-9
Sekaly, R.-P., 2008. The failed HIV Merck vaccine study: a step back or a launching point for future vaccine development? J. Exp. Med. 205, 7–12. https://doi.org/10.1084/jem.20072681
Shahbaznejad, L., Raeeskarami, S., Assari, R., Shakoori, A., Azhideh, H., Aghighi, Y., Tahghighi, F., Ziaee, V., 2018. Familial Mediterranean Gene (MEFV) Mutation in Parents of Children with Familial Mediterranean Fever : What Are the Exceptions ? Int. J. Inflamation 2018. https://doi.org/https://doi.org/10.1155/2018/1902791
Smirnova, L., Harris, G., Leist, M., Hartung, T., 2015. Cellular Resilience 32, 247–260. https://doi.org/https://dx.doi.org/10.14573/altex.1509271 A
Soboleski, M.R., Oaks, J., Halford, W.P., 2005. Green fluorescent protein is a quantitative reporter of gene expression in individual eukaryotic cells. FASEB J. 19, 440–442. https://doi.org/10.1096/fj.04-3180fje
Sompayrac, L.M., 2019. How the Immune System Works, 6th Editio. ed, Wiley Blackwell. John Wiley & Sons, Inc., Hoboken, NJ, USA.
Sousa, F., Prazeres, D.M.F., Queiroz, J.A., 2009. Improvement of transfection efficiency by using supercoiled plasmid DNA purified with arginine affinity chromatography. J. Gene Med. 11, 79–88. https://doi.org/10.1002/jgm.1272
Sparwasser, T., Peschel, C., Gross, O., Gewies, A., Finger, K., Scha, M., 2006. Card9 controls a non-TLR signalling pathway for innate anti-fungal immunity 442, 651–656. https://doi.org/10.1038/nature04926
Steinfeldt, T., Finsterbusch, T., Mankertz, A., 2007. Functional analysis of cis- and trans-acting replication factors of porcine circovirus type 1. J. Virol. 81, 5696–5704. https://doi.org/10.1128/JVI.02420-06
Stenger, D.C., Revington, G.N., Stevenson, M.C., Bisaro, D.M., 1991. Replicational release of geminivirus genomes from tandemly repeated copies: evidence for rolling-circle replication of a plant viral DNA. Proc. Natl. Acad. Sci. 88, 8029–8033. https://doi.org/10.1073/pnas.88.18.8029
Stephenson, K.E., Barouch, D.H., 2013. A global approach to HIV-1 vaccine development. Immunol. Rev. 254, 295–304. https://doi.org/10.1111/imr.12073
Stephenson, K.E., D'Couto, H.T., Barouch, D.H., 2016. New concepts in HIV-1 vaccine development. Curr. Opin. Immunol. 41, 39–46. https://doi.org/10.1016/j.coi.2016.05.011
Stoline, M.R., 1981. The status of multiple comparisons: Simultaneous estimation of all pairwise comparisons in one-way ANOVA designs. Am. Stat. 35, 134–141. https://doi.org/10.1080/00031305.1981.10479331
Stone, S.F., Isbister, G.K., Shahmy, S., Mohamed, F., Abeysinghe, C., Karunathilake, H., Ariaratnam,

A., Jacoby-Alner, T.E., Cotterell, C.L., Brown, S.G.A., 2013. Immune Response to Snake Envenoming and Treatment with Antivenom; Complement Activation, Cytokine Production and Mast Cell Degranulation. PLoS Negl. Trop. Dis. 7. https://doi.org/10.1371/journal.pntd.0002326

Su, X.Z., Wu, Y., Sifri, C.D., Wellems, T.E., 1996. Reduced extension temperatures required for PCR amplification of extremely A+T-rich DNA. Nucleic Acids Res. 24, 1574–5.

Tähtinen, M., Strengell, M., Collings, A., Pitkänen, J., Kjerrström, A., Hakkarainen, K., Peterson, P., Kohleisen, B., Wahren, B., Ranki, A., Ustav, M., Krohn, K., 2001. DNA vaccination in mice using HIV-1 nef, rev and tat genes in self-replicating pBN-vector. Vaccine 19, 2039–2047. https://doi.org/10.1016/S0264-410X(00)00420-5

Takeda, K., Akira, S., 2015. Toll-Like receptors. Curr. Protoc. Immunol. 2015, 14.12.1-14.12.10. https://doi.org/10.1002/0471142735.im1412s109

Tanzer, F.L., Shephard, E.G., Palmer, K.E., Burger, M., Williamson, A.-L., Rybicki, E.P., 2011. The porcine circovirus type 1 capsid gene promoter improves antigen expression and immunogenicity in a HIV-1 plasmid vaccine. Virol. J. 8, 51. https://doi.org/10.1186/1743-422X-8-51

Teng, M.W.L., Bowman, E.P., Mcelwee, J.J., Smyth, M.J., Casanova, J., Cooper, A.M., Cua, D.J., 2015. IL-12 and IL-23 cytokines : from discovery to targeted therapies for immune-mediated inflammatory diseases. https://doi.org/10.1038/nm.3895

Tisoncik, J.R., Korth, M.J., Simmons, C.P., Farrar, J., Martin, T.R., Katze, M.G., 2012. Into the Eye of the Cytokine Storm. Microbiol. Mol. Biol. Rev. 76, 16–32. https://doi.org/10.1128/mmbr.05015-11

Tokunaga, R., Zhang, W., Naseem, M., Puccini, A., Berger, M.D., Soni, S., Mcskane, M., Baba, H., Lenz, H., 2018. CXCL9 , CXCL10 , CXCL11 / CXCR3 axis for immune activation – A target for novel cancer therapy. Cancer Treat. Rev. 63, 40–47. https://doi.org/10.1016/j.ctrv.2017.11.007

Tomlin, H., Piccinini, A.M., 2018. A complex interplay between the extracellular matrix and the innate immune response to microbial pathogens. Immunology 155, 186–201. https://doi.org/10.1111/imm.12972

Toogood, P., 2002. Inhibition of protein-protein association by small molecules: approaches and progress. J. Med. Chem. 45, 1543–58.

Toubi, E., Vadasz, Z., 2019. Think autoimmunity, breath autoimmunity, and learn autoimmunity. Clin. Rheumatol. 33, 16–19. https://doi.org/10.1007/s10067-019-04540-2

Treveris, P., 1526. The grete herball.

Tzur, A., Moore, J.K., Jorgensen, P., Shapiro, H.M., Kirschner, M.W., 2011. Optimizing optical flow cytometry for cell volume-based sorting and analysis. PLoS One 6, 1–9. https://doi.org/10.1371/journal.pone.0016053

Ugolini, M., Gerhard, J., Burkert, S., Jensen, K.J., Georg, P., Ebner, F., Volkers, S.M., Thada, S., Dietert, K., Bauer, L., Schäfer, A., Helbig, E.T., Opitz, B., Kurth, F., Sur, S., Dittrich, N., Gaddam, S., Conrad, M.L., Benn, C.S., Blohm, U., Gruber, A.D., Hutloff, A., Hartmann, S., Boekschoten, M. V., Müller, M., Jungersen, G., Schumann, R.R., Suttorp, N., Sander, L.E., 2018. Recognition of microbial viability via TLR8 drives T FH cell differentiation and vaccine responses. Nat. Immunol. 19, 386–396. https://doi.org/10.1038/s41590-018-0068-4

Verhelst, J., Parthoens, E., Schepens, B., Fiers, W., Saelens, X., 2012. Interferon-Inducible Protein Mx1 Inhibits Influenza Virus by Interfering with Functional Viral Ribonucleoprotein Complex. J. Virol. 86, 13445–13455. https://doi.org/10.1128/JVI.01682-12

Vermaelen, K., 2019. Vaccine Strategies to Improve Anti-cancer Cellular Immune Responses 10, 1–17. https://doi.org/10.3389/fimmu.2019.00008

Virgin, H.W., Wherry, E.J., Ahmed, R., 2009. Redefining Chronic Viral Infection. Cell 138, 30–50. https://doi.org/10.1016/j.cell.2009.06.036

Volkman, H.E., Cambier, S., Gray, E.E., Stetson, D.B., 2018. cGAS is predominantly a nuclear protein. bioRxiv 58, 486118. https://doi.org/10.1101/486118

Vyas, S., Zaganjor, E., Haigis, M.C., 2016. Mitochondria and Cancer. Cell 166, 555–566. https://doi.org/10.1016/j.cell.2016.07.002

Wahren, B., Liu, M.A., 2014. DNA Vaccines: Recent Developments and the Future. Vaccines 785–796. https://doi.org/10.3390/vaccines2040785

Walther, W., Stein, U., 2009. Gene therapy of cancer: methods and protocols, 2nd ed, Trends in Genetics. https://doi.org/10.10007/9781597455619

Walton, A.H., Muenzer, J.T., Rasche, D., Boomer, J.S., Sato, B., Brownstein, B.H., Pachot, A., Brooks, T.L., Deych, E., Shannon, W.D., Green, J.M., Storch, G. a, Hotchkiss, R.S., 2014. Reactivation of multiple viruses in patients with sepsis. PLoS One 9, e98819. https://doi.org/10.1371/journal.pone.0098819

Wang, J., Chun, H.J., Wong, W., Spencer, D.M., Lenardo, M.J., 2001. Caspase-10 is an initiator caspase in death receptor signaling 98.

Wang, J., Shiels, C., Sasieni, P., Wu, P.J., Islam, S.A., Freemont, P.S., Sheer, D., 2004. Promyelocytic leukemia nuclear bodies associate with transcriptionally active genomic regions. J. Cell Biol. 164, 515–526. https://doi.org/10.1083/jcb.200305142

Wang, R., Brattain, M.G., 2007. The maximal size of protein to diffuse through the nuclear pore is larger than 60 kDa. FEBS Lett. 581, 3164–3170. https://doi.org/10.1016/j.febslet.2007.05.082

Ward, W.H., 1910. The seal cylinders of western Asia. The Carnegie Institution of Washington.

Wells, K.E., Maule, J., Kingston, R., Foster, K., McMahon, J., Damien, E., Poole, A., Wells, D.J., 1997. Immune responses, not promoter inactivation, are responsible for decreased long-term expression following plasmid gene transfer into skeletal muscle. FEBS Lett. 407, 164–168. https://doi.org/10.1016/S0014-5793(97)00329-3

Wen, J., Hao, W., Fan, Y., Du, J., Du, B., Qian, M., Jiang, W., 2014. Co-delivery of LIGHT expression plasmid enhances humoral and cellular immune responses to HIV-1 Nef in mice. Arch. Virol. 159, 1663–1669. https://doi.org/10.1007/s00705-014-1981-y

Wenzel, M., Wunderlich, M., Besch, R., Poeck, H., Willms, S., Schwantes, A., Kremer, M., Sutter, G., Endres, S., Schmidt, A., Rothenfusser, S., 2012. Cytosolic DNA triggers mitochondrial apoptosis via DNA damage signaling proteins independently of AIM2 and RNA polymerase III. J. Immunol. 188, 394–403. https://doi.org/10.4049/jimmunol.1100523

Wilcox, R.R., Wilcox, R.R., 2010. Understanding the Practical Advantages of Modern ANOVA Methods Understanding the Practical Advantages of Modern ANOVA Methods 4416, 37–41.

Williams, J., 2013. Vector Design for Improved DNA Vaccine Efficacy, Safety and Production. Vaccines 1, 225–249. https://doi.org/10.3390/vaccines1030225

Williamson, C., Swanstrom, R., 2015. HIV-1 replication capacity: Setting the pace of disease. Proc. Natl. Acad. Sci. 112, 201502208. https://doi.org/10.1073/pnas.1502208112

Wolff, J.A., Malone, R.W., Williams, P., Wang, C., Acsadi, G., Jani, A., Felgner, P.L., 1990. Direct gene transfer into mouse muscle in vivo. Science (80-.). 247, 1465–1468. https://doi.org/10.1126/science.1690918

Yamamoto, T., Kanuma, T., Takahama, S., Okamura, T., Moriishi, E., Ishii, K.J., Terahara, K., Yasutomi, Y., 2019. STING agonists activate latently infected cells and enhance SIV-specific responses ex vivo in naturally SIV controlled cynomolgus macaques. Sci. Rep. 9, 1–11. https://doi.org/10.1038/s41598-019-42253-3

Yang, Z.-Y., Kong, W.-P., Huang, Y., Roberts, A., Murphy, B.R., Subbarao, K., Nabel, G.J., 2004. A DNA vaccine induces SARS coronavirus neutralization and protective immunity in mice. Nature 428, 561–564. https://doi.org/10.1038/nature02463

Yi, L., Lee, Y., Izzard, L., Hurt, A.C., 2018. A Review of DNA Vaccines Against Influenza. Front. Immunol. 9, 1–8. https://doi.org/10.3389/fimmu.2018.01568

Yin, X., Wang, W., Zhu, X., Wang, Y., Wu, S., Wang, Z., Wang, L., Du, Z., Gao, J., Yu, J., 2015. Synergistic antitumor efficacy of combined DNA vaccines targeting tumor cells and angiogenesis. Biochem. Biophys. Res. Commun. 465, 239–244. https://doi.org/10.1016/j.bbrc.2015.08.003

Yoneyama, M., Kikuchi, M., Matsumoto, K., Imaizumi, T., Miyagishi, M., Taira, K., Foy, E., Loo, Y.-M., Gale, M., Akira, S., Yonehara, S., Kato, A., Fujita, T., Miyagishi, M., Taira, K., Foy, E., Loo, Y.-M., Gale, M., 2005. Shared and Unique Functions of the DExD/H-Box Helicases RIG-I, MDA5, and LGP2 in Antiviral Innate Immunity. J. Immunol. 175, 2851 LP – 2858. https://doi.org/10.4049/jimmunol.175.5.2851

Yuan, J., Najafov, A., Py, B.F., 2016. Roles of Caspases in Necrotic Cell Death. Cell 167, 1693–1704. https://doi.org/10.1016/j.cell.2016.11.047

Zapata, W., Aguilar-jim, W., Feng, Z., Weinberg, A., 2016. Identification of innate immune antiretroviral factors during in vivo and in vitro exposure to HIV-1 18, 211–219. https://doi.org/10.1016/j.micinf.2015.10.009

Zhang, Q., Lenardo, M.J., Baltimore, D., 2017. Review 30 Years of NF- k B : A Blossoming of

Relevance to Human Pathobiology. Cell 168, 37–57. https://doi.org/10.1016/j.cell.2016.12.012